The Role of the CCX-CKR Chemokine Receptor in Immunity and Tolerance

Elinor Julie Rae Anderson

A thesis submitted to the College of Medicine, Veterinary and Life Sciences, University of Glasgow in fulfilment of the requirements for the degree of Doctor of Philosophy

January 2011

Institute of Infection, Immunity and Inflammation
University of Glasgow
120 University Place
Glasgow
G12 8TA

Summary

CCX-CKR is an atypical chemokine receptor for the homeostatic chemokines CCL19, CCL21 and CCL25. CCL19 and CCL21 are also ligands for CCR7 and are crucial for the induction of antigen specific immunity and tolerance, whereas CCL25 is the sole ligand for CCR9 and is involved in the recruitment of immune effector cells to the small intestine. CCX-CKR does not signal after binding its ligands, as determined by a failure to induce the rapid increase in intracellular calcium that is typical of G-protein mediated signalling. CCX-CKR also does not become desensitised to chemokine binding and therefore is proposed to act as a scavenger receptor that can regulate the activity of CCR7 and CCR9 by affecting the availability of their ligands *in vivo*. At the time of starting my project, there were no published reports describing the biological function of CCX-CKR *in vivo* and the principal aim of my thesis was to characterise the immune system of the recently generated CCX-CKR KO mouse with particular focus on the intestinal immune compartment where all three of the chemokine ligands are expressed.

Firstly, as described in Chapter 3, I analysed the cellular composition of the secondary lymphoid organs of CCX-CKR KO mice. These studies revealed normal proportions and absolute numbers of lymphocytes, $CD11c^+$ dendritic cells (DC), macrophages and natural killer (NK) cells in the absence of CCX-CKR. The proliferative responses of lymphocytes to mitogenic or TCR stimulation *in vitro* were also normal, although there was a decreased production of IFNγ by $CD4^+$ T cells from CCX-CKR KO mice. Although most of the phenotypic subsets of conventional DC were present in comparable numbers in the mesenteric lymph nodes (MLN) of CCX-CKR KO and WT mice, there was a consistent and dramatic reduction in the numbers of $CD11c^{lo}$PDCA-1^+ plasmacytoid DC (pDC) in CCX-CKR KO MLN. In parallel, fewer $CD11c^{lo}B220^+$ cells from CCX-CKR KO MLN than WT expressed CCR9, despite this marker being expressed normally by lymphocytes in these mice. The proportions of pDC in CCX-CKR KO inguinal lymph nodes (ILN) were also significantly reduced compared to WT and pDC from CCX-CKR KO MLN, ILN and spleen all appeared to express higher levels of class II MHC than WT pDC. These data suggest that CCX-CKR may play an important role in the recruitment and/or survival of pDC in the LN and that in its absence, pDC in secondary lymphoid organs may have a more mature phenotype.

In Chapter 4, I examined the cellularity of the intestinal immune compartment in resting CCX-CKR KO mice, as well as the effects of Flt3L administration *in vivo*. Although CCX-CKR KO mice displayed no histological abnormalities in their small intestinal architecture and had normal numbers of T cells in the lamina propria, they did have significantly reduced numbers of intra-epithelial lymphocytes (IEL) as well as decreased proportions of $CD19^+$ B cells and increased proportions of $CD11c^+$ cells in the lamina propria compared with WT mice. The proportions and absolute numbers of $CD103^+$ DC were normal in the lamina propria and MLN of CCX-CKR KO mice, suggesting that CCX-CKR has little to no role in regulating DC migration from the lamina propria to the MLN, a process that is critically dependent on CCR7. Although the proportions and absolute numbers of B cells and $CD11c^+$ cells were normal in CCX-CKR KO Peyer's patches (PP), there were significantly decreased proportions of pDC compared with WT PP. *In vivo* treatment of CCX-CKR KO mice with the DC differentiation factor Flt3L, expanded $CD11c^+$ DC numbers dramatically in both CCX-CKR KO and WT small intestinal lamina propria, ILN, spleen, MLN and PP. Although Flt3L abolished the apparent defects in pDC populations in the ILN and PP, this was not the case for CCX-CKR KO MLN, which remained significantly deficient in pDC compared to WT MLN. Work in Chapter 6 examined parallel effects in the blood and bone marrow.

As the CCX-CKR ligands CCL19 and CCL21 are involved in the development of all adaptive immune responses, and together with the other CCX-CKR ligand, CCL25, orchestrate immune responses to antigen encountered in the gut, I next investigated the development of antigen specific immunity and tolerance in CCX-CKR KO mice. There were no significant differences in systemic immune responses to subcutaneous immunisation with ovalbumin (OVA) emulsified in complete Freunds adjuvant (CFA) between CCX-CKR KO and WT mice when assessed *in vivo* or *in vitro*. However, the development of oral tolerance in CCX-CKR KO mice was impaired, with no suppression of OVA specific delayed type hypersensitivity (DTH) responses or of serum OVA specific IgG2a as was seen in WT mice. In parallel with defective systemic tolerance after feeding OVA, CCX-CKR KO mice appeared to be more susceptible to priming of systemic and local antibody responses after feeding OVA with cholera toxin (CT) as a mucosal adjuvant. In addition, there was some evidence of priming of OVA specific antibody responses in CCX-CKR KO mice fed OVA alone, which was not seen in WT mice. Despite this evidence of abnormal mucosal immunity, CCX-CKR KO mice developed DSS colitis normally, with all indices of disease being identical in CCX-CKR KO and WT animals.

Together, these data suggest that there are selective defects in the regulation of antigen specific mucosal immune responses in the small intestine of CCX-CKR KO mice that may predispose these animals towards exaggerated active immune responses.

Finally, I performed some preliminary experiments to try and relate DC function to the immune dysregulation I observed in CCX-CKR KO mice and to explore the basis of the pDC defect in the MLN. Bone marrow derived and splenic DC from CCX-CKR KO mice showed a reduced ability to process and present intact protein antigens although endocytic activity was normal. MLN DC from normal and Flt3L treated CCX-CKR KO mice responded similarly to *in vitro* stimulation with the synthetic TLR7 agonist R848, showing an expansion in the numbers of $CD11c^{hi}PDCA\text{-}1^{+}$ cells that nearly all expressed CD40 and CD86. In addition, *in vivo* administration of R848 triggered identical migration of $CD11c^{hi}classIIMHC^{hi}CD103^{+}$ DC into the MLN of CCX-CKR KO and WT mice, suggesting that lamina propria pDC can effectively mobilise local DC to the MLN in the absence of CCX-CKR. There were no differences in the proportions or absolute numbers of pDC in the liver of CCX-CKR KO and WT mice despite the fact that liver pDC have been implicated in other studies of oral tolerance. Although the proportions of pDC were normal in the bone marrow of resting and Flt3L treated CCX-CKR KO mice, there did appear to be a defective recruitment of Flt3L expanded pDC into the blood of these animals. I used an adoptive transfer approach to study the *in vivo* localisation of pDC into lymphoid organs and although these experiments were not entirely conclusive, they indicated that WT pDC could enter the MLN and other lymphoid tissues of CCX-CKR KO mice normally and that pDC from CCX-CKR KO mice may have a defect in their ability to enter WT MLN.

Taken together, my data suggest that CCX-CKR is involved in the entry and/or survival of pDC in secondary lymphoid organs, a process that normally involves migration across high endothelial venules (HEV). This was associated with impaired oral tolerance induction and heightened immune responses to antigen delivered orally, indicating that CCX-CKR contributes to the regulation of mucosal immunity and tolerance by an as yet unclear mechanism. Further study of these animals will hopefully better define the relationship between pDC and the regulation of mucosal immune responses.

Table of Contents

List of Tables and Figures

Chapter 1

Chapter 2

Chapter 3

Chapter 4

Chapter 5

Chapter 6

Acknowledgements

Firstly, I would like to thank my PhD supervisors, Prof Allan Mowat and Dr Rob Nibbs for their guidance throughout my project. I would also like to thank the Oliver Bird Rheumatism Programme for funding my studies and its co-ordinator at the University of Glasgow, Prof Iain McInnes for his continued encouragement throughout my time in the department. In particular, I am eternally grateful to Allan as my principal supervisor for his tutelage and unwavering support. It was as an undergraduate student at the University of Edinburgh that I learned I had secured a place on the Oliver Bird Rheumatism Programme at the University of Glasgow and as a PhD programme with the opportunity to choose from a range of supervisors to work with, it was Allan who was repeatedly recommended to me.

Needless to say I have been most fortunate to have had worked with Allan and his group members throughout the years. I would like to thank the original "Team Mowat" members, Yvonne, Andy and the irrepressible Anne Donachie for welcoming me into the group and showing me the ropes as well as Angela, Mairi and Theresa from Prof Maggie Harnett's group. I would also like to thank the new wave of "Mowlings" that have joined "Team Mowat" and formed the Milling group over the latter part of my PhD, namely Calum and Aude as Mowat group interlopers, as well as Vuk and Lotta along with Dr Simon Milling as their group leader. It has truly been a pleasure to have had worked with you and I regard you all as dear lifelong friends (and of course respect you all as scientists especially after having seen all your antics in the pub!). I would also like to thank, Mairi Clarke, Chris, Ross, Laura, Rae, Catherine Hurson, Catherine Wilson and Derek of the Nibbs and Graham groups for being so welcoming and helpful. I especially want to thank, Vuk, Calum and Catherine for reading through my thesis chapters and Dr Carl Goodyear for being very patient when advising me on statistics. A special thank you goes to Catherine H for helping with printing. I would also like to thank the staff at the CRF, in particular, Joanne, Craig, Colin Chapman and Tony.

Thank you to my family, in particular my parents, grandmothers and great uncle Doug for always supporting me and providing a retreat as and when required. I love you all very much. To my very dear friends, Anona, Hayley, Nicola, Sarah, Ashley, Jude, Catherine H and Anne, I will always be grateful for keeping me in good humour throughout the highs and the lows of my PhD. I could not have done this without the support of my family and friends and would

like to dedicate this thesis to the memory of Gemma McLeod and her mother Agnes, two of the most incredible people I have ever known. I miss you every day Gemma.

Lastly, I suppose I should thank the long-suffering Martin especially for putting up with me over the last few months of this write up! I love you.

Author's Declaration

I declare that, except where explicit reference is made to the contribution of others, that this thesis is the result of my own work and has not been submitted for any other degree at the University of Glasgow or any other institution.

Signature: .....

Printed name: .....

Abbreviations

The following abbreviations are used throughout this thesis:

7-AAD	7-amino-actinomycin D
APC	allophycocyanin
APC	antigen presenting cells
BM	bone marrow
BMDC	bone marrow derived dendritic cells
CCL	CC-chemokine ligand
CCR	CC-chemokine receptor
CCX-CKR	Chemocentryx chemokine receptor
CD	cluster of differentiation
cDC	conventional dendritic cell
CFA	complete Freund's adjuvant
CMF-HBSS	calcium/magnesium free Hank's buffered salt solution
CP	cryptopatch
Con A	Concanavalin A
CXCL	CXC-chemokine ligand
CXCR	CXC-chemokine receptor
CX_3CL	CX_3C-chemokine ligand
CX_3CR	CX_3C-chemokine receptor
DAG	diacylglycerol
DARC	Duffy antigen receptor for chemokines
DC	dendritic cell
DNA	deoxyribonucleic acid
DP	double positive
DSS	dextran sulphate sodium
DTH	delayed type hypersensitivity
EAE	experimental autoimmune encephalitis
EDTA	ethylenediaminetetraacetic acid
ELISA	enzyme-linked immunosorbent assay
EMA	ethidium monoazide

FACS	fluorescence activated cell sorting
FAE	follicle associated epithelium
FCS	foetal calf serum
FDC	follicular dendritic cell
FGF	fibroblast growth factor
FITC	fluorescein isothiocyanate
FRC	fibroblastic reticular cell
FSC	forward scatter
Flt3	FMS-like tyrosine kinase 3
Flt3L	FMS-like tyrosine kinase 3 ligand
GAG	glycosaminoglycan
GALT	gastrointestinal associated lymphoid tissue
GC	germinal centre
GDP	guanosine diphosphate
GM-CSF	granulocyte macrophage colony-stimulating factor
GRK	G-protein coupled receptor kinase
GTP	guanosine triphosphate
HAO	heat aggregated ovalbumin
HBSS	Hank's buffered salt solution
HEV	high endothelial venule
IBD	inflammatory bowel disease
IDO	indoleamine-2,3-deoxygenase
IEL	intra-epithelial lymphocyte
IFN	interferon
Ig	immunoglobulin
IL	interleukin
ILF	isolated lymphoid follicle
ILN	inguinal lymph node
i.p.	intraperitoneal
IP_3	inositol triphosphate
IRF	interferon regulatory factor
i.v.	intravenous
kD	kilodaltons

KO	knock-out
LN	lymph node
LP	lamina propria
LPS	lipopolysaccharide
LT	lymphotoxin
LTi	lymphoid tissue inducer
LTin	lymphoid tissue initiator
LTo	lymphoid tissue organiser
M	microfold
MACS	magnetically activated cell sorter
MAPK	mitogen-activated protein kinase
MFI	mean fluorescence intensity
MHC	major histocompatibility complex
MLN	mesenteric lymph node
mRNA	messenger RNA
NK	natural killer
NKT	natural killer T
OD	optical density
OVA	ovalbumin
PAMP	pathogen associated molecular pattern
PBS	phosphate buffered solution
PCR	polymerase chain reaction
pDC	plasmacytoid dendritic cell
PE	phycoerythrin
PI3K	phosphatidylinositol biphosphate
PIgR	polymeric immunoglobulin receptor
PLC	phospholipase C
plt/plt	paucity of lymph node T cells
PMA	phorbol 12-myristate 13-acetate
Poly I:C	polyinosinic-polycytidylic acid
PP	Peyer's patches
PRR	pattern recognition receptor
R848	resiquimod

RA	retionic acid
RALDH	retinaldehyde dehydrogenase
RNA	ribonucleic acid
RPMI	Roswell Park Memorial Institute-1640 medium
RT-PCR	reverse transcriptase polymerase chain reaction
SA	streptavidin
SD	standard deviation
SP	spleen
SPF	specific pathogen free
SSC	side scatter
Tcm	central memory T cell
TEC	thymic epithelial cell
Tem	effector memory T cell
TGF	transforming growth factor
Tfh	follicular helper T cell
Th_1	T helper 1
Th_2	T helper 2
Th_{17}	T helper 17
TLR	Toll-like receptor
TMB	3,3,5,5-tetramethylbenzidine peroxides
TNF	tumour necrosis factor
TPA	12-O-tetradecanoylphorbol-13-acetate
TSLP	thymic stromal lymphopoietin
T reg	regulatory T cell
SED	sub-epithelial dome
VEGF	vascular endothelial growth factor
WT	wild type
XCL	XC-chemokine ligand
XCR	XC-chemokine receptor

Chapter 1
General Introduction

Introduction

The innate and adaptive arms of the immune system co-operate to discriminate between harmless and pathogenic antigens, tolerating and eradicating them respectively. Our immune systems are in a constantly dynamic state, employing growth factors to nurture and develop, cytokines to activate and polarise, and chemotactic molecules to guide and assemble leukocytes. Cells of the innate immune system respond to conserved microbial constituents and products of tissue damage, whereas lymphocytes of the adaptive immune system recognise specific epitopes so that targeted immunity can be implemented.

During an inflammatory immune response, antigen loaded dendritic cells (DC) are licensed at peripheral sites of infection and mature as they migrate via the afferent lymphatics to draining secondary lymphoid organs and alert circulating lymphocytes to the presence of their cognate antigen. Activated T cells and plasmablasts are then disseminated to the original site of antigen encounter to complement the innate effector mechanisms already in place, and memory T and B cells are generated to allow rapid antigen specific responses in the case of subsequent challenge. At all stages of these responses, cells must be motile and receptive to the directional cues provided by the combinational display of adhesion molecules and chemokines that allow their appropriate temporal and spatial positioning.

Chemokines regulate leukocyte organisation under homeostatic basal conditions and direct their recruitment and activation during infection and inflammation. The differential expression of chemokines and their receptors contributes to the strategic positioning of cells within their particular niches and directly influences whether immunity or tolerance ensue. As a result, chemokines must be tightly regulated to ensure appropriate immune activation and tolerance.

1.1 Chemokines – a superfamily of cytokines

Chemokines are small proteins between 8 and12 kDa in size that are best known for their ability to induce chemotaxis of leukocytes, allowing for the strategic positioning of cells during immune responses. Their sequence homology is variable, but their tertiary structure is highly conserved, comprising an N-terminus of 6-10 amino acids that serves as a crucial signalling domain (1). Most chemokines are secreted from the cell, with the exceptions of CX_3CL1 and CXCL16 that can also be tethered to extracellular surfaces by mucin-like stalks (2, 3). Chemokines and their receptors can vary dramatically in their homology between species, suggesting that there has been rapid and divergent evolution, and reflecting the ongoing "arms race" between hosts and their specific pathogens (3). Although best known as mediators of cell migration, chemokines are also involved in the processes of angiogenesis, fibrosis, cell proliferation and apoptosis (4). Chemokines can function as monomers, dimers, oligomers and even as hetero-oligomers, although oligomers appear to be needed to elicit cell migration, which is termed "haptotaxis" when movement is directional (1, 5). "Chemokinesis" is the random movement of cells in response to soluble chemokine, whereas "chemotaxis" is the directed movement of cells in response to chemokine gradients (6).

Classification of chemokines

The recent expansion in bioinformatics and gene discovery has heralded the rapid characterisation of numerous chemokines and their receptors. Such a boom in chemokine biology called for a consistency in their nomenclature, as many chemokines have several alternative names, often based on how they were originally defined functionally. Chemokines are now classified on the basis of the arrangement of four cysteine motifs in their amino acid sequence (2, 3). Approximately fifty chemokines have been characterised and they can be broadly categorized into four families. The CC chemokines (CCL1-28) comprise most of the chemokine superfamily and have the first two of their four cysteine molecules adjacent to each other. CXC chemokines (CXCL1-16) constitute the second family, and have a single amino acid between their first two cysteine residues. Three non conserved amino acids separate the first two cysteine residues of CX_3CL1, the sole member of the third family of chemokines. C chemokines (XCL1 and hXCL2) lack one of the first two cysteine residues and comprise the fourth family (3, 4, 7). The chemokine family members are summarised in Table 1.1.

Table 1.1: Systematic nomenclature of chemokines

CC Family Systematic Name	Alternative Name(s)	Systematic Receptor Name(s)
CCL1	(h)I-309 (m)TCA-3	CCR8
CCL2	(h)MCP-1 (m)JE	CCR2
CCL3	(h)MIP-1α	CCR1, CCR5
CCL4	(h)MIP-1β	CCR5
CCL5	(h)RANTES	CCR1, CCR3, CCR5
mCCL6	(m)C10	CCR1
CCL7	(h)MCP-3	CCR1, CCR2, CCR3, CCR5
CCL8	(h)MCP-2	CCR3
mCCL9	(m)MIP-1γ	CCR1
mCCL10	(m)MIP-1γ	CCR1
CCL11	Eotaxin	CCR3
mCCL12	(m)MCP-5	CCR2
hCCL13	(m)MCP-4	CCR2, CCR3
hCCL14	(h)HCC-1	CCR1
hCCL15	(h)HCC-2	CCR1, CCR3
hCCL16	(h)HCC-4	CCR1, CCR2, CCR5
CCL17	TARC	CCR4
hCCL18	(h)DC-CK1/PARC	unknown
CCL19	ELC/MIP-3β/exodus3	CCR7
CCL20	MIP3α/LARC/exodus1	CCR6
CCL21	SLC/6Ckine/exodus2	CCR7
CCL22	(h)MDC (m) ABCD-1	CCR4
hCCL23	(h)MPIF-1	CCR1
CCL24	Eotaxin-2/MPIF-2	CCR3
CCL25	TECK	CCR9
hCCL26	(h)Eotaxin-3	CCR3
CCL27	C-TACK (m)Eskine	CCR10
CCL28	(h)MEC	CCR10

C Family Systematic Name	Alternative Name(s)	Systematic Receptor Name(s)
XCL1	Lymphotactin/(h)SCM-1α	XCR1
hXCL2	(h)SCM-1β	XCR1

CX3C Systematic Name	Alternative Name(s)	Systematic Receptor Name(s)
CX3CL1	Fractalkine/ (m)Neurotactin	CX3CR1

CXC Family Systematic Name	Alternative Name(s)	Systematic Receptor Name(s)
CXCL1	(h)GROα (m)GRO/MIP-2/KC	CXCR1, CXCR2
CXCL2	(h)GROβ (m)GRO/MIP-2/KC	CXCR2
CXCL3	(h)GROγ (m)GRO/MIP-2/KC	CXCR2
CXCL4	PF4	CXCR3B
CXCL5	(h)ENA-78 (m)GCP-2/LIX	CXCR2
CXCL6	GCP-2	CXCR1, CXCR2
hCXCL7	(h)NAP-2	CXCR2
hCXCL8	(h)IL-8	CXCR1, CXCR2
CXCL9	Mig	CXCR3
CXCL10	IP-10	CXCR3
CXCL11	I-TAC	CXCR3, CXCR7
CXCL12	SDF-1	CXCR4, CXCR7
CXCL13	(h)BCA-1 (m)BLC	CXCR5
CXCL14	BRAK (h)Bolekine	unknown
mCXCL15	(m)Lungkine/WECHE	unknown
CXCL16	SCYB16, SR-PSOX	CXCR6

Preceded with (h) = applicable to humans only
Preceded with (m) = applicable to mice only
Not specified= applicable to both humans and mice

Glycosaminoglycans (GAGs) bind and localise chemokines

Most chemokines are produced as soluble molecules *in vivo*, although they are also found tethered to cell surface glycosaminoglycans (GAGs) that concentrate chemokines in localised areas and so help position cells bearing cognate chemokine receptors. GAGs are negatively charged polysaccharides attached to core proteins forming proteoglycans that interact with several circulating proteins. These are important in several complex processes such as blood coagulation and angiogenesis, as well as in modulating the signalling transduction events involved in cell development and proliferation (8, 9). Their electrostatic interactions with basic chemokines mean that GAGs such as heparan sulphate present and immobilise proteins in defiance of the shear forces found in blood vessels, allowing for the local retention of chemokines and development of putative chemokine gradients *in vivo* (8). The importance of this strategic display of chemokines as directional cues for migrating cells is apparent from observations that mice deficient in GAGs or their oligermization show impaired migration of leukocytes, as well as an inability to trigger adhesion of leukocytes to vascular endothelium in response to chemokines (5, 10, 11).

Chemokines mediate leukocyte extravasation and migration in interstitial spaces

The most familiar role of chemokines is to drive the movement of leukocytes out of blood vessels and through tissues. Leukocyte recruitment from the vasculature into lymphoid tissues is mediated via a multi-step sequential process involving selectin mediated rolling, chemokine dependent integrin activation, integrin induced arrest and cellular trans-migration across the endothelium (8, 12). This process is summarised in Figure 1.1. The co-ordinated efforts of selectins, chemokines and adhesion molecules can also result in tissue selectivity, depending on the combination and mode of molecules expressed (13). The essential role of chemokine receptors is emphasised by the fact that integrin activation, integrin mediated signalling and cellular extravasation can all be blocked using pertussis toxin to inhibit G-protein-signalling (14). Chemokine binding induces cytoskeletal rearrangements in responding cells via actin polymerisation that casues the formation of a polarised cellular morphology with chemokine receptor expression concentrated at the leading edge (6, 15, 16). This accounts for the directional movement of a cell towards chemokine and triggers a series of co-ordinated integrin activations that propel the cell onwards (17, 18). The directional movement of cells in response to chemokines has been extensively documented *in vitro* although it is not yet clear whether true chemokine gradients exist in organised lymphoid tissues *in vivo*. Lymphocytes can negotiate these sites in the absence of any such gradient, using chemokine immobilised on fibroblastic reticular cells (FRC) as a scaffolding to guide their migration (19-26). Nevertheless, it has been proposed that chemokine gradients may prevail at sites of inflammation, with evidence suggesting the formation of solid phase chemokine gradients on the GAGs of extracellular matrix of human rheumatoid synovium (27).

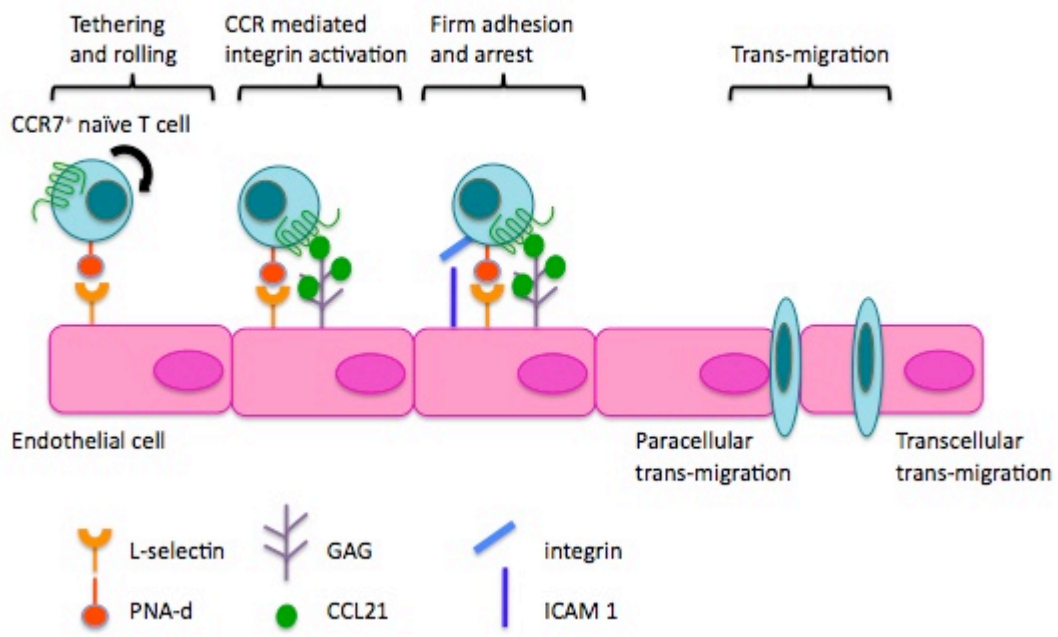

Fig 1.1 Role of chemokines in the extravasation of lymphocytes
Naïve circulating lymphocytes exit the blood via specialised high endothelial venules (HEV) into lymph nodes (LN) and Peyer's patches (PP) in search of dendritic cells (DC) presenting their cognate antigen. This is a multi-step process beginning with selectin mediated tethering that slows lymphocytes to roll along the endothelium. Rolling lymphocytes are activated via CCR7 by CCL19 and/or CCL21 presented by glycosaminoglycans (GAGs) on the luminal surface of HEV. This induces conformational changes in lymphocyte integrin molecules leading to their clustering in a high affinity state encouraging their firm arrest via interactions with endothelial expressed intracellular adhesion molecule 1 (ICAM 1). Lymphocytes then undertake paracellular or transcellular translocation between or across endothelial cells respectively, possibly in response to CCR7 ligands within the awaiting parenchyma.

1.2 Chemokine receptors

Chemokine receptors are part of the wider family of G protein linked coupled receptors (GPCR). GPCR are seven trans-membrane receptors that comprise the largest family of membrane associated receptors to have been characterised and are involved in several physiological processes such as neurotransmission, blood pressure maintenance and smooth muscle contraction (1, 5, 28). Despite no obviously conserved structural signature, chemokine receptors show up to 80% sequence homology, suggesting a common ancestor. Chemokine receptors are 340 to 370 amino acids in length, have an acidic N-terminal segment and a cysteine residue in each of their four extracellular domains. The sequence DRYLAIVHA, or a variation of it, lies in the second intracellular loop and is essential for the signal transduction events following chemokine receptor ligation (2).

In keeping with chemokine nomenclature, chemokine receptors are classified systematically based on the chemokine class they bind followed by a number. Thus, CXCR bind CXC chemokines, CCR bind CC chemokines, XCR1 binds the C chemokines XCL1 and hXCL2, and CX_3CR1 binds CX_3CL1 (3).

Chemokine receptor signal transduction

GPCR classically initiate signalling events via the activation of their associated G protein heterotrimer complexes that contain Gα, β and γ subunits. In the resting state, the Gα subunit has GDP bound rendering the G protein complex inactive. There are four families of α subunits, $G\alpha_s$, $G\alpha_q$, $G\alpha_i$ and $G\alpha_{12}$. Each family consists of several members, thus contributing to the complexity of chemokine receptor mediated signalling events. Chemotaxis is regulated primarily via the $G\alpha_i$ sub-family (29). After chemokine receptor ligation, the Gα subunit becomes phosphorylated, exchanges GDP for GTP and releases activated β and γ subunits which remain bound together. The targets of the now dissociated G protein components are usually enzymes or ion channels in the plasma membrane that ultimately lead to intracellular signalling events including activation of phosphatidylinositol 3-kinase (PI3K), phospholipase C (PLC), RAS and RHO GTPases and the mitogen-activated protein kinase (MAPK) pathways. In the case of most chemokine receptors, these processes induce cytoskeletal re-arrangement and migration (18). After signalling, the Gα subunit then hydrolyses its bound GTP back to GDP and re-associates with the βγ complex to re-form the inactive G protein

heterotrimer ready for further stimulation (17). These signalling pathways are summarised in Figure 1.2.

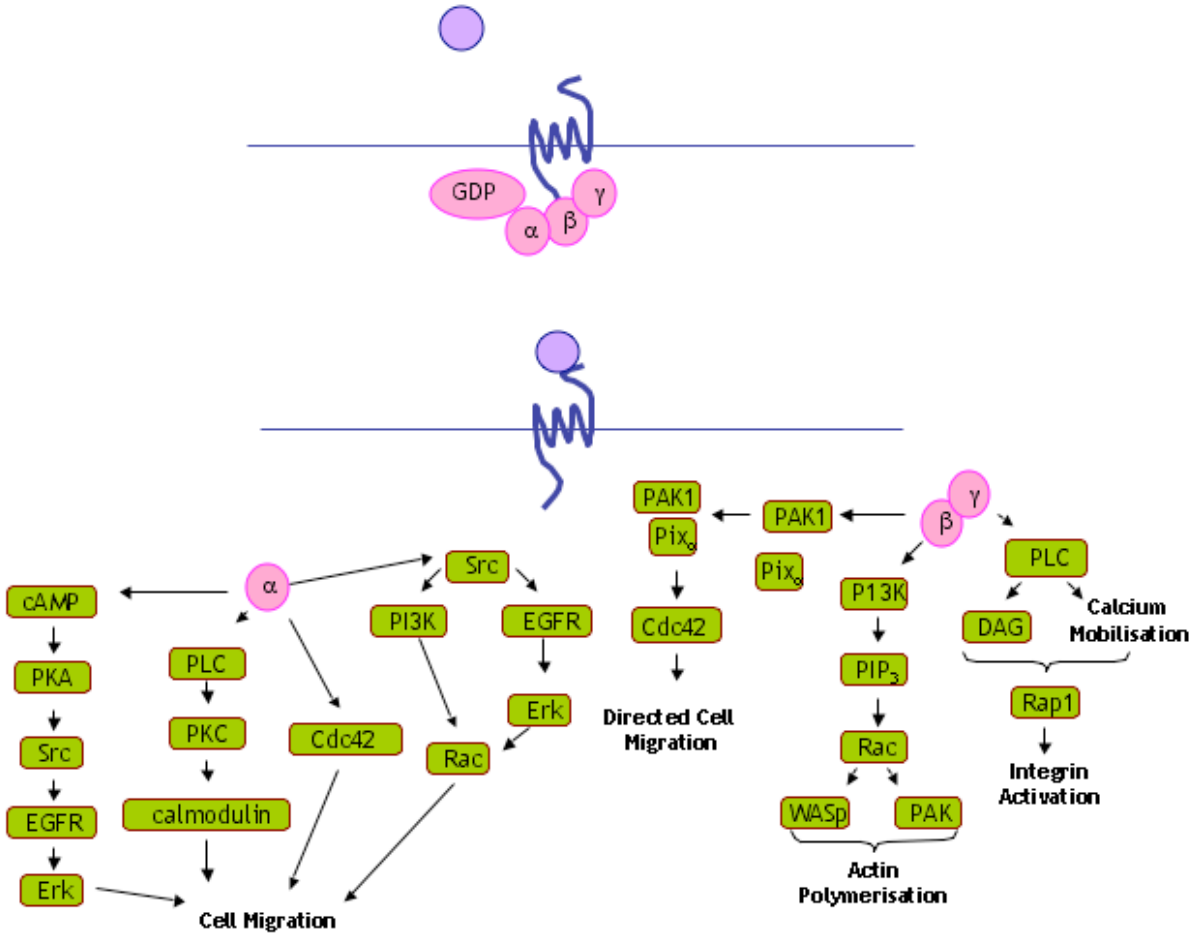

Fig 1.2 Schematic representation of chemokine receptor signalling cascades
In a resting state (top) the Gα subunit has GDP bound, rendering the G protein complex inactive. Chemokine binding (bottom) induces a conformational change, releasing the Gα protein and allowing the transduction of several signalling cascades. Arrows indicate downstream target signalling pathways that culminate in integrin activation, actin polymerisation and cell migration (15, 17, 18, 30).

The chemokine system can be characterised as one of redundancy, with several chemokines within the same sub-class binding multiple chemokine receptors (2). Further complexity is generated by the ability of chemokine receptors to function as homodimers and heterodimers (5).

Chemokine receptor desensitisation

GPCR become de-sensitised after prolonged ligand interactions and re-sensitise to binding when denied ligand exposure. G protein coupled receptor kinases (GRK) contribute to this mechanism by recognizing the activated GPCR, binding to and phosphorylating it and creating an arrestin binding substrate. β-arrestin binding effectively silences the GPCR even in the presence of chemokine ligand stimulation and targets the GPCR for recycling to endocytic pathways via clathrin coated pits. This allows for receptor degradation or re-sensitisation. Alternatively or in addition, arrestin binding can initiate additional intracellular signalling cascades independent of GPCR signalling events (28, 31). GRK themselves can also activate PI3K, MAPK and the Ezrin/Radexin/Moesin cascades, leading to cell migration events rivalling those induced by classical GPCR signalling (30).

1.3 Homeostatic versus inflammatory chemokines

Chemokines can be divided into two main functional groups. Those which co-ordinate cell trafficking throughout resting tissues and secondary lymphoid organs (homeostatic) and those which recruit cells to sites of inflammation (inflammatory) (12, 15). CCL19, CCL21, CXCL13 and CCL25 are examples of chemokines that are expressed constitutively within lymphoid tissues. However, it is a misconception to assume that homeostatic chemokines simply keep things "ticking over", as they underpin extremely active processes that determine the development of the immune system and allow naïve lymphocytes to survey the enormous antigen load delivered constantly to secondary lymphoid organs. In addition, homeostatic chemokines direct tissue tropic effector cells back to the original sites of their cognate antigen encounter, allowing for site specific and targeted immune responses. Inflammatory chemokines include CCL2, CCL3, CCL4 and CCL5. They are inducible during inflammatory responses and serve to activate and direct effector cells to and within peripheral tissues. This division of chemokines into homeostatic and inflammatory groups is becoming less clear, as increasing evidence suggests that homeostatic chemokines such as CCL19, CCL21 and CXCL13 can also be induced in peripheral tissues during inflammatory responses (32, 33).

Homeostatic chemokines in thymus organisation

CCR7 and its two ligands, CCL19 and CCL21, as well as CCR9 and its ligand CCL25 are involved at several stages of T cell development in the thymus. Proceedings begin after the CCR9 dependent entry of bone marrow derived haematopoietic precursors into the thymus via blood vessels in the cortico-medullary junction in response to the only known ligand for CCR9, CCL25. These cells then migrate through the cortex to the sub-capsular zone as double negative (DN) $CD4^-CD8^-$ thymocytes undergoing pre-T cell receptor mediated selection and maturing into double positive (DP) $CD4^+CD8^+$ cells (34-39). CCR7 and CCR9, along with CXCR4 and its ligand CXCL12, all appear to be involved in this outward migration, with CCR7 and CCR9 KO mice showing poor accumulation of DN thymocytes in the subcapsular zone (34, 40). At this point, DP thymocytes undergo positive selection by recognising self-peptides presented in MHC molecules on cortical thymic epithelial cells (TEC), before reversing their migration and returning to the cortico-medullary junction in response to CCL19 and CCL21 expressed by TEC in the medulla (34, 41). Once in the medulla, the developing thymocytes are exposed to tissue specific self-antigens presented by DC and AIRE expressing TEC leading to the deletion of self-reactive T cells. The surviving T cells then become single positive (SP) and migrate from the medulla to peripheral lymphoid organs (34, 42, 43). The importance of CCR7 in these latter processes is shown by the lack of migration towards the medulla and failed negative selection in CCR7 KO mice and in paucity of lymph node T cell (*plt*/*plt*) mice that are deficient for CCL19 and CCL21-Ser (43-45). These effects may partly account for the spontaneous autoimmunity seen in CCR7 KO mice (34, 46). Interestingly, CCL19 KO mice show no defects in cellular composition and architecture of the thymus, suggesting that as CCL19 and CCL21 are not compartmentalised in their expression, CCL21 may offer a compensatory role (12, 23).

Homeostatic chemokines in secondary lymphoid organ development

As well as organising cells within the thymus, homeostatic chemokines are also essential for the positioning of the progenitor cells that establish secondary lymphoid organs during embryogenesis. The development of secondary lymphoid organs occurs through the interactions between haematopoietic $CD4^+CD3^-$IL-$7R\alpha^+\alpha4\beta7^+$ lymphoid tissue inducer cells (LTi), and $CD4^-CD3^-$IL-$7R\alpha^-CD11c^-$ lymphoid tissue initiator (LTin) cells and mesenchymal lymphoid tissue organiser (LTo) cells that are positioned at designated sites of future lymphoid organ development. The homeostatic chemokines CCL19, CCL21 and the CXCR5

ligand, CXCL13, attract LTi cells to these sites and promote their expression of lymphotoxin-αβ (LTαβ) (47). The ligation of LTβR on mesenchymal cells by LTαβ on LTi cells promotes the expression of the vascular addressins MAdCAM, VCAM-1 and PNAd as well as inducing further production of CCL19, CCL21 and CXCL13. These homeostatic chemokines recruit more LTi cells, as well as mature lymphocytes that are required to establish T and B cell zones within secondary lymphoid organs. In addition to orchestrating the spatial and temporal positioning of LTi cells and lymphocytes, the CCR7 ligands CCL19 and CCL21 promote LTαβ expression by both LTi and mature $CD4^+$ T cells, triggering further chemokine release by mesenchymal and stromal cells. This in turn recruits further LTαβ producing cells and forms a powerful positive feedback loop that sustains lymphoid organ development (47). The importance of homeostatic chemokines in the development of secondary lymphoid organs is shown by findings that CXCL13 and CXCR5 KO mice fail to develop PP and most LN while CCL19 and CCL21 deficient *plt/plt* mice have small and poorly organised lymphoid organs (48-50).

Inflammatory chemokines and innate immune responses

Homeostatic chemokines regulate the development of secondary lymphoid organs and the thymic differentiation of the T cells that populate them, providing the infrastructure for antigen specific immunity. However, pathogenic organisms tend to invade at peripheral sites that are distant from these specialised lymphoid structures. Therefore mechanisms have evolved to alert lymphocytes in secondary lymphoid tissues to the presence of their cognate antigens in the periphery. The presence of invasive organisms at these peripheral sites induces local inflammatory responses that include chemokine production by stromal and parenchymal cells, recruiting innate effector cells from the blood as a first line of immune defence. These cells are alerted to the presence of microbes via activation of different families of conserved pathogen recognition receptors (PRR). Toll like receptors (TLR) comprise a major family of PRR and their activation results in the production of chemokines and inflammatory cytokines such as IL-1, TNFα and IL-6 that recruit and activate effector immune cells (15). Chemokines typically produced in response to pathogens include the ligands of CCR1, CCR2, CCR3, CCR5, CXCR2 and CXCR3 that recruit granulocytes, monocytes, DC, natural killer (NK) cells and effector T cells to their source. As a consequence, mice deficient in these chemokines or their chemokine receptors are often compromised in their immunity to pathogens (15, 51, 52). The inflammatory chemokine milieu at sites of infection and

inflammation can also play a role in polarising effector T cell responses, with CCL2 and CCL3 appearing to induce Th_1 and Th_2 differentiation respectively (15, 53, 54). Innate immune responses of this kind are rapid, but are often aggressive and indiscriminate. The development of antigen specific adaptive immunity allows more targeted responses and is highly dependent on chemokines and other mediators produced during the innate response.

Chemokines and DC in the link between innate and adaptive immunity

One of the most important of these processes is the carriage of antigen by DC from the site of infection to the naïve lymphocytes congregated in secondary lymphoid organs. DC are professional antigen presenting cells (APC) that are recruited to peripheral tissues from blood derived precursors by inflammatory chemokines. Circulating $Ly6C^{+}CCR2^{hi}CX_3CR1^{lo}$ monocytes recruited to inflamed tissues by the CCR2 ligand, CCL2, give rise to a variety of conventional DC (cDC) subsets (55). CCR2 expression by monocytes also facilitates their release from the bone marrow during inflammation (56). Immature DC express the inflammatory chemokine receptors CCR1, CCR2, CCR5, CCR6, CXCR1 and CXCR2 and only moderate levels of class II MHC and co-stimulatory molecules (57). Some immature DC also express inflammatory chemokine receptors particular to their local environment. For instance immature $CCR6^{+}$ DC are recruited to Peyer's patches (PP) and intestinal mucosa in response to CCL20 produced by epithelial cells under resting and inflamed conditions (58, 59). When tissues are inflamed, resident DC secrete potent immune enhancing cytokines such as TNFα, IL-6, IL-12 and IFNα to activate other innate effector cells including NK cells and natural killer T (NKT) cells. Activated DC then down-regulate their inflammatory chemokine receptors and tissue anchoring adhesion molecules such as E-cadherin, whilst concomitantly up-regulating CCR7. These processes promote their exit from tissues via afferent lymphatics towards the subcapsular sinus of the draining LN (60, 61). In parallel, the DC mature, assuming a dendritic like morphology and up-regulating class II MHC and co-stimulatory molecule expression so that they may activate and polarise T cells upon their arrival in the LN. They also secrete CCL19, which assists in their differentiation and contributes to the recruitment of naïve T cells and further activate DC once they have arrived in the LN (62, 63).

1.4 Chemokines and the generation of adaptive immune responses

Antigen specific immune responses are initiated in secondary lymphoid organs where lymphocytes are organised into a distinct T cell zone and B cell follicles under control of the CCR7 ligands, CCL19/CCL21 and the CXCR5 ligand, CXCL13. CCR7 and L-selectin co-expression on naïve lymphocytes directs their entry from the blood via specialised high endothelial venules (HEV) which punctuate the T cell zone (58, 64, 65). NK, NKT and γδ T cells also co-express CCR7 and L-selectin suggesting that they too enter LN via HEV (65). The spleen is devoid of HEV and instead lymphocytes and DC enter the red pulp via terminal arterioles and migrate into the T cell zone of the white pulp via the marginal sinus (63, 64, 66). Interestingly, some T cells can access LN from peripheral tissues via the afferent lymphatics in a CCR7 dependent manner reminiscent of DC (67, 68). The LN of CCR7 KO mice are lymphopaenic and deficient in DC, and the T cell areas in all secondary lymphoid organs are grossly disrupted, emphasising the indispensable role for CCR7 and its ligands in leukocyte recruitment to and positioning within these structures (40, 69). Once in the T cell zone, lymphocytes migrate around randomly under the control of CCL19 and CCL21 produced by radiation resistant stromal cells (58, 70). Interestingly, CCL21 protein levels are approximately 100 fold higher than of CCL19, and it remains to be clarified exactly why the two ligands for CCR7 are expressed together. However, this property is conserved across mammalian species, and so it would appear to be of biological importance (12, 66, 71). In mice there are two genetic variants of CCL21 distinguishable by the amino acid at position 65 of their sequence. CCL21-Ser is expressed by HEV and fibroblastic reticular cells (FRC) in T cell areas of secondary lymphoid organs, whereas CCL21-Leu is restricted to the lymphatic vessels in non-lymphoid organs such as the lung, colon and skin (12). Whereas CCL21 is produced directly by cells lining the HEV, CCL19 is not, and instead it is transcytosed from the basolateral region to the luminal endothelial surface. As described above, the presentation of the CCR7 ligands, CCL19 and CCL21 on HEV facilitates lymphocyte trans-migration by enhancing the affinity state of endothelial integrins such as LFA-1 and triggering increases in the expression of integrin ligands on lymphocytes (63, 66, 72, 73). Unlike CCL19, CCL21 has a long C-terminal tail that avidly binds to GAGs, in particular podoplanin expressed by lymphatic endothelial cells and reticular stromal cells. The expression of podoplanin might regulate CCL21 availability and thus contribute to the kinetics of leukocyte entry into secondary lymphoid organs (12). The need for such regulation is emphasised by findings that

transgenic over-expression of CCL21 correlates with a dramatic down-regulation of CCR7 on T cells and immune deficiency (74).

CCL19 and CCL21 introduce naïve T cells to DC

Naïve lymphocytes recirculate continuously between the blood and secondary lymphoid organs in search of DC bearing their cognate antigen. T and B cells spend approximately 12-18 and 24 hours respectively surveying any given secondary lymphoid organ and especially in the case of T cells, undertake a rapid and random migration guided by FRC under the control of CCR7 ligands. If unfulfilled in their search, lymphocytes exit LN and PP via the efferent lymph or from the spleen directly into the venous circulation. Efferent lymph collects in the thoracic duct and then returns lymphocytes to the blood where they continue their re-circulation and search for antigen (66, 75). As described above, activated DC loaded with antigen filter into the LN via the subcapsular sinus and then migrate deeper into the paracortex under the control of CCR7 ligands produced by and around the HEV. There the DC can greet as many T cells entering the LN as possible. As discussed above, DC within the paracortex produce CCL19 themselves, attracting even more DC and increasing the chances of any given lymphocyte to locate a DC bearing its cognate antigen (22, 76). The importance of CCL19 and CCL21 in this DC localisation is shown by findings that afferent lymph borne DC do not exit the sub-capsular sinus of CCL21-Ser and CCL19 deficient *plt/plt* mice and that CCR7 KO mice have reduced DC numbers in their LN paracortex, as well as defective development of antigen specific immunity and tolerance (69, 77, 78). T cells spend approximately 15 hours associated with DC presenting their cognate antigen, engaging co-stimulatory molecules and receiving signals from DC derived cytokines. CCL22 or CXCL16 secretion by DC maintains such contacts by binding to recently activated T cells expressing CCR4 or CXCR6 respectively (58).

Adaptable expression of CXCR5 and CCR7 allow T and B cells to interact

With adequate TCR affinity thresholds met, $CD4^+$ T cells proliferate and differentiate into effector Th_1, Th_2, Th_{17} or regulatory T cells (T regs), depending on the context of antigen presentation. A proportion of activated T cells migrates to the interface of the T and B cell zones and becomes follicular helper T cells (Tfh) that interact with and activate B cells possessing the same antigen specificity. Concurrently, naïve B cells encounter and internalise their cognate antigen by routes that remain controversial, but may involve subcapsular

macrophages, DC in the T cell dependent area or follicular dendritic cells (FDC) in the B cell follicles (79). The encounters between antigen specific T and B cells are prompted by the TCR-induced expression of CXCR5 and BCR-induced expression of CCR7, leading to the translocation of activated T and B cells to the boundary separating the CCL19/CCL21 rich T and CXCL13 rich B cell zones (63, 65). Up-regulation of CXCR5 accompanied by a down-regulation of CCR7 allows $CD4^+$ T lymphocytes to enter B cell follicles and interact with B cells specific for the same antigen, presented as peptides on surface class II MHC molecules. As the B cell follicle matures into a germinal centre (GC), the production of IL-4 and expression of co-stimulatory molecules such as ICOS and CD40L by T helper cells drives the differentiation of a proportion of B cells into CXCR4 expressing plasmablasts that migrate in response to CXCL12 to the red pulp of the spleen or the medulla of LN and ultimately enter the bloodstream. In addition, T cell help drives the affinity maturation and class switching of plasmablasts within the GC so that high affinity antibody can be produced upon their deployment to effector sites (66, 80). Other T cells differentiate into an effector phenotype in a process accompanied by down-regulation of CCR7 and concurrent up-regulation of the inflammatory chemokine receptors CCR3, CCR5 and CXCR3, allowing for their recruitment to peripheral sites of inflammation (81). Activated T cells can also express tissue specific chemokine receptors and adhesion molecules, guiding the effector T cells to the site of original antigen encounter. For instance, T cells activated in cutaneous draining LN acquire expression of CCR4 and CCR10 for which the ligands, CCL17 and CCL27 are expressed in the skin. Similarly, CCR9 expression is induced on T cells primed in the MLN, for which the ligand, CCL25 is produced in the small intestine (82) . The organisation of T and B cells in LN is briefly summarised in Fig 1.3.

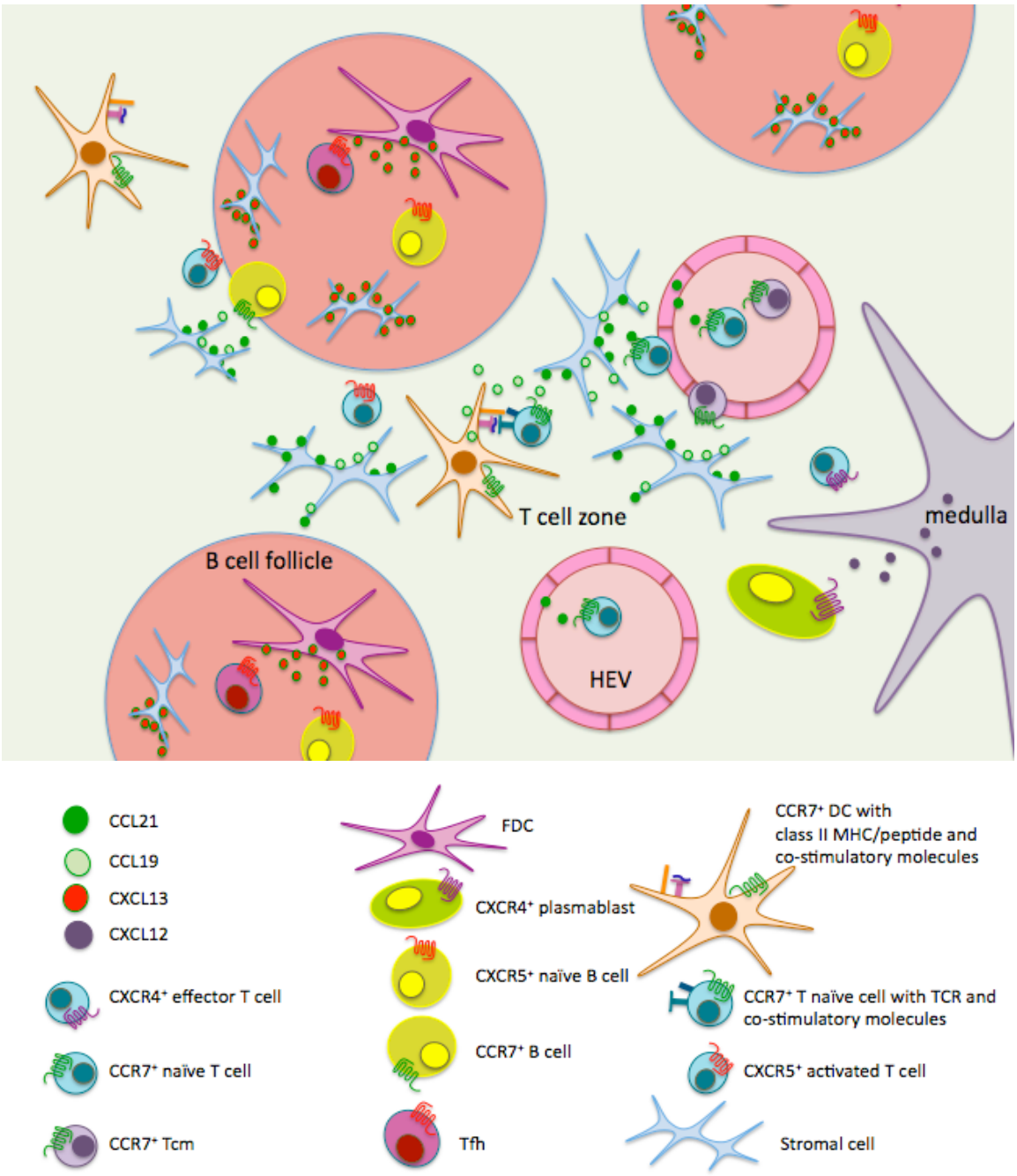

Fig 1.3 Schematic representation of lymph node organisation
The LN is made up of a T cell zone and B cell follicles. CCR7 expressing lymphocytes arriving from the blood via the HEV move around the T cell zone rapidly using CCL19 and CCL21 immobilised on stromal cells and meet up with CCR7 expressing antigen loaded DC that have arrived via the afferent lymphatics. CCR7 expression is down-regulated by T cells upon their activation and a proportion of cells then up-regulate CXCR4 and migrate towards the medulla to be released into the circulation. Other T cells up-regulate CXCR5 and migrate to the T/B cell boundary in response to CXCL13 secreted by FDC and stromal cells. Here they become Tfh and interact with CCR7 expressing B cells activated by antigen presented on FDC. B cells that receive T cell help then differentiate into plasmablasts, up-regulate CXCR4 and migrate to the medulla in response to CXCL12 for their release into the circulation.

Chemokines and the development of immunological memory

In addition to this immediate deployment of effector cells, a proportion of activated T and B cells contribute to immunological memory so that rapid responses to pathogen re-exposure can be implemented. Antigen specific memory T cells persist after the resolution of infection and can be divided into central memory (Tcm) and effector memory (Tem) subsets based on their differential expression of CCR7. Tcm express CCR7 and re-circulate throughout secondary lymphoid organs scanning DC for the presence of their cognate antigen, so that upon secondary encounter they can provide a rapid source of fresh effector T cells (83, 84). The importance of CCR7 in this re-circulation is demonstrated by the impaired homing of Tcm to secondary lymphoid organs in CCR7 KO mice (85). In contrast, Tem do not express CCR7 and so are denied access to secondary lymphoid organs. Instead, Tem express inflammatory chemokine receptors and localise preferentially in peripheral tissues, so that during re-infection they can activate local innate effector responses immediatey (86).

Memory T cell responses are also complemented by memory B cell responses generating high affinity antibody quickly in the event of re-infection. As described, during adaptive immune responses, B cell follicles can develop into germinal centres (GC) that are split into CXCL12 rich dark and CXCL13 rich light zones. Within GC, B cell derived centroblasts accumulate somatic mutations in their BCR affinity, driving affinity maturation and selection of B cells with high affinity and class switched BCR. Some of these B cells remain in the GC as memory cells, meaning that in the event of subsequent infection by the same pathogen, high affinity class switched antibody is available rapidly (77). Class-switched memory B cells express CCR7, CXCR4, CXCR5 and CCR6 that are thought to assist in their recirculation between the blood and secondary lymphoid organs (87). In addition, long-lived plasma cells that have already undergone differentiation to produce high affinity class switched antibody, accumulate in the bone marrow so that they may maintain serum antibody levels. This persistence is thought to be dependent on CXCR4 expression by plasma cells (88).

Chemokines and regulatory T cells

The immune system is designed to be a formidable adversary for pathogens, but it is important to remember that these responses also need to be regulated to ensure resolution of inflammation. In addition, tolerance has to be maintained against self-antigens and harmless antigens such commensal organisms and foodstuffs. Regulatory T cells (T regs) are key

players in tolerance, suppressing immune responses through their secretion of the cytokines TGFβ and IL-10, or by cell-cell contact dependent mechanisms. "Natural" T regs develop in the thymus under control of the forkhead family transcription factor, FoxP3 and are $FoxP3^{+}CD4^{+}CD25^{+}$. Similar cells, known as "adaptive' T regs can differentiate from naïve T cells in the periphery and these may be either $FoxP3^{+}CD4^{+}CD25^{+}$ or $FoxP3^{-}CD4^{+}CD25^{+}$ (89). Circulating T regs express CCR7 and although CCR7 deficient T regs are suppressive *in vitro*, they cannot function *in vivo* due to their inability to access LN via HEV (85, 90). After encountering antigen, T regs express a variety of inflammatory chemokine receptors, including CCR1, CCR2, CCR4 and CCR5 allowing them to enter tissues and assist in the resolution of inflammation at peripheral sites (91).

1.5 Dendritic cells shape immune responses

As discussed above, DC are specialised APC, dedicated to sampling antigens in tissues and processing and presenting them as peptides in class II MHC molecules after migrating to meet T cells in draining secondary lymphoid organs. DC are the only APC that can do this and so provide the sole means of alerting naive T cells to the presence of their cognate antigen, DC also alert T cells to the presence of dangerous pathogenic organisms by up-regulating co-stimulatory molecules in response to PRR activation. The co-expression of peptide bound MHC and co-stimulatory molecules induces antigen specific naïve T cells to undergo IL-2 dependent clonal expansion. Although macrophages and B cells also express class II MHC and can process and present antigen with this molecule, DC are the only APC that can induce clonal expansion of naïve $CD4^{+}$ T cells directly. DC also instruct the development of the resultant effector T cells via the secretion of cytokines such as IL-12 and, IL-6 and IL-23 which instruct Th_1 and Th_{17} type responses respectively (89, 92). IL-4 is required for the polarisation of Th_2 responses but as DC do not produce this cytokine themselves, its source is unclear although, basophils have been suggested (93, 94). Several subsets of DC have now been characterised based on their surface markers and anatomical positioning and are summarised in Table 1.2 (55). Broadly, these can be divided into conventional and plasmacytoid DC, although some controversy surrounds the division of tissue resident mononuclear antigen sampling cells into conventional DC (cDC) and other CD11c expressing subsets such as activated macrophages (95, 96).

Table 1.2: DC subsets

Differentiated DC Subset	Cell Surface Marker Phenotype
CD8α^+ DC	CD8α^+, class II MHC$^+$, CD11c$^+$, CD4$^-$, CD205$^+$ SIRP-1α^-
pDC	B220$^+$, CD11c^{lo}, Ly6C$^+$, class II MHC^{lo}, CD4$^{-/+}$, CD8$\alpha^{-/+}$, PDCA-1$^+$
Langerhan's Cells	Langerin$^+$, class II MHC$^+$, Dectin-1$^+$, CD1a$^+$, CD11b$^+$, CD11c$^+$, CD24a$^+$, CD205$^+$, CD45^{lo}, CD8$\alpha^{+/-}$, CD103$^-$
Dermal DC (Langerin$^+$ subset)	Langerin (CD207)$^+$, class II MHC$^+$, CD103$^+$, CD11b^{lo}, CD11c^{int}, CD45^{hi}, CD8α^-
Dermal DC (Langerin$^-$ subset)	Langerin (CD207)$^-$, class II MHC$^+$, CD11c$^+$, CD4$^-$, DEC205 (CD205)$^+$, CD24a$^-$
CD8α^- DC	CD8α^-, class II MHC$^+$, CD11c$^+$, CD11b$^+$, CD4$^-$, SIRP-1α^+, DCIR2$^+$
CD8α^-CD4$^+$ DC	CD8α^-, CD4$^+$, CD11b$^+$, class II MHC$^+$, DCIR2$^+$
Lung DC	
Conducting airways	CD11b^{hi}, CD11c$^+$, CD103$^-$
Lung interstitium	CD11b^{lo}, CD11c$^+$, CD103$^+$
Lamina propria DC	
	CD11c^{int}, CD11b^{int}, CD205$^-$, CD103$^-$ CD11c^{int}, CD11b$^+$, CD205$^-$, CD103$^-$ CD11c^{hi}, CD11b$^-$, CD205$^+$, CD103$^+$ CD11c^{hi}, CD11b$^+$, CD205$^+$, CD103$^+$
Peyer's patch DC	
	CD11c$^+$ CD8α^- CD11b$^-$ CD11c$^+$ CD8α^+ CD11b$^-$ CD11c$^+$ CD8α^- CD11b$^+$

Conventional DC subsets

DC develop from myeloid precursors in the bone marrow and in mice, all DC express CD11c integrin and class II MHC molecules to some extent. In mammalian species, several subsets of DC can be distinguished by their surface markers and cytokine secretion profiles and in mice there are two main subsets of conventional DC, CD8α^+ and CD8α^- (97). CD8α^- DC usually express CD11b and/or CD4 and are the principal DC found in non-lymphoid tissues. These are derived from myeloid precursors, are under control of the transcription factor IRF4 and seem to be closely related to monocytes. CD8α^- DC are proficient in the capture of antigens and in presenting them with class II MHC to CD4$^+$ T cells after migrating to LN (93, 98, 99). In contrast, CD8α^+ DC are generally found in the T cell zones of secondary lymphoid organs and were once believed to be derived from a lymphoid precursor. However, it is now clear that like CD8α^-CD11b$^+$ DC, CD8α^+ DC develop from a common myeloid precursor, but differ in that they are under the control of Batf3 and IRF8 transcription factors (100, 101). CD8α^+ DC are

also thought to enter LN directly from the bloodstream via HEV and generally do not migrate from tissues in afferent lymph. Initial studies suggested that $CD8\alpha^+$ DC and $CD8\alpha^-CD11b^+$ DC primed different subsets of $CD4^+$ T cells, but it is now clear that they can both produce IL-12 and other polarising mediators under appropriate circumstances (93, 99, 102). However, one striking difference is that $CD8\alpha^+$ DC are the only DC capable of cross presenting exogenous antigen in class I MHC to $CD8^+$ T cells, making them important in the development of adaptive immune responses to viral and tumour antigens (101, 103-105).

Plasmacytoid DC

Plasmacytoid DC (pDC) are a subset of DC that are the principal sources of type 1 IFN in viral infections in most species. In mice, pDC are $CD11c^{lo}$ and co-express B220, PDCA-1 and Ly6C and they are functionally, genetically and morphologically distinct from the conventional DC described above. pDC are thought to migrate from the bone marrow to the periphery as fully matured cells and recognise unmethylated cytosine phosphate guanine (CpG) motifs and single stranded (ss) RNA from viruses via TLR9 and TLR7 respectively. Upon activation via these TLR, pDC become potent secretors of type 1 IFN and contribute significantly to the development of anti-viral immunity (106-112). Moreover, IFNα and IFNβ promote $CD8^+$ T cell and natural killer (NK) cell cytotoxicity, Th_1 polarisation and the differentiation of B cells into antibody secreting plasma cells. In addition to type 1 IFN, activated pDC also secrete the pro-inflammatory chemokines CCL3, CCL4, CCL5, CXCL8 and CXCL10, that can recruit activated T cells and NK cells. Activated pDC can also secrete IL-12 and are capable of presenting antigen in class II MHC to T cells (113-117). In addition, pDC have been reported to have tolerogenic properties in a variety of inflammatory disease models (118-120). pDC are scarce in resting non-lymphoid tissues with the exception of the small intestine, but are readily detectable in the blood, bone marrow and secondary lymphoid organs. pDC enter LN via HEV using L-selectin which they constitutively express (106). pDC numbers are dramatically increased in non-lymphoid organs during inflammatory responses, but unlike conventional DC, pDC do not exit tissues via the afferent lymphatics (29). Instead it is proposed that pDC serve to activate and mobilise tissue DC, directing their migration into afferent lymphatics (121). pDC express CCR7 and CCR9 and although the former seems to be only upon activation, the expression of CCR9 is thought to account for their presence in the resting small intestinal lamina propria where there are high levels of the CCR9 ligand, CCL25 (29, 121-124). As a result, CCR9 KO mice are devoid of lamina propria pDC (121).

DC mediate immunological tolerance

Although DC are potent activators of adaptive immune responses, together with T regs they also play crucial roles in the maintenance of immunological tolerance. This is partly due to their role in negative selection of self-reactive T cells in the thymus and may involve resident $CD8\alpha^+$ DC. However, recent studies suggest that circulating immature $CD8\alpha^-$ DC can enter the thymus carrying self-antigens from peripheral tissues (55). DC are also crucial in the maintenance of peripheral tolerance where their role is to minimise activation of any mature T cells in the periphery that might recognise self-antigens or innocuous foreign antigens. This is particularly important at sites of chronic exposure to harmless environmental antigens such as the airways and gut. Peripheral tolerance relies on DC to present antigen to T cells and as for the induction of active immunity, requires CCR7 dependent interactions between antigen loaded DC and antigen specific T cells in secondary lymphoid organs (125-128). Recent studies have revealed that tissue derived DC constitutively enter the afferent lymph under resting conditions (129, 130). The precise mechanisms governing the migration of these non-inflammatory steady state DC are yet to be elucidated, but the continuous migration of steady state DC from the lungs, skin and small intestine is CCR7 dependent as is the ensuing development of T cell tolerance (125, 131-133).

There are a number of ways in which DC can induce peripheral tolerance. Autoreactive T cells can be deleted directly by DC especially those specific for antigens targeted to endocytic pathways via DEC-205 (CD205) (126, 134). Antigen presentation by immature DC in the absence of co-stimulation can lead to impaired clonal expansion and T cell anergy or to the induction of T regs (92, 126, 135, 136). DC can also direct the differentiation of T regs through the secretion of IL-10, TGFβ or retinoic acid (RA). This is a particular trait of $CD103^+$ DC from the gut and respiratory tract, where chronic exposure to environmental antigen may lead to preferential production of IL-10 that inhibits secretion of IL-12 (60, 89, 128). A further mechanism by which DC can induce tolerance is via indolamine-2-3-deoxygenase (IDO), a tryptophan metabolising enzyme that depletes this essential amino acid, which is required by activated T cells for their proliferation and function. As well as depleting local tryptophan, IDO leads to the accumulation of toxic metabolites and together these effects encourage cell cycle arrest and anergy in T cells and the generation of T regs (92, 137, 138). IDO production by DC may be induced by IFNγ, TNFα or PGE_2 and by ligation of CD80 by CTLA-4 on T regs (139-142). Whether or not a specialised subset of tolerogenic DC exists is

controversial. Initially, CD8α^+ LN resident DC were believed to be dedicated to tolerance induction but, as described above, these DC can actively prime T cells and more recent evidence shows that constitutive CCR7 dependent migration of CD11b$^+$ DC from tissues is critical for inducing and maintaining peripheral tolerance (92, 126, 143-147). In the intestine, this function is associated specifically with DC expressing CD103 (the α_E component of $\alpha_E\beta_7$ integrin). As DC are so plastic in their function, whether or not priming or tolerance occurs probably reflects the local environment at the time of antigen sampling as opposed to dedicated lineages of DC.

1.6 Regulation of chemokine function

As I have discussed, chemokines have many crucial roles in the organisation of innate and adaptive immune responses, and so they must be regulated stringently to avert the development of aberrant immune responses and a number of mechanisms exist to achieve this. The bioactivity of chemokines can be regulated by post-translational modifications of the amino acid terminus and this provides a means of regulating chemokine function more rapidly than transcriptional control, as it allows targeting of pre-formed biologically active chemokines that have already been secreted. After secretion, chemokine bioactivity, distribution and bioavailabilty can also be regulated by enzymatic cleavage and glycosylation (7, 148).

In addition, chemokine receptors can be antagonised directly (148, 149). CCL7 naturally antagonises CCR5, while CCL11 and CCL26 antagonise CCR2 mediated chemotaxis (150-153). CCR3 ligands can antagonise CXCR3 and vice versa, suggesting that as CXCR3 and CCR3 are associated with opposing types of Th responses, this antagonism may play a role in polarising immune response (153-156). Soluble chemokine receptors can also antagonise chemokine responses, a phenomenon that has been exploited by several viruses and parasites that produce soluble decoy cytokine and chemokine receptors (157).

The immune system itself produces cytokine and chemokine receptor homologues that regulate the responses of their relevant ligands. For instance, atypical TNF and IL-1 receptors exist as soluble and membrane bound forms that do not conduct signals following ligand engagement, but are thought to scavenge these pro-inflammatory cytokines, promoting the resolution of inflammatory responses. Several atypical chemokine receptors have now also

been identified and are proposed to function as scavenging decoy receptors (7). One of these, CCX-CKR, is the focus of this thesis.

Atypical chemokine receptors

Over the last decade, a number of atypical chemokine receptors with hypothesised decoy functions have been identified. Such receptors do not couple to the typical G protein signalling pathways and so generally do not induce chemotaxis or calcium flux within cells. Atypical chemokine receptors of this kind include DARC, D6, CXCR7 and CCX-CKR (149, 157-162). The distribution and ligands of these atypical chemokine receptors are summarised in Table 1.3. Atypical chemokine receptors have been proposed to function as decoy receptors or "sinks" in a manner somewhat similar to the IL-1 receptor type II which binds to IL-1β with high affinity and specificity without triggering signal transduction (163). However with the increasing characterisation of atypical chemokine receptors, mounting evidence suggests that their function may be more complex than simply to remove chemokine.

Table 1.3: Atypical chemokine receptor ligands and distribution

Atypical Chemokine Receptor	Chemokine Ligands	Receptor Expression Sites
DARC	CCL2, CCL5, CCL7, CCL11, CCL13, CCL14, CCL17, CXCL5, CXCL6, CXCL8, CXCL11	Erythrocytes, endothelial cells, Purkinjie cells, kidney epithelial cells, type II pneumocytes
D6	CCL2, CCL3, CCL3L1, CCL4, CCL5, CCL7, CCL8, CCL11, CCL13, CCL17, CCL22, CCL23, CCL24	Lymphatic endothelium, lungs, innate B cells, trophoblasts
CXCR7	CXCL11, CXCL12	Somatic cells during development, adult tumour cells
CCX-CKR	CCL19, CCL21, CCL25, hCXCL13, mCCL1	Lymph nodes, thymus, spleen, skin, heart, small intestine
CCRL2 (aka CRAM in humans)	CCL19, (also binds the chemo-attractant molecule, chemerin)	Mast cells, macrophages, T cells (humans only), bronchial epithelium, astrocytes, microglia

Duffy antigen receptor for chemokines (DARC)

Duffy antigen receptor for chemokines (DARC) was originally characterised as an entry receptor for malarial parasites on erythrocytes (149, 157, 158, 162). It is a seven trans-membrane spanning receptor lacking the DRY motif on the second intracellular loop that is essential for G protein coupling and signal transduction by conventional chemokine receptors (162). Thus, ligand binding does not cause detectable signalling events or chemotaxis (149). As well as being expressed by erythrocytes, DARC is found on venular endothelial cells, and binds to most inflammatory CC and CXC chemokines, but not to homeostatic chemokines (164, 165). This promiscuity in ligand binding has been attributed primarily to the amino terminal extracellular domain (166). Upon chemokine binding and internalisation, DARC associates with caveolae vesicles that are usually involved in trans-cellular transport. Thus it has been suggested that DARC is involved in transcytosis of chemokines on to the luminal surface of endothelium, a notion supported by evidence that DARC can transcytose intact ligand from basal to apical endothelial cell surfaces (149, 164). Interestingly, DARC can hetero-oligeromize with CCR5 and prevent chemotaxis and calcium flux in response to CCR5 ligands, indicating that DARC can directly and specifically over-rule CCR5 mediated chemotactic activity (167).

An inhibitory role for DARC is supported by the findings that DARC KO mice develop exaggerated inflammatory responses and leukocyte infiltrates into tissues in response to LPS, as well as accumulating elevated levels of DARC chemokine ligands in the blood (168, 169). Such reports have led to suggestions that DARC expression on erythrocytes may serve to buffer plasma chemokine levels (149, 164). In parallel, transgenic over-expression of DARC is associated with reduced angiogenesis and tumourogenesis, as well as reduced levels of CCL2 (149). Thus, DARC appears to play an important role in the recruitment of leukocytes to sites of inflammation by regulating local concentrations and distribution of its chemokine ligands.

D6, an inflammatory chemokine receptor

D6 is an atypical chemokine receptor expressed by lymphatic endothelium, placental trophoblasts and some leukocytes. It binds inflammatory CC chemokines, sharing most of its ligands with CCR1-5 and is proposed to function as a “decoy” chemokine receptor that resolves inflammation by scavenging chemokines (149, 157, 159, 160, 162, 170). D6 is a

close structural homlogue of CCR1 and CCR5, but does not couple to the major signalling pathways normally induced by ligand engagement of chemokine receptors and so does not induce chemotaxis. This is thought to be due to an altered DRYLAIV motif in the second intracellular loop of D6 that is instead present as DKYLEIV. D6 constitutively binds and internalises ligand into clathrin-coated pits before entering recycling endosomes in a β-arrestin dependent manner and then returning to the cell surface. This process prevents de-sensitisation of D6 and occurs in the absence of ligand binding, allowing constitutive expression of D6 on the cell surface. Any bound chemokines dissociate readily from internalised D6 receptors during vesicle acidification and are then targeted for degradation (171-173). Unlike DARC, D6 expressed on lymphatic endothelium does not appear to transcytose its chemokine ligands *in vivo* (174). Taken together with its continual recycling and ligand degradation, chemokine scavenging seems the most likely role for D6.

D6 KO mice have been shown to have heightened inflammatory responses in the skin, together with increased leukocyte infiltrates and delayed clearance of D6 chemokine ligands from the tissue and draining LN (175, 176). D6 KO mice are also more susceptible to lethal *Mycobacterium tuberculosis* infection, with exaggerated local and systemic inflammatory responses and elevated levels of the D6 ligands, CCL2-5. Importantly, these effects of D6 deletion could be reversed by blocking the inflammatory chemokines (177).

However, some studies have reported opposite effects of D6 deletion on inflammation, with resistance to the induction of experimental autoimmune encephalomyelitis (EAE) and to dextran sodium sulphate (DSS) induced colitis (178, 179). As the latter finding has been contradicted recently by another study, it would appear that the exact biological role of D6 in inflammation requires more investigation (180).

CXCR7

CXCR7 is expressed on somatic cells during development and has been implicated in regulating the trans-endothelial migration of cells, as well as angiogenesis (158, 181). Adult mice appear to lack CXCR7, although it is expressed by some tumours, suggesting it may support the rapid angiogenesis necessary for tumour survival (182). CXCR7 lacks a canonical DRYLAIV motif, instead expressing DRYLSIT and consequently, does not signal conventionally following binding of its ligands, CXCL11 and CXCL12 (183).

CCRL2 and CRAM

CCRL2 is a further atypical receptor that binds the chemoattractant molecule, chemerin and has recently been identified on a variety of leukocytes and non-haematopoietic cells such as mast cells, macrophages, human T cells, astrocytes, microglia and bronchial epithelial cells. CCRL2 is thought to present and concentrate chemerin, enhancing the attraction of cells expressing the chemerin receptor, ChemR23 which is also known as CMKLR1 (184). CCRL2 KO mice have reduced IgE responses to allergen sensitisation, but its exact biological roles remain unknown (184-186). Confusingly, the literature also cites CRAM as an atypical chemokine receptor encoded by the CCRL2 gene and existing as the splice variants CRAM-A and CRAM-B. CRAM is expressed by human peripheral blood and bone marrow derived B cells and binds CCL19 with a similar affinity to CCR7, constitutively recycling via clathrin-coated pits to the cell surface (187, 188).

CCX-CKR, a homeostatic chemokine receptor

ChemoCentryx chemokine receptor (CCX-CKR) was originally named CCR11 and first identified from a screen of orphan receptors transfected into human embryonic kidney (HEK) cells. Upon interrogation with immobilised chemokines, CCX-CKR showed high affinity binding to the murine and human forms of the CCR7 ligands CCL19 and CCL21, as well as the CCR9 ligand CCL25. mCCL9/CCL10 and hCXCL13 also bound to CCX-CKR transfected HEK cells, but with far weaker affinity (189).

As there is no antibody available for CCX-CKR, its expression has only been investigated using molecular approaches. Initial RT-PCR studies suggested that CCX-CKR mRNA was expressed in human primary T cells and monocyte derived DC, as well as in whole spleen, LN, heart, kidney, placenta, trachea and brain (189). Northern blot analysis then revealed expression in the mouse lung and heart as well as lower levels in the spleen and skeletal muscle. Equivalent analysis in humans also revealed abundant expression in the heart, lung, small intestine, colon and skeletal muscle, but no CCX-CKR RNA was detectable in human leukocytes (190). In mice, CCX-CKR exists as a single gene, whereas two CCX-CKR genes have been identified in humans, one on chromosome 3 and the other on chromosome 6. Northern blot analysis showed the chromosome 6 hCCX-CKR gene to be primarily expressed in the heart (190).

The only published studies of CCX-CKR protein expression have used CCX-CKR1-EGFP knock-in mice and they suggested that CCX-CKR was expressed by non-haematopoietic cells of the thymus, intestine, LN and epidermis. Specifically these cells were identified as TEC, intestinal lymph vessels and the marginal sinus of LN. However, no CCX-CKR protein expression was found in the heart, kidney, liver, spleen or brain (191). As these findings contradict the original analyses of CCX-CKR mRNA expression, they emphasise the need for reliable methods of detecting CCX-CKR protein *in vivo*.

The discovery that CCX-CKR binds the same chemokines as CCR7 and CCR9 led to the idea that CCX-CKR may act as a scavenger receptor that might regulate the activity of these receptors by affecting the availability of their ligands *in vivo*. This is supported by the available evidence that demonstrates that CCX-CKR does not signal after binding its ligands or induce a rapid increase in intracellular calcium. Instead it appears to target bound chemokine for degradation after internalisation (191, 192). This process is extremely efficient, allowing scavenging and degradation of around 80% of biotinylated CCL19 from culture medium after 24 hours. This is quite distinct from when CCR7 binds CCL19, which as one of two ligands of CCR7, selectively leads to receptor desensitisation after prolonged ligand exposure and impaired clearance of exogenous CCL19 from culture medium (12, 192-194). The uptake and sequestration of CCL19 by CCX-CKR occurs via a caveolae dependent mechanism that does not appear to require β-arrestin-1 or clathrin mediated endocytosis (192).

At the time my project started, very little was known about the biological role of CCX-CKR *in vivo,* although the Nibbs group had generated a CCX-CKR KO mouse and their preliminary findings suggested that CCX-CKR KO mice developed normally, with no gross abnormalities in the architecture of secondary lymphoid organs, although the ILN were found to be smaller in CCX-CKR KO mice compared to WT. However, there were no significant differences in the proportions of T cells and B cells in the spleens or ILN of CCX-CKR KO mice. In parallel, CCX-CKR KO ILN failed to enlarge normally in response to the skin irritant, PMA.

Subsequent published studies have confirmed a trend towards lower cell numbers in CCX-CKR KO lymphoid tissue, with lower numbers of migratory $CD11c^{+}MHCII^{hi}$ DC in the skin draining LN of resting CCX-CKR KO mice compared with WT animals. However, the numbers of $CD11c^{+}MHCII^{hi}$ isolated from epidermal sheets and their mobilisation into skin

draining LN upon FITC skin sensitisation were normal. Although CCX-CKR is expressed in the thymus and all of its ligands play important roles in T cell development, this process appears to be normal in CCX-CKR KO mice. Transgenic over-expression of CCX-CKR targeted to thymic epithelial cells revealed no alterations in the expression levels of thymic chemokines, or in the expression pattern of CCL25 in the embryonic thymic anlagen. However, there were significantly reduced numbers of haematopoietic precursors entering the thymus, consistent with disruptions to these normally CCR9 dependent processes although T cell development in adult CCX-CKR transgenic mice was normal (191). In addition, a separate study has reported that the over-expression of CCX-CKR by cancer cell lines inhibited their proliferative and invasive capacity (195).

Thus, no clear role for CCX-CKR *in vivo* has been elucidated and there have been no studies of the intestinal immune compartment, a site where all three ligands of CCX-CKR are known to play crucial roles in the regulation of immunity and tolerance. Therefore, investigating these tissues in CCX-CKR KO mice was the principal aim of my project.

1.7 The intestinal immune system

The physiological role of the intestinal epithelium requires that it is selectively permeable to nutrients and water, but not permissive to invasion by potentially pathogenic luminal microbes (196). The intestinal mucosa is exposed to the greatest antigenic burden of the whole body, which includes dietary proteins, commensal flora and self-antigens as well as pathogenic organisms. As discussed above, these different types of antigens must be distinguished, so that active tolerance or immunity are induced accordingly. As in the rest of the immune system, CCL19 and CCL21 are critical for these processes, as is the other CCX-CKR ligand, CCL25.

The layout of the intestinal immune system

The immune apparatus of the intestine can be divided into organised and scattered lymphoid tissues. The organised tissues comprise the PP, MLN and isolated lymphoid follicles (ILF), and are the sites where immune responses are initiated. PP are macroscopic structures lying in the wall of the small intestine and like other secondary lymphoid organs, have a distinct T cell zone and B cell follicles, but differ by lacking afferent lymphatics. Instead, luminal antigens gain access to PP by specialised epithelial cells known as microfold (M) cells, found in the follicle associated epithelium (FAE) overlying the lymphoid compartments of the PP. Antigen

from M cells is delivered to DC in the underlying sub-epithelial dome (SED) area, which then interact with T and B cells deeper in the PP or migrate to MLN (197). ILF are microscopic cellular aggregates that are structurally very similar to PP, with FAE and M cells, but consist of only one or two B cell follicles. Although ILF are smaller than PP, they can increase dramatically in size in response to local antigen burden. There are many hundreds of them in both the small and large intestine, and thus they can make a substantial contribution to local immune responses (198). MLN are the draining LN of the intestine and are connected to PP and the intestinal mucosa by lymphatics. In keeping with the enormous load of antigen in the gut, MLN are the largest LN in the body. Cryptopatches (CP) are a further group of organised lymphoid tissues found in the intestinal mucosa. Once thought to be sites of extra-thymic T cell differentiation they are now seen as immature ILF, containing $CCR9^+$ LTi recruited by CCL25 producing DC (197). The scattered lymphoid tissues comprise the lamina propria and epithelium, where effector leukocytes are found. In the lamina propria, there are macrophages, plasma cells, DC, $CD4^+$ T cells, $CD8^+$ T cells and eosinophils. The epithelium contains mostly $CD8^+$ T cells, which are found immediately above the basement membrane and are known as intra-epithelial lymphocytes (IEL). IEL express CCR9 and have been shown to up-regulate CD103 in response to CCL25, which is secreted by intestinal epithelial cells. CD103 expression mediates IEL adhesion to E-cadherin, a molecule that is abundant on intestinal epithelium, and such interactions appear to be important in the localisation of IEL, as CD103 KO and CCR9 KO mice have reduced numbers of these cells (199-201). With its constant leukocyte infiltrate arising from a bombardment of luminal antigen, the healthy intestinal mucosa could be described as being in a chronic state of inflammation. However, symptomatic inflammatory bowel disease is a rare occurrence thanks to stringent regulatory mechanisms.

The induction of intestinal immune responses

As described above, invasive antigens such as bacteria are delivered directly from the intestinal lumen to PP DC which then mature and migrate to the T cell zone of the PP, or to the MLN where they prime effector T and B cells (202). As in all mucosal tissues, the antibody response in the intestine is dominated by IgA which is produced by plasma cells in the lamina propria. IgA secreted as a J chain linked dimer, interacts with polymeric immunoglobulin receptors (pIgR) expressed on epithelial cells and is transcytosed across them into the lumen where it can neutralise pathogens and their products (203). IgA class switching occurs in the GC of PP and MLN under the influence of T cells, TGFβ and RA production

from mucosal DC. In mice but not humans, there is also a significant production of T independent IgA induced by direct interactions between DC and B1 B cells (203-206).

Homing of small intestinal effector cells

An essential component of mucosal immunity is the homing of effector T cells, T regs and plasmablasts from inductive sites to the mucosal surface. In the small intestine, this is directed by the expression of CCR9 and $\alpha_4\beta_7$ integrin on lymphocytes. These recognise CCL25 secreted by small intestinal epithelial cells and MadCAM-1 expressed selectively by vascular endothelial cells at mucosal surfaces. Evidence suggests that the induction of these receptors on naive lymphocytes occurs in the MLN and is controlled by RA production by a population of $CD103^+$ DC that is unique to the intestine (133, 197, 205, 207-215). Although CCR9 controls T cell and IgA plasma cell migration into the small intestine, it is not involved in the colon or other mucosal sites. The specific factors controlling entry to these tissues are yet to be elucidated, but in the case of the colon, CCR10 and CCL28 may be important (82, 216-218). CCR9 KO mice have decreased numbers of IgA plasma cells in the small intestinal lamina propria and show decreased IgA responses after oral immunisation with antigen, although they do have normal numbers of $\alpha_4\beta_7$ expressing $CD4^+$ and $CD8^+$ T cells in the lamina propria. Intriguingly, CCR9 deficient T cells can retain some ability to migrate into the lamina propria (219). Together, these data suggest that the requirement of CCR9 expression for T cell entry into the small intestine is not absolute and that it is the combined display of chemokine receptors and integrins that affords tissue specific localisation (82).

Intestinal DC

PP are not the sole source of mucosal DC as these are also abundant in the lamina propria, MLN and ILF. Several DC subsets have been characterised in the intestine, including $CD103^+$, $CD8\alpha^+$ and $CD8\alpha^-CD11b^+$ DC, as well as pDC (133, 208, 209). However there has been much debate recently over the definition of DC in the gut. This is particularly so in the lamina propria, where the majority of $CD11c^+CD103^-$ cells originally classed as DC are in fact CX_3CR1^+ cells derived from inflammatory monocytes and are genetically and morphologically identical to tissue resident macrophages. As a result, many workers consider that only $CD11c^+CD103^+$ cells and pDC are genuine DC in the intestinal mucosa. However, the situation is different in the PP and MLN, where conventional $CD103^-$ DC are found (95, 96).

CD103$^+$ DC

CD103$^+$ DC are found throughout the intestinal immune compartment and in some peripheral secondary lymphoid organs although in much fewer numbers. They are the dominant DC in the lamina propria, have several unique functional properties and are the only population of DC to migrate from the lamina propria to the MLN. Under resting conditions, CD103$^+$ DC generally promote tolerance and appear to be conditioned to be anti-inflammatory by soluble factors such as thymic stromal lymphpoietin (TSLP) secreted by intestinal epithelial cells (205). CD103$^+$ DC contribute to peripheral tolerance to innocuous proteins within the small intestine by driving the development of antigen specific FoxP3$^+$ T regs from naïve T cells during antigen presentation in the MLN in a TGF-β and RA dependent manner (220). CCR7 KO mice have defective migration of CD103$^+$ DC to MLN and fail to develop peripheral tolerance to orally administered antigens (125, 132).

As CD103$^+$ DC are also the only APC to induce the expression of CCR9 and $\alpha_4\beta_7$ on T cells including FoxP3$^+$ T regs, they play a crucial role in instructing antigen experienced T cells to return to the mucosa. This property also requires the production of retinoic acid (RA) by CD103$^+$ DC, which is generated from the metabolism of dietary vitamin A by the retinal dehydrogenase (RALDH) and ALDH families of enzymes. Consequently, the long-term withdrawal of vitamin A from the diet of mice results in a selective reduction in $\alpha_4\beta_7$ expressing CD4$^+$ T cells in secondary lymphoid organs and a defect in total lamina propria T cell numbers (212, 221). Other intestinal DC cannot produce vitamin A metabolising enzymes and neither can CD103$^+$ DC from peripheral secondary lymphoid organs. Although it is suggested that CD103$^+$ DC are intrinsically capable of generating RA while in the mucosa, other recent work suggests this property may be induced in DC by stromal cells in the MLN. Intriguingly, this effect appears to be unique to MLN stroma, as peripheral LN transplanted into the intestinal mesentery are unable to promote the expansion of gut tropic effector T cells (222). Although it now appears that many CD11c$^+$CD103$^-$ cells in the lamina propria may be inflammatory macrophages, conventional CD11c$^+$CD103$^-$ DC are also present in the MLN and are thought to develop from blood derived DC precursors that have not been exposed to non-inflammatory conditioning in the gut. As a result they have potent immunogenic potential and in contrast to CD103$^+$ DC, these CD11c$^+$CD103$^-$ DC possess high levels of mRNA coding for TLR, so are more sensitive to activation by PAMPs and inclined to produce pro-inflammatory cytokines driving Th_1 and Th_{17} type immune responses (206). However as CD103$^-$ DC cannot

induce the expression of gut homing molecules on the effector T cells, it brings into question how they can instruct the appropriate migration of T cells to the lamina propria which would be required for protective immunity.

Intestinal pDC

pDC can be found in the MLN, PP and small intestinal lamina propria. CCR9 expressing pDC are thought to migrate to the small intestinal lamina propria in response to CCL25 and are largely absent from the small intestine of CCR9 KO mice. Competitive transfers confirm that CCR9 deficient pDC are impaired in their ability to seed the small intestine of WT recipients. In contrast, pDC are present in normal numbers in the lung, liver and secondary lymphoid organs of CCR9 KO mice (121). pDC do not themselves migrate in lymph to MLN, but appear to control the mobilisation of $CD103^+$ DC from the mucosa via type 1 IFN and TNFα dependent mechanisms (121, 223, 224). In addition, $CCR9^+$ pDC have been reported to be capable of inducing T regs *in vivo* and *in vitro,* whereas $CCR9^-$ pDC fail to induce T cell tolerance (118). Recent work also suggests that pDC in the liver play a direct role in oral tolerance by virtue of their ability to delete $CD8^+$ T cells or drive the differentiation of T regs (225, 226). Thus, pDC may play a central but as yet not fully defined role in regulating mucosal immune responses.

Oral tolerance

Many of the antigens encountered by the gastrointestinal tract are harmless, such as the commensal bacteria and dietary antigens that are essential to our existence. It would be wasteful to induce active immunity against such antigens and in fact this can lead to inflammatory bowel disease (IBD) and coeliac disease. Therefore the default response to these antigens is the induction of peripheral tolerance. Oral tolerance is the phenomenon by which immunological tolerance is induced by oral administration of an innocuous antigen such as soluble protein or commensal bacteria. In the case of proteins, this is manifest as a systemic hypo-responsiveness upon challenge with the same antigen in an immunogenic form (146, 227-235). It can also affect local immune responses such as IgA responses and in the case of commensal bacteria, local tolerance may be the only aspect of immunity that is altered, while the systemic immune system remains ignorant to these antigens (236). The mechanisms of oral tolerance remain unclear, although initial studies reported that high doses of a protein antigen induced T cell anergy and/or deletion, whereas lower doses of proteins induced active

suppression by expanding T regs and enhancing TGFβ, IL-4 and IL-10 release (227, 237-240). More recently, this distinction has become less accepted and most work has focussed on the role of T regs which may be $FoxP3^+$ or $FoxP3^-$ (146, 235). Irrespective of the mechanism, the MLN appear to be the main site of oral tolerance induction, as deletion of PP has no consistent effect on the phenomenon, whereas removal of MLN ablates tolerance to both bacteria and proteins. Preventing cell emigration from the MLN also prevents the development of systemic tolerance to orally administered proteins by as yet undefined mechanisms (241, 242).

Thesis Aims

The homeostatic chemokines CCL19, CCL21 and CCL25 are all crucial for immune development and function. In particular the development of adaptive immunity and tolerance are dependent on CCR7 and its ligands CCL19 and CCL21, while CCL25 is important in the recruitment of CCR9 expressing pDC and effector cells to the gut. With such integral roles in immune activation and suppression, the regulation of these chemokines' bioavailability is essential. The atypical chemokine receptor CCX-CKR binds all three of these chemokines and has been proposed to assist in this regulation by scavenging excess chemokine.

At the time of starting my project, studies of CCX-CKR function were limited and characterisations of the CCX-CKR KO mouse were in their infancy. The aims of this thesis were therefore to characterise the immune system of CCX-CKR KO mice and to determine the effects of CCX-CKR deletion on mucosal immunity in particular.

I began my investigations by examining the cellularity of secondary lymphoid organs in CCX-CKR KO mice and this work is described in Chapter 3. Subsequently, in Chapter 4, I describe my characterisation of the intestinal immune compartment and in Chapter 5, I detail my investigations of antigen specific immune responses and tolerance in CCX-CKR KO mice after systemic and oral challenge, and explore the development of oral tolerance and intestinal inflammation. Finally in Chapter 6, I describe some preliminary investigations into DC function in CCX-CKR KO mice.

Chapter 2
Materials and Methods

2.1 Mice

CCX-CKR knock-out (KO) and CCR9 KO mice ($CD45.1^-CD45.2^+$) were bred and maintained on a C57Bl/6 genetic background ($H\text{-}2^b$) under specific pathogen free (SPF) conditions in the Central Research Facility, University of Glasgow. C57Bl/6 (B6) wild-type (WT) mice ($CD45.1^-CD45.2^+$) (originally littermates of the CCX-CKR KO mice) were bred and maintained in these conditions as a separate colony. C57B1/6 SJL mice ($CD45.1^+CD45.2^-$) and OT2 CD4 T-cell receptor (TCR) transgenic mice ($CD45.1^-CD45.2^+$) specific for the ovalbumin (OVA) peptide sequence 323-339 complexed to the $I\text{-}A^b$ class II MHC molecule were bred under SPF conditions at the Veterinary Research Facility, University of Glasgow.
All mice used were female and first used between 6-8 weeks of age. All procedures were performed in accordance with United Kingdom Home Office regulations.

2.2 Flt3L mediated expansion of dendritic cells *in vivo*

In vivo expansion of DC was achieved by the administration of 10μg human recombinant CHO derived Flt3L (kind gift of Amgen Corp, Seattle, USA) in 0.2ml sterile PBS (Invitrogen, Paisley, UK) i.p. for 10 consecutive days. Mice were sacrificed the day after the final administration.

2.3 R848 administration

10μg or 100μg of the synthetic TLR7/8 agonist R848 (Enzo Life Sciences UK Ltd, Exeter, UK) were administered via gavage in 0.2ml sterile PBS (Invitrogen) as a single dose. 18 or 24 hours later, mice were sacrificed and their MLN and small intestines removed to assess $CD11c^+$ cell content.

2.4 Induction of systemic immune responses *in vivo*

Mice were immunized in the right hind footpad with a single 50μl subcutaneous injection of 100μg ovalbumin (OVA) (Sigma, Poole, UK) dissolved in sterile PBS (Invitrogen) and emulsified in Complete Freund's Adjuvant (CFA) (Sigma) in a 1:1 ratio of antigen to adjuvant.

2.5 Measurement of antigen specific delayed type hypersensitivity responses

DTH responses were assessed three weeks after immunisation in the footpad with OVA/CFA by measuring the increase in thickness of the opposite footpad 24 hours after challenge with

100µg heat aggregated OVA (HAO) in 50µl sterile PBS (Invitrogen) using callipers. HAO was prepared by heating a 2% solution of OVA (Sigma) in sterile PBS at 70°C for an hour. The precipitated OVA formed was then centrifuged for 10 minutes at 400G at 4°C and the supernatant discarded. HAO pellets were suspended in sterile PBS (Invitrogen) at a concentration of 20mg/ml until further use.

2.6 Measurement of antigen specific antibody production and total serum antibody titres

Serum was separated from blood by centrifugation at 13000g for 20 minutes and was stored at -20°C until use. Immulon-4 ELISA plates (Corning, Amsterdam, the Netherlands) were coated overnight at 4°C either with 50µl per well 10µg/ml OVA (Sigma) or purified capture antibodies for the detection of OVA specific IgA, IgG, IgG1 and IgG2a and total IgA and IgG respectively. The next day, plates were washed a minimum of five times with PBS 0.05% Tween 20 (Sigma) before blocking with PBS 3% BSA (Sigma) for 1 hour at room temperature. Plates were washed and 50µl of diluted serum samples added in doubling dilutions in duplicate before leaving overnight at 4°C. The next day, plates were washed and 75µl biotin conjugated detection antibodies added and incubated at room temperature for 1 hour. Plates were then washed and incubated with 1:1000 extravidin-peroxidase (Sigma) for 1 hour at room temperature before washing and being developed using TMB substrate (KPL, Middlesex, UK) and read at 630nm using a MRX II microplate reader (Dynex, West Sussex, UK). A list of the capture and detection antibodies used are shown in Table 2.1.

2.7 Isolation and measurement of intestinal IgA antibodies

Faeces were removed from the colon and transferred to Eppendorfs containing ice cold PBS (Invitrogen) with 0.1mg/ml soybean trypsin inhibitor type II (Sigma) and 50mM EDTA (Sigma). Tubes were centrifuged at 1500g for 10 minutes and the supernatants collected into fresh Eppendorfs, to which 10µl of 100mM phenylmethylsulfonyl (PMSF) (Sigma) in 95% ethanol solution was added before being centrifuged at 14000g for 30 minutes at 4°C. 10µl PMSF solution, 10µl of 1% sodium azide (Sigma) solution and 50µl FCS (Invitrogen) were then added to the resulting supernatants which were stored at –20°C until required. The total protein content of these preparations was determined using a BCA assay kit (Pierce, Loughborough, UK) according to the manufacturer's guidelines and using two-fold dilutions of BSA as standards. Samples were added neat and in duplicate. Immulon-4 ELISA plates

(Corning) were coated overnight at 4°C either with 50µl per well 10µg/ml OVA (Sigma) or purified rat anti-mouse IgA (BD Biosciences, Oxford, UK) for the detection of OVA specific IgA and total IgA respectively. The next day, the plates were washed a minimum of five times with PBS 0.05% Tween 20 (Sigma), before blocking with PBS 3% BSA for 1 hour at room temperature. Plates were washed and 50µl of neat faecal samples preparations added in duplicate before leaving overnight at 4°C. The next day, the plates were washed and 75µl biotin conjugated rat anti-mouse IgA (BD Biosciences) was added before being incubated at room temperature for 1 hour. Plates were then washed and incubated with 1:1000 extravidin-peroxidase (Sigma) for 1 hour at room temperature before washing and were developed using tetramethylbenzidine (TMB) substrate (KPL) and read at 630nm using a MRX II microplate reader (Dynex).

2.8 Induction of tolerance or priming by oral administration of antigen

To induce tolerance, mice were fed OVA, either as a single high dose feed of 25mg or as five daily feeds of 1mg dissolved in 0.2ml sterile PBS (Invitrogen) using a rigid steel curved gavage tube. Control mice received 0.2ml sterile PBS alone. One week after feeding, all mice were immunized in the right hind footpad with 100µg OVA/CFA and 2 weeks later, OVA specific DTH and antibody responses were assessed. To induce oral priming, mice received three feeds of 10mg OVA (Sigma) together with 10µg cholera toxin (CT) (Sigma) in 0.2ml sterile PBS ten days apart. Control mice received either 10mg OVA in 0.2ml sterile PBS or 0.2ml sterile PBS alone. Ten days after the final feed, OVA specific DTH and antibody responses were assessed.

2.9 Isolation of lymphocytes from secondary lymphoid organs

Single cell suspensions were prepared from the spleen (SP), inguinal lymph nodes (ILN) and mesenteric lymph nodes (MLN) by mashing through sterile 50µm Nitex mesh (Cadisch, London, UK) in RPMI 1640 medium (Invitrogen). Cells were subsequently washed by centrifugation at 400g for 5 minutes at 4°C and re-suspended in complete medium (RPMI 1640, 2mM L-glutamine, 100µg/ml penicillin, 100µg/ml streptomycin, 1.25µg/ml Fungizone and 10% foetal calf serum (FCS) (all Gibco)). Red blood cells were removed from spleen cell preparations by re-suspending cell pellets in 1ml Red Blood Cell Lysing Buffer Hybri-Max (Sigma) for 1 minute at room temperature followed by washing in RPMI 1640 (Invitrogen) for 5 minutes at 4°C prior to re-suspension in complete medium. Viable cell counts were

performed using a Neubauer haemocytometer and phase contrast microscope (Nikon Labophot, UK). Cell suspensions were kept on ice until required.

2.10 Isolation of dendritic cells (DC) and macrophages from secondary lymphoid organs

Lymphoid tissues were chopped up using a sterile scalpel blade and digested in 1mg/ml collagenase D and 30μg/ml DNase I (both Roche, Hertfordshire, UK) calcium-magnesium free (CMF) HBSS (Invitrogen) for 30 minutes in a 37°C cell shaker. Cells were subsequently homogenised into a single cell suspension as outlined above.

2.11 Isolation of Peyer's patch (PP) leukocytes

PP were removed from the small intestine and cells were isolated from PP as for secondary lymphoid organs with an additional step prior to collagenase digestion comprising an incubation with CMF-HBSS (Invitrogen) 2mM EDTA (Sigma) in a 37°C cell shaker for 15 minutes to remove surface epithelium.

2.12 Isolation of small intestine lamina propria leukocytes

Whole small intestines were removed, soaked in CMF-HBSS (Invitrogen), placed on a CMF-HBSS soaked paper towel and stripped of Peyer's patches and fat by careful dissection. Intestines were opened longitudinally, cut into 1cm sections and placed in 20ml CMF-HBSS (one intestine per tube) in a 37°C shaker for approximately 10 minutes to remove mucus and intestinal content. To remove the epithelial cell layer, the CMF-HBSS was aspirated from the tissue before being replenished with 20ml fresh CMF-HBSS supplemented with 2mM EDTA (Sigma). Following 15 minutes incubation in the 37°C shaker, the EDTA CMF-HBSS was removed and discarded. 20ml fresh CMF-HBSS was added, the tube shaken vigorously by hand and then aspirated before addition of 20ml fresh 2mM EDTA CMF-HBSS for a further incubation. A total of four EDTA incubations and washes were performed. Tissue was then washed in 20ml sterile PBS and aspirated before addition of 20ml CMF-HBSS containing 100U/ml collagenase type V111 from *Clostridium histolyticum* (Sigma), 30μg/ml DNase (Roche) and 20% FCS. Tissues were digested for 45 minutes to an hour at 37°C in a shaker. Resultant suspensions were passed through cell strainers to generate a single cell suspension, washed for 5 minutes, re-suspended in complete medium and placed on ice until use.

2.13 Isolation of liver leukocytes

Livers were chopped into approximately 5mm^2 pieces and incubated in a shaker at 37°C for 30 minutes with 1mg/ml type IA collagenase (Sigma) and 0.1mg/ml DNase I (Roche) in CMF-HBSS (Invitrogen). Following digestion, the solution and any remaining tissue were mashed through a 40μm cell strainer to generate a single cell suspension.

2.14 Purification of CD4$^+$ lymphocytes

Cells were purified by negative selection using a CD4$^+$ T cell isolation kit according to the manufacturer's instructions (Miltenyi Biotec Ltd, Surrey UK). Briefly, single cell suspensions of LN cells were prepared as described and up to 10^7 total cells were suspended in 40μl MACS buffer (2mM EDTA, 0.5% BSA PBS). 10μl of biotin-antibody cocktail was then added per 10^7 total cells and incubated for 10 minutes at 4°C. 30μl of MACS buffer and 20μl of anti-biotin magnetic microbeads were then added per 10^7 total cells, mixed well and incubated for 15 minutes at 4°C. Cells were then washed by centrifugation at 300g for 10 minutes and re-suspended in 500μl of MACS buffer per 10^8 cells and passed through a MACS column placed within the magnetic field of the MACS separator. Magnetically labelled cells were retained there and the effluent containing the fraction of unlabelled CD4$^+$ cells was collected.

2.15 Generation of bone marrow derived dendritic cells (BMDC)

To obtain bone marrow cells, mouse femurs and tibias were flushed out with RPMI 1640 (Invitrogen) using a syringe and 21G needle. Cells were filtered through sterile Nitex and suspended at 3x10^6 cells/ml. 1ml of cells were seeded into 90cm low-adherence Petri dishes (Sterilin, UK) along with 8ml complete medium and 1ml GM-CSF derived from the filtered supernatant of the X-63 fibroblast GM-CSF transfected cell line. Cells were incubated at 37°C in 5% CO_2 and after 3 and 6 days of culture, the medium was supplemented with 5ml complete medium and 0.5ml GM-CSF supernatant. BMDC were harvested by gentle washing of the Petri dishes after 7 to 9 days of culture and were typically >70% CD11c$^+$ as determined by flow cytometry.

2.16 Assessment of endocytic activity of BMDC

BMDC were cultured in complete medium with 1mg/ml FITC dextran (MW 4400; Sigma) in ultra low adherence 24 well flat-bottomed plates (Corning) for 0-60 minutes at either 4°C or

37°C. Cells were then washed twice in ice-cold FACS buffer (PBS 2% FCS 5mM EDTA) before staining with anti-CD11c-PE (BD Biosciences) for 30 minutes at 4°C in the dark and analysis by flow cytometry. The uptake of FITC dextran was expressed as the ΔMFI, calculated by subtracting the FITC specific mean fluorescent intensity of cells cultured at 4°C from that of cells cultured at 37°C.

2.17 Activation of BMDC *in vitro*

$1x10^6$ BMDC per well were cultured overnight in 24 well flat bottom low adherence plates (Corning) in either complete medium alone or with 2μg/ml *Escherichia coli* LPS (Sigma). Cells were harvested by aspiration of supernatants, washed in complete medium and stained for CD11c and a selection of co-stimulatory molecules and class II MHC for analysis by flow cytometry.

2.18 Assessment of antigen presenting activity of DC

B6 BMDC or spleen cells were pulsed with 5mg/ml OVA (Sigma) by incubating in low adherence 24 well plates (Corning) at $3x10^6$ cells per well at 37°C in 5% CO_2 for 2 hours. Excess OVA was then washed off by centrifugation at 4°C for 5 minutes at 400g and the cells irradiated at a dose of 3000Gy to inhibit proliferative capacity. The pulsed cells were then cultured with OVA specific OT2 LN cells in a 1:1 or 1:5 ratio in flat-bottomed 96 well plates at $2x10^5$ cells per 200μl T cell medium per well. Unpulsed BMDC or spleen cells were also cultured with T cells and 1μg/ml OVA peptide 323-339 (Genosys, Sigma). Cells were cultured for 120h and pulsed with 1μCi/well tritiated thymidine (^{3}H-TdR) for the final 18 hours of culture and harvested as above.

2.19 Proliferative responses of lymphocytes to Concanavalin-A and anti-CD3/CD28

Aliquots of $2x10^5$ lymphoid cells were cultured in 200μl of T cell medium (complete medium supplemented with 1% non-essential amino acids (NEAA), 1mM sodium pyruvate and 50μM 2-ME (all Gibco, Invitrogen)). Cells were either cultured alone or in the presence of 1μg/ml anti-CD3 and 1μg/ml anti-CD28 (both from BD Biosciences), or with 5μg/ml concanavalin-A (ConA) (Sigma). Cells were cultured in triplicate for 48-120h at 37°C in 5% CO_2 in 96-well flat-bottomed tissue culture plates (Corning). After 48h of culture, cell supernatants were

removed and stored at –20°C for measurement of cytokines by ELISA and the wells replenished with fresh medium. To assess proliferation, cells were pulsed with 1μCi/well tritiated thymidine (^{3}H-TdR) (West of Scotland Radionucleotide Dispensary) for the final 18 hours of culture. Cellular DNA was harvested on to glass fibre filter mats (Wallac, Perkin-Elmer, Cambridge, UK) and ^{3}H-TdR uptake was measured by a Betaplate scintillation counter (Wallac) using the Microbeta programme.

2.20 Assessment of antigen specific cell proliferation and activation *in vitro*

Aliquots of $2x10^5$ lymphoid cells were cultured in 200μl of T cell medium. Cells were cultured in the presence of 1mg/ml, 500μg/ml or 100 μg/ml OVA, or with 1μg/ml OVA peptide 323-339 (Genosys, Sigma) to assess antigen specific proliferation and cytokine production. Cells cultured in medium alone or in the presence of 1μg/ml anti-CD3 and 1μg/ml anti-CD28 (both from BD Biosciences) were used as negative and positive controls respectively. Cells were cultured in triplicate for 96h at 37°C in 5% CO_2 in 96-well flat-bottomed tissue culture plates (Corning). After 48h of culture, cell supernatants were removed and stored at –20°C for measurement of cytokines by ELISA and the wells replenished with fresh medium. To assess proliferation, cells were pulsed with 1μCi/well tritiated thymidine (^{3}H-TdR) for the final 18 hours of culture as above.

2.21 Stimulation of MLN cells with R848 *in vitro*

Single cell suspensions were prepared from the MLN of normal resting or Flt3L treated mice by mashing through sterile 50μm Nitex mesh (Cadisch) in RPMI 1640 medium (Invitrogen). Cells were subsequently washed by centrifugation at 400g for 5 minutes at 4°C and re-suspended in complete medium. Aliquots of $1x10^6$ viable MLN cells were cultured in 1ml of T cell medium alone, or in the presence of 1μg/ml R848 (Alexis Biochemicals). Cells were cultured in triplicate for 24h at 37°C in 5% CO_2 in 24-well flat-bottomed tissue culture plates (Corning). After 24 hours, cells were harvested and stained for expression of CD11c, PDCA-1 and CD40 or CD86 for analysis by flow cytometry.

2.22 Flow cytometry

Cells were washed by centrifugation at 400g at 4°C for 5 minutes in ice cold FACS buffer, suspended at $1x10^6$ cells per tube in 5ml round-bottomed tubes (BD Biosciences) and

incubated with 1:200 anti-CD16/CD32 (BD Biosciences) in FACS buffer for 15 minutes at 4°C to block non-specific binding. Cells were washed in FACS buffer and stained for a further 30-60 minutes with fluorescein isothiocyanate (FITC), phycoerythrin (PE), allophycophycoerythrin (APC) or biotin-conjugated antibodies specific for selected cell markers (Table 2.2). Biotin-conjugated antibodies were detected by the addition of streptavidin allophycophycoerythrin (SA-APC) (BD Biosciences). All FACS antibodies were used at 1:200 in FACS buffer with the exception of anti-PDCA-1 which was used at 1:11. All incubations were performed in 200µl at 4°C in the dark. After washing, dead cell exclusion was carried out by addition of 10µl 7-AAD (BD Biosciences) to each tube immediately prior to acquisition and analysis using a dual laser (488nm argon laser, 635nm red diode laser) FACSCalibur flow cytometer and CELLQuest software (BD Biosicences). Data were analysed using FlowJo software (Tree Star Inc, OR, USA).

2.23 Chemokine receptor staining for flow cytometry

Surface CCR9 was detected using monoclonal antibodies kindly provided by Dr Oliver Pabst (Institute of Immunology, Hannover Medical School, Hannover, Germany). Non specific binding by cells was blocked by incubating in PBS 2% FCS 10% mouse serum for 1 hour at 4°C, then cells were washed by centrifugation in PBS 2% FCS three times before staining for a further hour at 4°C with 5µg/ml anti-CCR9 antibody or purified ratIgG2b (as an isotype control). Cells were washed three times, stained with biotinylated polyclonal anti-rat IgG (BD Biosciences) for 30 minutes at 4°C, washed again and then stained with SA-APC (BD Biosciences) for 15 minutes at 4°C before washing three times.

2.24 Assessment of intracellular cytokine production

To assess cell specific IFNγ production, $2x10^6$ LN and spleen cell suspensions were stimulated for 4 hours with 0.1µM PMA and 1µM ionomycin (both Sigma) per well in 6 well tissue culture plates (Corning) in complete medium. 1µM monensin and 10µg/ml Brefeldin A (both Sigma) were added to the culture to prevent protein secretion by blocking the Golgi apparatus. Cells were harvested and re-suspended in 200µl "Block Wash" solution (PBS 0.1% sodium azide (Sigma), 1% heat inactivated FCS (Invitrogen) and 0.1% BSA (Sigma)). To allow for dead cell exclusion, 800µl 0.11µg/ml ethidium monoazide (EMA; Molecular Probes, Paisley, UK) was added to the tubes before their incubation for 10 minutes in the dark, followed by exposure to bright light for a further 10 minutes all at room temperature. Cells were stained for

surface markers as described above then washed in "Block Wash" solution. 250µl of 1% formaldehyde (BDH Laboratory Supplies, Poole, England) in PBS was then added for 10 minutes at 4°C to fix cells. Cells were then permeabilised in "Perm Wash" solution (PBS 0.1% saponin (Sigma) 0.1% sodium azide, 0.2% heat inactivated FCS and 0.1% BSA) before their incubation with purified anti-mouse CD16/CD32 (Fc block) (BD Biosciences) at 4°C for 15 minutes to block intracellular Fc receptor binding. Cells were then suspended in "Perm Stain" solution (PBS 0.1% saponin (Sigma) 0.1% sodium azide, 1% heat inactivated FCS and 0.1% BSA) with anti-cytokine antibodies or appropriate isotype controls added at 1:200 dilutions and incubated in the dark at 4°C for 30 minutes. Finally, cells were washed in "Perm Wash" and analysed by flow cytometry.

2.25 Assessment of intracellular FoxP3 staining by flow cytometry

Cells were stained for intracellular expression of the regulatory T cell specific transcription factor FoxP3 using an APC-anti mouse/rat FoxP3 staining kit according to the manufacturer's instructions (Ebioscience). Briefly, $1x10^6$ cells were added per tube in 100µl FACS buffer and stained with EMA as above to exclude dead cells. Surface markers were stained for as above and cells washed in the flow cytometry buffer provided. 1ml of freshly prepared fixation/permeabilisation working solution was then added to the cells which were then incubated in the dark at 4°C for 30 minutes. Cells were then washed in the permeabilisation buffer provided and blocked with 100µl Fc block in permeabilisation buffer at 4°C for 15 minutes. Without further washing, anti-FoxP3 antibody or the isotype control antibody was added at 0.5µg per 100µl of sample and incubated in the dark at 4°C for 30 minutes. Cells were then washed twice in permeabilisation buffer before re-suspension in FACS buffer and analysis by flow cytometry as above.

2.26 Measurement of cytokine production by ELISA

IFNγ levels in culture supernatants were determined by sandwich ELISA. Immulon-4 ELISA plates (Corning) were coated overnight at 4°C with anti-IFNγ capture antibody diluted in carbonate buffer (Sigma). Plates were washed a minimum of three times with PBS 0.05% Tween 20 (Sigma) before blocking with PBS 10% FCS for 1 hour at room temperature. Plates were washed and incubated with samples and recombinant IFNγ standards (BD Biosciences) for 2 hours at room temperature before further washing and addition of biotinylated anti-IFNγ detection antibody (BD Biosciences) for 1 hour at room temperature. Plates were then washed

and incubated with 1:1000 extravidin-peroxidase (Sigma) for 1 hour at room temperature before washing and being developed using tetramethylbenzidine (TMB) substrate (KPL) and read at 630nm or 450nm in the presence of stop solution (R&D Systems, Abingdon, UK). The optical density (OD) of each well at 450nm was determined using a MRX II microplate reader (Dynex) and sample cytokine concentrations calculated from the standard curve obtained. A list of the capture and detection antibodies used is shown in Table 2.1.

2.27 Measurement of chemokine production by ELISA

CCL21 protein levels were measured by ELISA according to the manufacturer's instructions (R&D Systems). Capture antibody was coated onto plates overnight at 4°C. Plates were then washed with PBS 0.05% Tween 20 (Sigma) before being blocked with PBS 1% BSA (Sigma) for 3 hours at room temperature. Plates were washed again, samples and standards added for 2 hours and after washing, detection antibody was added for a further 2 hours at room temperature. Plates were then washed and streptavidin-HRP was added at room temperature for 1 hour. Following washing, substrate solution (R&D Systems) was added for 20 minutes before stop solution (R&D Systems) was applied. The optical density (OD) of each well at 450nm was determined using a MRX II microplate reader (Dynex) and sample chemokine concentrations calculated from the standard curve obtained. A list of the capture and detection antibodies used is shown in Table 2.1.

2.28 Purification of PDCA-1$^+$ plasmacytoid DC

Cells from the spleens of Flt3L treated CD45.1$^+$CD45.2$^-$ C57Bl/6, WT and CCX-CKR KO mice were purified by negative selection using the plasmacytoid dendritic cell isolation kit II according to the manufacturer's instructions (Miltenyi Biotec Ltd). Briefly, single cell suspensions of spleen cells were prepared as described and 10^8 cells were re-suspended per 350µl MACS buffer (2mM EDTA, 0.5% BSA PBS). 50µ1 FcR blocking reagent and 100µl plasmacytoid dendritic cell (pDC) biotin cocktail were added per 10^8 cells and the cells incubated for 10 minutes at 4°C. Cells were then washed by centrifugation at 300g for 10 minutes before 800µ1 MACS buffer and 200µ1 of anti-biotin microbeads per 10^8 cells were added. Cells were incubated for 10 minutes at 4°C, then washed by centrifugation at 300g for 10 minutes and re-suspended in 500µl of MACS buffer per 10^8 cells. Cells were then passed through a MACS column placed within the magnetic field of a MACS separator and unlabelled PDCA-1$^+$ cells were collected in the effluent.

2.29 Adoptive transfer of plasmacytoid DC

Intact spleen cells from $CD45.1^+CD45.2^-$ C57Bl/6 mice or enriched pDC from Flt3L treated $CD45.1^+CD45.2^-$ C57Bl/6, WT C57Bl/6 or CCX-CKR KO mice were passed through Nitex and an aliquot of cells was stained with anti-PDCA-1 antibody (Miltenyi Biotec Ltd, Surrey, UK) to assess pDC numbers by flow cytometry. The proportion of PDCA-1 expressing cells was calculated and the equivalent of $1x10^6$ $PDCA\text{-}1^+$ pDC were transferred in sterile PBS (Invitrogen) i.p. (in the case of intact spleen cells) or i.v. (in the case of enriched pDC) per recipient.

2.30 Induction of dextran sulphate sodium mediated colitis

To induce acute colitis, mice received 2% dextran sulphate sodium (DSS) (reagent grade; MW 36,000-50,000 kDa; MP Biomedicals, Ohio) in sterile drinking water for 7 days. The amount of water consumed per animal was estimated by dividing the total water intake by the number of animals per cage. Mice were monitored for weight change, rectal bleeding and diarrhoea, which were scored according to the criteria shown in Table 2.3. Colon shortening was determined immediately after sacrifice by measuring colon length and histological analysis was performed on paraffin embedded sections stained with haematoxylin and eosin (H&E) processed by technical staff in the department of veterinary medicine at the University of Glasgow.

2.31 Measurement of cytokine and chemokine production in colon explant cultures by Luminex

Colons were opened longitudinally and 1cm long samples of proximal and distal colons were washed in PBS supplemented with 100μg/ml penicillin and streptomycin. Colon tissues were then cultured in RPMI-1640 with 100μg/ml penicillin and streptomycin for 24 hours at 37°C in 5% CO_2 and supernatants removed and stored at -20°C. The supernatants were assayed for the presence of FGF, GM-CSF, IFNγ, TNFα, IL-1α, IL-1β, IL-2, IL-4, IL-5, IL-6, IL-10, IL-12 (p40 and p70), IL-13, IL-17, CCL2, CCL3, CCL4, CCL5, CXCL1, CXCL9 and CXCL10 using the Multiplex Bead Assay (Biosource, Paisley, UK) according to the manufacturer's guidelines. Briefly, supernatant samples were incubated with antibody coated microspheres expressing distinct fluorophores specific for designated chemokines/cytokines in 96 well plates (Corning). After washing, biotinylated detection antibodies were added for 1 hour at room temperature before the addition of SA-PE for 30 minutes at room temperature.

Following washing, the fluorescence intensity bound to microspheres was detected and measured using a Luminex XMAP system.

2.32 Statistical analysis

Results are shown as means +1 standard deviation (SD) unless stated otherwise and groups were compared using either a Student's unpaired two-tailed t test, Mann-Whitney test, one-way Anova or two-way Anova with Bonferroni post tests. The distribution of data was assessed using a D'Agostino and Pearson omnibus normality test. Values of $p<0.05$ were considered to be statistically significant.

Table 2.1 Monoclonal antibodies used for ELISA.

Antibody	**Capture/ Detection**	**Working Concentration**	**Supplier**
Anti mouse IgG (Fc specific) Alkaline phosphatase antibody produced in goat	Capture	1:40000 dilution	Sigma
Purified rat anti-mouse IgA	Capture	1:500 dilution	BD Biosciences
Biotin rat anti-mouse IgG2a	Detection	1:1000 dilution	BD Biosciences
Biotin rat anti-mouse IgG1	Detection	1:16000 dilution	BD Biosciences
Anti-mouse IgG (Fab specific) biotin antibody produced in goat	Detection	1:200000 dilution	Sigma
Biotin rat anti-mouse IgA	Detection	1:500 dilution	BD Biosciences
Anti- mouse IFNγ	Capture	1:250 dilution	BD Biosciences
Biotin anti-mouse IFNγ	Detection	1:250 dilution	BD Biosciences
Rat anti-mouse CCL21	Capture	4 μg/ml	R&D Systems
Biotin goat anti-mouse CCL21	Detection	50 ng/ml	R&D Systems
Rat anti-mouse CCL21	Capture	4 μg/ml	R&D Systems
Biotin goat anti-mouse CCL21	Detection	50 ng/ml	R&D Systems

Table 2.2 Monoclonal antibodies and isotype controls used for flow cytometry

Antigen	Clone	Isotype	Supplier
B220	RA3-6B2	Rat IgG2a	BD Biosciences
CD3	145-2C11	Hamster IgG1	BD Biosciences
CD4	GK1.5	Rat IgG2b	BD Biosciences
CD8	53-6.7	Rat IgG2a	BD Biosciences
CD11b	M1/70	Rat IgG2b	BD Biosciences
CD11c	HL3	Hamster IgG1	BD Biosciences
CD19	1D3	Rat IgG2a	BD Biosciences
CD25	7D4	Rat IgG2b	BD Biosciences
CD40	3/23	Rat IgG2a	BD Biosciences
CD45	30-F11	Rat IgG2b	Ebioscience
CD69	C9B7W	Rat IgG1	BD Biosciences
CD80	16-10A1	Hamster IgG2a	BD Biosciences
CD86	GL1	Rat IgG2a	BD Biosciences
CD103	M290	Rat IgG2a	BD Biosciences
DX5	DX5	Rat IgM	BD Biosciences
IFNγ	XMG1.2	Rat IgG1	BD Biosciences
IL-4	11B11	Rat IgG1	BD Biosciences
F4/80	BM8	Rat IgG2a	Ebioscience
FoxP3	FJK-16s	Rat IgG2a	Ebioscience
KJ	KJ1-26	Murine IgG2a	BD Biosciences
CD45.1	A20	Murine IgG2a	BD Biosciences
MHC class II (I-A^b)	25-9-17	Murine IgG2a	BD Biosciences
PDCA-1	JF05-IC24.1	Rat IgG2b	Miltenyi-Biotec
Vα2 TCR	KB5-C20	Rat IgG2a	BD Biosciences
CCR9	7E7	Rat IgG2b	Dr Oliver Pabst

Table 2.3 Disease score criteria for DSS induced colitis.

Points	Weight Loss as % of total starting body weight	Rectal Bleeding	Stools
0	none	none	well-formed pellet
1	1-5		
2	5-10	blood stain around anus	pasty soft pellets that do no adhere to the anus
3	10-20		
4	> 20	gross bleeding	diarrhoea that adheres to anus

Chapter 3
Characterisation of the Secondary Lymphoid Organs of CCX-CKR KO Mice

Introduction

Chemokines are essential for inflammatory processes, as well as the maintenance of homeostasis. CCR7 and CCR9 are examples of chemokine receptors that mediate leukocyte localisation within lymphoid organs and tissues (12, 82). Previous data from an earlier PhD student has indicated that CCX-CKR may function as a scavenger of the CCR7 ligand CCL19, suggesting a role for CCX-CKR in the regulation of the availability of its chemokine ligands. As CCR7 is the principal chemokine receptor involved in leukocyte entry into secondary lymphoid organs, CCX-CKR could play a role in regulating the recruitment of CCR7 expressing DC and naïve lymphocytes from tissues and the bloodstream into secondary lymphoid organs. Therefore, I investigated the architecture and composition of the LN and spleen in CCX-CKR KO mice and assessed the proliferative capacity of and cytokine production by lymphocytes in response to a selection of stimuli.

3.1 Analysis of CCX-CKR KO secondary lymphoid architecture

To begin my characterisation of the secondary lymphoid organs of CCX-CKR KO mice, I carried out a histological analysis of ILN, MLN and spleens of CCX-CKR KO and WT mice. No gross abnormalities could be seen in CCX-CKR KO mice, with B cell follicles being apparent along the outer edge of LN, as well as densely populated T cell zones in the surrounding areas. Lymphoid white pulp areas also appeared normal in the spleens of CCX-CKR KO mice (Fig 3.1).

3.2 Analysis of CCX-CKR KO secondary lymphoid organ cellularity and lymphocyte composition

At the time of starting my project, preliminary work had suggested there might be reduced size and cellularity of secondary lymphoid organs in CCX-CKR KO FVB mice. I therefore extended this work using large numbers of CCX-CKR KO mice backcrossed thoroughly onto the C57Bl/6 genetic background but I found no significant differences in the total cell numbers recovered from the MLN, ILN or spleens of CCX-CKR KO and WT mice (Fig 3.2).

There were also no significant differences in the proportions or absolute numbers of $CD4^+$ and $CD8^+$ T cells, or of $CD19^+$ B cells in these tissues (Fig 3.3). As CCX-CKR expression could also potentially affect the availability of CCL25, a ligand recognised by CCR9, I assessed CCR9 expression by lymphocytes within secondary lymphoid organs. As expected, most $CD8^+$ T cells in WT mice expressed CCR9, as did a proportion of $CD4^+$ T cells and $B220^+$ B

cells, but there were no significant differences in the proportions of CCR9 expressing lymphocytes between CCX-CKR KO and WT mice (Fig 3.4). Unfortunately attempts to assess CCR7 expression by lymphocytes from CCX-CKR KO mice using flow cytometry were unsuccessful.

$CD4^+CD25^+FoxP3^+$ T regs are a further subset of lymphocytes that are dependent on CCR7 for efficient migration into secondary lymphoid organs (90). Comparable proportions and absolute numbers of total $CD4^+CD25^+FoxP3^+$ cells, and of $FoxP3^+$ cells amongst $CD4^+CD25^+$ cells were present within the MLN and ILN of CCX-CKR KO and WT mice. However, the proportion of $CD4^+CD25^+FoxP3^+$ cells in the spleens of CCX-CKR KO mice was significantly increased compared with controls, although this did not translate into a difference in the absolute numbers of T regs (Fig 3.5).

3.3 Proliferative and cytokine responses of CCX-CKR KO lymphocytes *in vitro*

Having determined that the lymphocyte composition of secondary lymphoid organs is not significantly different between CCX-CKR KO and WT mice, I went on to assess lymphocyte function, as measured by their proliferative capacity and cytokine responses *in vitro*.

Cells isolated from the MLN, ILN and spleens of CCX-CKR KO and WT mice were cultured either in complete medium alone, or with 1μg/ml anti-CD3 and anti-CD28 antibodies. The proliferative responses of spleen and LN cells from WT and CCX-CKR KO mice were not significantly different at any time point after stimulation (Fig 3.6). Similar results were observed when MLN and spleen cells were stimulated with 5μg/ml Con A (Fig 3.7).

In contrast, CCX-CKR KO MLN and spleen cells produced significantly lower levels of IFNγ after 48 hours stimulation with anti-CD3 and anti-CD28 antibodies. A similar defect was seen when CCX-CKR KO MLN cells were stimulated with 5μg/ml Con A. The same trend was found with spleen cells, although the difference was not statistically significant in this case (Fig 3.8).

To extend these studies, I analysed intracellular IFNγ expression by MLN and spleen cells stimulated for 4 hours with PMA and ionomycin. This revealed a significant reduction of IFNγ production by CCX-CKR KO $CD4^+$ cells compared with WT T cells. However, IFNγ

production by $CD8^+$ cells was comparable between CCX-CKR KO and WT (Fig 3.9). Unfortunately, I was unable to assess production of the Th2 associated cytokine, IL-4 using this approach.

3.4 Analysis of DC populations in secondary lymphoid organs of CCX-CKR KO mice

I next investigated whether the absence of CCX-CKR affected the composition of $CD11c^+$ DC subsets within the MLN, ILN and spleen from which there were no significant differences in the proportions or numbers of total $CD11c^+$ cells recovered (Fig 3.10). I also examined the presence of $CD11c^{hi}$classIIMHC^{hi} and $CD11c^{hi}$class11MHC^{lo} DC in the MLN, on the basis that these are believed to represent DC that have migrated from tissues into secondary lymphoid organs, or which are "resident" DC derived from the blood stream respectively. Again no differences were found in either of these populations between CCX-CKR KO and WT mice (Fig 3.11).

I next assessed the abundance of conventional DC subsets in the MLN that are characterised by their expression of CD11c and CD4, CD8 or CD11b (98). The proportions of total live cells co-expressing CD11c and CD4 or CD8 were significantly reduced in CCX-CKR KO mice, although the proportion co-expressing CD11c and CD11b were unaffected by CCX-CKR deletion. When expression of these markers was examined directly on $CD11c^+$ cells, similar numbers and proportions of cells co-expressing CD11c and CD11b or CD4 were seen in the MLN of CCX-CKR KO and WT mice. However the proportion of $CD11c^+$ cells expressing CD8 was reduced significantly in the MLN of CCX-CKR KO mice, although this did not manifest as a difference in their absolute numbers (Fig 3.12).

Finally, I assessed the prevalence of pDC, as they are reported to express both CCR7 and CCR9 (121, 122). pDC have been characterised as being $CD11c^{lo}B220^+PDCA\text{-}1^+$ cells. On examining the total LN cells, I found populations of $CD11c^{lo}$ cells which expressed B220 or PDCA-1 (Fig 3.13A) and when $CD11c^{lo}$ cells were analysed directly I found two distinct subsets, one of which were $B220^+PDCA\text{-}1^+$ and the other $B220^+PDCA\text{-}1^-$ (Fig 3.13.B). Preliminary studies using these criteria showed an apparent decrease in the absolute numbers and proportions of the $CD11c^{lo}B220^+PDCA\text{-}1^+$ cell subset in the MLN of CCX-CKR KO mice but there were no differences in the absolute numbers or proportions of the $B220^+PDCA\text{-}1^-$

cell subset (Fig 3.13 C, D). Recent work suggests that only the PDCA-1$^+$ cell subset are bona fide pDC, whereas the CD11c^{lo}B220$^+$PDCA-1$^-$ cells may be DC precursors (243). As I found that all CD11c^{lo}PDCA-1$^+$ cells co-expressed B220, I used CD11c^{lo} and PDCA-1 expression alone to identify pDC more simply in more extensive studies. This approach confirmed the virtual absence of pDC in the MLN of CCX-CKR KO mice, whereas around 10-20% of total CD11c$^+$ cells were of this phenotype in WT MLN (Figs 3.14 and 3.15)

A similar, but somewhat smaller reduction was also seen in the proportions of pDC in the ILN of CCX-CKR KO mice, although the absolute numbers of pDC were not significantly reduced in this case. There were no differences in the proportions or numbers of pDC in the spleens of CCX-CKR KO mice compared with WT, where pDC were relatively scarce in both strains (Fig 3.15).

Further analysis indicated that compared with WT, higher proportions of pDC from CCX-CKR KO lymphoid organs expressed class II MHC and that the level of class II MHC expression by pDC was also significantly higher in CCX-CKR KO mice as assessed by ΔMFI (Fig 3.16).

I next assessed CCR9 expression by pDC in CCX-CKR KO mice. CCR9 expressing total CD11c^{lo} cells were identifiable in the MLN and spleens of both WT and CCX-CKR KO mice. Staining was absent in CCR9 KO mice, confirming the specificity of the CCR9 antibody used in analysis. There were no significant differences in the proportions or numbers of CD11c^{lo}CCR9$^+$ cells in the spleens of CCX-CKR KO and WT mice, but these were significantly reduced by approximately 40% in the MLN of CCX-CKR KO mice compared with WT MLN (Fig 3.17). Because of staining difficulties, I was unable to use PDCA-1 to identify these CD11c^{lo}CCR9$^+$ cells as pDC directly. Therefore I used the co-expression of CD11c^{lo} and B220, although as discussed earlier, this population will also contain additional cells. In agreement with this, the numbers of CD11c^{lo}B220$^+$ cells in CCX-CKR KO tissues were not reduced as dramatically as I had found for the numbers of CD11c^{lo}PDCA-1$^+$ cells (Figs 3.15 and 3.18B). 40-50% of CD11c^{lo}B220$^+$ cells expressed CCR9 in the MLN and spleens of WT mice and this proportion was significantly reduced in the MLN of CCX-CKR KO mice. In parallel there was a significant reduction in the total numbers and proportions of CD11c^{lo}B220$^+$CCR9$^+$ pDC in CCX-CKR KO MLN. This contrasts with the normal

expression of CCR9 by lymphocytes in CCX-CKR KO tissues. Similar trends were observed in the spleen, but these were not statistically significant (Fig 3.18).

3.5 Analysis of macrophages and NK cells in lymphoid tissues of CCX-CKR KO mice

Having assessed the relative proportions and numbers of lymphocytes and DC in CCX-CKR KO secondary lymphoid organs, I decided to determine whether a deficiency of CCX-CKR affected the numbers of macrophages and NK cells. Macrophages were identified by expression of F480, while NK cells were identified as $CD3^{-}DX5^{+}$ cells. No differences were seen in the proportions or numbers of either cell type in any tissues from CCX-CKR KO and WT mice (Figs 3.19 and 3.20).

Summary

In this chapter, I have characterised the cellular composition of secondary lymphoid organs from CCX-CKR KO mice. My results have indicated that there are no differences in the proportions and numbers of $CD4^{+}$ and $CD8^{+}$ T cells, $CD19^{+}$ B cells, macrophages or NK cells between WT and CCX-CKR KO mice. In addition, proliferative responses to mitogenic or TCR stimulation *in vitro* were comparable. However there was a decreased production of IFNγ by $CD4^{+}$ T cells from CCX-CKR KO mice.

In addition, most of the phenotypic subsets of conventional DC were comparable in CCX-CKR KO and WT MLN, apart from a significant reduction in the proportion of $CD11c^{+}CD8^{+}$ DC. The numbers and proportions of "migratory" and "resident" DC were also normal in CCX-CKR KO MLN. The most significant finding from my studies was a consistent and dramatic reduction in the numbers of pDC in the MLN of CCX-CKR KO mice, despite the fact that the proportions and numbers of total $CD11c^{+}$ cells were comparable with WT mice. In parallel, fewer $CD11c^{lo}B220^{+}$ cells from the MLN of CCX-CKR KO mice than WT expressed CCR9, despite this marker being expressed normally by lymphocytes in these mice. Interestingly however, pDC from CCX-CKR KO mice appeared to express higher levels of class II MHC than WT pDC.

Taken together, these data indicate that CCX-CKR plays an important and selective role in the recruitment and/or maintenance and/or function of pDC into/within MLN. CCX-CKR may also play a subtle role in regulating Th1 function in secondary lymphoid organs.

In the next chapter I went on to examine the effects of CCX-CKR deletion on the cellular composition of the intestinal immune compartment, an environment in which all three CCX-CKR ligands, CCL19, CCL21 and CCL25 are abundant.

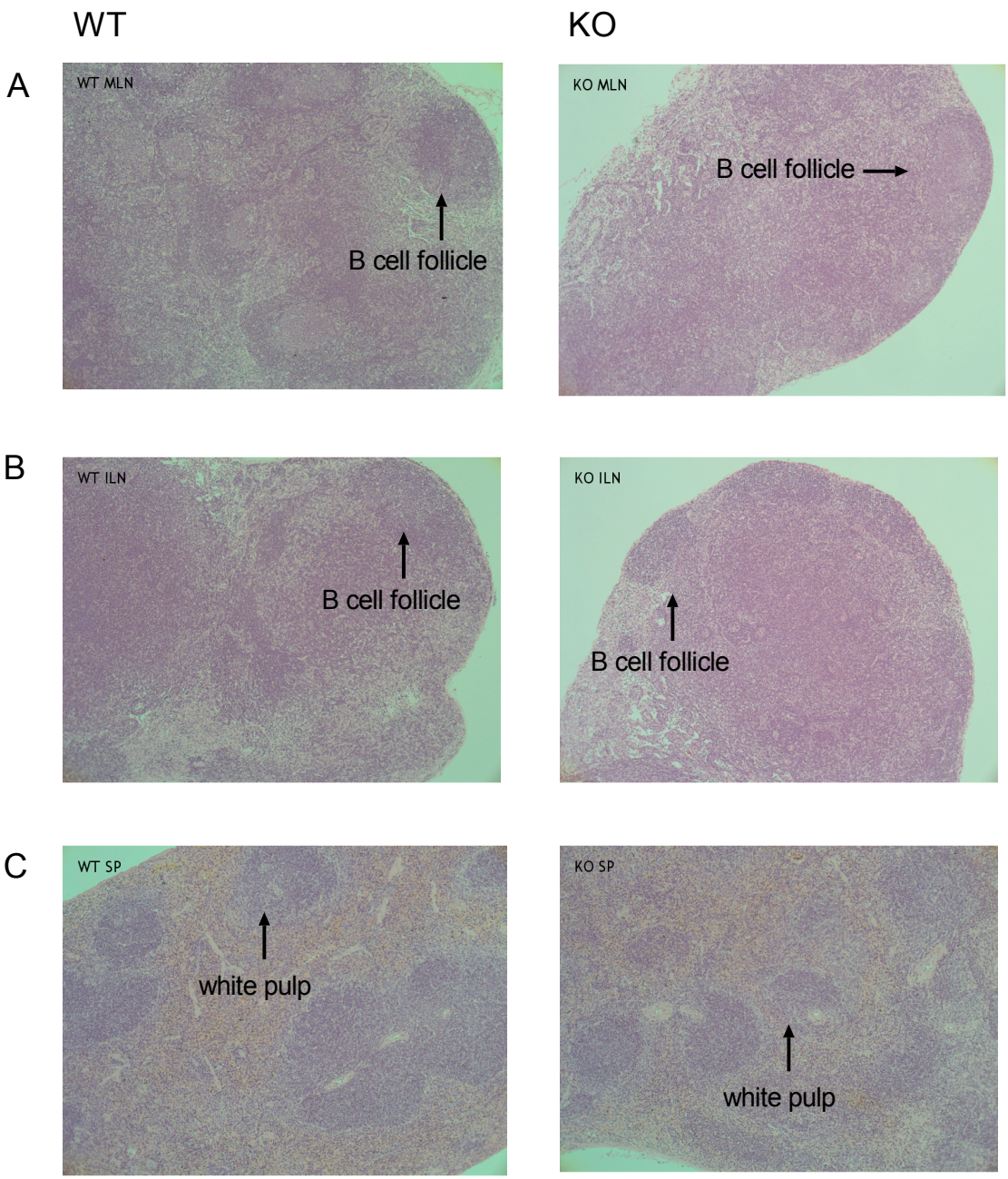

Figure 3.1
Normal Architecture of Secondary Lymphoid Organs in Resting CCX-CKR KO Mice
MLN (A), inguinal lymph nodes (ILN) (B) and spleens (C) from resting WT and CCX-CKR KO mice were removed, fixed in 10% formalin, embedded in paraffin and stained with haematoxylin and eosin for histological analysis. Distinct B cell follicles, T cell areas and white pulp can be seen in both WT and CCX-CKR KO tissue. Representative histology from 3 mice per group is shown. (Final magnification x100).

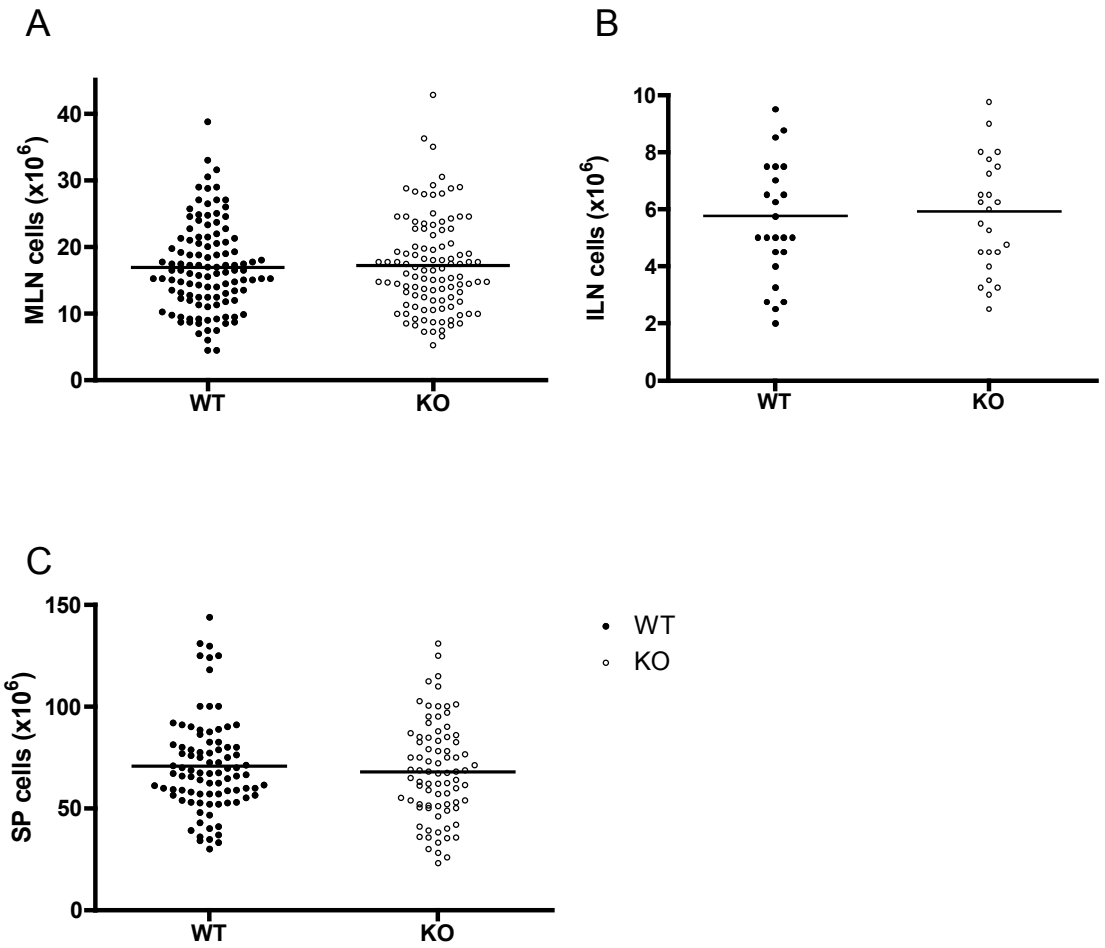

Figure 3.2
Total Cell Numbers in CCX-CKR KO and WT Secondary Lymphoid Organs
Cells were isolated from MLN (A), ILN (B) and spleens (C) of CCX-CKR KO and WT mice and viable cells counted by phase contrast microscopy. Results show means of between 25-113 mice per group used in 33 individual experiments.

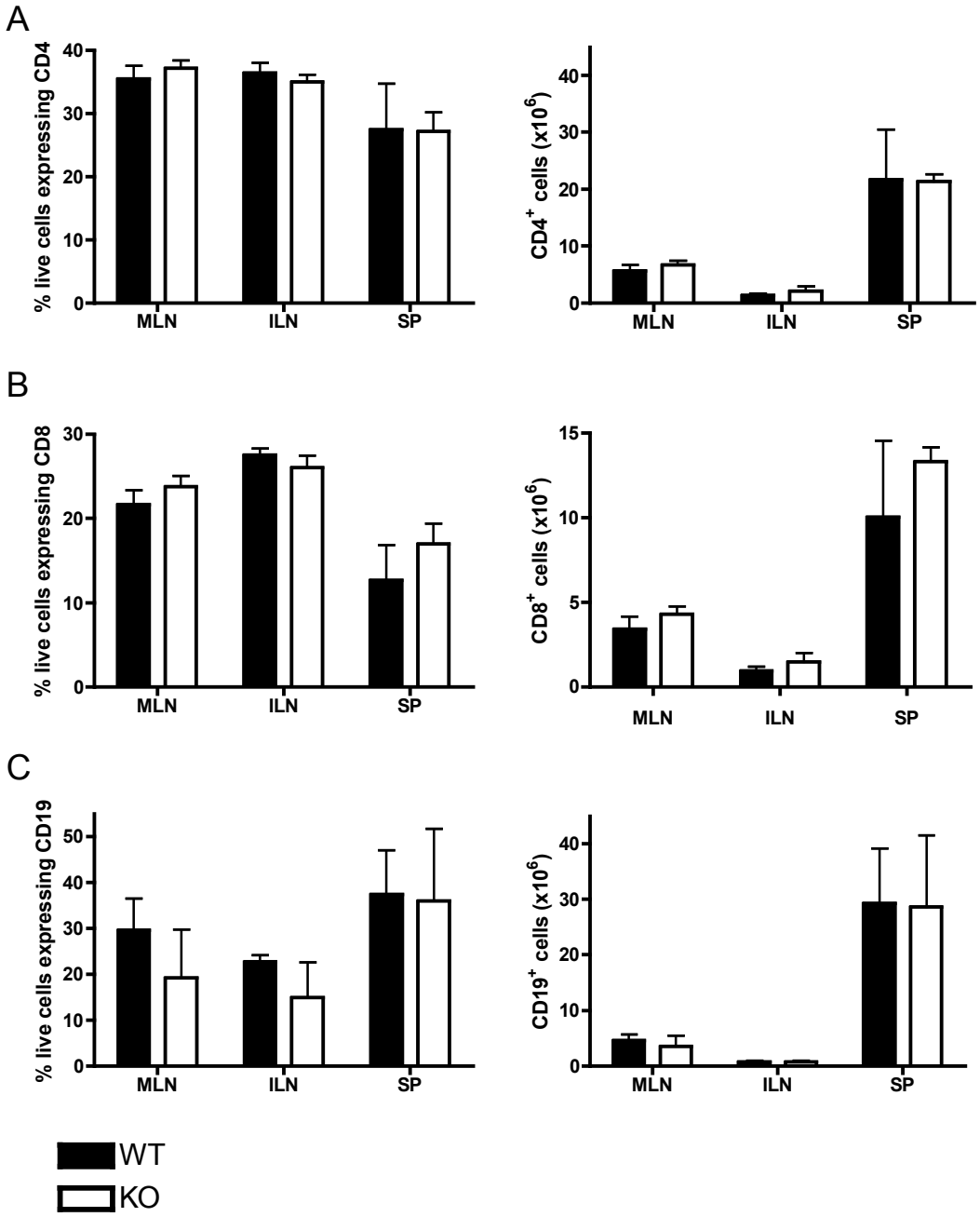

Figure 3.3
Lymphocyte Composition of CCX-CKR KO and WT Secondary Lymphoid Organs
Cells were isolated from the MLN, ILN and spleens of CCX-CKR KO and WT mice and analysed for cell surface expression of CD4 (A), CD8 (B) and CD19 (C) by flow cytometry. Left hand graphs show the proportions of each cell type within live cell gates, while right hand graphs show absolute cell numbers. Results show means +1 SD of 3 mice per group.

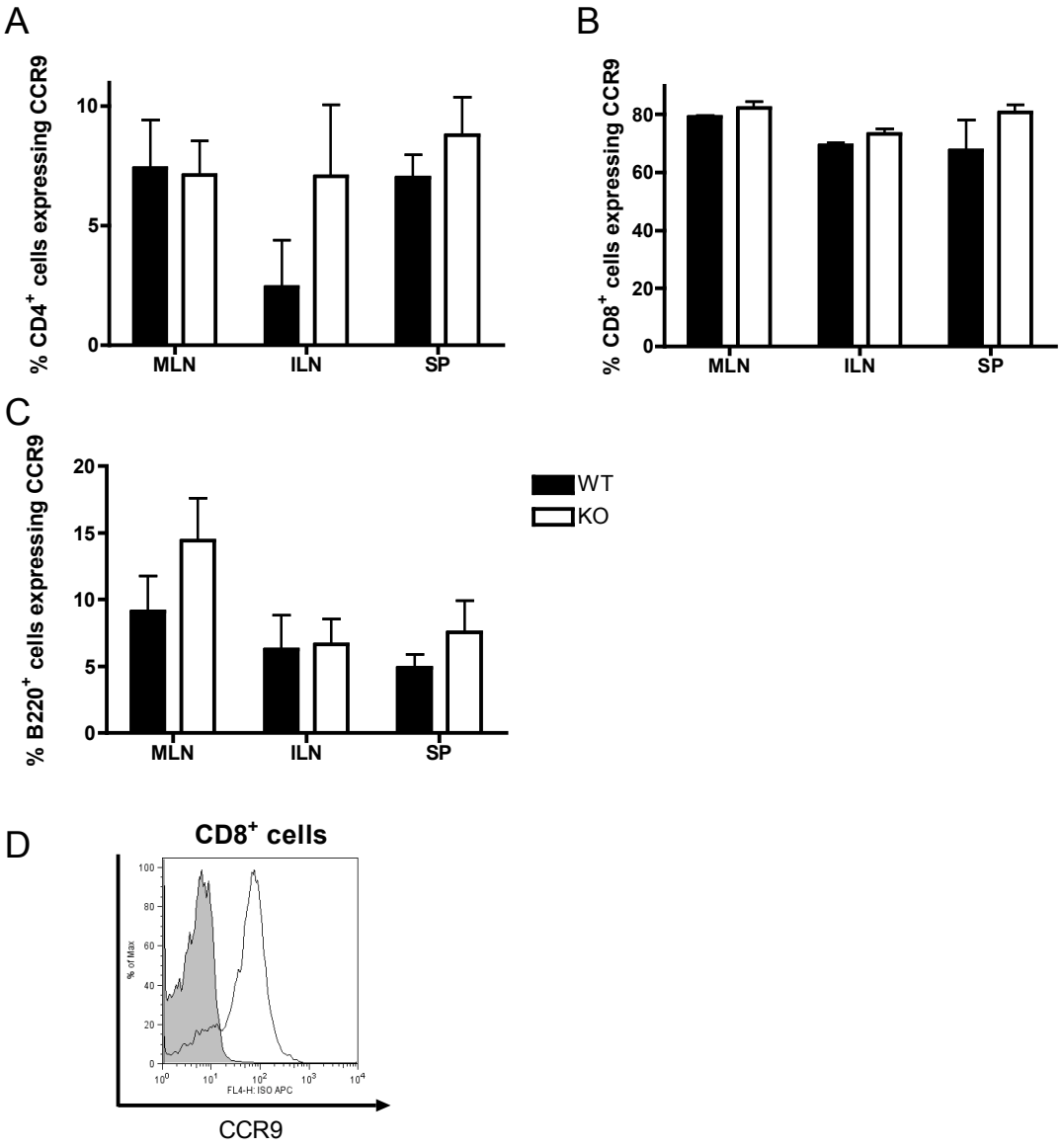

Figure 3.4
Expression of CCR9 by CCX-CKR KO and WT Lymphocytes
Cells isolated from MLN, ILN and spleens of WT and CCX-CKR KO mice were analysed for surface expression of CCR9 on $CD4^+$ (A) $CD8^+$ (B) and $B220^+$ (C) cells. Results show the mean proportion of each subset expressing CCR9 +1 SD of 3 mice per group. (D) Representative histograms show CCR9 isotype (shaded) and CCR9 specific staining of $CD8^+$ T cells from WT MLN.

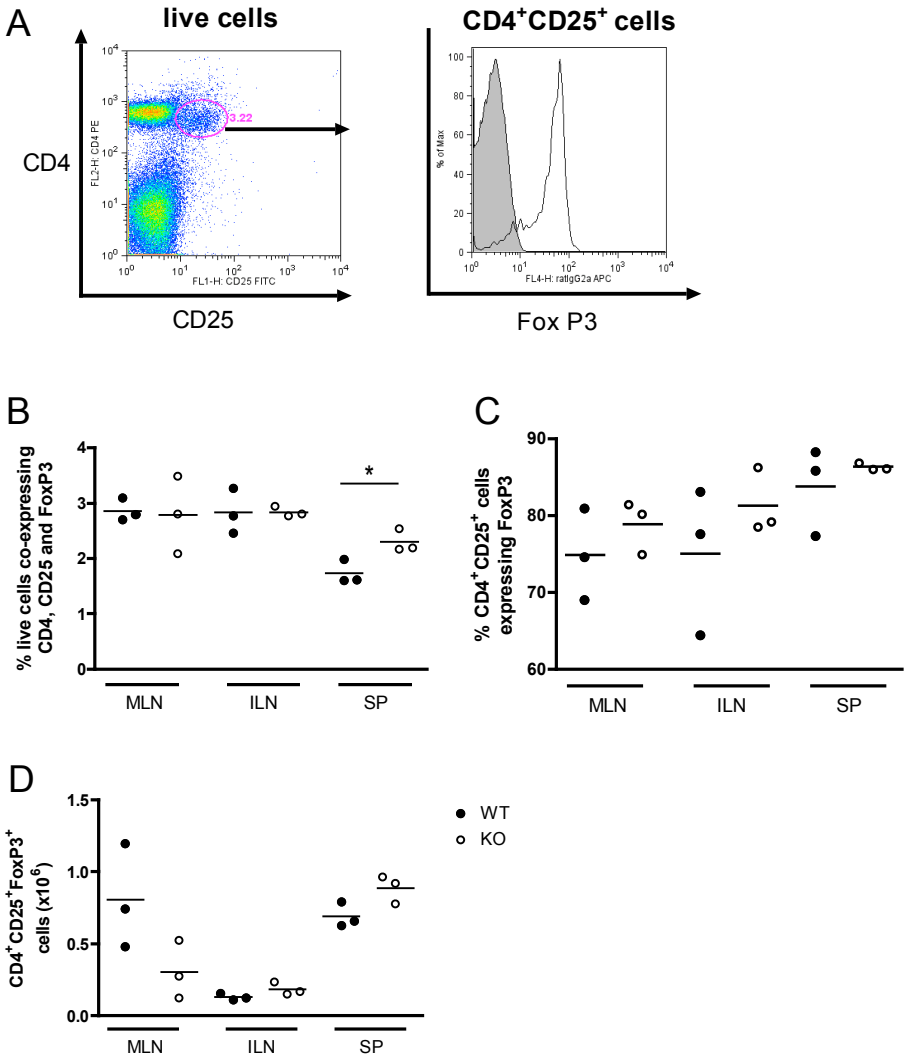

Figure 3.5
FoxP3$^+$ Regulatory T Cells in the Secondary Lymphoid Organs of CCX-CKR KO and WT mice
Intacellular expression of FoxP3 by CD4$^+$CD25$^+$ T cells from the MLN, ILN and spleens of CCX-CKR KO and WT mice was determined by flow cytometry. (A) A representative FACS plot (left) shows the gated CD4$^+$CD25$^+$ population within total live WT MLN cells while the histogram (right) shows FoxP3 isotype (shaded) and FoxP3 specific staining of CD4$^+$CD25$^+$ cells from WT MLN. (B) The proportions of live cells co-expressing CD4, CD25 and FoxP3 and of (C) CD4$^+$CD25$^+$ cells expressing FoxP3 along with (D) their absolute numbers are shown. Results show the means of 3 mice per group.

*p<0.05 Unpaired t test

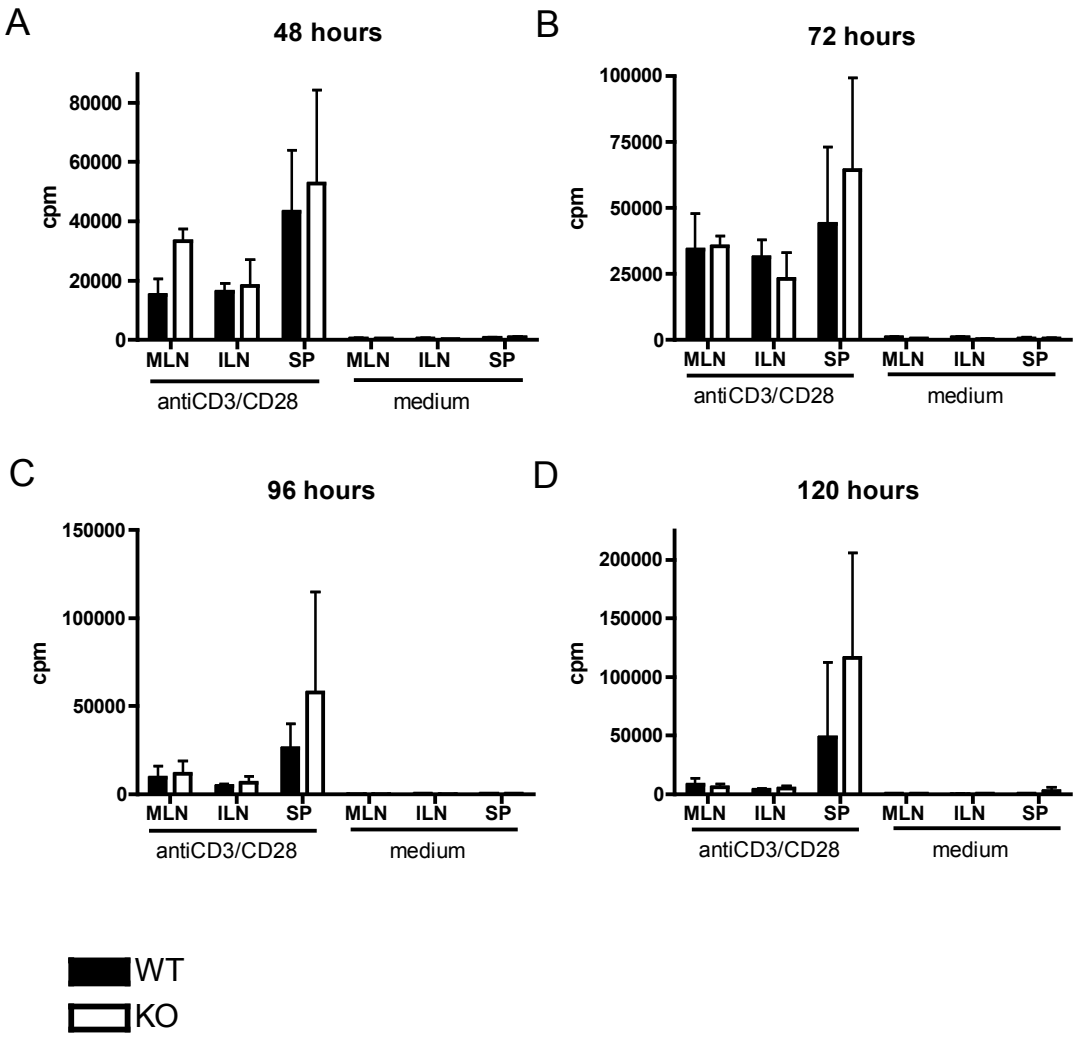

Figure 3.6
Proliferative Responses of CCX-CKR KO and WT T Cells to anti-CD3/CD28 Antibodies *In Vitro*
Cells were isolated from MLN, ILN and spleens of CCX-CKR KO and WT mice and cultured either in medium alone, or with anti-CD3 and anti-CD28 antibodies for 48 (A) 72 (B) 96 (C) and 120 hours (D). Proliferation was assessed by ^{3}H-TdR incorporation and results represent the mean cpm + 1 SD of 3 mice per group.

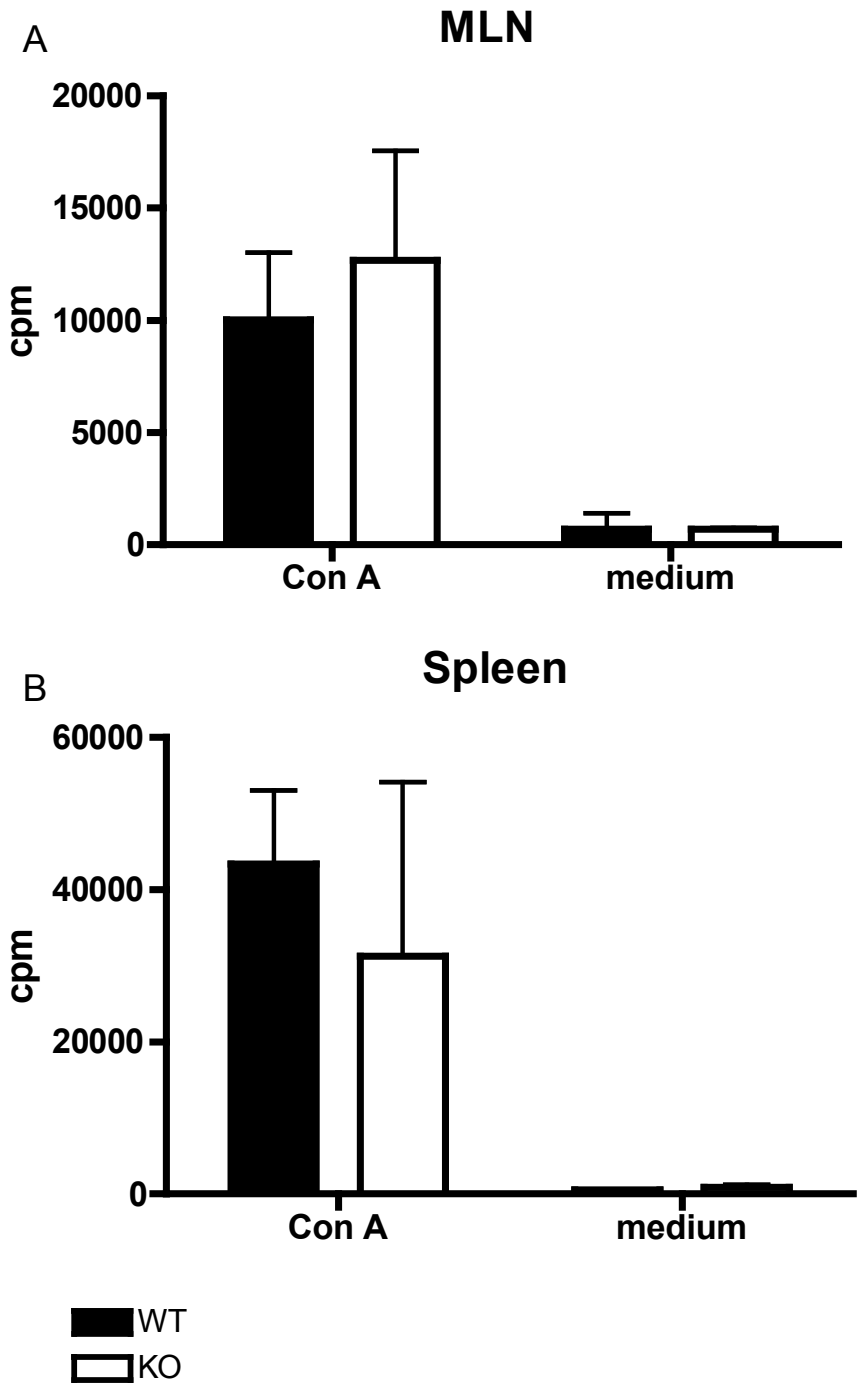

Figure 3.7
Proliferative Responses of Lymphocytes from CCX-CKR KO and WT Mice to Con A *In Vitro*
Cells were isolated from the MLN (A) and spleens (B) of CCX-CKR KO and WT mice and cultured either in complete medium alone or with 5μg/ml Con A for 72 hours. Proliferation was assessed by ^{3}H-TdR incorporation and results represent the mean cpm +1 SD of 3 mice per group.

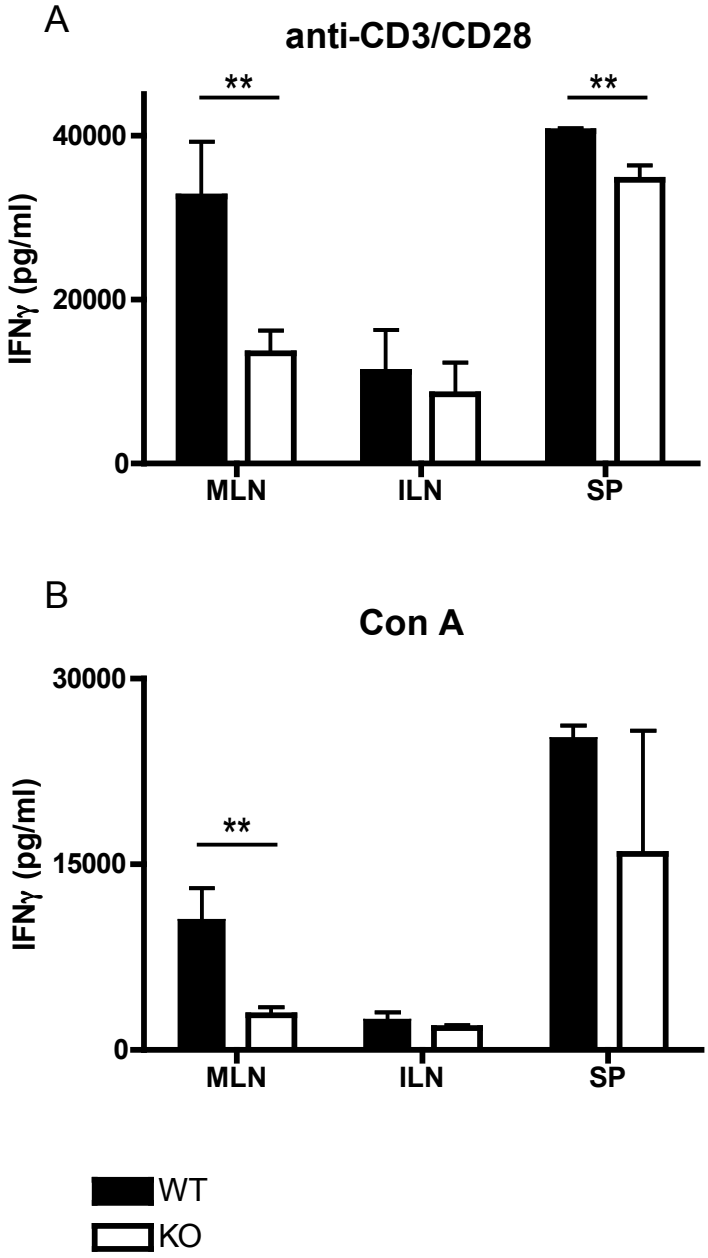

Figure 3.8
IFNγ Production by CCX-CKR KO and WT Lymphocytes *In Vitro*
Cells were isolated from the MLN, ILN and spleens of CCX-CKR KO and WT mice and cultured either in medium alone or with (A) 1μg/ml antiCD3/CD28 or (B) 5μg/ml ConA for 48 hours. Cytokine production was assessed by ELISA and results show the mean IFNγ production in pg/ml +1 SD of 3 mice per group.

**p<0.01 Unpaired t test

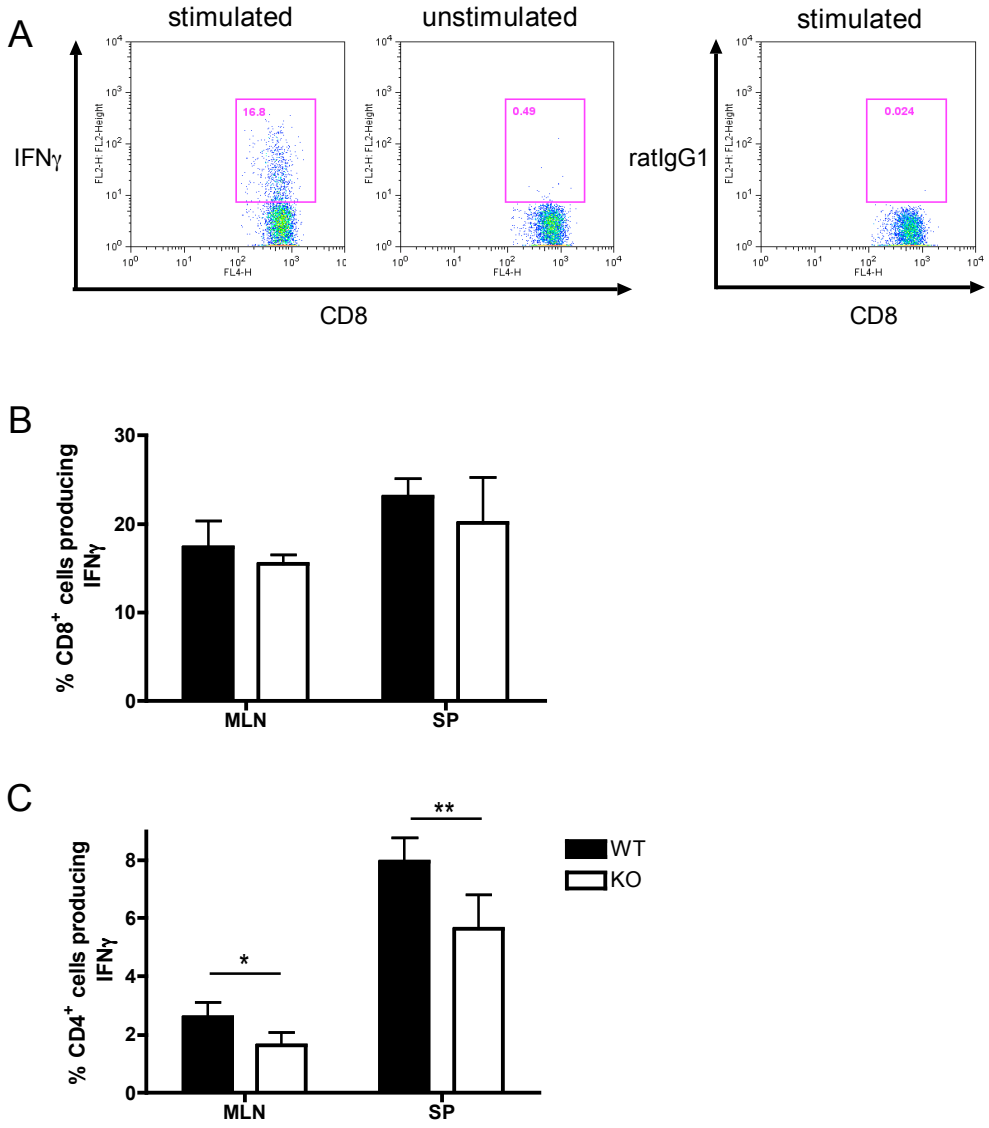

Figure 3.9
Intracellular Cytokine Analysis of IFNγ Production by CCX-CKR KO and WT T Cells *In Vitro*
Cells were isolated from the MLN and spleens of CCX-CKR KO and WT mice and cultured for 4 hours in complete medium with 0.1μM PMA+1mM ionomycin+10mg/ml Brefeldin A+1μM monesin. Cells were then stained for surface expression of CD4 and CD8, fixed and permeabilised to detect intracellular IFNγ. (A) Representative FACS plots of WT MLN $CD8^+$ T cells show IFNγ specific staining of stimulated cells (left) unstimulated cells (middle) and isotype staining of stimulated cells (right). Results show the mean proportions of live $CD8^+$ (B) and $CD4^+$ (C) T cells expressing IFNγ +1 SD of 5 mice per group.

*p<0.05 **p<0.01 Unpaired t test

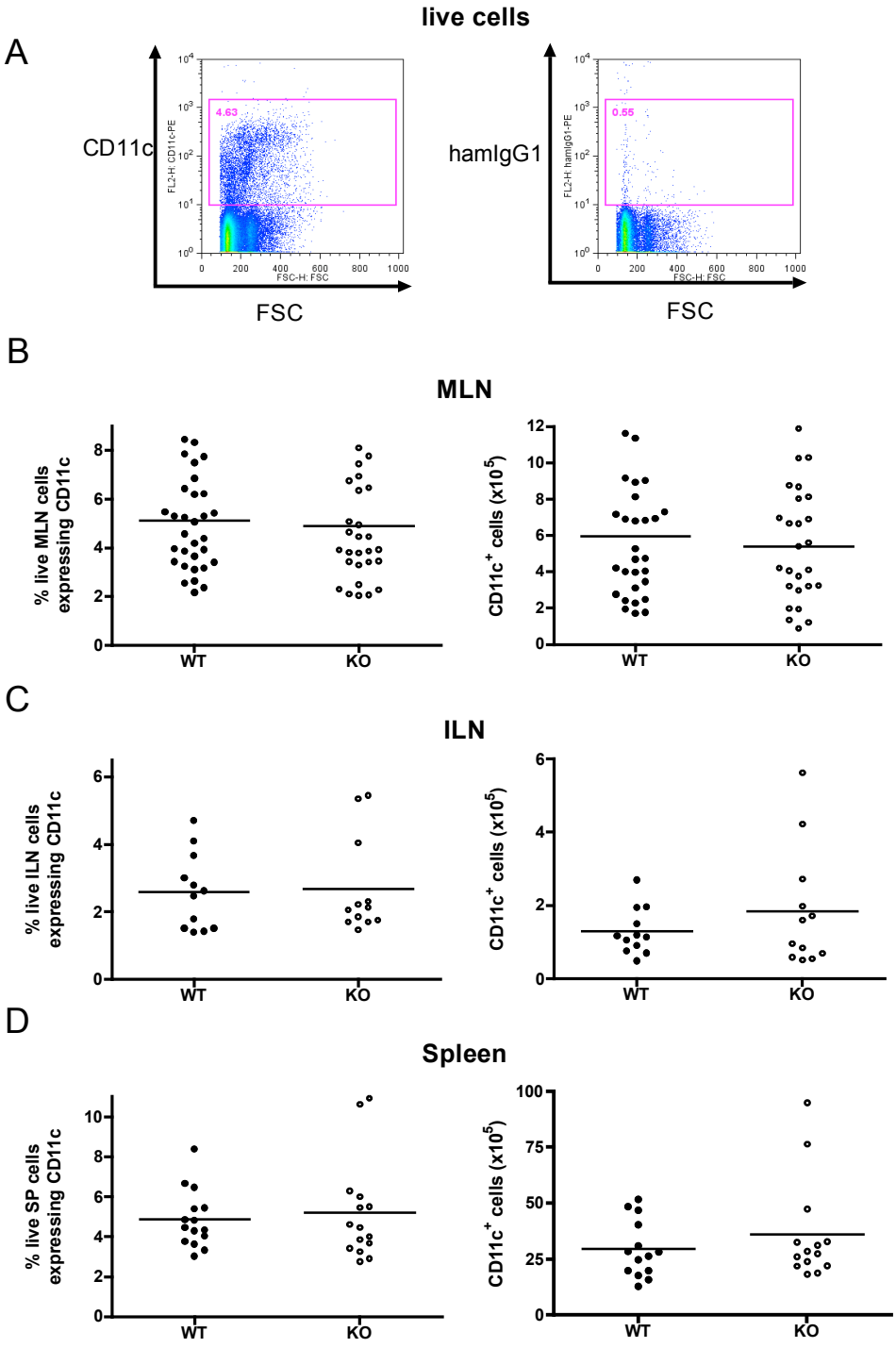

Figure 3.10
CD11c$^+$ Cells in the Secondary Lymphoid Organs of CCX-CKR KO and WT Mice
MLN, ILN and spleens from CCX-CKR KO and WT mice were digested with 1mg/ml collagenase D and 30μg/ml DNase I and cells analysed for surface expression of CD11c by flow cytometry. (A) Representative FACS plots of CD11c specific (left) and isotype staining (right) of WT MLN cells show the CD11c$^+$ cell population. (B), (C) and (D) show the proportions (left) and numbers (right) of live cells expressing CD11c in MLN, ILN and spleens respectively. Results show the mean cell numbers and proportions of 12-32 mice per group and are pooled from 8 individual experiments.

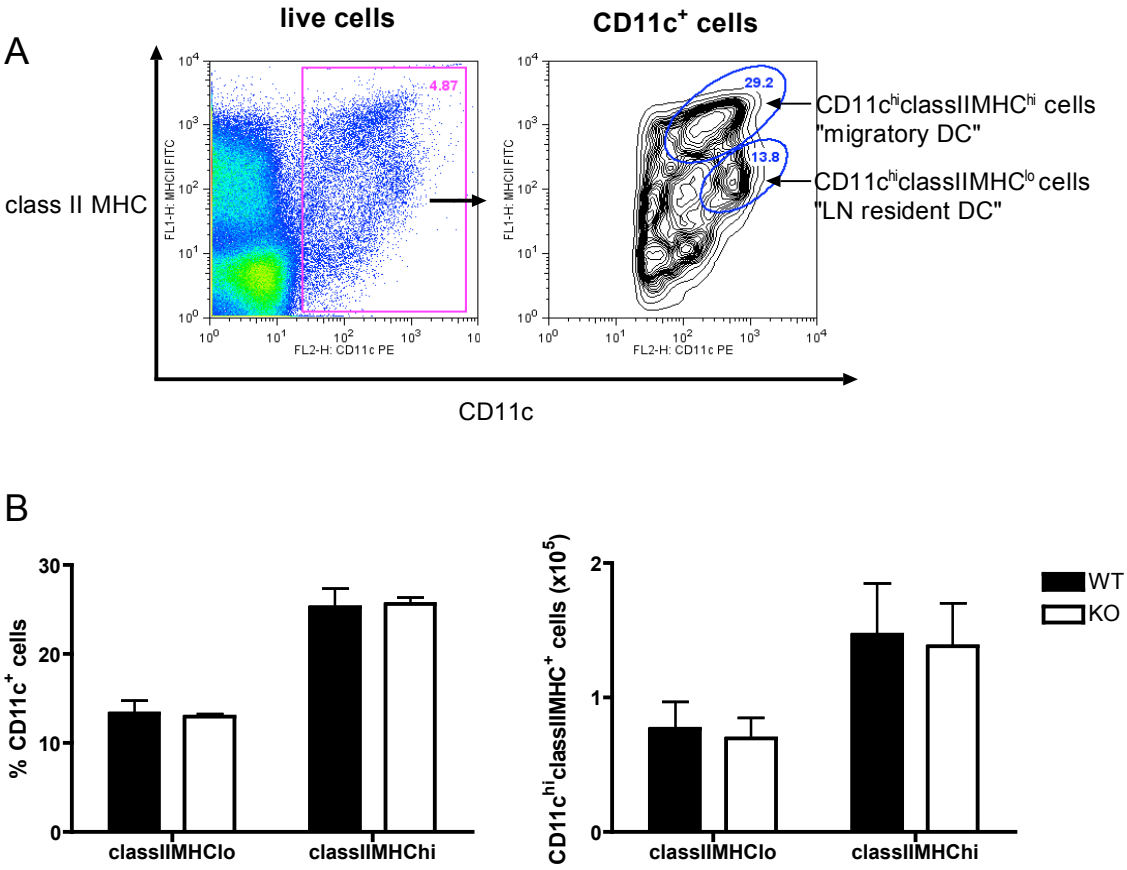

Figure 3.11
Migratory and Resident DC in the MLN of CCX-CKR KO and WT Mice
Cells were isolated from the MLN of CCX-CKR KO and WT mice and analysed for surface expression of CD11c and class II MHC by flow cytometry. (A) Representative FACS plots show $CD11c^{+}$ cells amongst live WT MLN cells (left), sub-divided into $CD11c^{hi}$class II MHC^{hi} "migratory DC" and $CD11c^{hi}$class II MHC^{lo} "LN resident DC" subsets (right). (B) The proportions (left) and absolute numbers (right) of each $CD11c^{hi}$ cell subset were determined. Results show the means +1 SD of 3 mice per group.

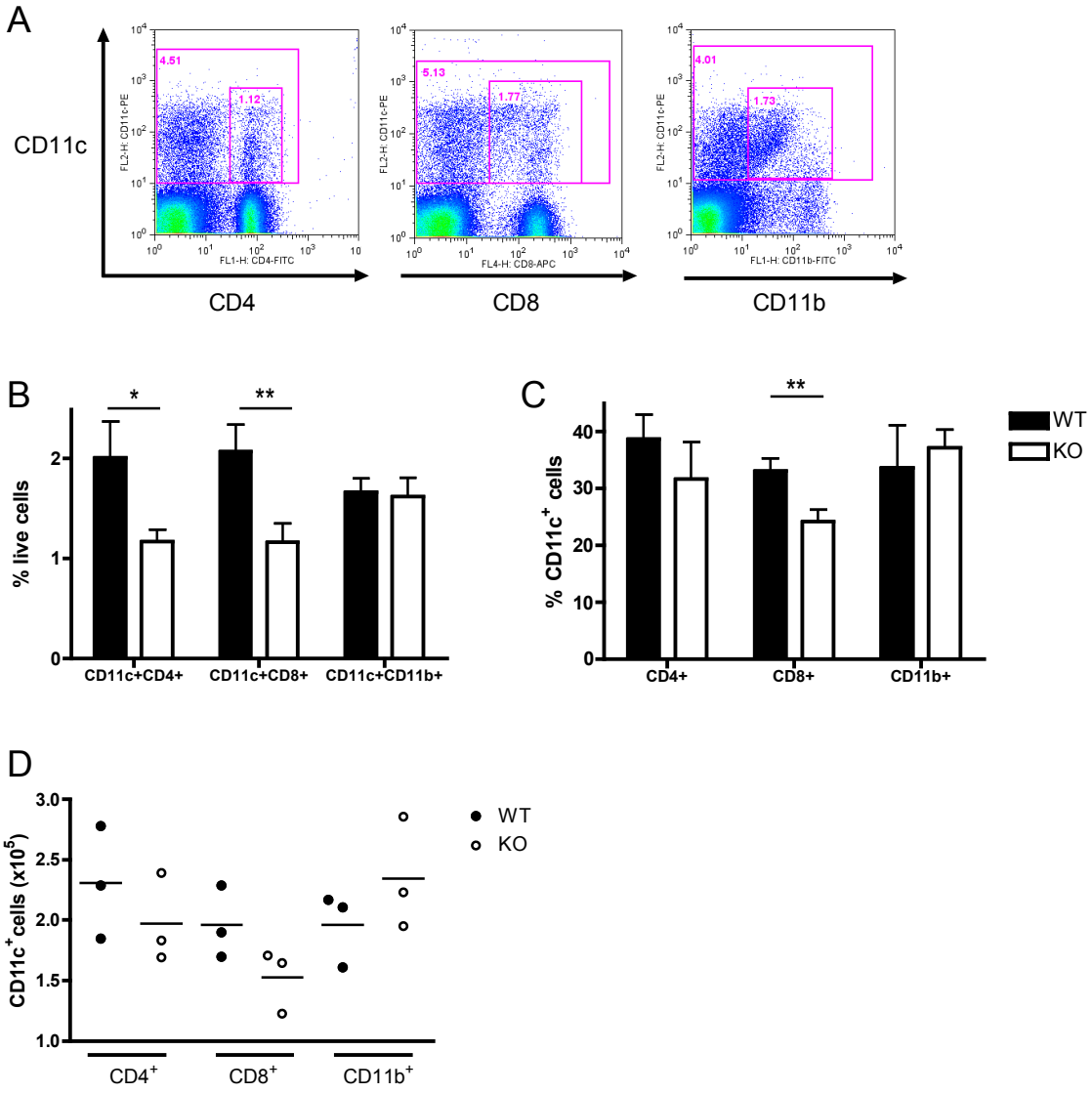

Figure 3.12
DC Subsets in the MLN of CCX-CKR KO and WT Mice
Cells were isolated from the MLN of CCX-CKR KO and WT mice and analysed for surface expression of CD11c and CD4, CD8 or CD11b by flow cytometry. (A) Representative FACS plots of WT MLN cells show the proportions of live cells expressing CD11c in the large gates and of those co-expressing CD11c and CD4 (left), CD8 (middle) or CD11b in smaller gates. The proportions of live cells co-expressing CD11c and CD4, CD8 or CD11b are shown in (B).The proportions of $CD11c^+$ cells expressing CD4, CD8 and CD11b are shown in (C) and the absolute numbers of cells within each $CD11c^+$ cell subset in (D). Results show the means +1 SD of 3 mice per group.

*p<0.05 **p<0.01 Unpaired t test

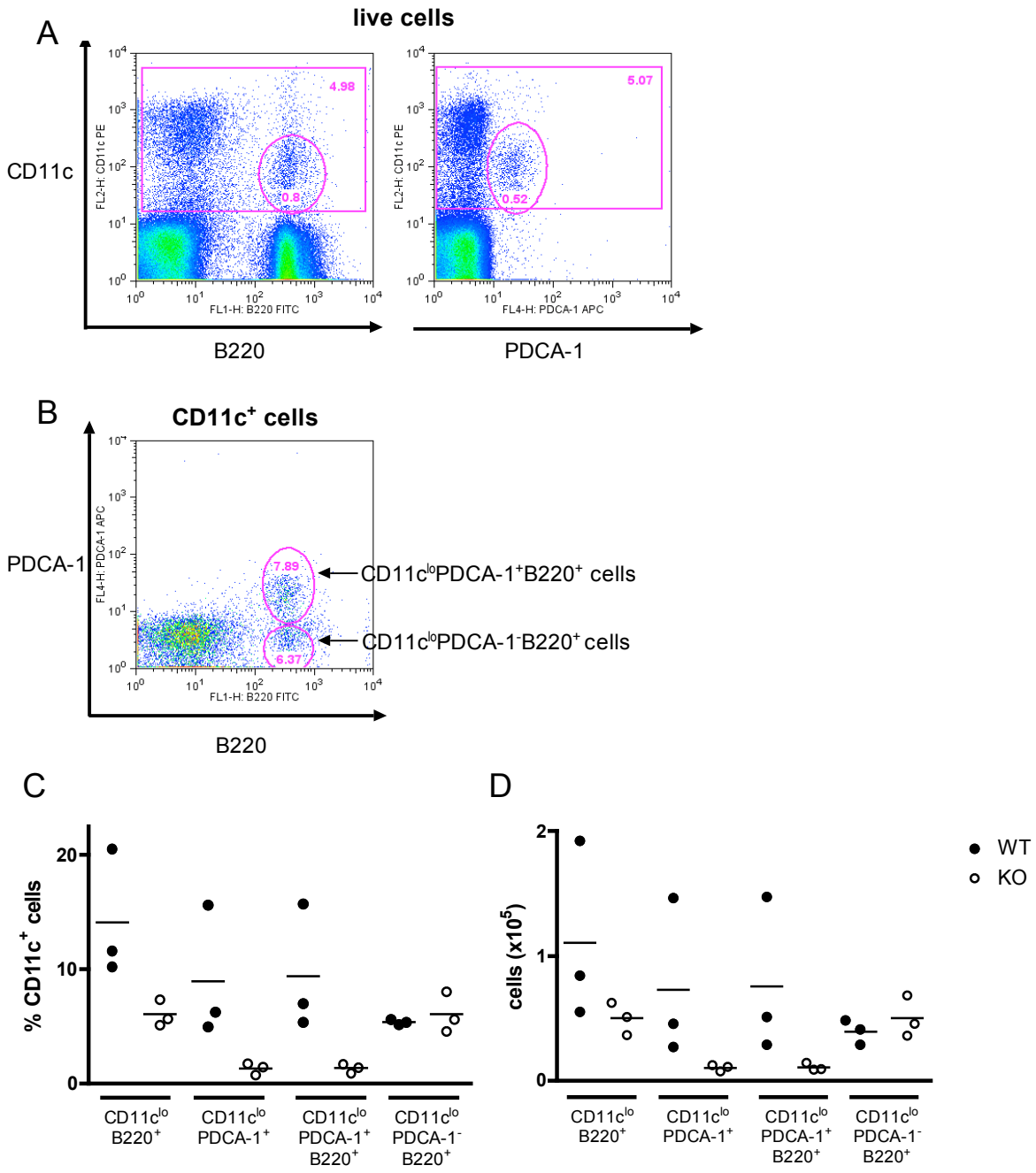

Figure 3.13
pDC in CCX-CKR KO and WT Mice
Cells isolated from the MLN of WT and CCX-CKR KO mice were analysed for surface expression of CD11c, B220 and PDCA-1 by flow cytometry. (A) Representative FACS plots of live WT MLN cells show the proportion of total live cells expressing CD11c in the large rectangular gates and $CD11c^{lo}B220^{+}$ (left) or $CD11c^{lo}PDCA\text{-}1^{+}$ (right) populations in smaller oval gates. (B) A representative FACS plot of live WT MLN $CD11c^{+}$ cells shows the proportions of $CD11c^{+}$ cells in $CD11c^{lo}B220^{+}PDCA\text{-}1^{+}$ and $CD11c^{lo}B220^{+}PDCA\text{-}1^{-}$ populations. (C) and (D) show the mean proportions and absolute numbers of $CD11c^{+}$ cells in $CD11c^{lo}B220^{+}$, $CD11c^{lo}PDCA\text{-}1^{+}$, $CD11c^{lo}B220^{+}PDCA\text{-}1^{+}$ and $CD11c^{lo}B220^{+}PDCA\text{-}1^{-}$ cell subsets. Results show the means of 3 mice per group.

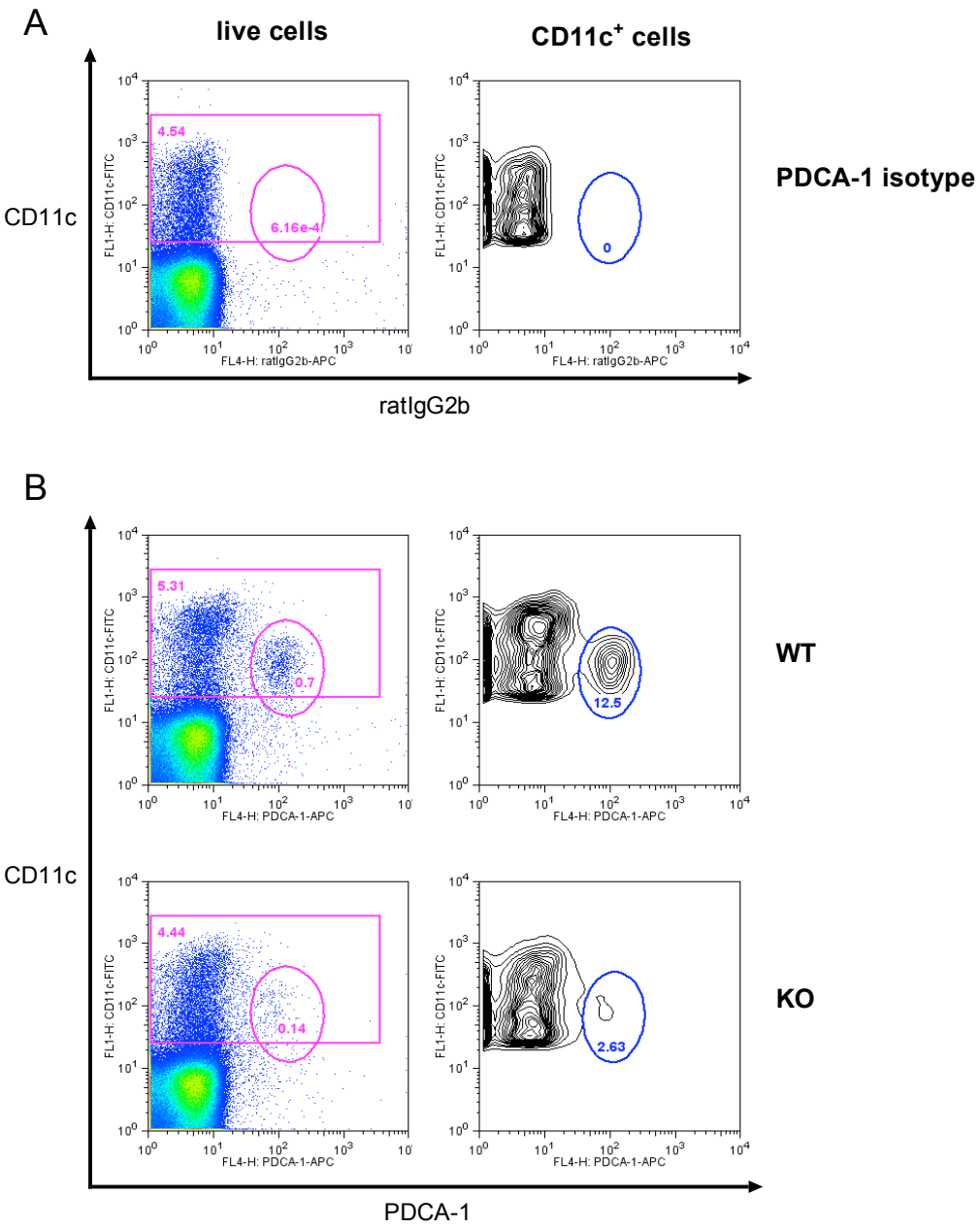

Figure 3.14
CD11c^{lo}PDCA-1^{+} pDC in the MLN of CCX-CKR KO and WT Mice
Cells isolated from the MLN of CCX-CKR KO and WT mice were analysed for cell surface expression of CD11c and PDCA-1 by flow cytometry to identify pDC. Representative FACS plots show the proportion of total live cells expressing CD11c in large rectangular gates and the CD11c^{lo}PDCA-1^{+} cell population in small oval gates (left). Contour plots are shown to more clearly define the CD11c^{lo}PDCA-1^{+} cell population in small oval gates (right). (A) CD11c specific staining and isotype staining for PDCA-1. (B) CD11c and PDCA-1 specific staining for WT and CCX-CKR KO cells.

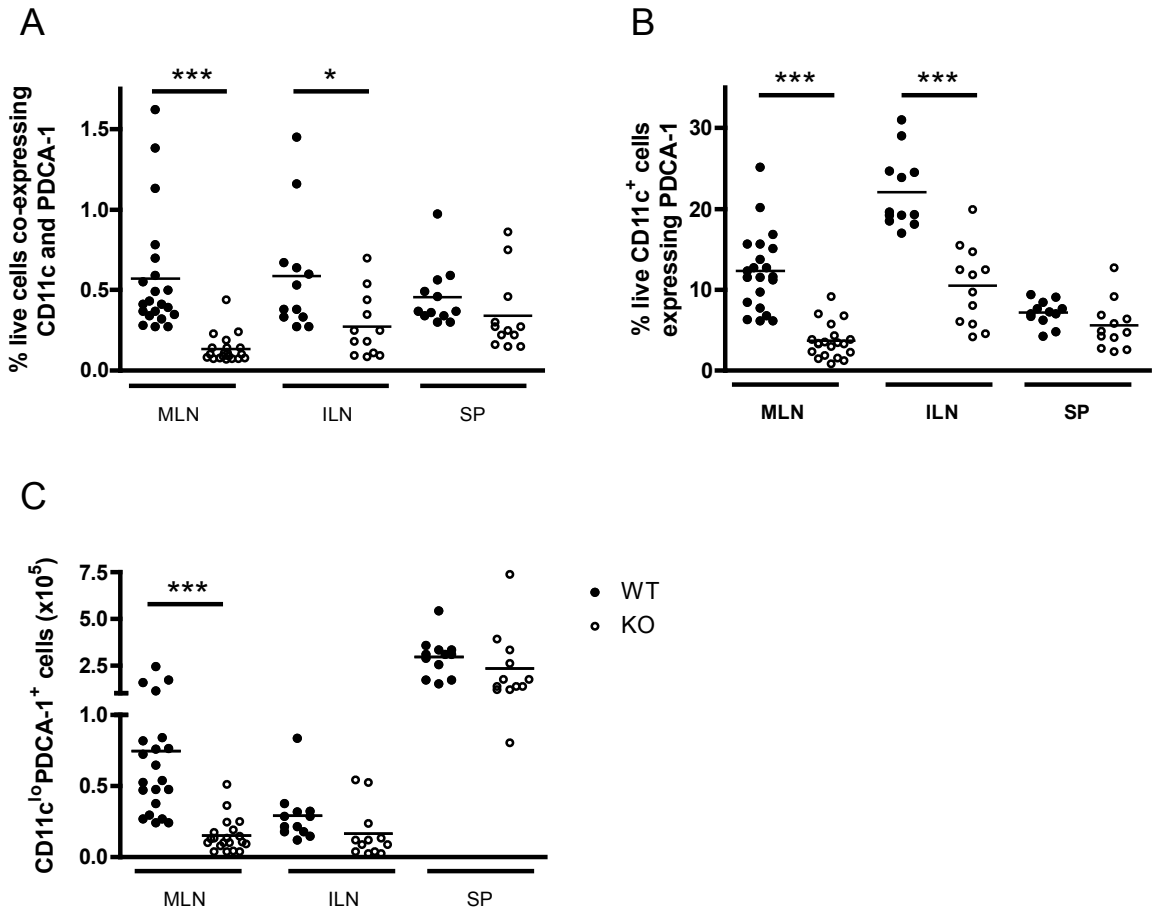

Figure 3.15
pDC in the Secondary Lymphoid Organs of CCX-CKR KO and WT Mice
Cells from the MLN, ILN and spleens of CCX-CKR KO and WT mice were analysed for cell surface expression of CD11c and PDCA-1. pDC were identified as $CD11c^{lo}PDCA\text{-}1^{+}$ cells. Results show the mean proportions of pDC amongst total live MLN cells (A) and $CD11c^{+}$ cells (B) and the absolute numbers of pDC (C) for 12-21 mice per group, pooled from 7 individual experiments.

***p<0.001 *p<0.05 Mann-Whitney test

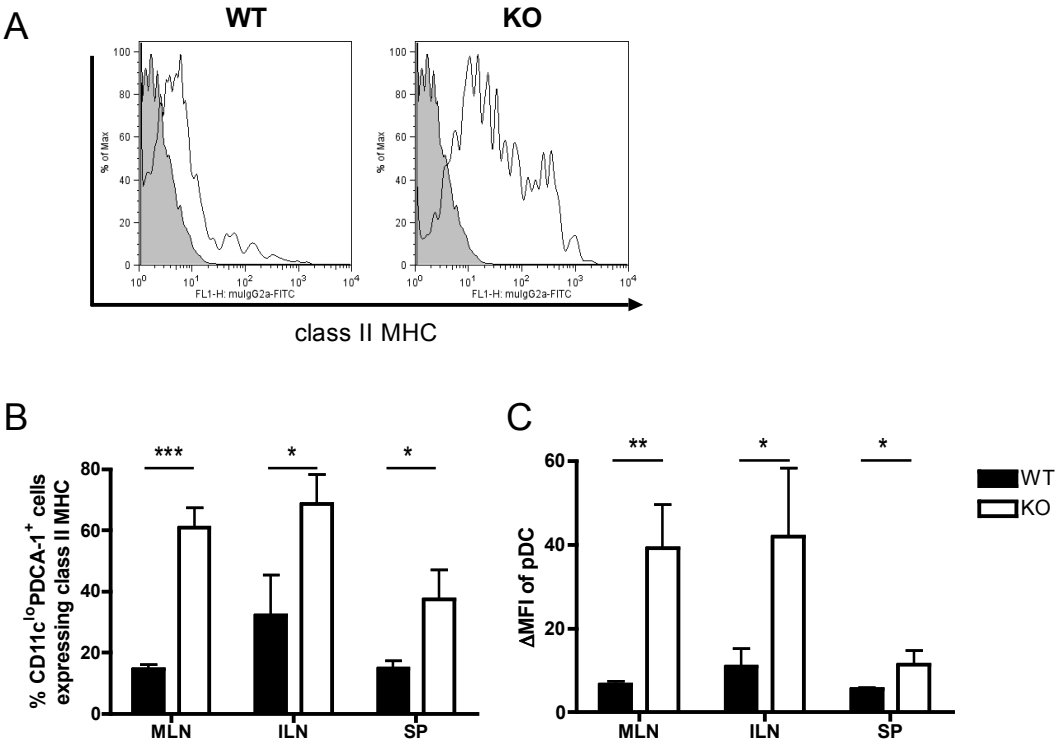

Figure 3.16
Class II MHC Expression on pDC in Secondary Lymphoid Organs of CCX-CKR KO and WT Mice
Cells isolated from the MLN, ILN and spleens of CCX-CKR KO and WT mice were analysed for surface expression of CD11c, PDCA-1 and class II MHC. (A) Representative histograms show class II MHC isotype (shaded) and specific staining of $CD11c^{lo}PDCA\text{-}1^{+}$ cells from CCX-CKR KO and WT mice. The proportions of $CD11c^{lo}PDCA\text{-}1^{+}$ pDC expressing class II MHC (B) and the levels of class II MHC expression on pDC as determined by ΔMFI (C) are shown. Results show means +1 SD of 3 mice per group.

***p<0.001 **p<0.01 *p<0.05 Unpaired t test

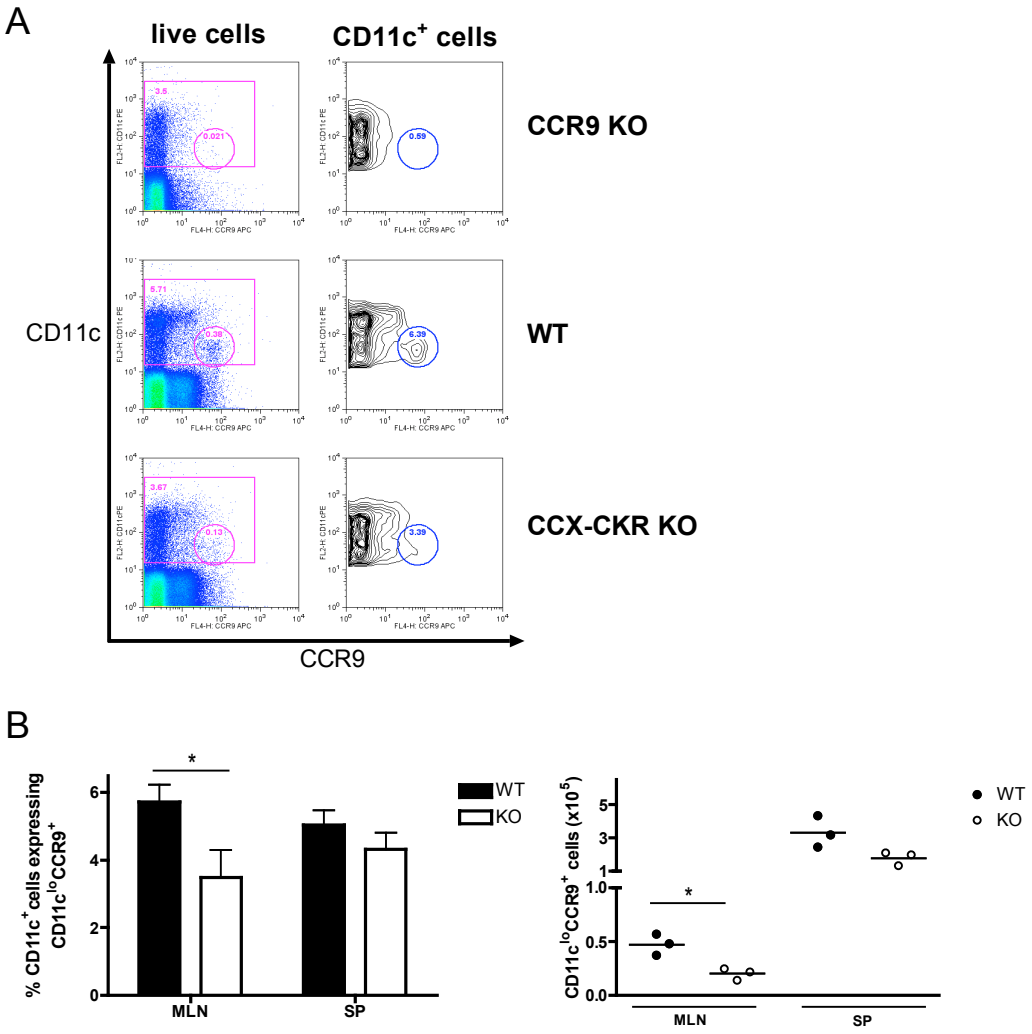

Figure 3.17
CCR9 expression on CD11c^{lo} Cells in CCX-CKR KO and WT Mice
Cells isolated from the MLN and spleens of CCX-CKR KO and WT mice were analysed for surface expression of CD11c and CCR9. (A) Representative FACS plots show live MLN cells from WT, CCX-CKR KO and CCR9 KO mice. The proportions of total live cells expressing CD11c are shown in the large rectangular gates and the proportions of total live cells (left) or CD11c^{+} cells (right) within the CD11c^{lo}CCR9^{+} cell population are shown in the smaller oval gates.(B) Proportions and absolute numbers of CD11c^{lo}CCR9^{+} cells in the MLN and spleens of CCX-CKR KO and WT mice are shown. Results show the means +1SD of 3 mice per group.

*p<0.05 Unpaired t test

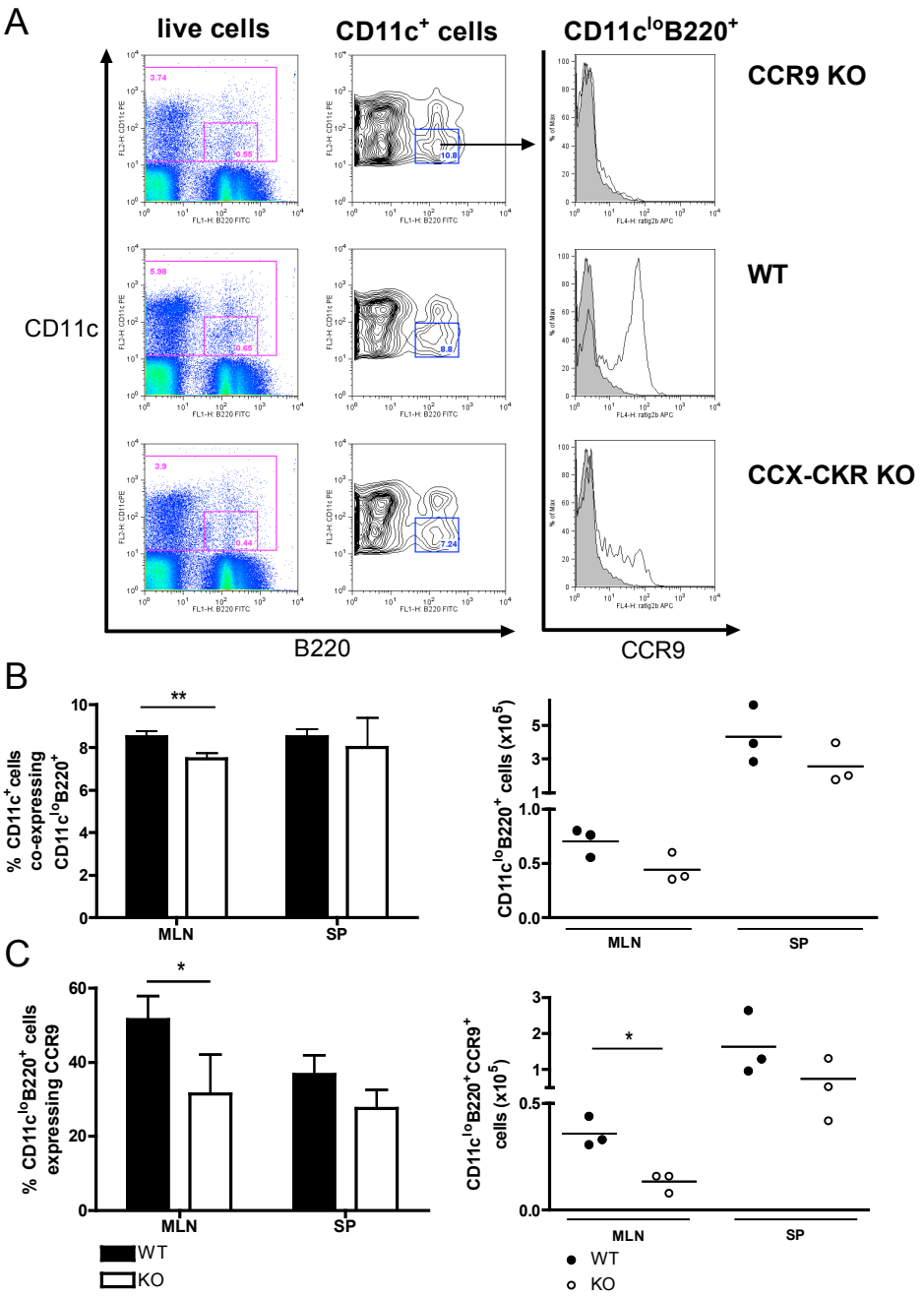

Figure 3.18

CCR9 expression on CD11c^{lo}B220^{+} Cells in CCX-CKR KO and WT Mice

Cells isolated from the MLN and spleens of CCX-CKR KO and WT mice were analysed for surface expression of CD11c, B220 and CCR9. Specifically, a CD11c^{lo}B220^{+} cell subset was identified and their CCR9 expression determined. (A) Representative FACS plots show live MLN cells from WT, CCX-CKR KO and CCR9 KO mice. The proportions of total live cells expressing CD11c are shown in large rectangular gates (left). The proportions of CD11c^{lo}B220^{+} cells amongst total live cells (left) and CD11c^{+} cells (middle) are shown in smaller oval gates. Histograms show the proportion of CD11c^{lo}B220^{+} cells expressing CCR9 (right). (B) The proportions and absolute numbers of CD11c^{+} cells that are CD11c^{lo}B220^{+} in the MLN and spleens of CCX-CKR KO and WT mice are shown as well as (C) the proportions and absolute numbers of CD11c^{lo}B220^{+} cells expressing CCR9.

**p<0.01 *p<0.05 Unpaired t test

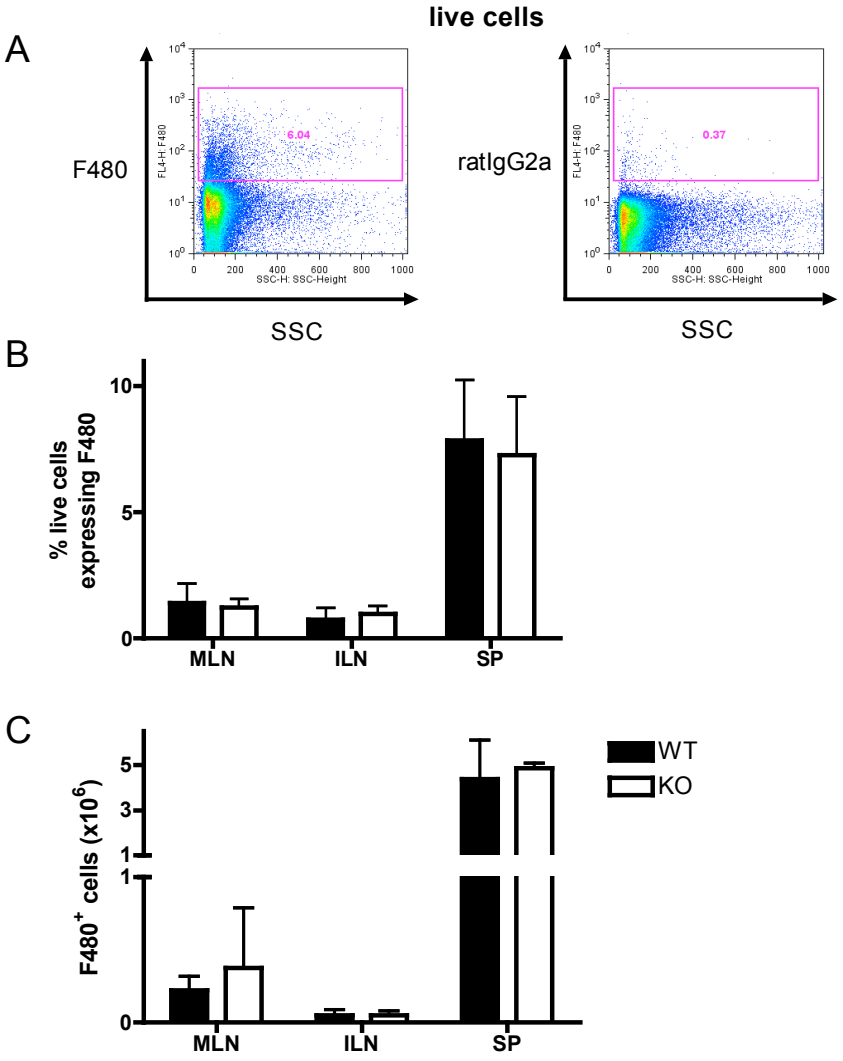

Figure 3.19
Macrophages in the Secondary Lymphoid Organs of CCX-CKR KO and WT Mice
MLN, ILN and spleens from CCX-CKR KO and WT mice were digested with 1mg/ml collagenase D and 30μg/ml DNase I and cells analysed for surface expression of F480 by flow cytometry.(A) Representative FACS plots of F480 specific (left) and isotype staining (right) of WT spleen cells show the $F480^+$ cell population. The proportions (B) and absolute numbers (C) of $F480^+$ cells isolated from MLN, ILN and spleens are shown. Results show means +1 SD of 3 mice per group.

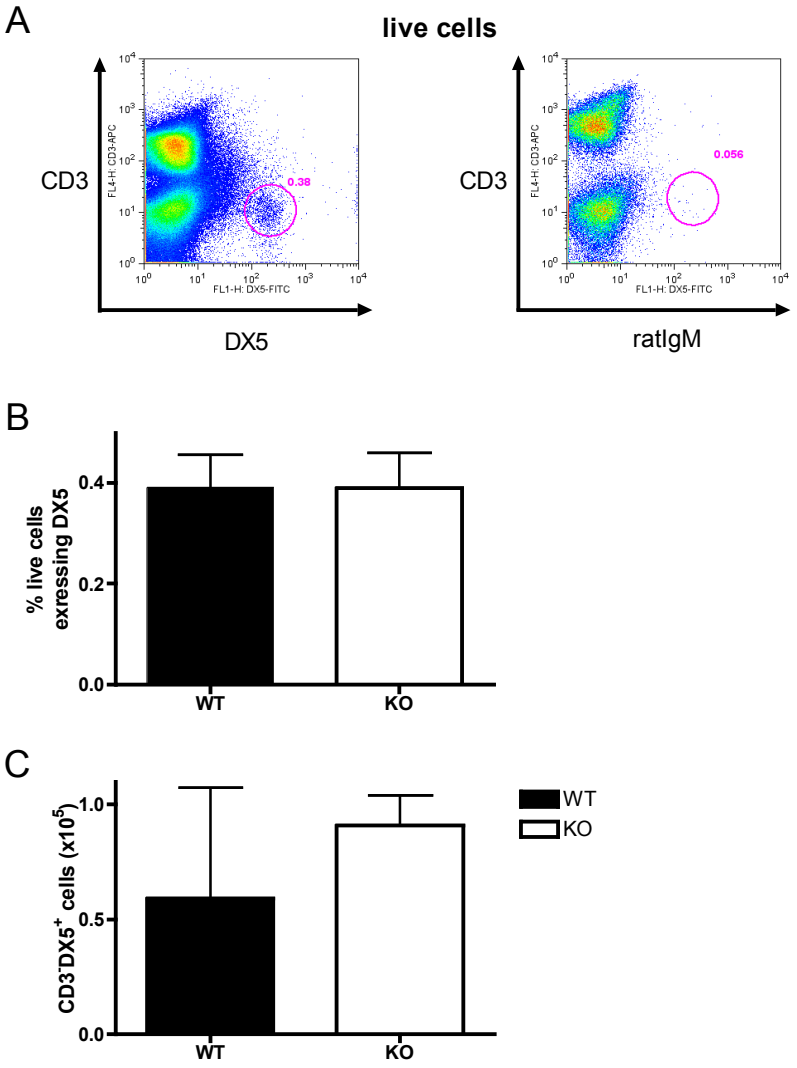

Figure 3.20
NK cells in the MLN of CCX-CKR KO and WT Mice
MLN from CCX-CKR KO and WT mice were digested with 1mg/ml collagenase and 30μg/ml DNase I and cells analysed for surface expression of CD3 and DX5 by flow cytometry. (A) Representative FACS plots of DX5 specific (left) and isotype staining (right) of WT MLN cells show the $CD3^{-}DX5^{+}$ cell population. The proportions (B) and absolute numbers (C) of $CD3^{-}DX5^{+}$ cell isolated from MLN are shown. Results show means +1 SD of 3 mice per group.

Chapter 4

Characterisation of the Small Intestinal Immune Compartment of CCX-CKR KO Mice

Introduction

In the previous chapter I described the effects of CCX-CKR deletion on the composition of lymphocyte and DC subsets in secondary lymphoid organs where the CCX-CKR ligands, CCL19 and CCL21 are abundant. In this chapter I have turned my attention to the small intestine where the other ligand for CCX-CKR, CCL25, is expressed constitutively by small intestinal epithelial cells and plays an important role in recruiting effector T cells to the small intestine (82, 133). CCR9, the receptor for CCL25 is induced on effector lymphocytes during priming by $CD103^+$ DC within the MLN and PP and is important for their gut tropism. CCL19 and CCL21 are also critical for cell positioning and immune responses in the intestine, as their receptor, CCR7 controls the migration of $CD103^+$ DC from the mucosa to MLN. This is required for the effective induction of tolerance and immunity to oral antigens (125, 133). Therefore here, I carried out initial investigations into the composition of the small intestinal immune compartment in CCX-CKR KO mice, examining lymphocytes and DC populations in the mucosa, MLN and PP.

4.1 Small intestinal lamina propria cellularity of CCX-CKR KO mice

The small intestine hosts a multitude of CCR9 expressing cells including effector T cells, pDC and plasma cells. Therefore, I first explored the leukocyte composition of the small intestinal lamina propria of CCX-CKR KO mice. Histological examinations of the small intestine revealed no obvious abnormalities in its architecture in CCX-CKR KO mice (Fig 4.1). Leukocytes were present in normal numbers in the villus and lamina propria and IEL were present in their normal position on the basement membrane. The numbers of IEL, however, were significantly decreased in CCX-CKR KO mice compared with WT mice (Fig 4.2).

The total numbers of live leukocytes identified by their expression of CD45 and lack of 7-AAD uptake in preparations obtained by collagenase and DNase digestion of small intestinal mucosa were comparable in CCX-CKR KO and WT mice (Figs 4.3A and B). Leukocyte populations were further analysed for the presence of T cells, B cells and DC (Fig 4.3A) and revealed no differences between CCX-CKR KO and WT mice in the proportions or absolute numbers of $CD3^+$, $CD4^+$ and $CD8^+$ T cells. However, the proportions of $CD11c^+$ and $CD19^+$ cells were significantly increased and decreased respectively in CCX-CKR KO lamina propria compared with WT mice. Although a similar trend was observed in the absolute numbers of these cells, this was not statistically significant (Figs 4.3C and D).

Having previously observed a significant reduction of $CD11c^{lo}PDCA\text{-}1^{+}$ pDC in the MLN of CCX-CKR KO mice, I next went on to determine whether CCX-CKR deletion affected the proportion of $CD11c^{+}$ cell subsets in the lamina propria, in particular that of pDC. Unfortunately, the small numbers of $CD11c^{+}$ cells obtained from resting mice made identification of individual DC subsets unreliable and I was unable to assess the numbers of $CD11b^{+}$ and $CD8\alpha^{+}$ DC. Attempts to identify a $CD11c^{lo}PDCA\text{-}1^{+}$ population of pDC were also inconclusive, although I was able to identify the $CD11c^{lo}B220^{+}$ cell population that should contain pDC (Fig 4.4A). No significant differences were seen in the proportions or absolute numbers of $CD11c^{lo}B220^{+}$ cells between CCX-CKR KO and WT mice, with approximately 7-15% of CD11c expressing cells comprising this DC subset in both cases (Figs 4.4B and C).

I was also able to determine the proportions and absolute numbers of the CD103 expressing DC which make up a substantial proportion of lamina propria DC (Fig 4.5A). There were no differences in the absolute numbers of $CD11c^{+}CD103^{+}$ DC between CCX-CKR KO and WT mice, with 30-40% of $CD11c^{+}$ cells expressing CD103 in both strains (Fig4.5B). $CD11c^{+}CD103^{+}$ cells could be divided into $CD11c^{int}CD103^{lo}$ and $CD11c^{hi}CD103^{hi}$ subsets and the proportions and absolute numbers of these subsets amongst $CD11c^{+}CD103^{+}$ DC were identical in the lamina propria of CCX-CKR KO and WT mice (Fig 4.5B and C).

4.2 Analysis of CD103 expression on MLN DC in CCX-CKR KO mice

Because $CD103^{+}$ DC from the lamina propria are known to migrate to the MLN (133, 197, 209). I extended my studies of the intestinal immune compartment by assessing the proportions and absolute numbers of $CD11c^{int}CD103^{lo}$ and $CD11c^{hi}CD103^{hi}$ subsets within the MLN. This was particularly relevant, as CCR7 KO mice have reduced numbers of $CD103^{+}$ DC in their MLN resulting in a failure to generate CCR9 expressing gut tropic effector T cells (125, 244). In agreement with published work (82), approximately 40% of $CD11c^{+}$ cells from the MLN of WT mice expressed CD103. The proportions and absolute numbers of $CD11c^{+}$ cells expressing CD103 were comparable between CCX-CKR KO and WT mice, as were the proportions and absolute numbers of $CD11c^{int}CD103^{lo}$ and $CD11c^{hi}CD103^{hi}$ cells amongst the $CD11c^{+}CD103^{+}$ population (Fig 4.6).

4.3 Peyer's patch cellularity in CCX-CKR KO mice

As the Peyer's patches (PP) are a major site of antigen presentation and T cell priming in the gut, any disruption of CCL19 or CCL21 availability could potentially affect lymphocyte and/or DC distribution there. Therefore I next assessed DC subsets and B cell abundance in the PP of CCX-CKR KO and WT mice. There were no differences in the total numbers of live leukocytes, or in the proportions and absolute numbers of $B220^+$ B cells between CCX-CKR KO and WT mice. For both strains, approximately 75% of live cells comprised B cells. However, there was a statistically significant increase in the proportions of $CD11c^+$ cells in CCX-CKR KO PP compared to WT but although the absolute numbers of $CD11c^+$ cells in CCX-CKR KO PP appeared increased compared to WT, this was not statistically significant (Fig 4.7). As before, there were insufficient numbers of $CD11c^+$ cells in resting PP to allow a detailed assessment of most individual DC subsets. However, the proportion of pDC identifiable as $CD11c^{lo}B220^+PDCA\text{-}1^+$ cells was reduced in the PP of CCX-CKR KO mice (Figs 4.8A, B and D). A similar reduction was seen in the absolute numbers of pDC, although this did not attain statistical significance (Fig 4.8C).

4.4 Flt3L expanded $CD11c^+$ cell populations in CCX-CKR KO mice

Due to the difficulties I experienced in obtaining sufficient DC from lamina propria and PP to conduct a detailed analysis of DC subsets in resting mice, I decided to expand DC numbers *in vivo* using fms-like tyrosine kinase ligand (Flt3L). Flt3L is a growth factor for DC precursors and is responsible for the homeostatic proliferation of DC in lymphoid tissues (245-247). By administering an exogenous source of Flt3L I could expand DC *in vivo* with the aim of being able to detect cell subsets more easily. In addition, it would allow me to determine whether the defect in pDC numbers within the secondary lymphoid organs of CCX-CKR KO mice could be overcome.

After 10 daily injections of Flt3L i.p, the total numbers of leukocytes were comparable in the lamina propria of Flt3L treated mice and were elevated compared with resting mice (Figs 4.3B and 4.9B). As expected, the proportion of live leukocytes expressing CD11c expanded dramatically from approximately 15% of WT and 25% of CCX-CKR KO live leukocytes to about 65% in both strains. In contrast to resting mice, there were no differences in the absolute numbers or proportions of total CD11c expressing cells in CCX-CKR KO and WT lamina propria after Flt3L treatment (Fig 4.9).

The expansion of DC numbers allowed me to characterise individual DC subsets within the lamina propria of Flt3L treated mice. The proportions and absolute numbers of $CD11c^+$ cells co-expressing B220, CD4, CD8, CD11b, CD103 or PDCA-1 were identical in CCX-CKR KO and WT mice (Fig 4.10). The proportions and absolute numbers of $CD103^+$ DC subsets amongst total live cells were also expanded in Flt3L treated mice, with both $CD11c^{int}CD103^{lo}$ and $CD11c^{hi}CD103^{hi}$ cell subsets being apparent. The proportions of $CD11c^{int}CD103^{lo}$ and $CD11c^{hi}$ $CD103^{hi}$ cells amongst $CD11c^+CD103^+$ cells in the lamina propria were significantly decreased and increased respectively in Flt3L treated CCX-CKR KO mice compared to WT however this did not translate into a significant difference in absolute numbers (Fig 4.11).

Next I investigated the effects of Flt3L mediated DC expansion in the PP of CCX-CKR KO mice. The total numbers of leukocytes were comparable in CCX-CKR KO and WT mice as was the proportion of $CD11c^+$ cells. The absolute numbers of $CD11c^+$ cells were elevated in CCX-CKR KO mice, although this was not statistically significant (Fig 4.12). $CD11c^+$ cells co-expressing B220, CD103 and PDCA-1 were readily definable in the PP of Flt3L treated mice and there were no significant differences in the proportions of these $CD11c^+$ cell subsets in the PP of CCX-CKR KO and WT mice (Fig 4.13A,B and D). However the absolute numbers of pDC, defined as $CD11c^{lo}B220^+$ or $CD11c^{lo}PDCA\text{-}1^+$ cells were significantly increased in CCX-CKR KO mice (Fig 4.13C). Perhaps reflecting the slightly elevated total cell numbers, the absolute numbers of $CD11c^{hi}CD103^{hi}$ DC were also significantly elevated in CCX-CKR KO mice, although no significant difference was seen in the proportions of the $CD11c^{hi}CD103^{hi}$ or $CD11c^{int}CD103^{lo}$ cell subsets amongst $CD11c^+CD103^+$ DC (Fig 4.14).

The total cell numbers obtained from the MLN of Flt3L treated CCX-CKR KO and WT mice were similar, as were the proportions and absolute numbers of $CD11c^+$ cells (Fig 4.15A). In both cases, the proportion of CD11c expressing cells rose dramatically from approximately 5% in resting mice to between 50 and 60% with Flt3L treatment (Figs 3.10B, 4.15B and C). The relative proportions and absolute numbers of $CD11c^+$ cells co-expressing CD8, CD11b and B220 in the MLN of Flt3L treated CCX-CKR KO mice were comparable with those in WT MLN (Fig 4.16A and B). Approximately 40% of MLN cells in Flt3L treated WT mice were $CD11c^+CD103^+$ and this proportion was significantly decreased in CCX-CKR KO mice, where approximately 25% of cells were $CD11c^+CD103^+$ (Fig 4.16B). However, this did not

translate into absolute numbers and the proportions of $CD11c^+$ cells co-expressing CD103 were the same in the MLN of Flt3L treated CCX-CKR KO and WT mice (Fig 4.16C and D).

As in the MLN of resting CCX-CKR KO mice, the proportion of $CD11c^+$ cells expressing PDCA-1 was significantly reduced in Flt3L treated CCX-CKR KO mice compared to WT. However, again this did not translate into absolute numbers or in differences in the proportions of total cells co-expressing CD11c and PDCA-1 (Fig 4.16). As in resting mice, a $CD103^+$ DC population was apparent, but there were no significant differences in the proportions or absolute numbers of $CD11c^{hi}CD103^{hi}$ or $CD11c^{int}CD103^{lo}$ cells in Flt3L treated CCX-CKR KO and WT mice (Fig 4.17).

Finally, I examined DC populations in the ILN and spleens of Flt3L treated mice. The total numbers of ILN cells, as well as the proportions and absolute numbers of $CD11c^+$ cells were similar in CCX-CKR KO and WT mice. As in the intestine, PP and MLN, $CD11c^+$ cells were expanded in the ILN of both CCX-CKR KO and WT mice, increasing from approximately 2% of total ILN cells in resting mice to 20-25% after Flt3L treatment (Fig 4.18).

The greater numbers of $CD11c^+$ cells recoverable from the ILN of Flt3L treated mice, allowed me to analyse DC subsets. The proportions and absolute numbers of $CD8^+$ and $CD11b^+$ DC subsets were similar in CCX-CKR KO and WT mice with $CD8^+$ DC predominating. In contrast to the resting ILN, the proportion of cells co-expressing CD11c and PDCA-1 was not significantly reduced in the ILN of Flt3L treated CCX-CKR KO mice compared to WT (Figs 3.15 and 4.19).

There were no significant differences in the proportions or absolute numbers of $CD11c^+$ cells in the spleens of Flt3L treated CCX-CKR KO and WT mice (Fig 4.20). Again, the proportion of live spleen cells expressing CD11c rose substantially from around 5% to 30% after Flt3L treatment (Figs 3.10 and 4.20). There were no differences in the proportions or absolute numbers of splenic $CD11c^+$ cells, or of $CD11c^+$ cells co-expressing CD8, CD11b or PDCA-1 between CCX-CKR KO and WT mice (Fig 4.21).

Summary

In this chapter I expanded on my finding of decreased pDC numbers in the MLN of resting CCX-CKR KO mice by carrying out an extensive analysis of DC subsets in the small intestinal lamina propria and its associated lymphoid tissues. I have also explored the effect of the DC growth factor, Flt3L on DC subsets in the intestine and secondary lymphoid organs of CCX-CKR KO mice.

Although CCX-CKR KO mice displayed no histological abnormalities in their small intestinal architecture, they do have significantly fewer IEL than WT mice. However, the T cell composition of the lamina propria of CCX-CKR KO appeared to be normal. The proportions of $CD19^+$ and $CD11c^+$ cells were significantly decreased and increased respectively in the lamina propria of resting CCX-CKR KO mice compared with WT and although my attempts to investigate DC subsets in the resting lamina propria were largely unsuccessful, the proportions and absolute numbers of $CD11c^{lo}B220^+$ and $CD103^+$ DC subsets were comparable between the strains. $CD103^+$ DC subsets in the MLN of resting CCX-CKR KO and WT mice were also similar. Interestingly, however, CCX-CKR KO mice had a significantly decreased proportion of pDC in PP compared with WT mice, although there were no differences in total $CD11c^+$ DC or B cells.

As expected, *in vivo* treatment with Flt3L led to a large expansion of all DC subsets including pDC in all the tissues I analysed. There were no differences in DC subsets including pDC in the ILN or spleen of CCX-CKR KO and WT mice however the proportions of $CD11c^{hi}CD103^{hi}$ and $CD11c^{int}CD103^{lo}$ cells amongst total $CD11c^+CD103^+$ DC in the lamina propria were significantly decreased and increased respectively. In addition, Flt3L overcame the decreased numbers of pDC seen in the PP of resting CCX-CKR KO mice. Indeed, the numbers of $CD11c^+$ cells expressing B220 or PDCA-1 in the PP of Flt3L treated CCX-CKR KO mice were actually significantly increased compared with WT, as were the numbers of $CD11c^{hi}CD103^{hi}$ cells. In contrast, the numbers of pDC remained significantly decreased in the MLN of CCX-CKR KO mice, despite the normal expansion of other DC subsets. The proportion of total $CD11c^+$ cells co-expressing CD103 was also significantly decreased in the MLN of Flt3L treated CCX-CKR KO mice compared with WT.

Together, these results indicated that the principal finding of the previous chapter of decreased pDC in the MLN in the absence of CCX-CKR was shared by PP. However this could be rescued in PP and other tissues by Flt3L, but not in the MLN.

Having assessed the phenotypic effects of CCX-CKR deletion on the cellularity of secondary lymphoid organs and the small intestinal lamina propria, in the next chapter I go on to explore the functional consequences of CCX-CKR deletion in the development of antigen specific immunity and tolerance.

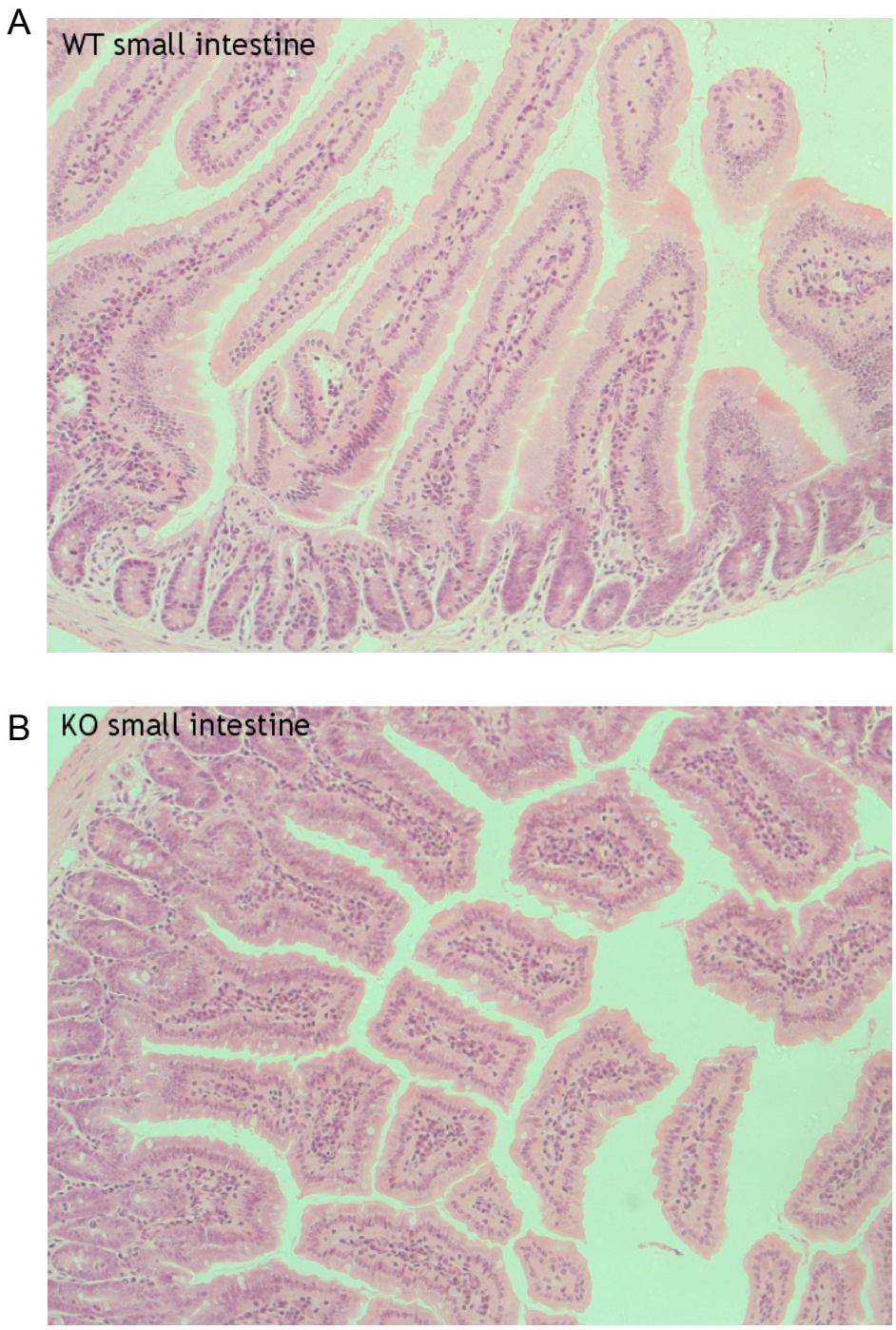

Figure 4.1
Histology of the Small Intestine of CCX-CKR KO and WT Mice
Sections of small intestine from WT (A) and CCX-CKR KO (B) mice were fixed in 10% formalin, embedded in paraffin and stained with haematoxylin and eosin for histolgical analysis.(Final magnification x 200)

A

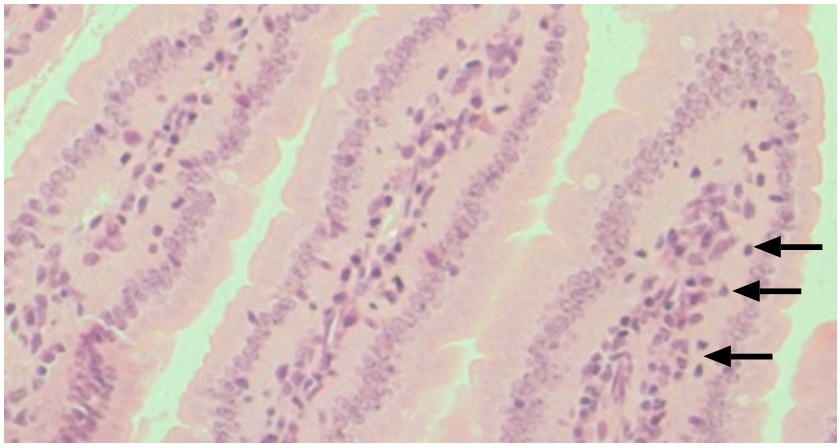

B

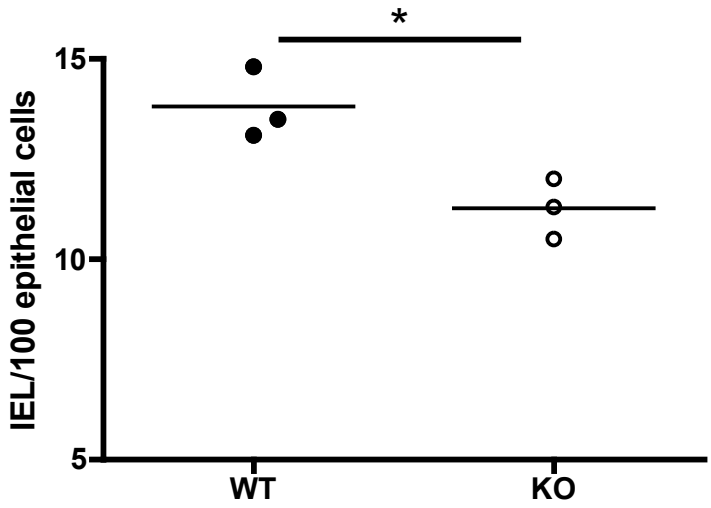

Figure 4.2
Frequency of Small Intestinal IEL in CCX-CKR KO and WT Mice
Sections of small intestine from CCX-CKR KO and WT mice were fixed in 10% formalin, embedded in paraffin and stained with haematoxylin and eosin to identify IEL (indicated by arrows) (A). The numbers of IEL per 100 epitheilal cells on sections were determined by counting (B).

*p<0.05 Unpaired t test

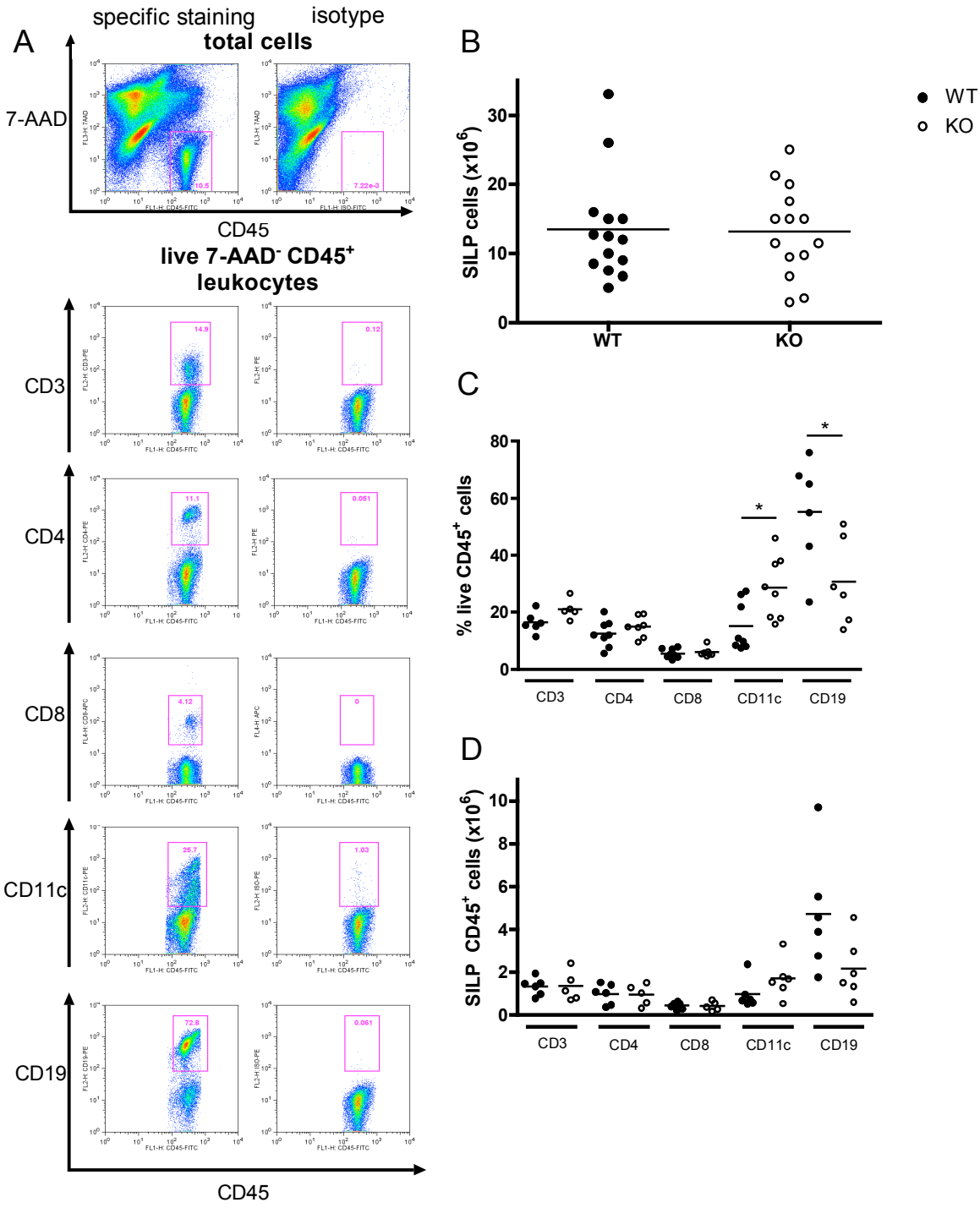

Figure 4.3
Phenotypic Analysis of Small Intestine Lamina Propia Cells from CCX-CKR KO and WT Mice
Small intestinal lamina propria cells from CCX-CKR KO and WT mice were analysed for expression of CD45 and 7-AAD uptake to identify $CD45^{+}7\text{-}AAD^{-}$ cells as live leukocytes.(A) Representative FACS plots are shown of live leukocytes and their expression of CD3, CD4, CD8, CD11c or CD19 with respective isotype controls. (B) The total numbers of live leukocytes, the (C) proportions of $CD3^{+}$, $CD4^{+}$, $CD8^{+}$ T cells, $CD11c^{+}$ DC and $CD19^{+}$ B cells and (D) their absolute numbers are shown. Results show the means of 5-14 mice per group and are pooled from 3 individual experiments.

*p<0.05 Unpaired t test

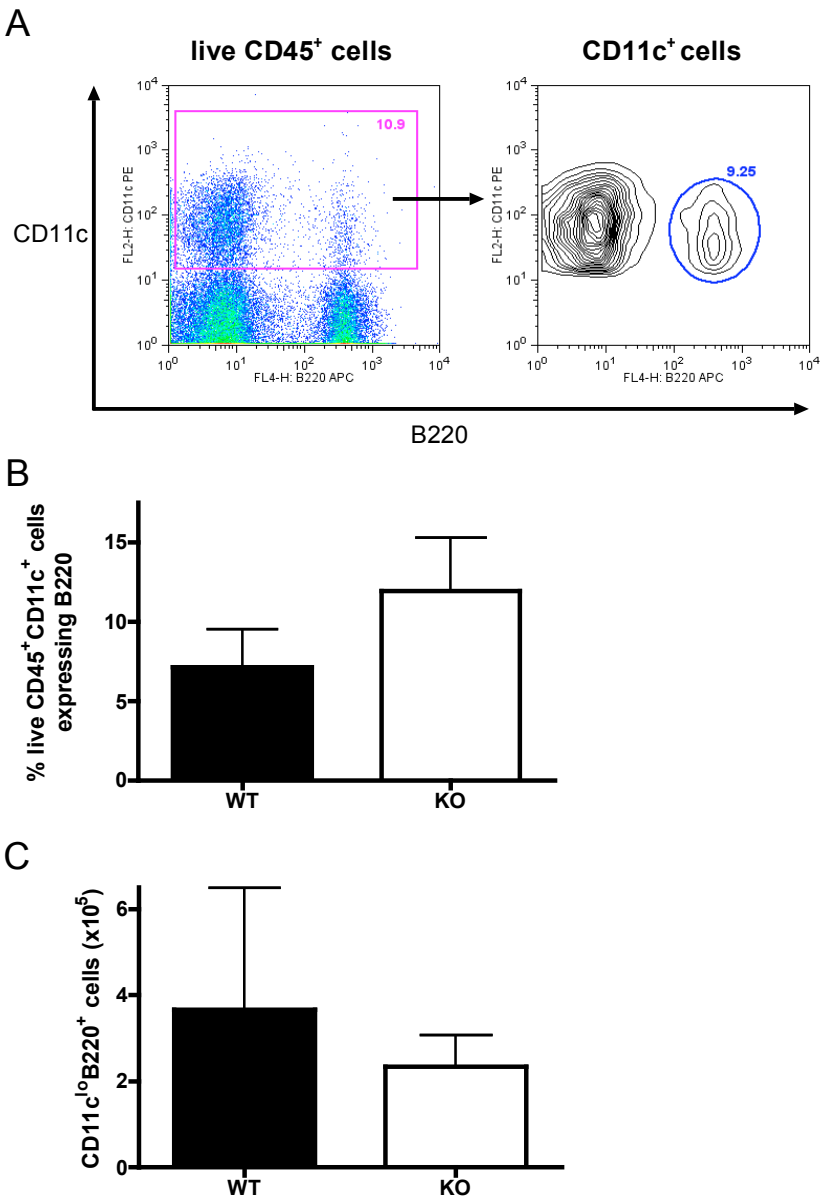

Figure 4.4
pDC in the Small Intestinal Lamina Propia of CCX-CKR KO and WT Mice
pDC were identified amongst live $CD45^+$ cells based on CD11c and B220 expression. (A) Representative FACS plots show the proportion of $7\text{-}AAD^-CD45^+$ live leukocytes expressing CD11c and the proportion of $CD11c^+$ cells expressing B220 (putatively termed pDC). The proportions of live $CD45^+CD11c^+$ cells expressing B220 and the total numbers of $CD11c^{lo}B220^+$ cells are shown in (B) and (C) respectively. Results show the means + 1 SD of 3 mice per group.

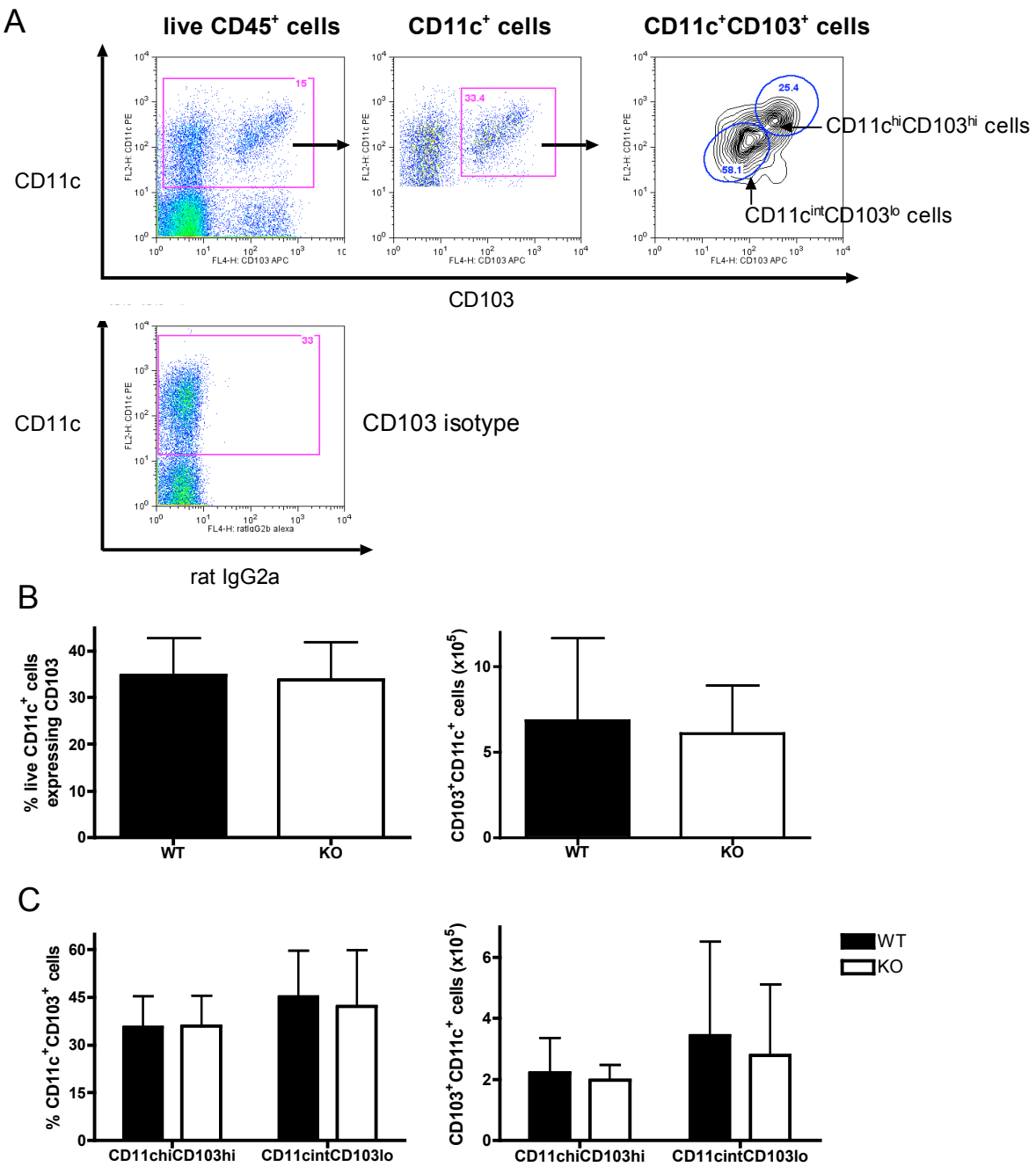

Figure 4.5
CD103 Expressing DC in the Small Intestinal Lamina Propria of CCX-CKR KO and WT Mice

(A) Representative FACS plots show the proportion of total 7-AAD$^-$CD45$^+$ live lamina propria leukocytes expressing CD11c (left), the proportions of CD11c$^+$ cells co-expressing CD103 (middle) and the proportions of CD11c^{hi}CD103^{hi} and CD11c^{int}CD103^{lo} cells amongst CD11c$^+$CD103$^+$ cells (right). CD103 isotype staining is shown immediately below. (B) The proportions of live CD11c$^+$ cells expressing CD103 (left), and their absolute numbers (right) are shown along with (C) the proportions (left) and absolute numbers of cells (right) in CD11c^{hi}CD103^{hi} and CD11c^{int}CD103^{lo} cell subsets. Results show the means +1 SD of 3 mice per group.

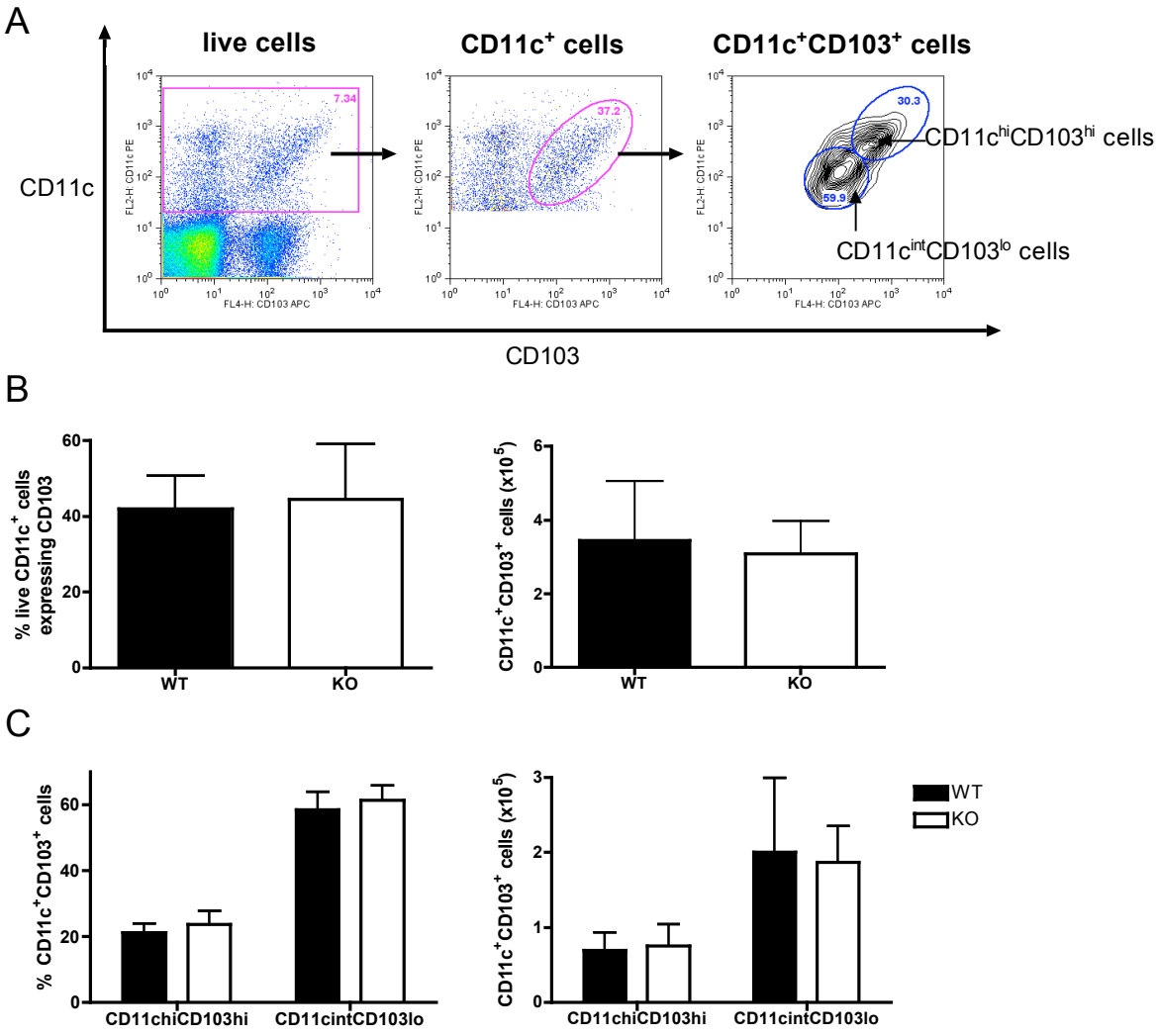

Figure 4.6
CD103 Expressing DC in the MLN of CCX-CKR KO and WT Mice
(A) Representative FACS plots show the proportion of total live MLN cells expressing CD11c (left), the proportions of $CD11c^{+}$ cells co-expressing CD103 (middle) and the proportions of $CD11c^{hi}CD103^{hi}$ and $CD11c^{int}CD103^{lo}$ cells amongst $CD11c^{+}CD103^{+}$ cells (right). (B) The proportions of live $CD11c^{+}$ cells expressing CD103 (left), and their absolute numbers (right) are shown along with (C) the proportions (left) and absolute numbers of cells (right) in $CD11c^{hi}CD103^{hi}$ and $CD11c^{int}CD103^{lo}$ cell subsets. Results show the means +1 SD of 3 mice per group.

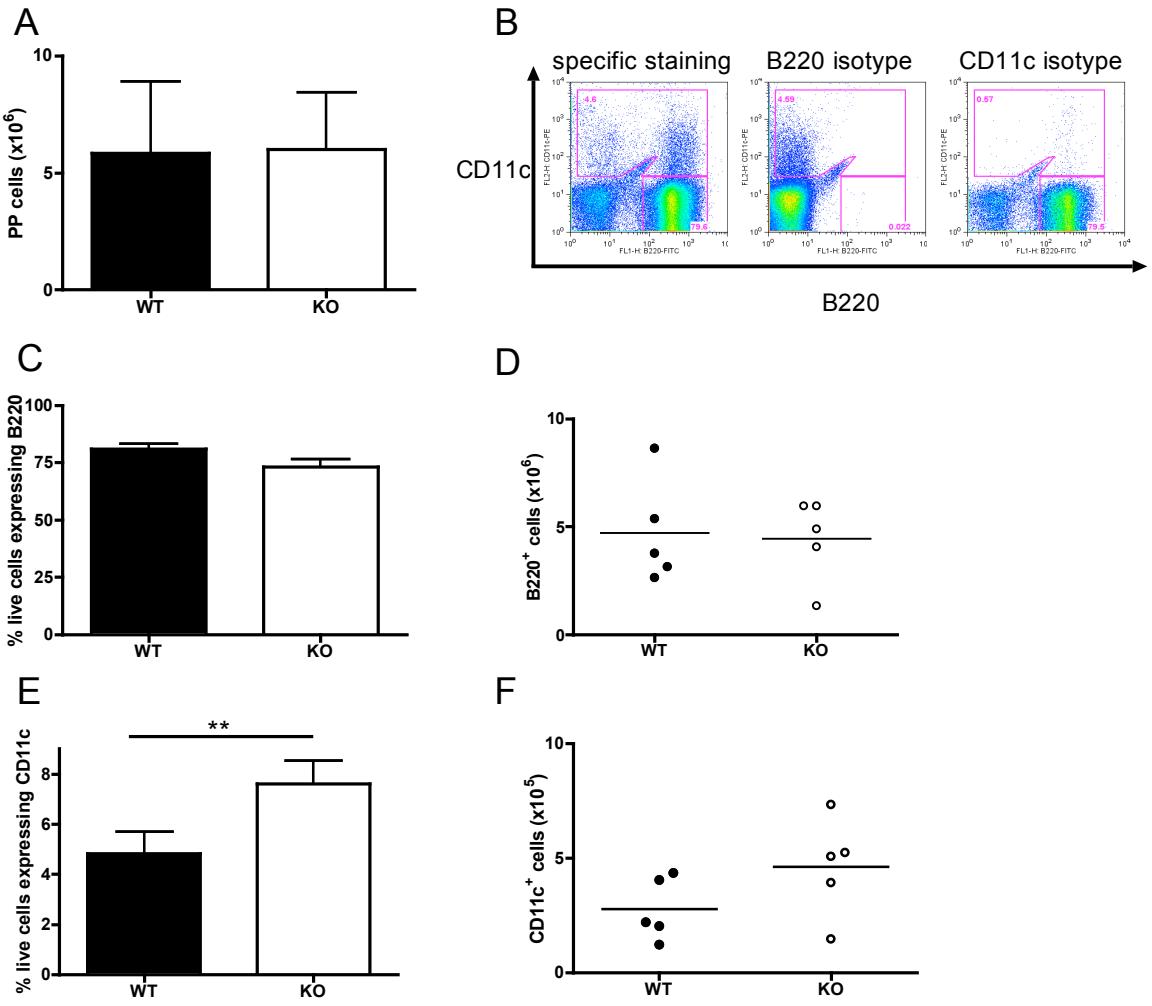

Figure 4.7
DC and B Cells in the PP of CCX-CKR KO and WT Mice
(A)Total numbers of Peyer's patch (PP) cells were determined and analysed for cell surface expression of CD11c and B220. (B) Representative FACS plots show the proportions of total live cells expressing CD11c and B220 (after excluding autofluorescent cells). CD11c and B220 isotype staining is also shown. (C,E) The proportions and absolute numbers (D,F) of live PP cells expressing B220 or CD11c are shown. Results show means +1 SD of 5 mice per group.

**p<0.01 Unpaired t test

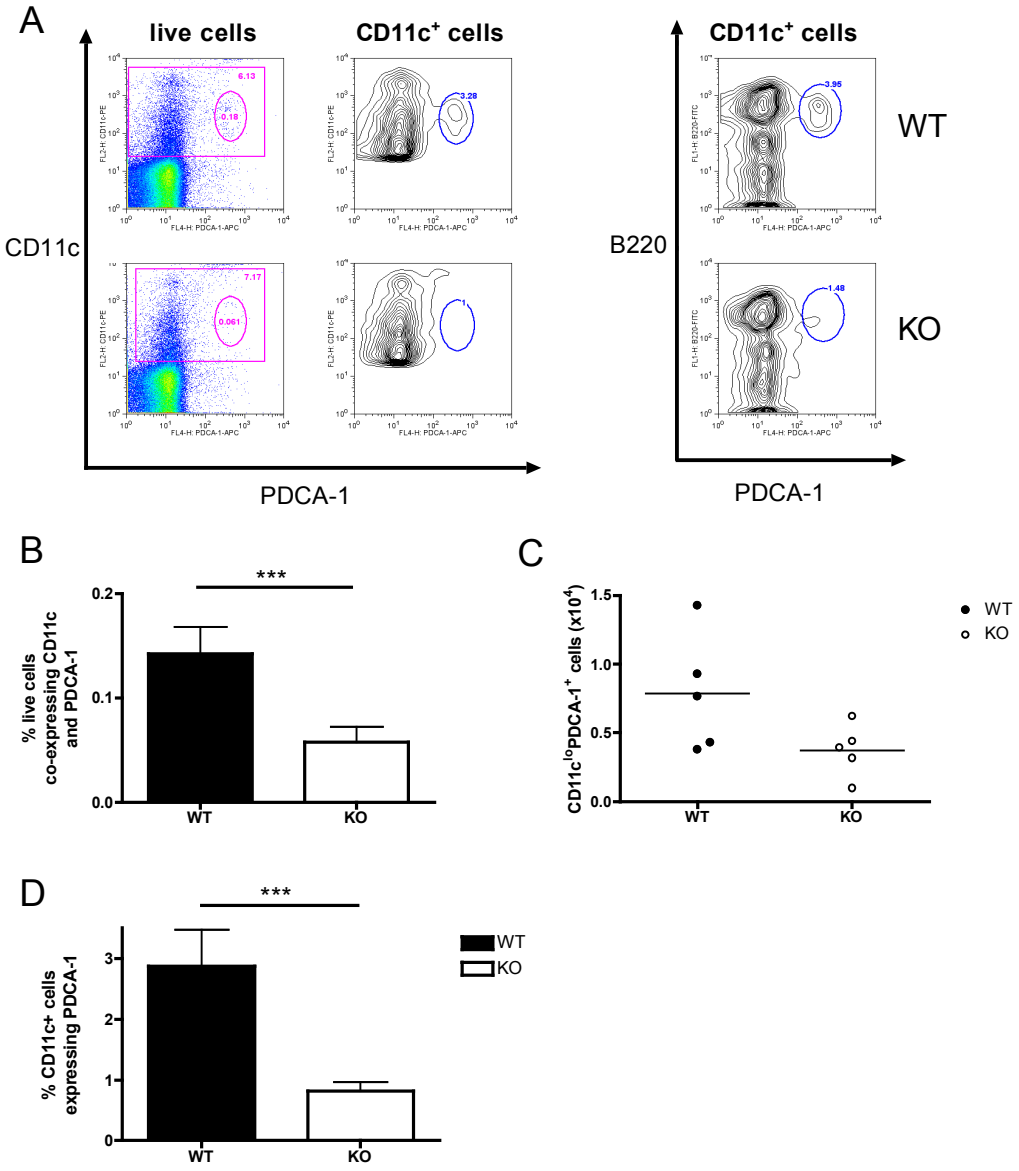

Figure 4.8
pDC in the PP of CCX-CKR KO and WT Mice
(A) Representative FACS plots of total live PP cells show the proportions expressing CD11c and co-expressing CD11c with PDCA-1 in rectangular and oval gates respectively (left panels) in WT (upper panels) and CCX-CKR KO (lower panels) mice. The proportions of $CD11c^+$ cells co-expressing B220 and PDCA-1 are also shown (right panels). (B) The proportions and (C) absolute numbers of $CD11c^{lo}PDCA\text{-}1^+$ pDC amongst live cells are shown along with (D) the proportions of $PDCA\text{-}1^+$ cells amongst gated $CD11c^+$ cells. Results show means +1 SD of 5 mice per group

***p<0.001 Unpaired t test

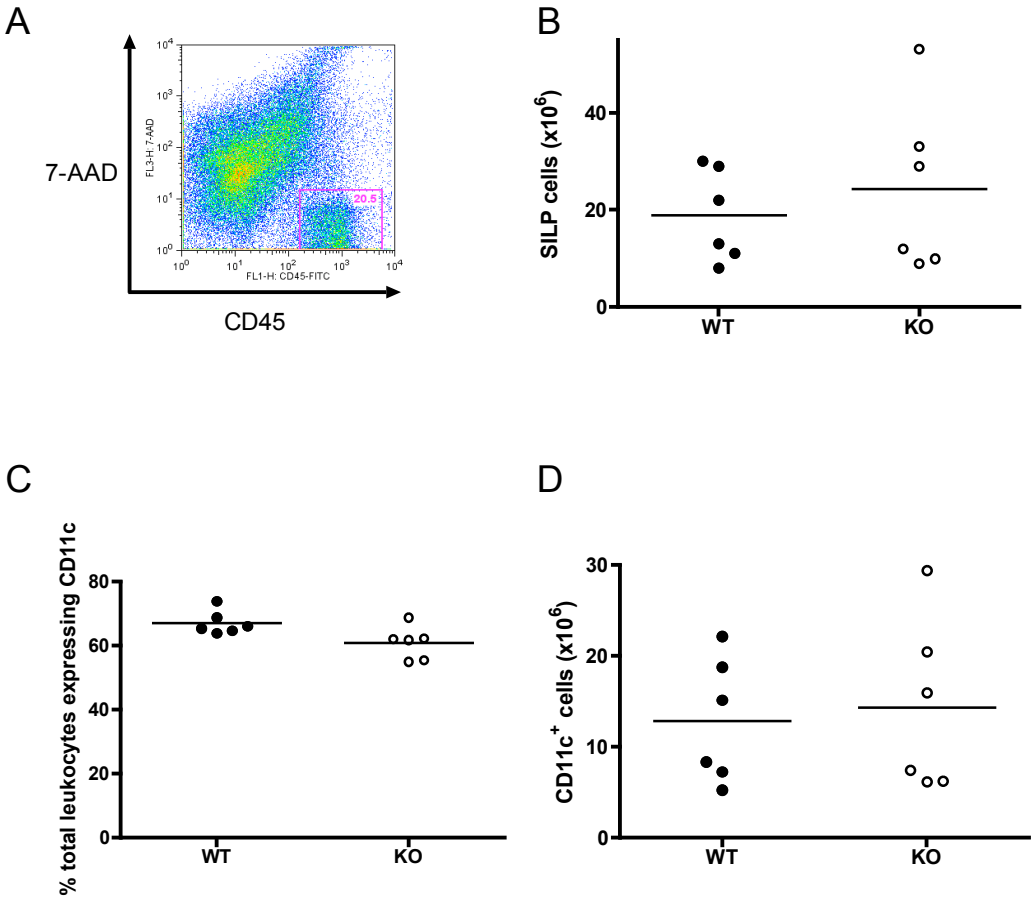

Figure 4.9
DC in the Small Intestinal Lamina Propria of CCX-CKR KO and WT Mice After Treatment With Flt3L
CCX-CKR KO and WT mice were injected daily with Flt3L for 10 days after which small intestines were removed and live leukocytes were analysed for CD11c expression. (A) Representative FACS plot showing the proportion of total 7-AAD$^-$CD45$^+$ cells. (B) Total numbers of live leukocytes in the lamina propria as well as (C) the proportions and (D) absolute numbers of CD11c$^+$ cells are shown. Results show means +1 SD of 6 mice per group.

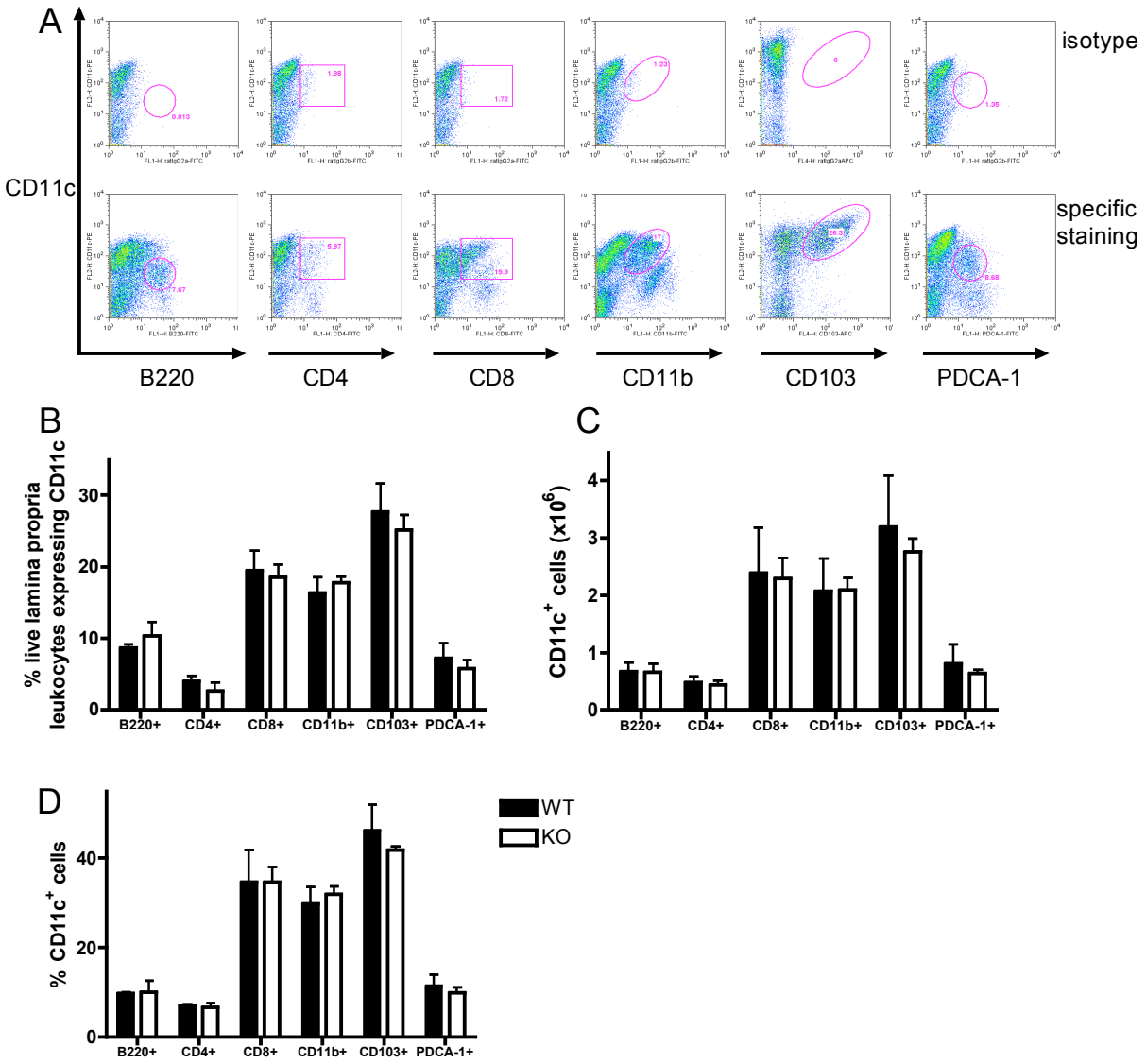

Figure 4.10
DC Subsets in the Small Intestinal Lamina Propria of Flt3L Treated CCX-CKR KO and WT Mice
Live gated lamina propria cells from Flt3L treated CCX-CKR KO and WT mice were analysed for surface expression of B220, CD4, CD8, CD11b, CD103 or PDCA-1 on $CD11c^+$ cells. (A) Representative FACS plots show the proportions of total live cells co-expressing CD11c and B220, CD4, CD8, CD11b, CD103 or PDCA-1. Isotype staining for each $CD11c^+$ cell subset is shown in the top row. (B) The proportions and (C) absolute numbers of live cells co-expressing CD11c and individual subset markers are shown. (D) The proportions of $CD11c^+$ cells expressing individual subset markers are shown. Results show means +1 SD of 3-9 mice per group.

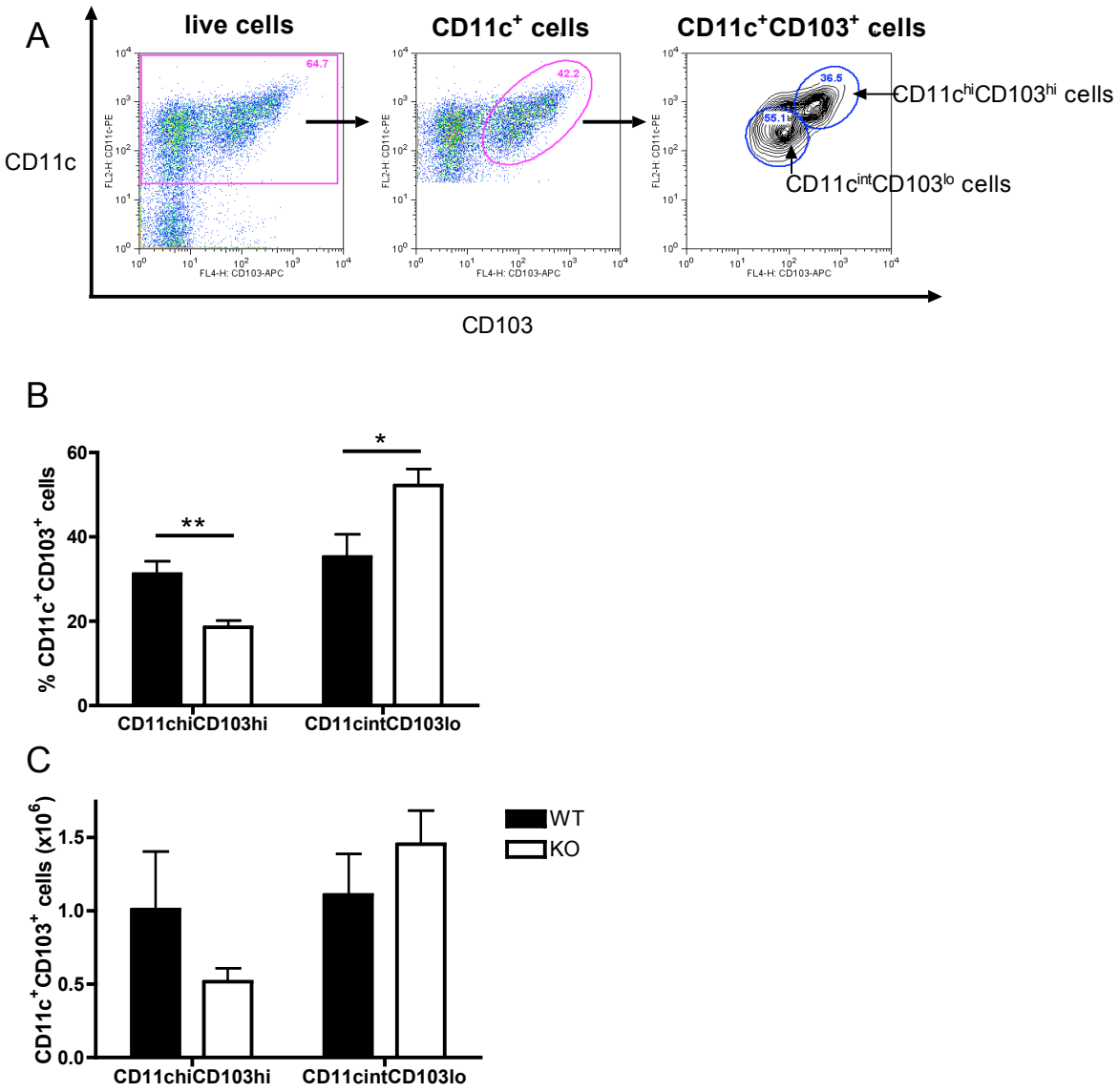

Figure 4.11
CD103 Expressing DC in the Small Intestine Lamina Propria of CCX-CKR KO and WT Mice After Treatment With Flt3L
Live gated cells from the small intestines of Flt3L treated CCX-CKR KO and WT mice were analysed for co-expression of CD11c and CD103. (A) Representative FACS plots show the proportion of total live leukocytes expressing CD11c (left), the proportion of $CD11c^+$ cells expressing CD103 (middle) and the proportions of $CD11c^+CD103^+$ cells that are $CD11c^{hi}CD103^{hi}$ and $CD11c^{int}CD103^{lo}$ cells (right). The proportion of $CD11c^+CD103^+$ cells in $CD11c^{hi}CD103^{hi}$ and $CD11c^{int}CD103^{lo}$ cell subsets and their absolute numbers are shown in (B) and (C) respectively. Results show the means +1 SD of 3 mice per group.

*p<0.05 **p<0.01 Unpaired t test

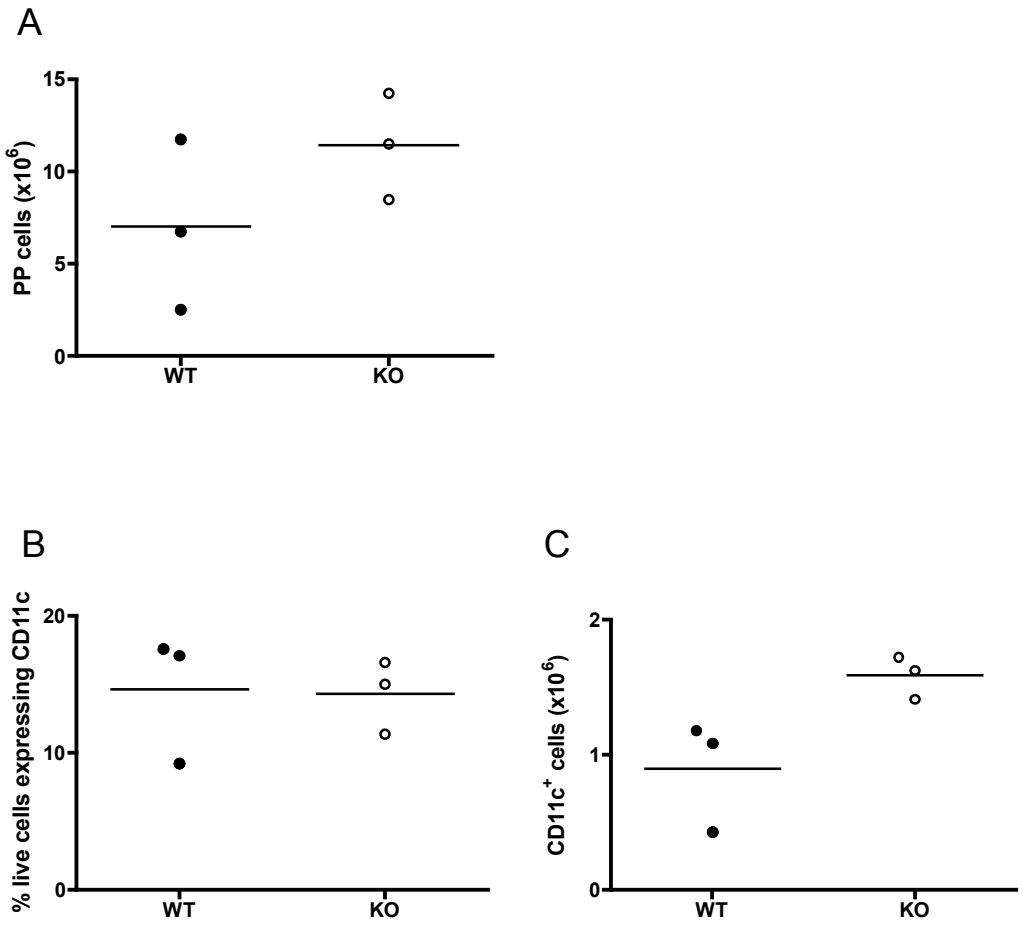

Figure 4.12
DC in the PP of CCX-CKR KO and WT Mice After Treatment With Flt3L
CCX-CKR KO and WT mice were injected daily with Flt3L for 10 days and the total numbers of live cells recovered from PP were determined (A). The proportions (B) and absolute numbers (C) of $CD11c^+$ cells were analysed by flow cytometry. Results show means of 3 mice per group.

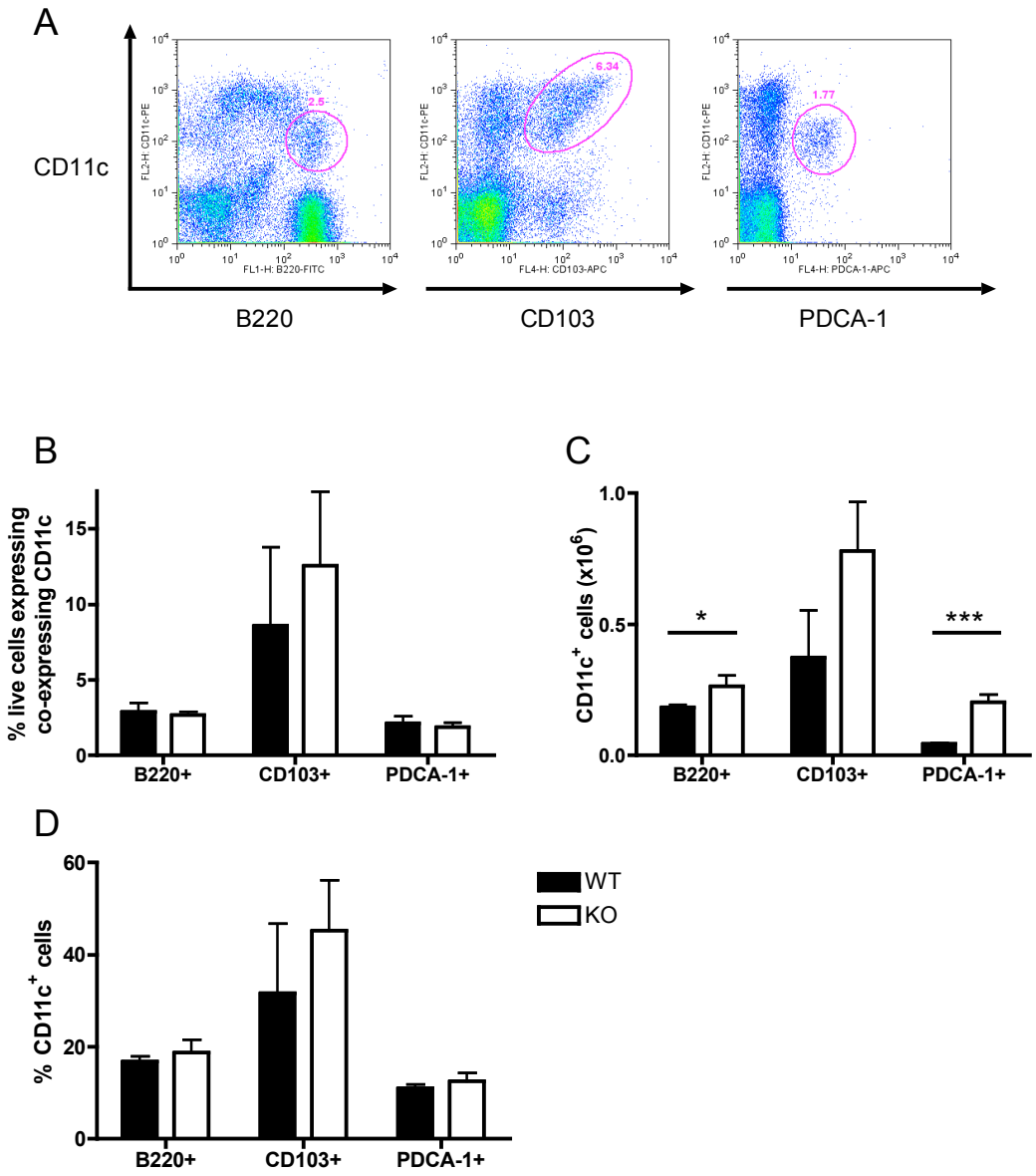

Figure 4.13
DC Subsets in the PP of CCX-CKR KO and WT Mice After Treatment With Flt3L
Live gated PP cells from Flt3L treated CCX-CKR KO and WT mice were analysed for surface expression of B220, CD103 or PDCA-1 on $CD11c^+$ cells. (A) Representative FACS plots show the proportions of total live cells co-expressing CD11c and B220, CD103 or PDCA-1. (B) The proportions and (C) absolute numbers of live cells co-expressing CD11c and individual subset markers are shown. (D) The proportions of $CD11c^+$ cells expressing individual subset markers are shown. Results show means +1 SD of 3 mice per group.

*p<0.05 ***p<0.001 Unpaired t test

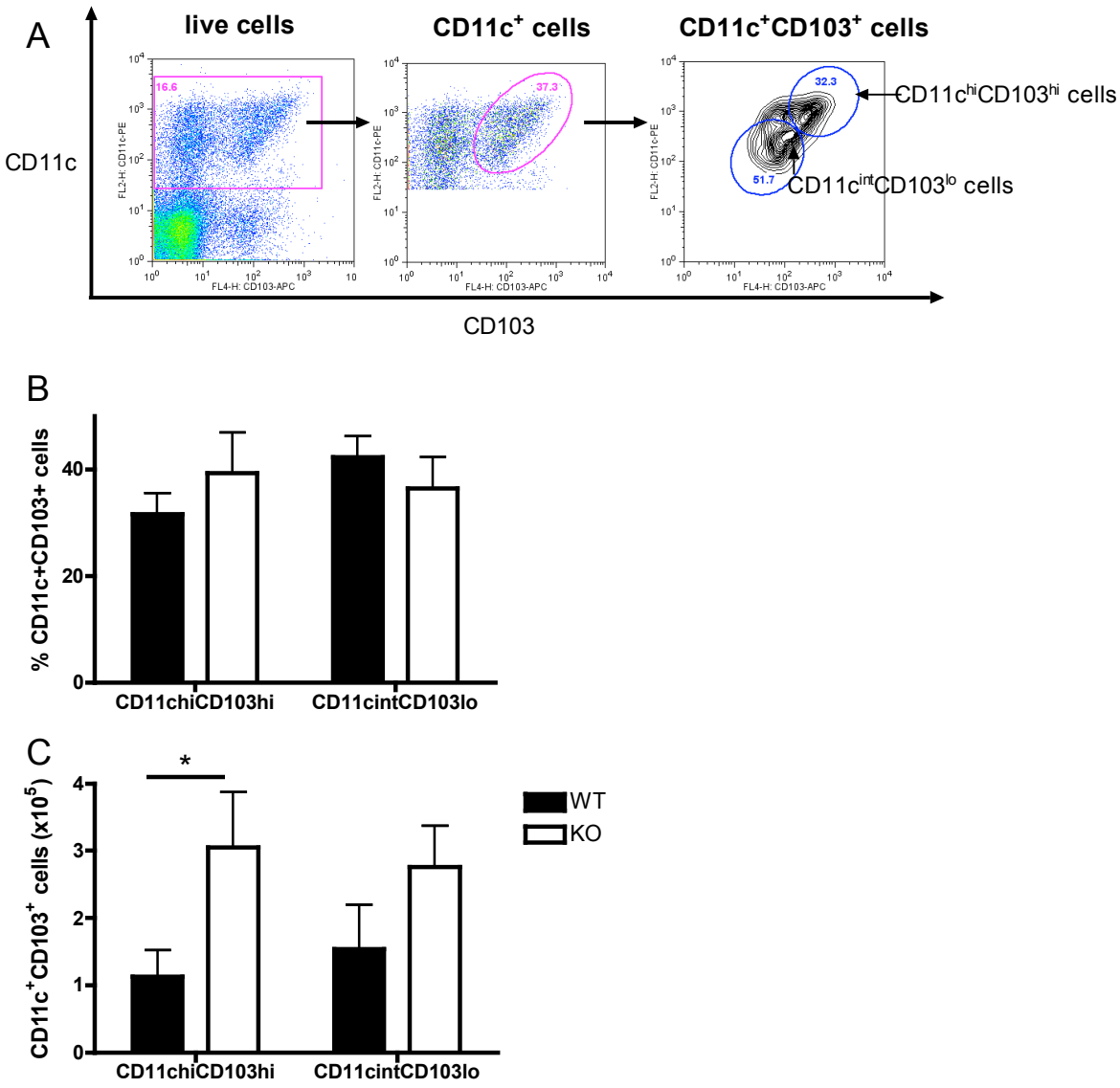

Figure 4.14
CD103 Expressing DC in the PP of CCX-CKR KO and WT Mice After Treatment With Flt3L
Live gated cells from the PP of Flt3L treated CCX-CKR KO and WT mice were analysed for co-expression of CD11c and CD103. (A) Representative FACS plots show the proportion of total live leukocytes expressing CD11c (left), the proportion of $CD11c^+$ cells expressing CD103 (middle) and the proportions of $CD11c^+CD103^+$ cells that are $CD11c^{hi}CD103^{hi}$ and $CD11c^{int}CD103^{lo}$ cells (right). The proportion of $CD11c^+CD103^+$ cells in $CD11c^{hi}CD103^{hi}$ and $CD11c^{int}CD103^{lo}$ cell subsets and their absolute numbers are shown in (B) and (C) respectively. Results show the means +1 SD of 3 mice per group.

*p<0.05 Unpaired t test

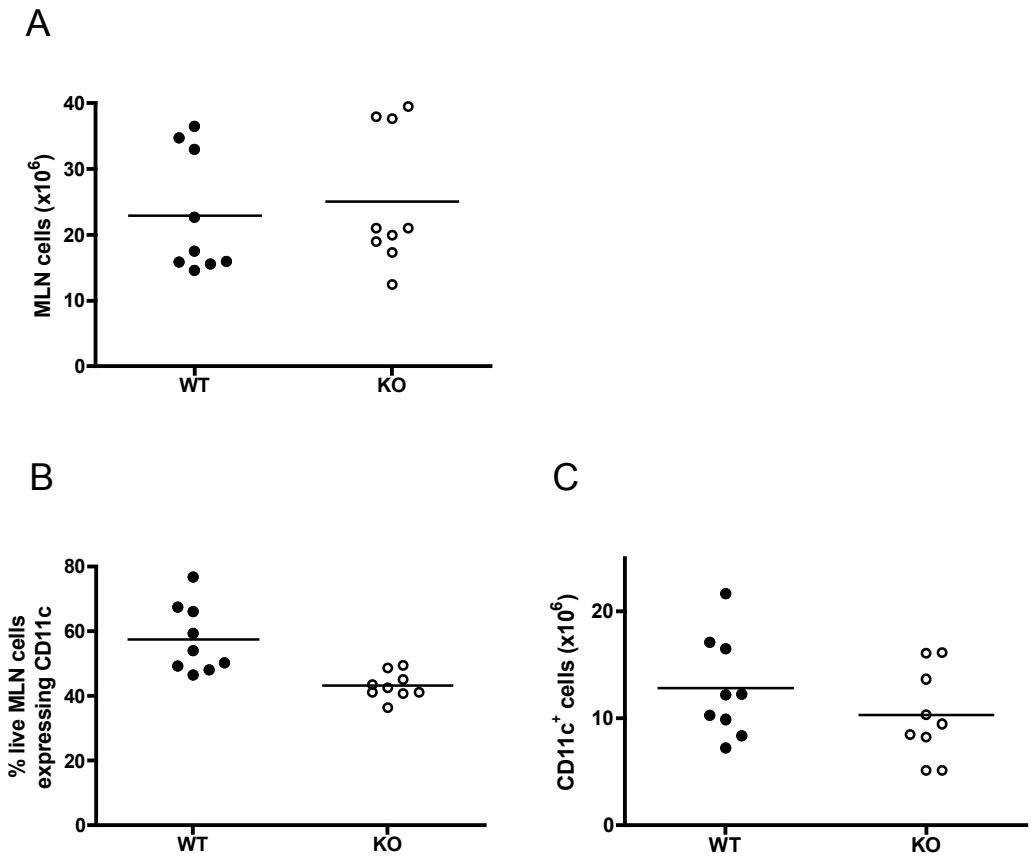

Figure 4.15
DC in the MLN of CCX-CKR KO and WT Mice After Treatment With Flt3L
CCX-CKR KO and WT mice were injected daily with Flt3L for 10 days and the total numbers of live cells recovered from MLN were determined (A). The proportions (B) and numbers (C) of $CD11c^+$ cells were analysed by flow cytometry. Results show means of 9 mice per group and are pooled from 3 separate experiments.

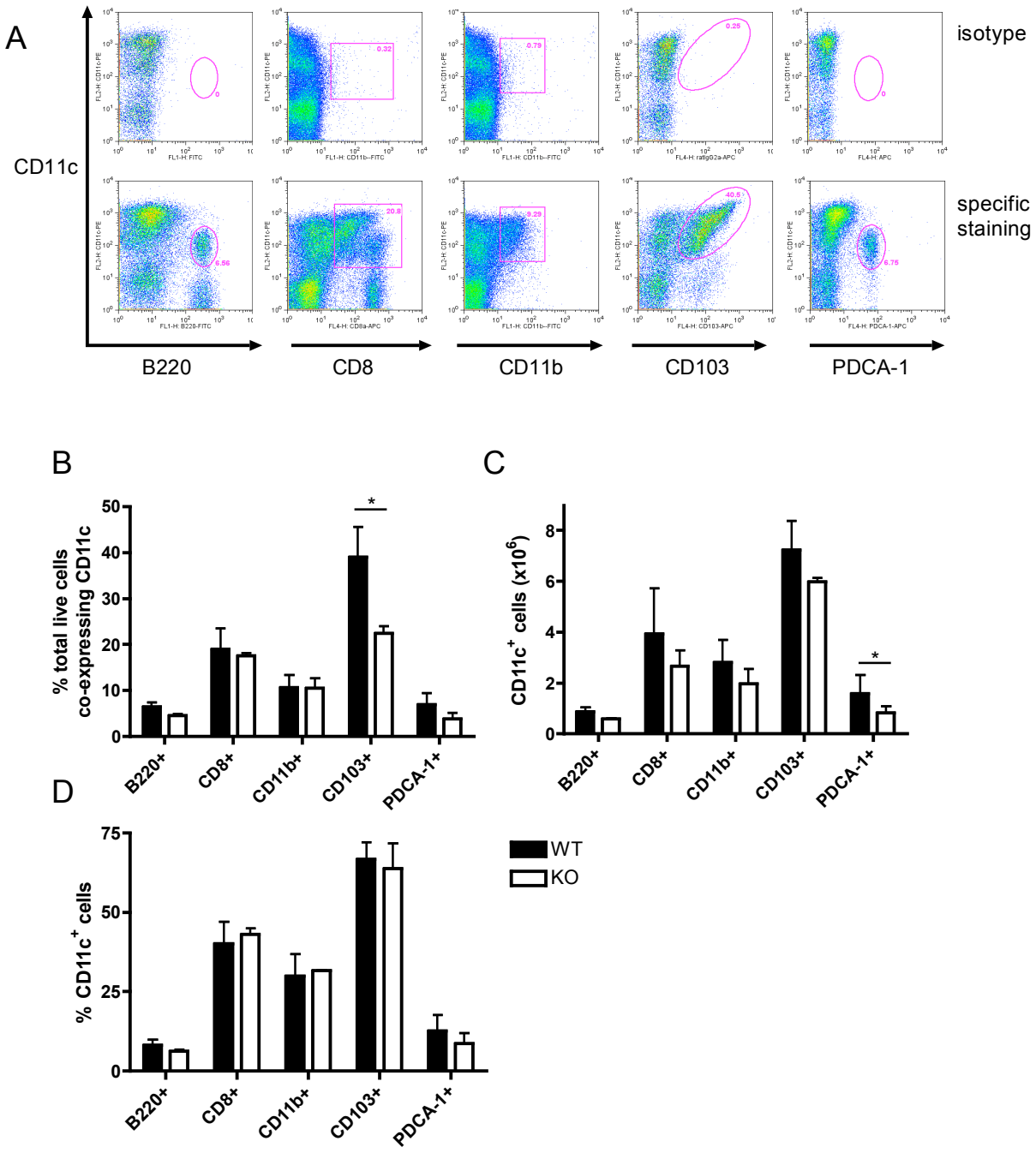

Figure 4.16
DC Subsets in the MLN of CCX-CKR KO and WT Mice After Treatment With Flt3L

Live gated MLN cells from Flt3L treated CCX-CKR KO and WT mice were analysed for surface expression of B220, CD8, CD11b, CD103 or PDCA-1 on $CD11c^+$ cells. (A) Representative FACS plots show the proportions of total live cells co-expressing CD11c and B220, CD8, CD11b, CD103 or PDCA-1. Isotype staining for each $CD11c^+$ cell subset is shown in the top row (B) The proportions and (C) absolute numbers of live cells co-expressing CD11c and individual subset markers are shown. (D) The proportions of $CD11c^+$ cells expressing individual subset markers are shown in (D). Results show means +1 SD of between 3 and 9 mice per group.

*p<0.05 Unpaired t test

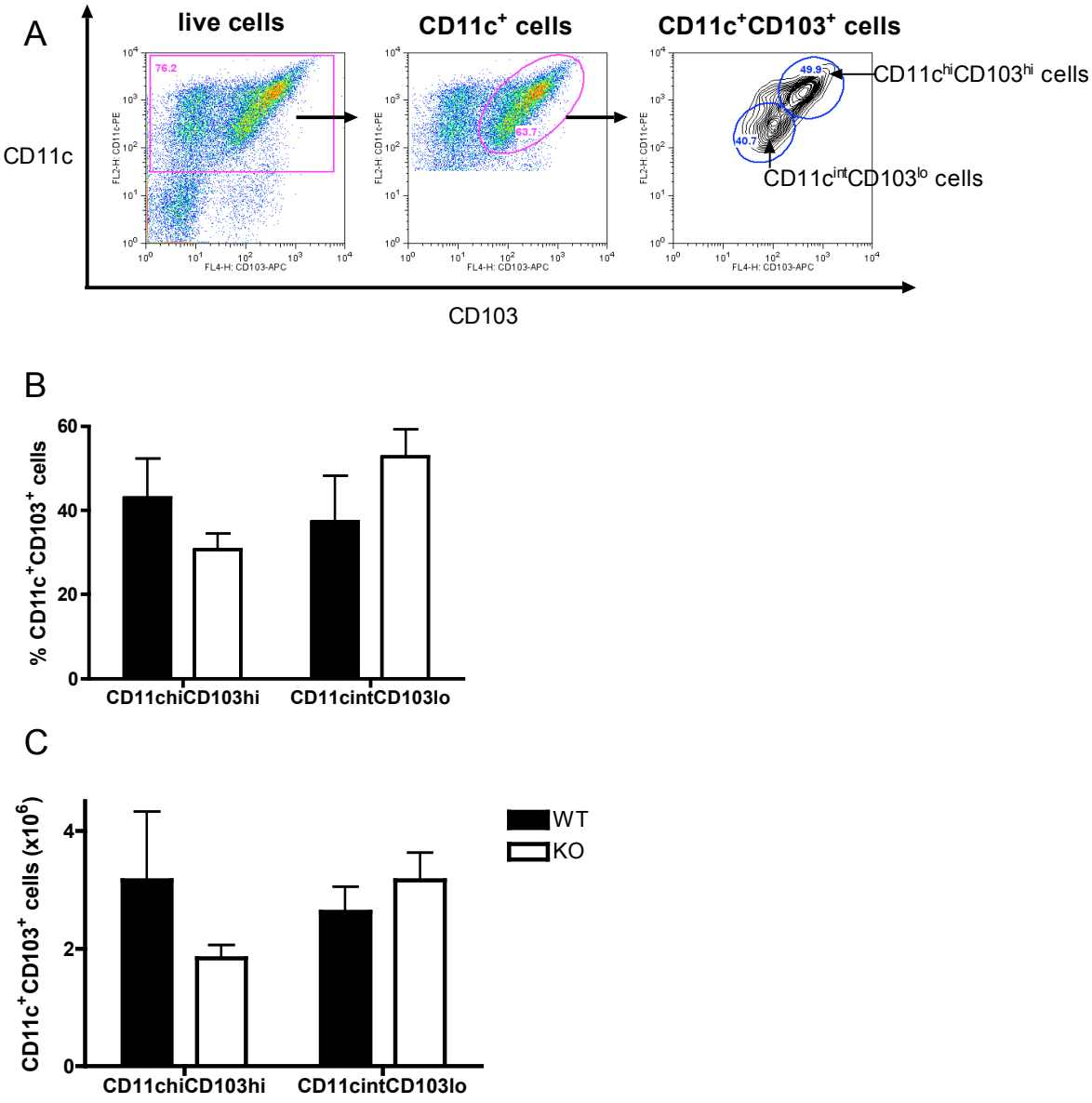

Figure 4.17
CD103 Expressing DC in the MLN of CCX-CKR KO and WT Mice After Treatment With Flt3L
Live gated cells from the MLN of Flt3L treated CCX-CKR KO and WT mice were analysed for co-expression of CD11c and CD103. (A) Representative FACS plots show the proportion of total live leukocytes expressing CD11c (left), the proportion of $CD11c^+$ cells expressing CD103 (middle) and the proportions of $CD11c^+CD103^+$ cells that are $CD11c^{hi}CD103^{hi}$ and $CD11c^{int}CD103^{lo}$ cells (right). The proportion of $CD11c^+CD103^+$ cells in $CD11c^{hi}CD103^{hi}$ and $CD11c^{int}CD103^{lo}$ cell subsets and their absolute numbers are shown in (B) and (C) respectively. Results show the means +1 SD of 3 mice per group.

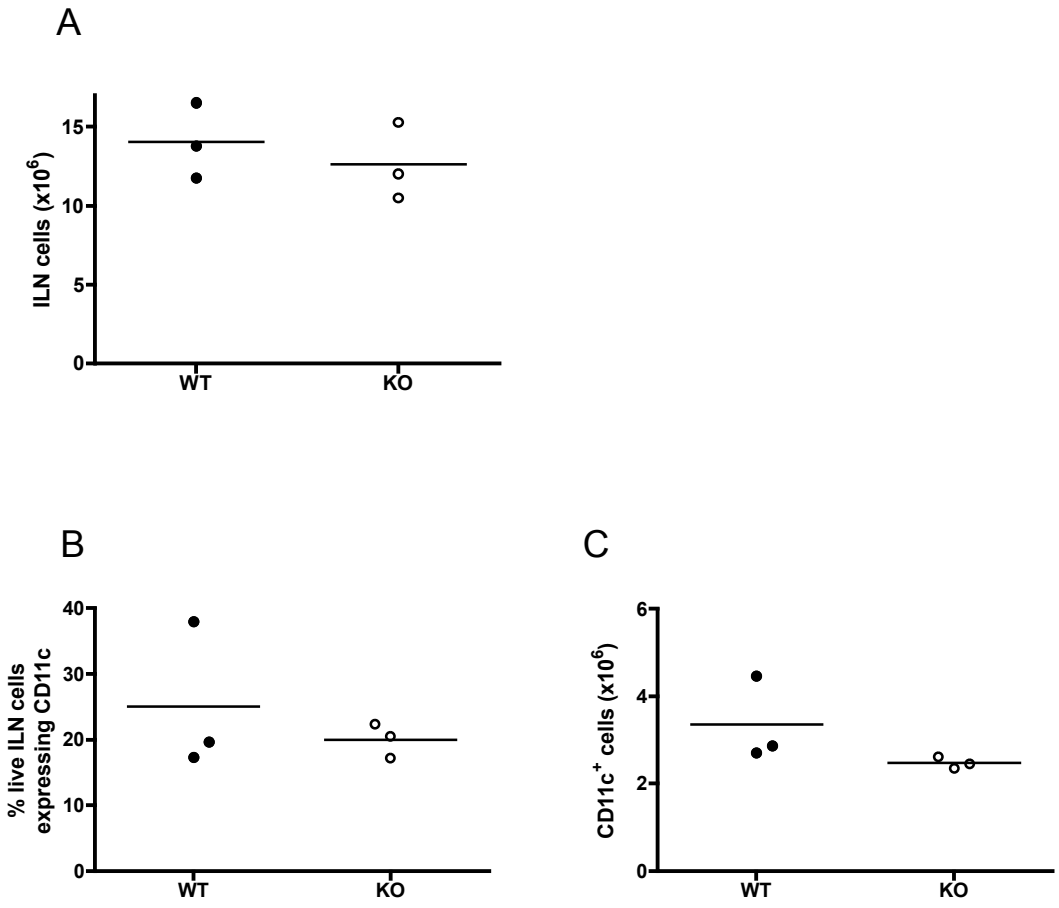

Figure 4.18
DC in the ILN of CCX-CKR KO and WT Mice After Treatment With Flt3L
CCX-CKR KO and WT mice were injected daily with Flt3L for 10 days and the total numbers of live cells recovered from ILN were determined (A). The proportions (B) and numbers (C) of $CD11c^+$ cells were analysed by flow cytometry. Results show means of 3 mice per group.

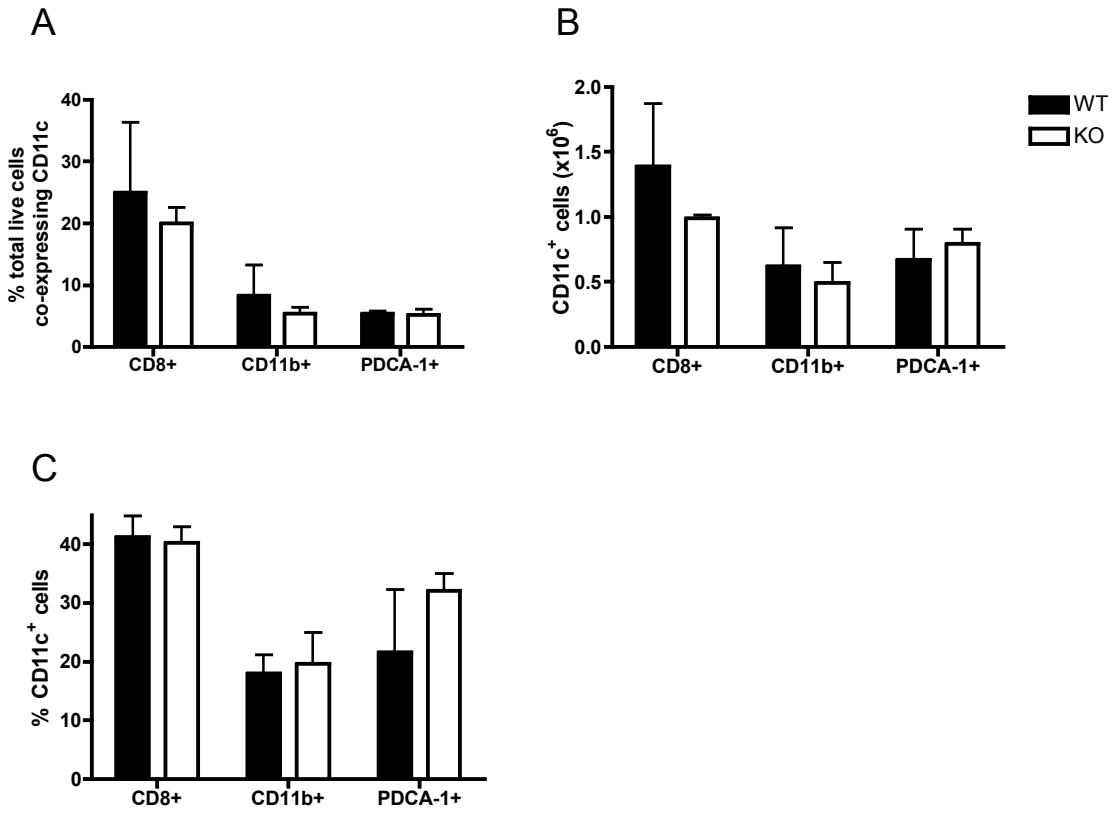

Figure 4.19
DC Subsets in the ILN of CCX-CKR KO and WT Mice After Treatment With Flt3L
Live gated ILN cells from Flt3L treated CCX-CKR KO and WT mice were analysed for surface expression of CD8, CD11b or PDCA-1 on $CD11c^+$ cells. (A) The proportions and (B) absolute numbers of live cells co-expressing CD11c and individual subset markers are shown (C) The proportions of $CD11c^+$ cells expressing individual subset markers. Results show means +1 SD of 3 mice per group.

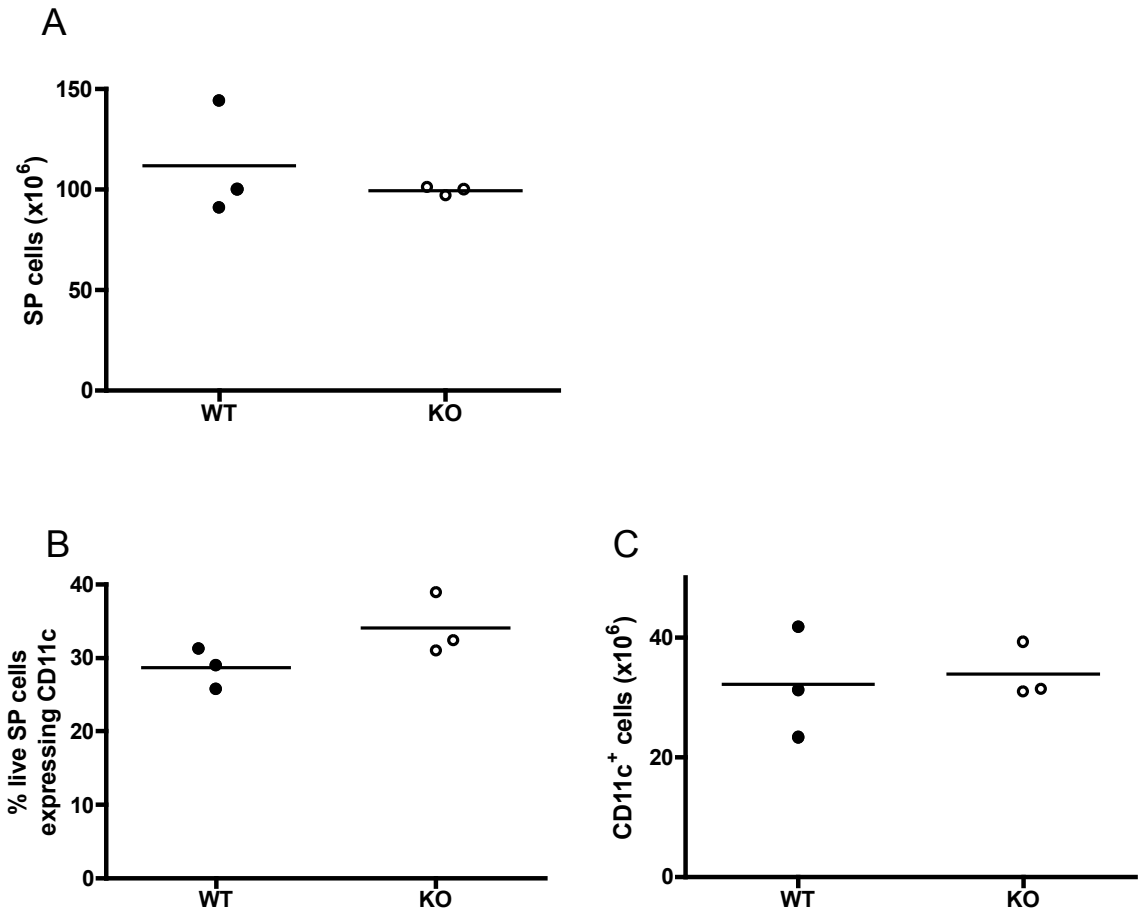

Figure 4.20
DC in the Spleens of CCX-CKR KO and WT Mice After Treatment With Flt3L
CCX-CKR KO and WT mice were injected daily with Flt3L for 10 days and the total numbers of live cells recovered from spleens were determined (A). The proportions (B) and numbers (C) of $CD11c^+$ cells were analysed by flow cytometry. Results show means of 3 mice per group.

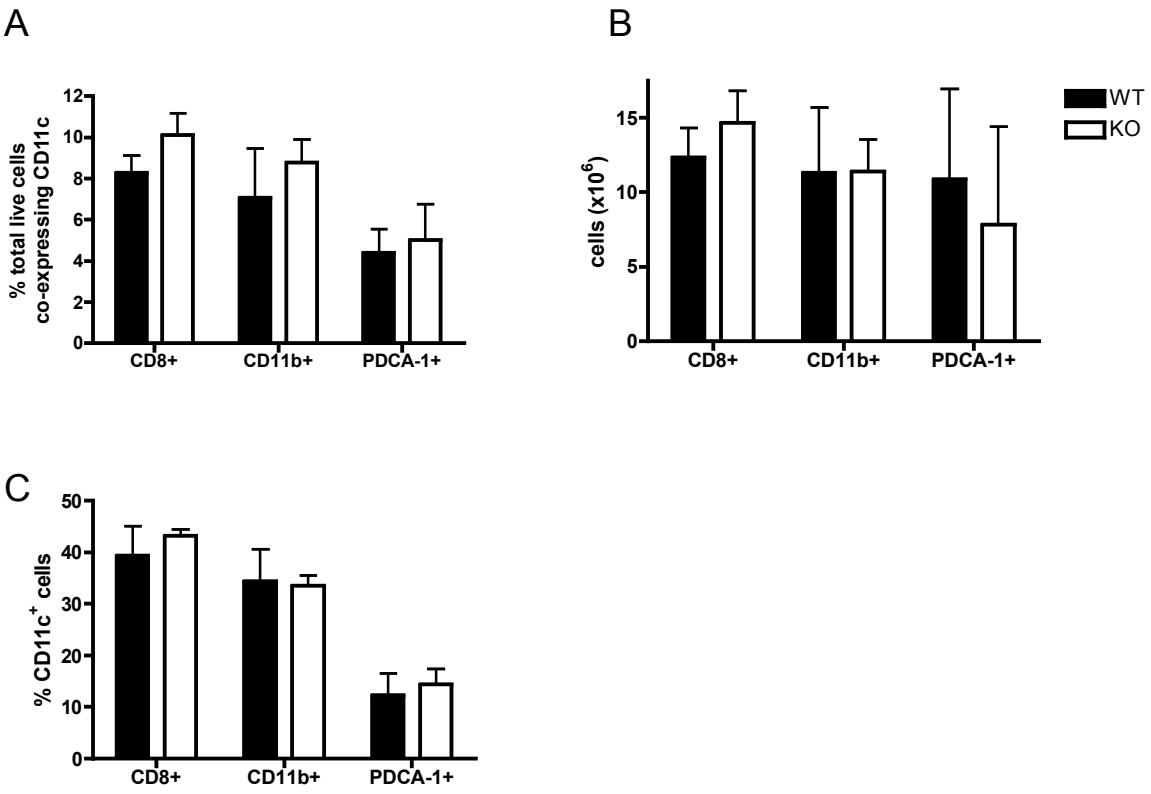

Figure 4.21
DC Subsets in the Spleens of CCX-CKR KO and WT Mice After Treatment With Flt3L
Live gated spleen cells from Flt3L treated CCX-CKR KO and WT mice were analysed for surface expression of CD8, CD11b or PDCA-1 on $CD11c^+$ cells. (A) The proportions and (B) absolute numbers of live cells co-expressing CD11c and individual subset markers are shown (C) The proportions of $CD11c^+$ cells expressing individual subset markers are shown. Results show means +1 SD of 3 mice per group.

Chapter 5

Analysis of Antigen Specific Immune Responses in CCX-CKR KO Mice

Introduction

The CCX-CKR ligands, CCL19 and CCL21 are crucial for co-ordinating liaisons between CCR7 expressing antigen loaded DC and naïve T cells, as well as for regulating B cell interactions with CCR7 expressing primed T cells within secondary lymphoid organs (22, 29, 67, 80). Such prominent roles in the development of adaptive immunity suggest that CCL19 and CCL21 bioavailability and activity must be tightly regulated to avoid the initiation of aberrant and potentially damaging immune responses. As CCX-CKR has been proposed to function as a regulator of CCL19 and CCL21 availability, I thought it would be of interest to explore the effects of CCX-CKR deletion on antigen specific immunity.

The immune system generates active immunity to dangerous foreign antigens and just as importantly, establishes immunological tolerance to innocuous and self-antigens. In the small intestine, this phenomenon is known as oral tolerance and an important manifestation of this is the suppression of antigen specific immune responses to a subsequent systemic challenge (146, 227, 228). Recent work shows that oral tolerance requires CCR7 dependent migration of DC from the gut wall to the draining MLN, indicating a central role for CCR7 and its ligands in regulating homeostasis within the gut (125). The CCX-CKR ligand CCL25 is also important in co-ordinating mucosal immunity. CCR9 co-expression with the integrin $\alpha_4\beta_7$ confers effector T cells with the ability to migrate to the mucosa from the blood in response to CCL25 produced by small intestine epithelial cells (212, 221). CCR9 is also expressed on pDC and plasma cells within the small intestinal lamina propria and both T cells and pDC are decreased in numbers in the lamina propria of CCR9 KO mice (121).

For these reasons, I hypothesised that CCX-CKR may play an important role in co-ordinating immune responses and tolerance, especially those originating in the intestine. I therefore explored systemic immune responses to subcutaneous immunisation with OVA in adjuvant, the generation of tolerance and immunity by feeding OVA and the induction of intestinal inflammation by oral administration of DSS.

5.1 Assessment of antigen specific immune responses in CCX-CKR KO mice

WT and CCX-CKR KO mice were immunised subcutaneously in the hind footpad with OVA emulsified in CFA. 3 weeks later, systemic DTH responses were measured by challenging the

opposite hind footpad with heat aggregated OVA (HAO) and blood was taken to assess OVA specific IgG1 and IgG2a antibody production (Fig 5.1A).

Both CCX-CKR KO and WT mice developed good DTH responses, as well as OVA specific IgG1 and IgG2a antibodies after immunisation and there were no significant differences between mouse strains (Fig 5.1B-D). In a separate experiment, mice received OVA emulsified in CFA in the footpad as above and 2 weeks later the draining popliteal LN were removed, the numbers of $CD4^+$, $CD8^+$ and $CD19^+$ lymphocytes were assessed by FACS and LN cells were re-stimulated *in vitro* with OVA or anti-CD3/CD28 (Fig 5.2A). The draining popliteal LN of immunised mice contained approximately 25% $CD4^+$ T cells, 20% $CD8^+$ T cells and 50% $CD19^+$ B cells, with no significant differences between CCX-CKR KO and WT mice. The absolute numbers of total cells and individual cell subsets were also identical (Figs 5.2B and C). Both WT and CCX-CKR KO popliteal LN cells proliferated and produced IFNγ robustly in response to anti-CD3/CD28 with no significant differences between the strains. Lesser, but still considerable proliferation and IFNγ production occurred in a dose dependent manner after re-stimulation of popliteal LN cells with OVA and again, these responses were not affected by the absence of CCX-CKR (Figs 5.2D and E). Together these results indicate that CCX-CKR does not have an essential role in priming of systemic T or B cell responses.

5.2 Assessment of oral tolerance induction in CCX-CKR KO mice using a single high dose feed

I next decided to investigate whether oral tolerance induction is affected by CCX-CKR deletion using a single high dose of protein.

WT and CCX-CKR KO mice were fed a single dose of 25mg OVA or PBS as a negative control. 1 week later, mice were immunised in the footpad with OVA emulsified in CFA and 3 weeks later, systemic DTH and serum antibody responses were assessed as described above (Fig 5.3A). As before, control CCX-CKR KO and WT mice that were fed PBS, developed good OVA specific DTH, IgG1 and IgG2a responses that did not differ between the strains. In each of the 3 experiments performed, WT mice that received OVA orally prior to immunisation showed a significantly reduced DTH response compared with PBS controls, indicating the induction of oral tolerance (Fig 5.3B). OVA specific IgG2a antibody responses were also lower in OVA fed WT mice than in PBS controls, although this was only significant

in one experiment (Fig 5.4). In contrast, OVA fed CCX-CKR KO mice did not show significant oral tolerance induction in any of the experiments, with identical OVA specific DTH and IgG2a responses in OVA fed and PBS fed groups (Figs 5.3B, 5.4). There was no significant suppression of OVA specific IgG1 antibody responses in WT or CCX-CKR KO OVA fed mice in any experiment.

In a further experiment, WT and CCX-CKR KO mice were fed PBS or 25mg OVA and 1 week later immunised in the hind footpad with OVA emulsified in CFA. 2 weeks after this, the draining popliteal LN were removed, cells isolated and re-stimulated *in vitro* with different doses of OVA to assess proliferation and IFNγ production (Fig 5.5A). Both CCX-CKR KO and WT cells from PBS fed mice proliferated in response to different doses of OVA. In both strains, these responses were reduced in OVA fed mice compared with PBS fed mice, although these effects were not statistically significant (Figs 5.5B and C). Similar results were obtained when IFNγ production was assessed, with OVA specific cytokine levels being reduced to similar extents in OVA fed CCX-CKR KO and WT mice compared with PBS fed controls. Again however these effects were not statistically significant (Fig 5.6).

5.3 Assessment of oral tolerance induction in CCX-CKR KO mice using multiple low dose feeds

As it has been suggested that different mechanisms may cause oral tolerance depending on the feeding regime employed, I went on to investigate if the apparent defect in oral tolerance development I had observed in CCX-CKR KO mice could be reproduced using a different protocol. CCX-CKR KO and WT mice were fed 1mg OVA daily over 5 consecutive days and immunised in the footpad with OVA/CFA 1 week after the last feed. 3 weeks later, systemic OVA specific DTH and antibody responses were assessed and as before, there were no significant differences in these responses between PBS fed CCX-CKR KO and WT mice (Fig 5.7). As with feeding a single high dose of antigen, DTH responses were reduced in WT mice fed multiple low doses of OVA compared with PBS controls, although this effect was not statistically significant in this instance. In contrast, DTH responses were not reduced in CCX-CKR KO mice fed multiple low doses of OVA compared with PBS controls and, if anything, appeared slightly elevated, although this was not statistically significant (Fig 5.7B).

As I found with high dose OVA feeding, WT mice fed multiple low doses of OVA had significantly reduced OVA specific IgG2a antibody levels compared with PBS fed controls whereas OVA specific IgG1 levels were identical in the two groups. OVA specific IgG1 and IgG2a levels were not significantly different between CCX-CKR KO mice fed OVA or PBS (Fig 5.8).

Together these findings indicate there is a defect in oral tolerance in CCX-CKR KO mice that is not influenced by the feeding regime used.

5.4 Assessment of oral priming in CCX-CKR KO mice

In view of the apparent defect in oral tolerance in CCX-CKR KO mice, I decided to investigate if there was also a difference in the ability of these mice to be primed by feeding antigen with a mucosal adjuvant.

WT and CCX-CKR KO mice were fed PBS, 10mg OVA alone, or 10mg OVA together with 10μg CT on three occasions 10 days apart. 10 days after the last feed, all groups were challenged in the footpad with HAO to assess priming of systemic DTH responses and serum was taken for the measurement of OVA specific IgG, IgG1, IgG2a and IgA responses (Fig 5.9A). Both CCX-CKR KO and WT mice fed OVA+CT appeared to show priming of OVA specific DTH responses, with increases in footpad thickness approximately twice or three times those in the negative controls fed OVA or PBS alone for WT and CCX-CKR KO mice respectively. However, this increase was only statistically significant for CCX-CKR KO mice although, there were no significant differences in the OVA specific DTH responses between primed CCX-CKR KO and WT mice (Fig 5.9B).

OVA specific antibody responses were assessed in 3 separate experiments (Figs 5.10-5.12). In the first, CCX-CKR KO mice fed OVA+CT showed elevated levels of OVA specific serum total IgG, IgG1, IgG2a and IgA antibodies compared with WT OVA+CT fed mice, which showed little evidence of priming in this experiment, apart from slightly elevated levels of IgG1 compared with OVA or PBS fed controls. However, levels of OVA specific total IgG and IgG2a were significantly elevated in OVA+CT fed CCX-CKR KO mice compared to primed WT mice and to OVA or PBS fed controls (Fig 5.10). In the second experiment, virtually no OVA specific serum antibody was detectable in PBS fed mice for either strain,

while OVA+CT fed CCX-CKR KO and WT mice showed some OVA specific IgG and IgG1 antibody production. CCX-CKR KO but not WT mice fed OVA alone also had detectable OVA specific IgG, IgG1 and IgA antibodies. Again, CCX-CKR KO mice fed OVA+CT had consistent levels of OVA specific antibody production of all kinds, which were much higher than those of PBS or OVA fed CCX-CKR KO mice. The OVA specific total IgG, IgG2a and IgA responses of OVA+CT fed CCX-CKR KO mice were higher than in OVA+CT fed WT, although only their OVA specific IgA responses were significantly increased. Robust OVA specific IgG1 responses were found in both OVA+CT fed CCX-CKR KO and WT mice (Fig 5.11). In the third experiment, there was also evidence of priming of OVA specific IgG antibody in OVA+CT fed CCX-CKR KO and WT mice with the levels of OVA specific total IgG and IgG1 being identical in both strains of mice. However, again, the levels of OVA specific IgG2a and IgA were elevated in primed CCX-CKR KO mice compared with WT mice fed OVA+CT although this was not statistically significant. WT mice fed OVA alone, had little or no OVA specific antibodies but again OVA fed CCX-CKR KO mice showed elevated levels of OVA specific total IgG and IgG1 compared with PBS fed controls, although this was not statistically significant (Fig 5.12). Collectively these experiments indicated an enhanced ability to prime systemic antibody production by feeding antigen with adjuvant to CCX-CKR KO mice, especially with respect to serum IgG2a and IgA.

As my results suggested that antigen specific IgG antibody titres might be higher in CCX-CKR KO mice, I thought it important to ensure that this did not reflect a generalised increase in circulating immunoglobulin levels. Therefore I assessed total IgG levels in the CCX-CKR KO and WT mice fed OVA+CT, OVA alone or PBS in the second of the oral priming experiments described above. All these samples had identical levels of total serum IgG, suggesting that the differences I observed were due to genuine variations in antigen specific mucosal priming of immune responses (Fig 5.13).

To examine whether the susceptibility of CCX-CKR KO mice to priming by oral administration of antigen extended to mucosal immune responses, I determined the levels of OVA specific intestinal IgA in the faeces of CT primed CCX-CKR KO and WT mice. CCX-CKR KO and WT mice fed OVA alone showed no OVA specific IgA antibody levels above those of PBS fed controls. There was no significant production of OVA specific IgA in WT mice fed OVA+CT, with only two mice showing any IgA above background. However, the

majority of CCX-CKR KO mice fed OVA+CT had detectable OVA specific IgA antibodies, with a significant difference between this group and all other groups (Fig 5.14A). Again, this seemed to be due to priming of specific immunity, as there were no differences in total intestinal IgA levels between any of the six groups (Fig 5.14B).

5.5 Assessment of DSS colitis in CCX-CKR KO mice

So far, I have addressed the induction of antigen specific mucosal immunity and tolerance in CCX-CKR KO mice, responses that are induced predominantly via the small intestine. In the next experiments, I decided to explore whether inflammatory effector responses in the large intestine were also affected in these animals. To do this I used a model of colitis induced by the oral administration of DSS.

Mice received 2% DSS in their drinking water for 7 days, while control mice received normal drinking water. As expected, WT mice lost weight after administration of DSS from day 5 onwards, losing approximately 15% of their body weight by day 7. An identical pattern of weight loss was also seen in CCX-CKR KO mice (Fig 5.15A). Clinical disease was determined by monitoring weight loss, the presence of diarrhoea and rectal bleeding. The combined clinical scores showed progressive disease in all mice and there were no significant differences between CCX-CKR KO and WT mice (Fig 5.15B). Both groups also had similar and significant reductions in colon length compared with controls when sacrificed on day 7 (Fig 5.15C).

Sections of distal colon segments from CCX-CKR KO and WT control and DSS treated mice on day 7 were stained with haematoxylin and eosin (H&E) to visualise mucosal architecture integrity and cellular infiltrates. The colons of CCX-CKR KO and WT mice given DSS both showed gross disruption of colon crypts and loss of the surface epithelial layer, together with extensive cellular infiltration of the mucosa (Fig 5.16). Thus there were no obvious differences in the colon inflammation induced by oral administration of DSS between CCX-CKR KO and WT mice.

To extend these findings, I used Luminex analysis to assess the production of cytokines and chemokines from explants of distal and proximal colons of DSS treated CCX-CKR KO and WT mice. As expected, this showed the presence of inflammatory cytokines such as IL-1α,

IL-1β, IL-6 and TNFα and VEGF in supernatants of distal colon explants, with no significant differences between CCX-CKR KO and WT mice. Other cytokines such as IL-10 and IFN-γ (Fig 5.17) as well as GMCSF and FGF (Fig 5.18) were also detectable, but much less consistently and generally at lower levels. In most cases, cytokines were produced at much lower levels than from the proximal colon explants, confirming the pattern of disease pathology in this model. Similar patterns of production of the chemokines CCL2, CCL3, CCL4, CCL5, CXCL1, CXCL9 and CXCL10 were seen, with generally higher levels in inflamed distal colon. Again, there were no significant differences between CCX-CKR KO and WT mice (Fig 5.19).

Summary

In this chapter, I have begun to characterise the development of systemic and mucosal immunity and tolerance in CCX-CKR KO mice.

There were no significant differences in systemic immune responses to subcutaneous immunisation with OVA/CFA between CCX-CKR KO and WT mice when assessed *in vivo* or *in vitro*. However, the development of oral tolerance in CCX-CKR KO mice was impaired, with a lack of the suppression of OVA specific DTH responses seen in WT mice fed a single high dose of OVA. In addition, IgG2a antibody responses were not suppressed in CCX-CKR KO mice fed a single high dose or multiple low doses of OVA, but were tolerised in WT mice. However, both groups of OVA fed mice showed similar suppression of T cell proliferation and IFNγ production following re-stimulation *in vitro*, while serum OVA specific IgG1 antibody responses were not significantly suppressed by feeding either CCX-CKR KO or WT mice. Together these data suggest that the suppression of antigen specific Th_1 responses by oral tolerance may be dependent on CCX-CKR *in vivo*.

In parallel with defective systemic tolerance after feeding OVA, CCX-CKR KO mice appeared much more susceptible to priming of systemic and local antibody responses after feeding OVA with CT as a mucosal adjuvant. Although both CCX-CKR KO and WT mice developed robust systemic OVA specific IgG1 responses after feeding OVA+CT, only CCX-CKR KO mice showed evidence of systemic OVA specific IgG2a and IgA or intestinal OVA-specific IgA. In addition, there was some evidence of priming of OVA specific antibody responses in CCX-CKR KO mice fed OVA alone which was not seen in WT mice.

Despite this evidence of abnormal mucosal immunity, CCX-CKR KO mice developed DSS colitis normally, with all indices of disease being identical in CCX-CKR KO and WT animals.

Together these results indicate that there are selective defects in the regulation of mucosal immune responses in CCX-CKR KO mice and in the next chapter I went on to investigate the cellular basis of this, examining in particular the role of pDC function and migration.

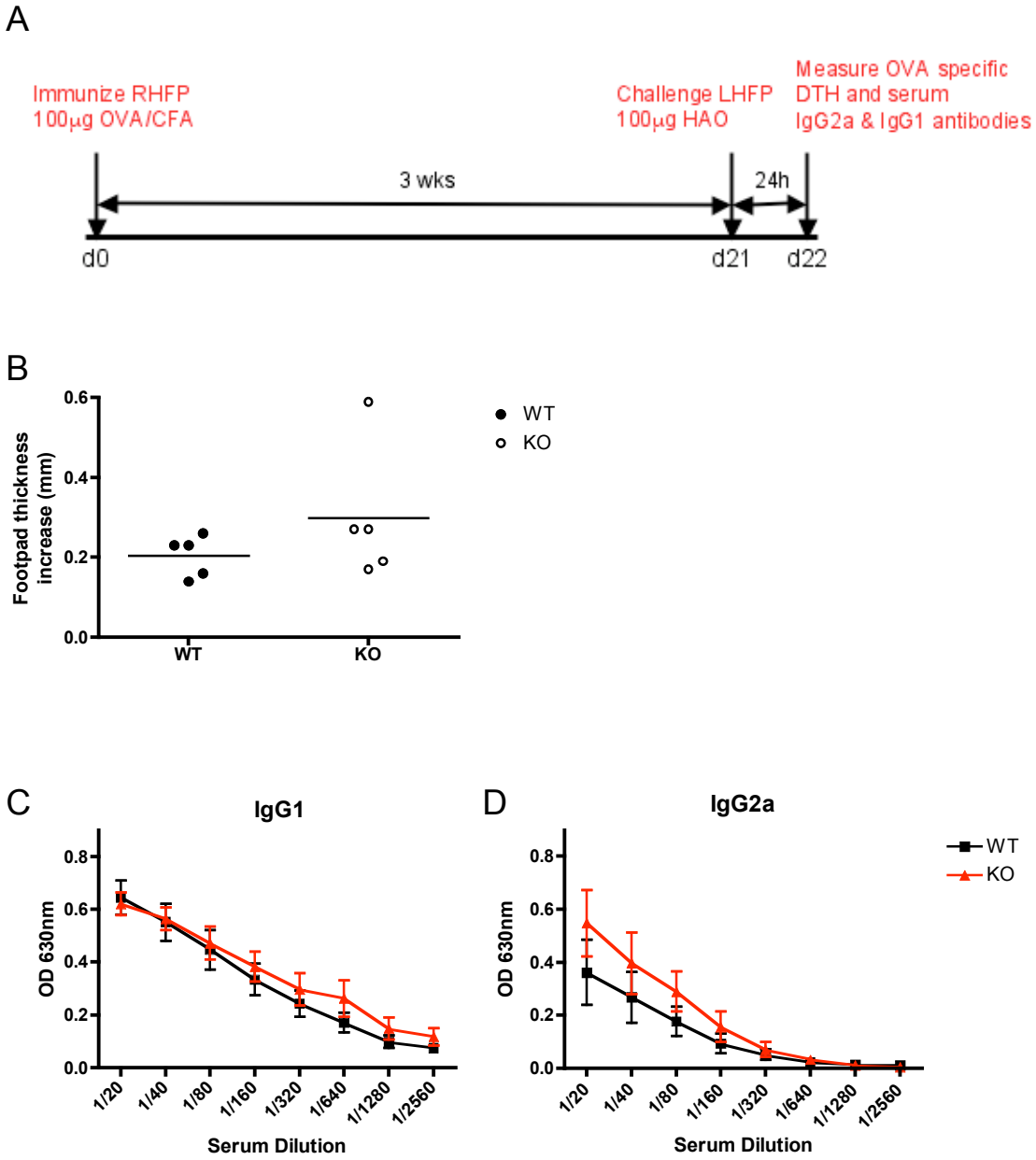

Figure 5.1
Priming of DTH and Antibody Responses by Systemic Immunisation of CCX-CKR KO and WT Mice
(A) CCX-CKR KO and WT mice were immunised in the right hind footpad (RHFP) with ovalbumin (OVA) emulsified in complete Freund's adjuvant (CFA). 21 days later, mice were challenged in the contralateral footpad with heat-aggregated OVA (HAO) and 24 hours later, OVA specific DTH responses were assessed by measuring footpad swelling (B). OVA specific serum IgG1 (C) and IgG2a antibodies (D) were determined by ELISA. Results show the individual footpad increments and mean OD 630nm +/- 1 SEM of serially diluted sera of 5 mice per group.

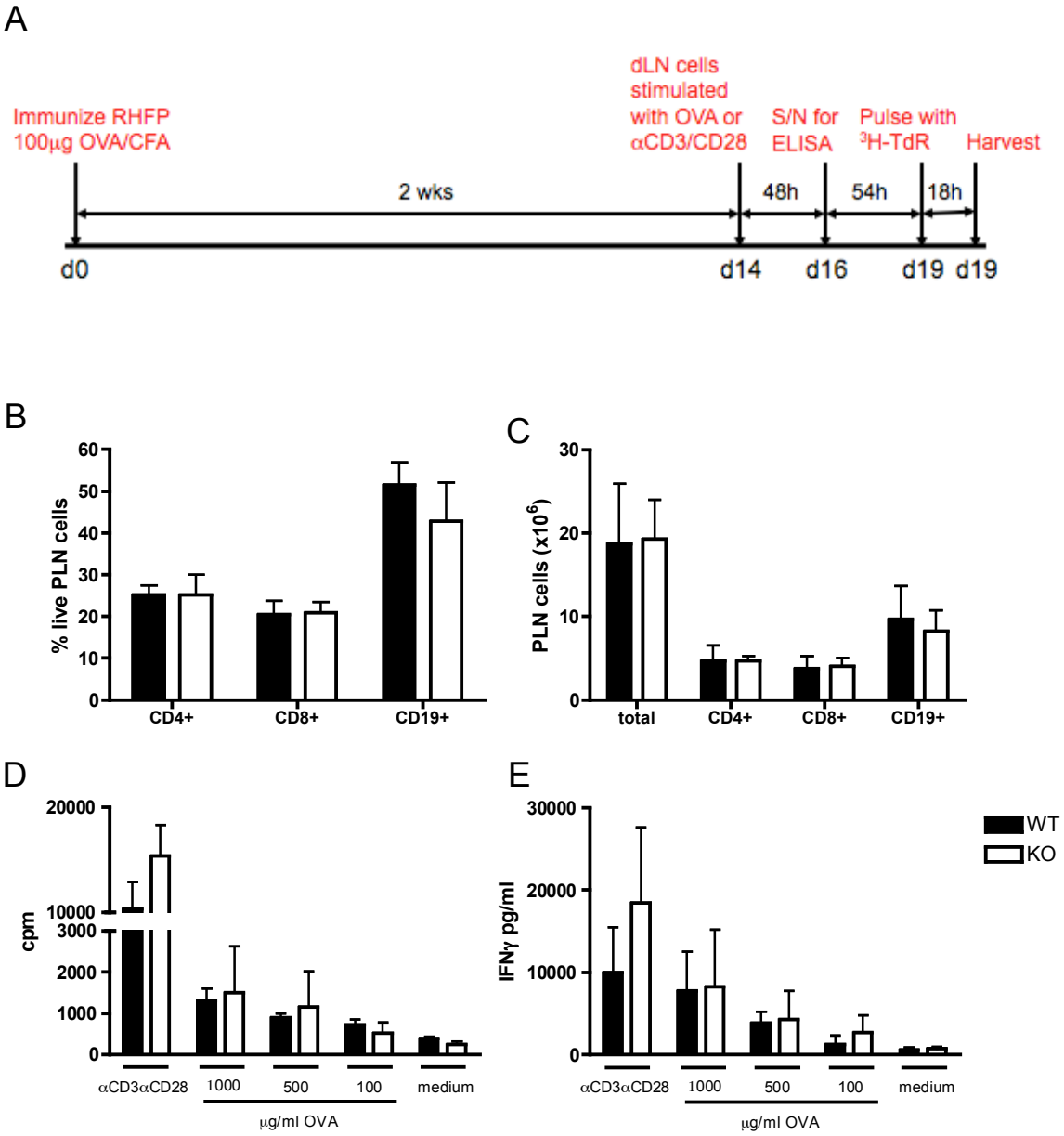

Figure 5.2
Priming of *In Vitro* Immune Responses by Systemic Immunisation of CCX-CKR KO and WT Mice
(A) CCX-CKR KO and WT mice were immunised in the hind footpad with OVA emulsified in CFA. 14 days later, the draining popliteal lymph nodes were removed, cells isolated and restimulated with either αCD3/CD28, different concentrations of OVA, or medium alone *in vitro*. Cells were cultured for 120 hours and ^{3}H-TdR was added for the final 18 hours of culture. The proportions (B) and numbers (C) of $CD4^{+}$, $CD8^{+}$ and $CD19^{+}$ cells from draining popliteal lymph nodes (dLN) were determined by flow cytometry. Proliferation was assessed by ^{3}H-TdR incorporation (D) and IFNγ production was measured by ELISA (E). Results show means +1 SD of 4 mice per group.

A

B

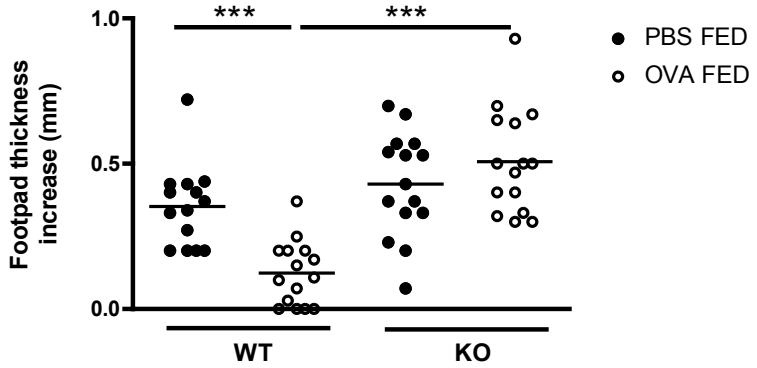

Figure 5.3
***In Vivo* Assessment of High Dose Oral Tolerance Induction in CCX-CKR KO and WT Mice**
(A) CCX-CKR KO and WT mice were fed a single dose of 25mg OVA or PBS and immunised in the right hind footpad with OVA emulsified in CFA 7 days later. 21 days later, mice were challenged in the contralateral footpad with HAO and 24 hours later, OVA specific DTH responses were assessed. (B) OVA specific DTH responses are shown as the mean footpad increments of 14-15 mice per group and are pooled from 3 individual experiments.

Two way Anova with Bonferroni post tests ***$p<0.001$

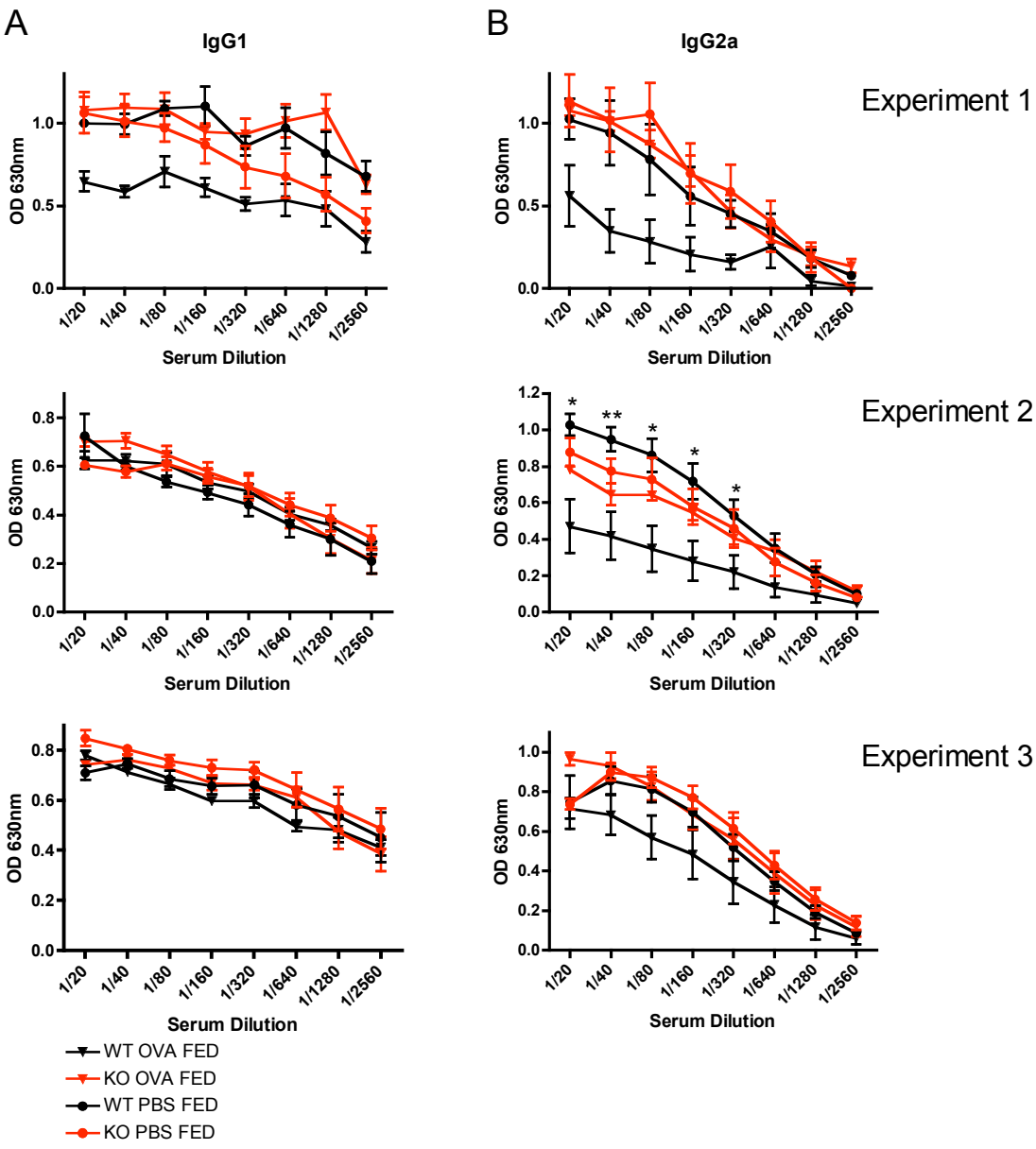

Figure 5.4
***In Vivo* Assessment of High Dose Oral Tolerance Induction in CCX-CKR KO and WT Mice**
CCX-CKR KO and WT mice were fed a single dose of 25mg OVA or PBS and immunised in the hind footpad with OVA emulsified in CFA 7 days later. 21 days later, mice were challenged in the contralateral footpad with HAO and 24 hours later, OVA specific serum IgG1 (A) and IgG2a (B) antibody responses were assessed by ELISA in 3 separate experiments. Results show the mean OD 630nm +/- 1 SEM of serially diluted sera from 4-5 mice per group for each experiment.

**p<0.01 *p<0.05 Mann Whitney test comparing WT OVA and PBS fed groups

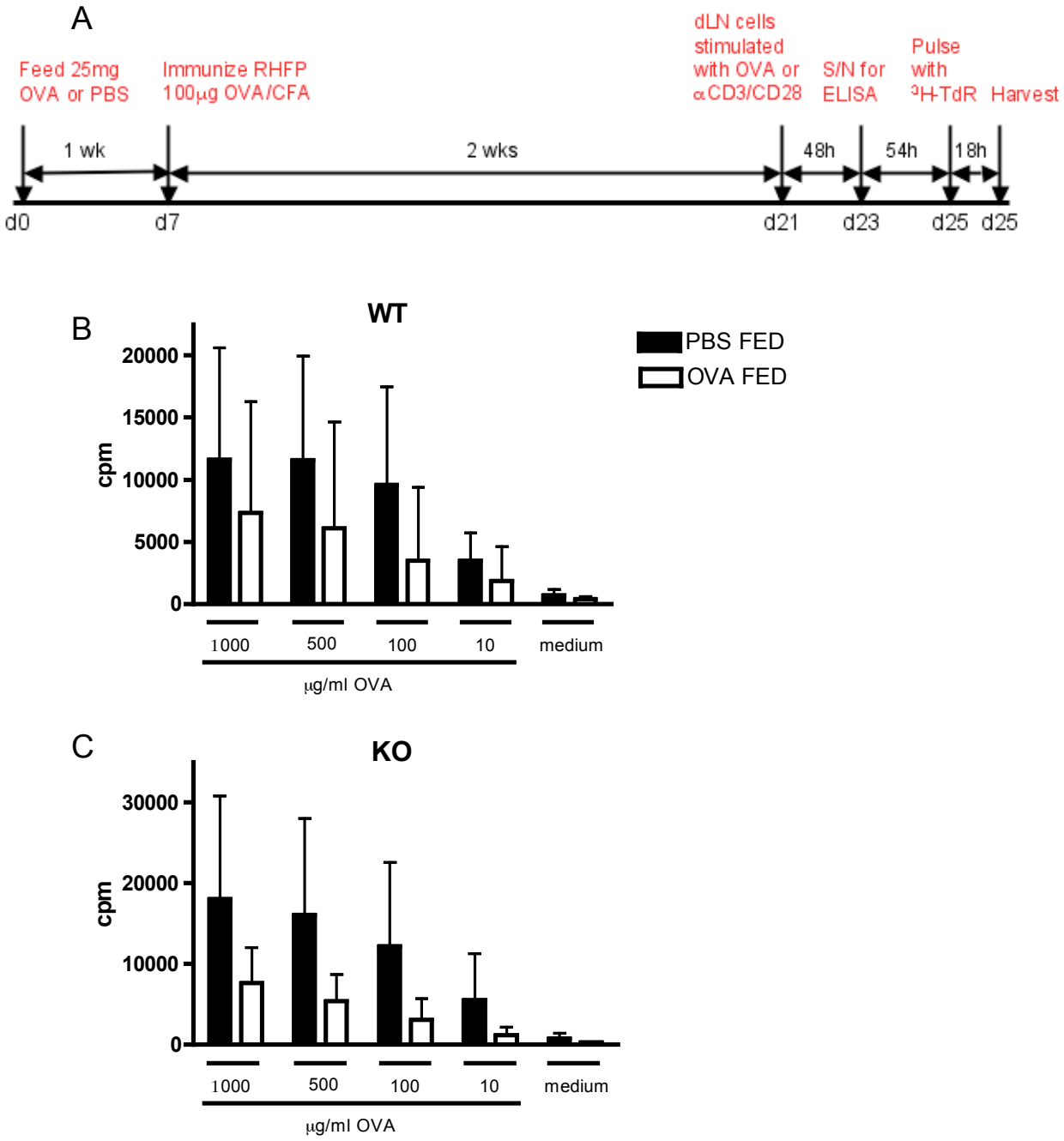

Figure 5.5
***In Vitro* Assessment of High Dose Oral Tolerance Induction in CCX-CKR KO and WT Mice**
(A) CCX-CKR KO and WT mice were fed a single high dose of 25mg OVA or PBS and immunised in the right hind footpad with OVA emulsified in CFA 7 days later. 14 days later, the draining popliteal lymph nodes were removed, cells isolated and restimulated with either αCD3/CD28, different concentrations of OVA, or with medium alone *in vitro*. WT (B) and CCX-CKR KO (C) cells were cultured for 120 hours and ^{3}H-TdR was added for the final 18 hours of culture. Results show mean cpm +1 SD of 4 mice per group.

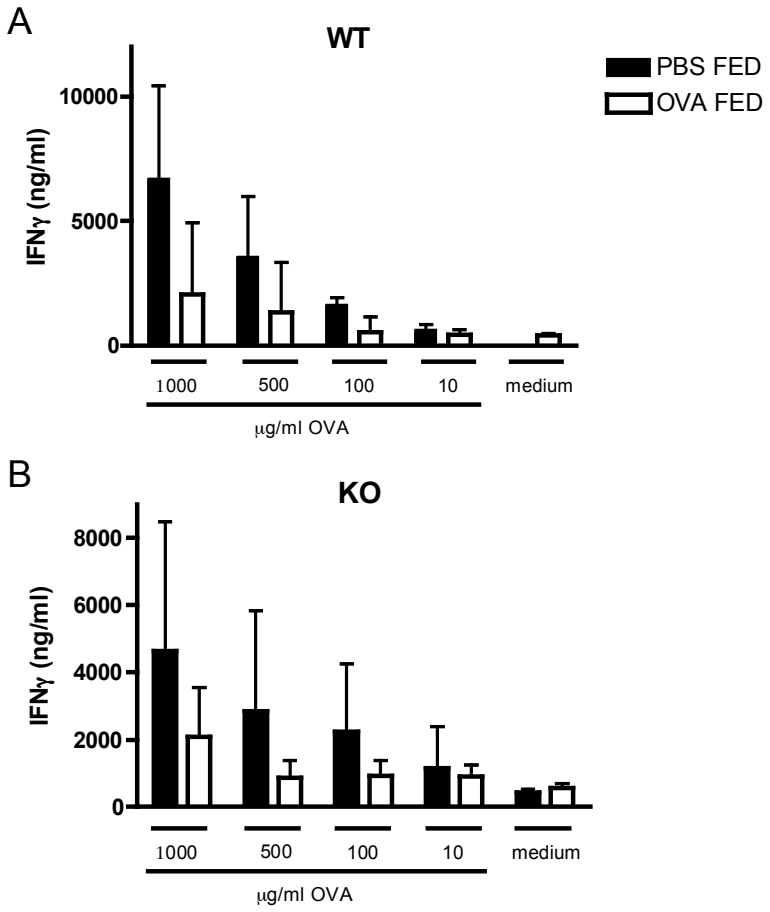

Figure 5.6
***In Vitro* Assessment of High Dose Oral Tolerance Induction in CCX-CKR KO and WT Mice**
(A) CCX-CKR KO and WT mice were fed a single high dose of 25mg OVA or PBS and immunised in the right hind footpad with OVA emulsified in CFA 7 days later. 14 days later, the draining popliteal lymph nodes were removed, cells isolated and restimulated with either αCD3/CD28, different concentrations of OVA or with medium alone *in vitro*. (B) WT and (C) KO cells were cultured for 48 hours before supernatants were removed for analysis of IFNγ production by ELISA. Results show means +1 SD of 4 mice per group.

A

B

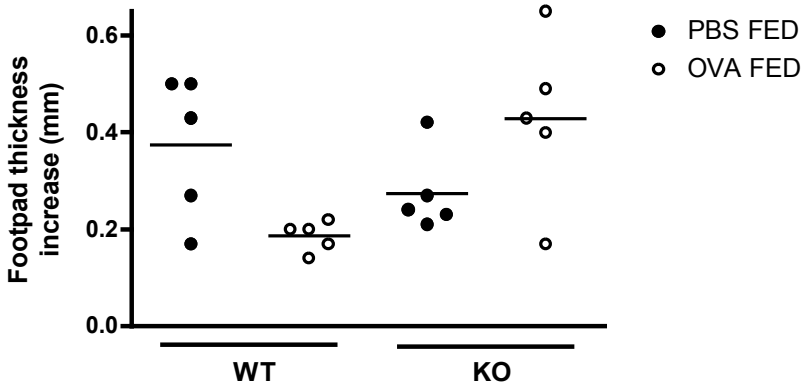

Figure 5.7
***In Vivo* Assessment of Low Dose Oral Tolerance Induction in CCX-CKR KO and WT Mice**
(A) CCX-CKR KO and WT mice were fed a daily dose of 1mg OVA or PBS over 5 consecutive days and immunised in the right hand footpad with OVA emulsified in CFA 7 days after the final feed. 21 days later, mice were challenged in the contralateral footpad with HAO and 24 hours later, OVA specific DTH responses were assessed. (B) OVA specific DTH responses are shown as the mean footpad increments of 5 mice per group.

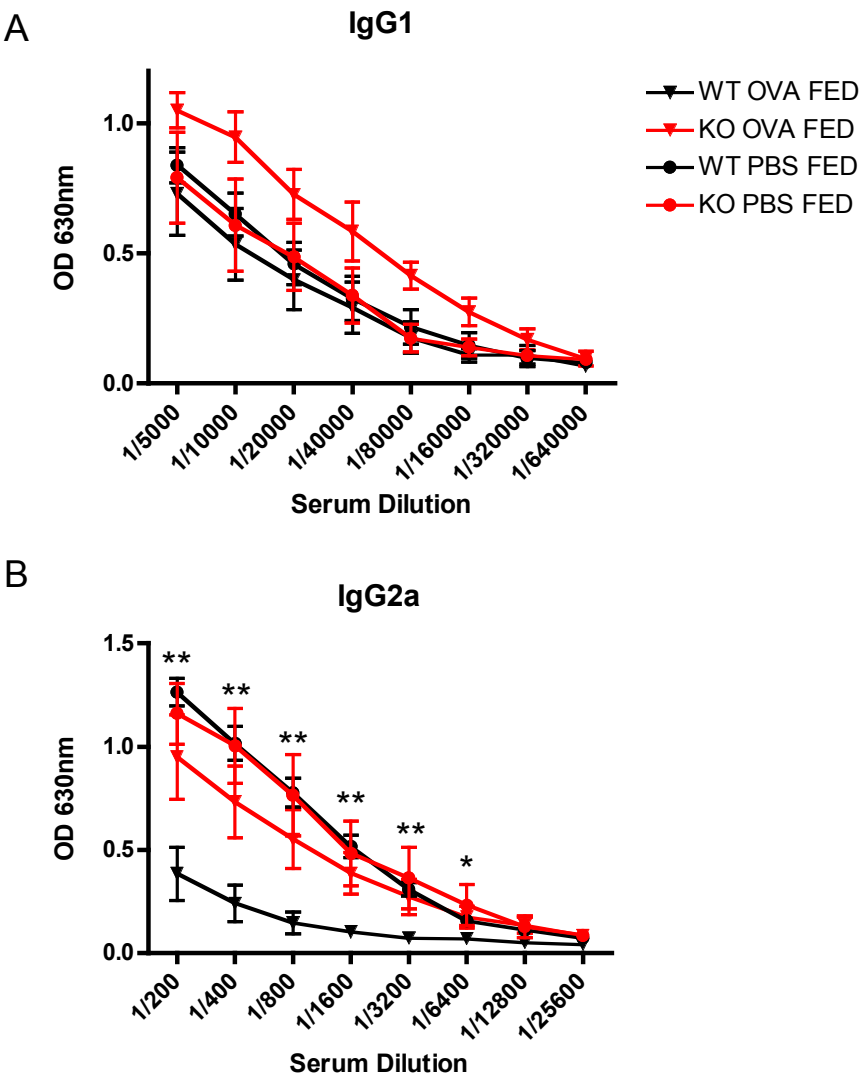

Figure 5.8
***In Vivo* Assessment of Low Dose Oral Tolerance Induction in CCX-CKR KO and WT Mice**
(A) CCX-CKR KO and WT mice were fed a daily dose of 1mg OVA or PBS over 5 consecutive days and immunised in the right hand footpad with OVA emulsified in CFA 7 days later. 21 days later, mice were challenged in the contralateral footpad and 24 hours later, OVA specific serum IgG1 (A) and IgG2a (B) antibody responses were assessed by ELISA. Results show the mean OD 630nm +/- 1 SEM of serially diluted sera from 5 mice per group.

**p<0.01 *p<0.05 Mann Whitney test comparing WT OVA and PBS fed groups

A

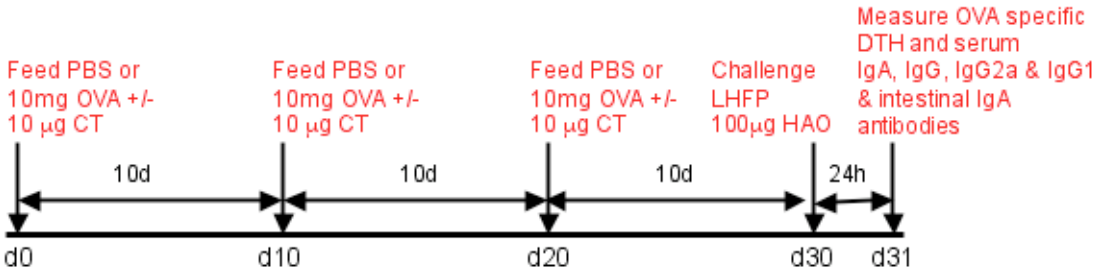

B

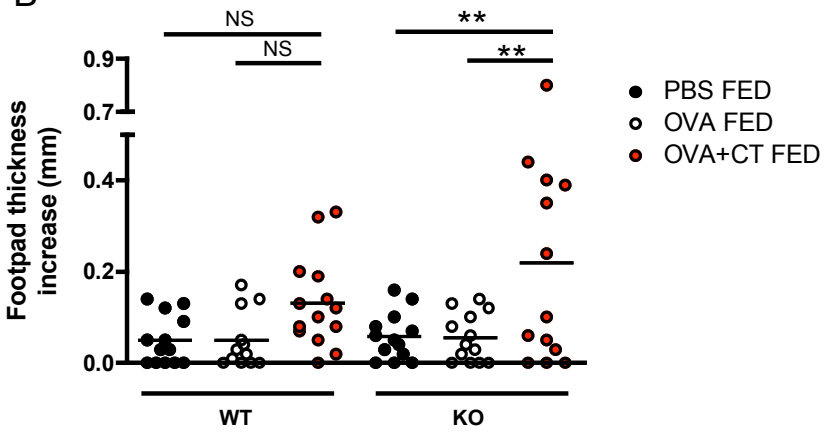

Figure 5.9
Priming of CCX-CKR KO and WT Mice by Oral Administration of Antigen
CCX-CKR KO and WT mice were fed 3 doses of 10mg OVA alone or together with 10μg CT or PBS alone 10 days apart. 10 days after the final feed, mice were challenged in the footpad with HAO and 24 hours later, OVA specific DTH responses were assessed. (B) OVA specific increases in footpad thickness are shown as the mean footpad increments of 11-14 mice per group and are pooled from 3 individual experiments.

Two way Anova with Bonferroni post tests **p<0.01

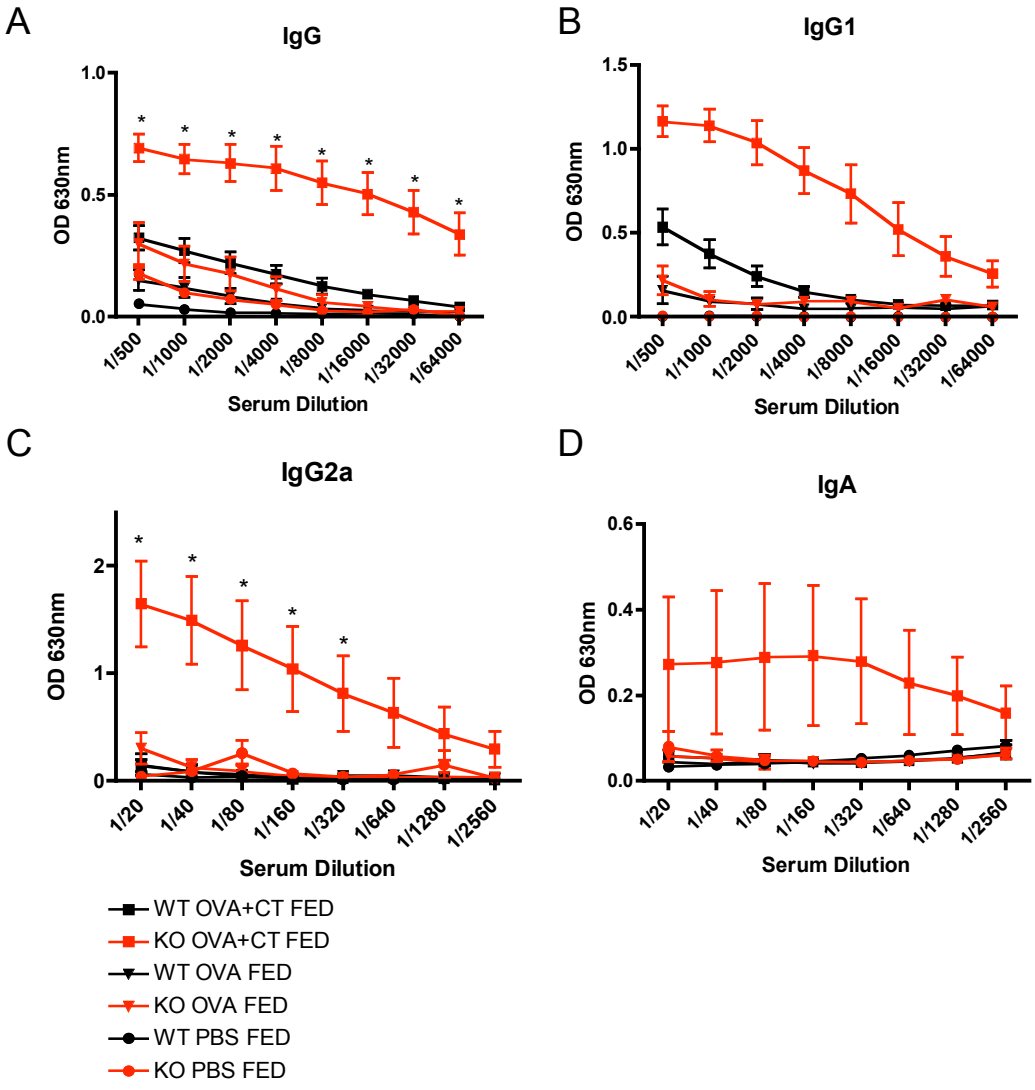

Figure 5.10
Priming of CCX-CKR KO and WT Mice by Oral Administration of Antigen
CCX-CKR KO and WT mice were fed 3 doses of 10mg OVA+10μg CT, 10mg OVA, or PBS alone 10 days apart. 11 days after the final feed, OVA specific IgG (A), IgG1 (B), IgG2a (C) and IgA (D) levels in the serum were determined by ELISA. Results show mean OD 630nm +/- 1 SEM of serially diluted sera from 4-5 mice per group.

*p<0.01 Mann Whitney test comparing WT OVA+CT FED and KO OVA+CT FED groups

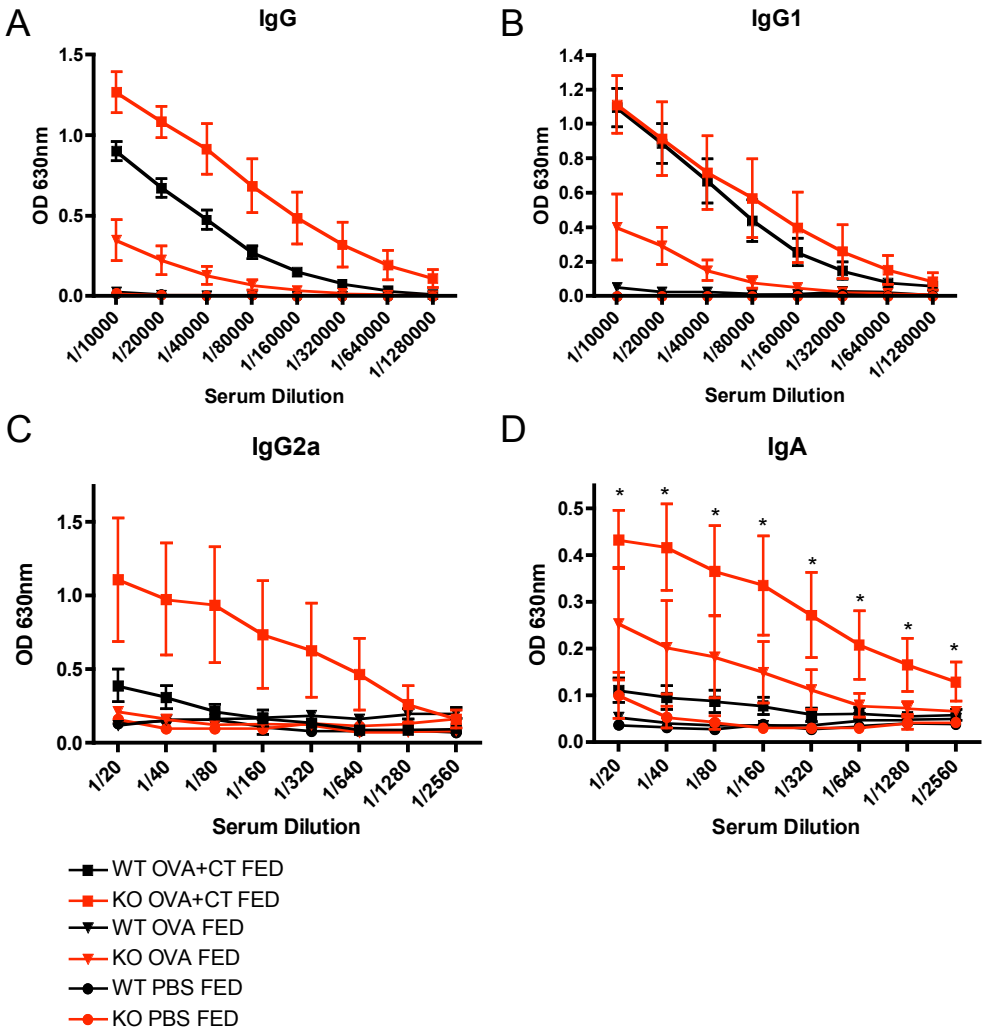

Figure 5.11
Priming of CCX-CKR KO and WT Mice by Oral Administration of Antigen
CCX-CKR KO and WT mice were fed 3 doses of 10mg OVA+10μg CT, 10mg OVA or, PBS alone 10 days apart. 11 days after the final feed, OVA specific IgG (A), IgG1 (B), IgG2a (C) and IgA (D) levels in the serum were determined by ELISA. Results show mean OD 630nm +/- 1 SEM of serially diluted sera from 4-5 mice per group.

*p<0.01 Mann Whitney test comparing WT OVA+CT FED and KO OVA+CT FED groups

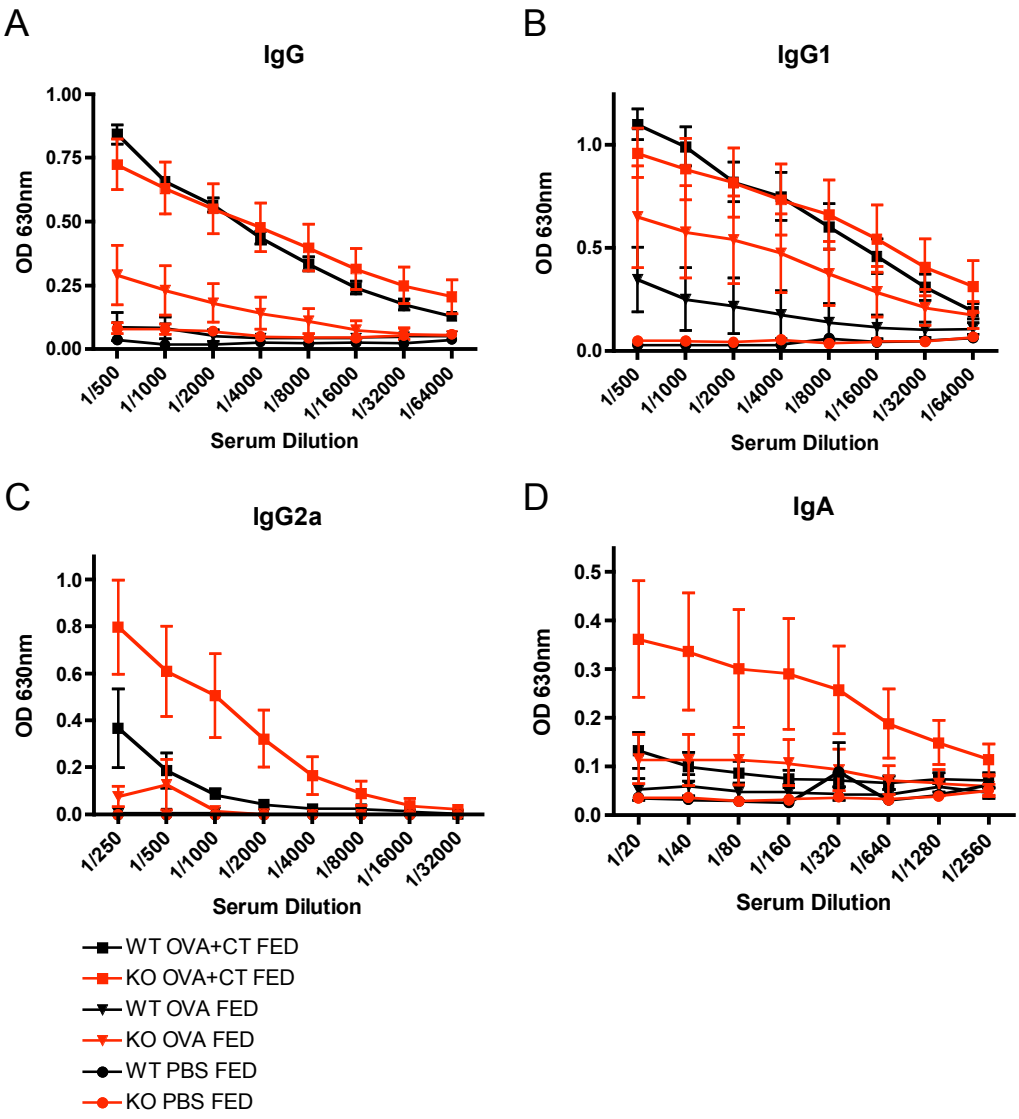

Figure 5.12
Priming of CCX-CKR KO and WT Mice by Oral Administration of Antigen
CCX-CKR KO and WT mice were fed 3 doses of 10mg OVA+10μg CT, 10mg OVA, or PBS alone 10 days apart. 11 days after the final feed, OVA specific IgG (A), IgG1 (B), IgG2a (C) and IgA (D) levels in the serum were determined by ELISA. Results show mean OD 630nm +/- 1 SEM of serially diluted sera from 4-5 mice per group.

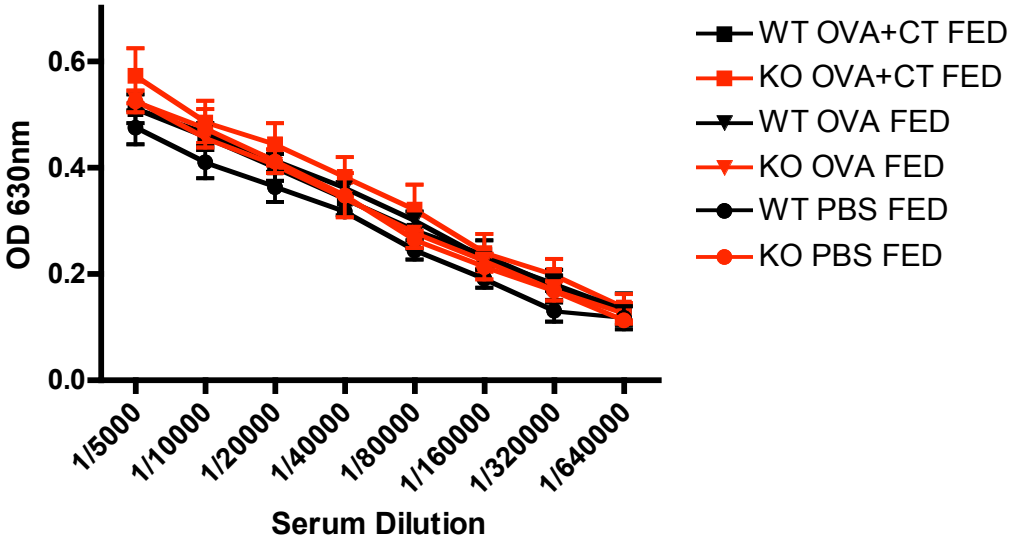

Figure 5.13
Total Serum IgG Levels in in CCX-CKR KO and WT Mice
CCX-CKR KO and WT mice were fed 3 doses of 10mg OVA+10μg CT, 10mg OVA, or PBS alone 10 days apart. 11 days after the final feed, total IgG levels in the serum were determined by ELISA. Results show mean OD 630nm +/- 1 SEM of serially diluted sera from 4-5 mice per group.

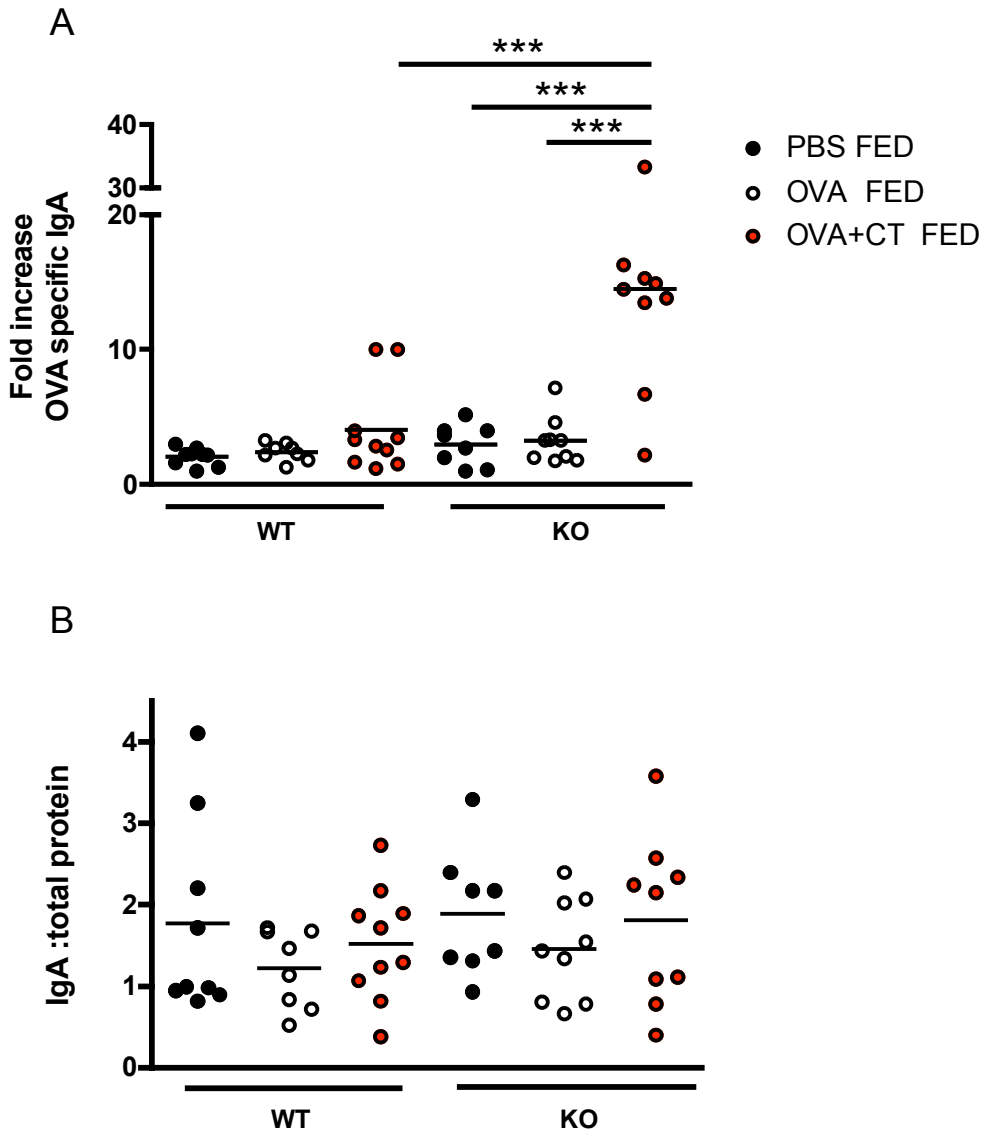

Figure 5.14
Priming of Local IgA Antibody Responses by Oral Administration of OVA+CT in CCX-CKR KO and WT Mice
(A) OVA specific IgA levels in the faeces were measured 11 days after the final feed of antigen, calculated as the fold increase in the ratio of specific IgA:total protein relative to that of PBS fed mice. (B) Mean IgA levels in faeces are shown, calculated as the ratio of OD 630nm of specific IgA relative to the total protein levels of 9-10 mice per group.

Two way Anova with Bonferroni post tests *** $p<0.001$

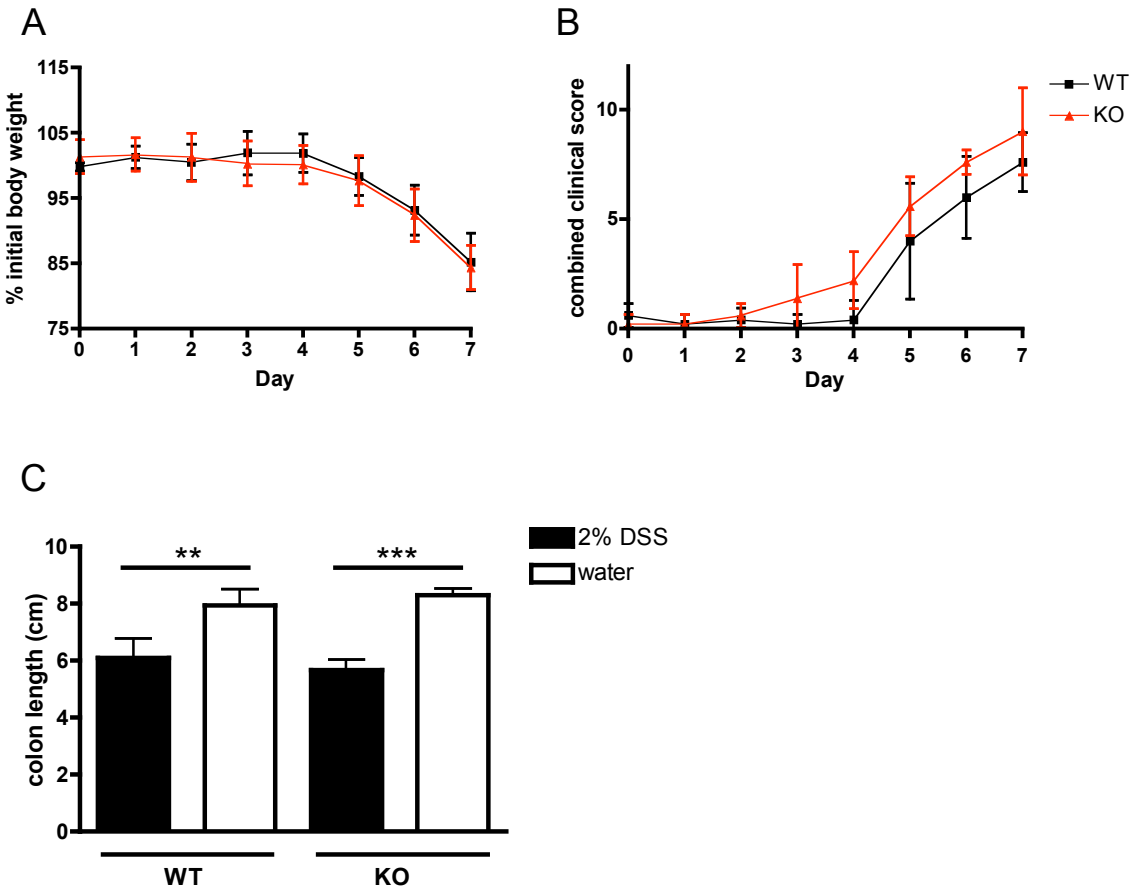

Figure 5.15
Induction of DSS Colitis in CCX-CKR KO and WT Mice
WT and CCX-CKR KO mice received 2% DSS in their drinking water for 7 days to induce colitis. Control mice received normal drinking water throughout. Body weight (A) and clinical disease (B) were assessed daily. Clinical disease score was determined by monitoring diarrhoea (score 0-4) and rectal bleeding (score 0-4). Colon lengths were assessed after sacrifice on day 7 (C). Results show the mean +/- 1SD of 4-5 mice per group.

** $p<0.01$ ***$p<0.001$ Unpaired t test

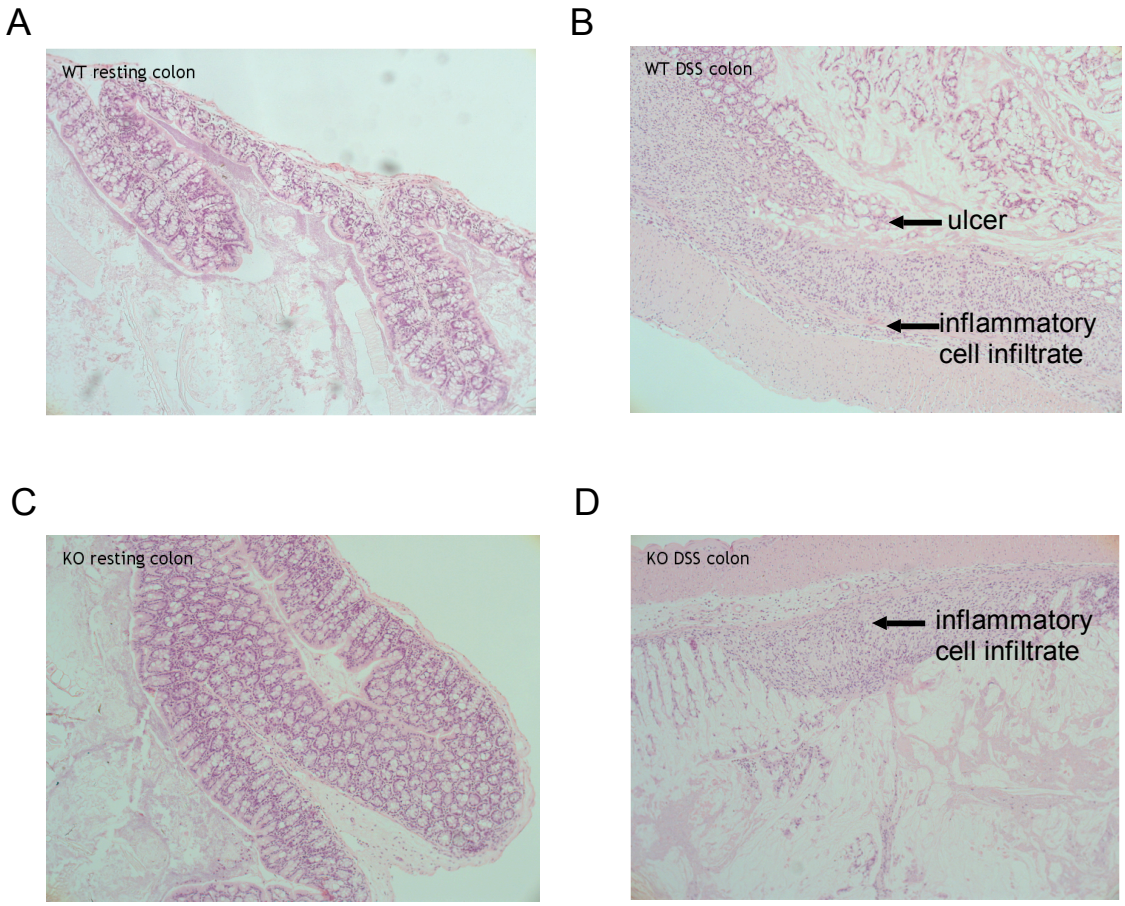

Figure 5.16
Induction of DSS Colitis in CCX-CKR KO and WT Mice
WT and CCX-CKR KO mice received 2% DSS in their drinking water for 7 days to induce colitis.Control mice received normal drinking water throughout. After 7 days, colons were excised and fixed in 10% formalin, embedded in paraffin and sections stained with haematoxylin and eosin for histological analysis. WT control (A), WT DSS treated (B), KO control (C) and KO DSS treated (D) colon sections are shown. DSS treated mice show crypt hyperplasia, goblet cell loss, ulceration and inflammatory cell infiltrate. (Final magnification x100)

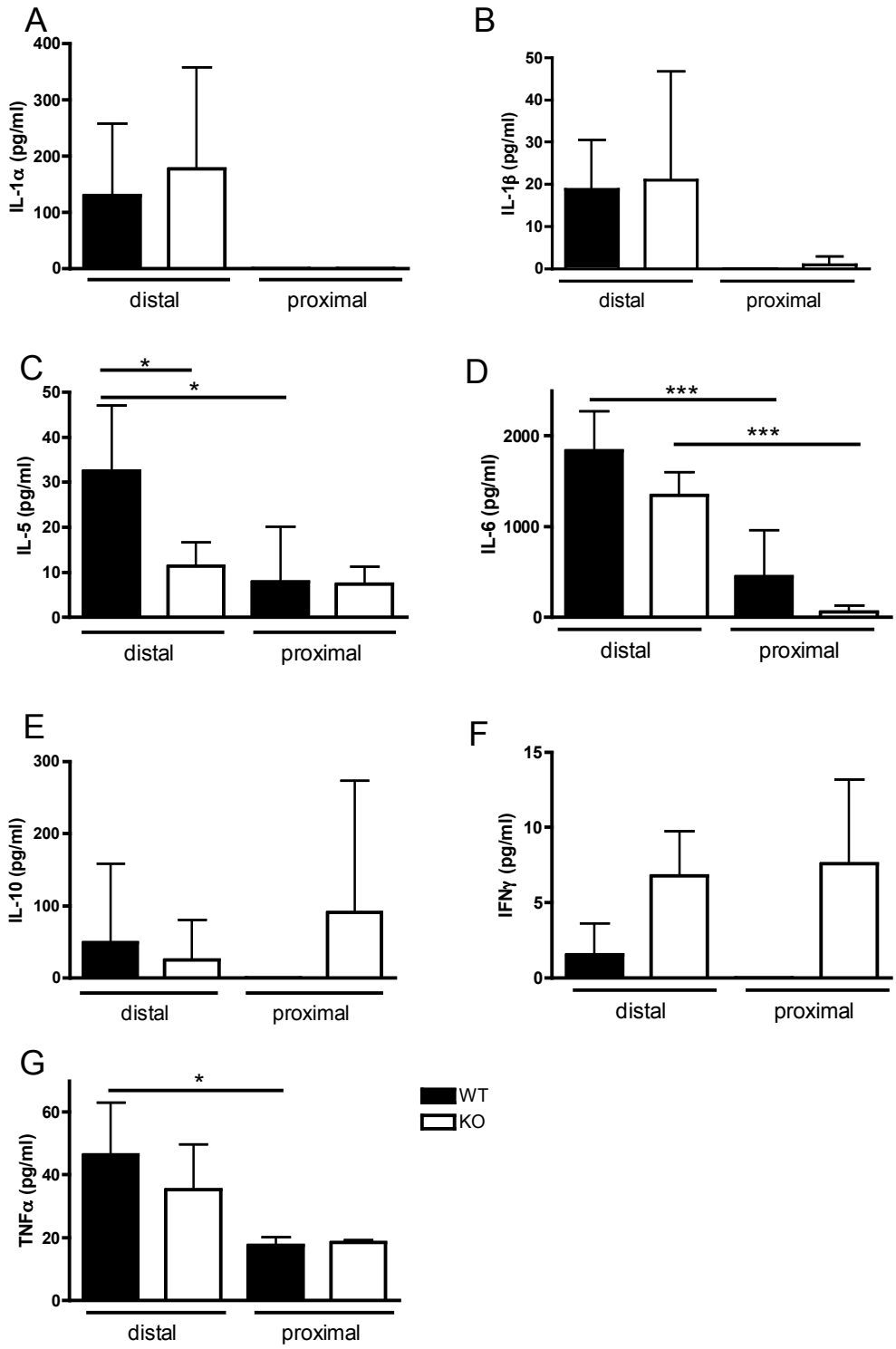

Figure 5.17
Production of Cytokines by Colon Explants from CCX-CKR KO and WT Mice with DSS Colitis
CCX-CKR KO and WT mice received 2% DSS in their drinking water for 7 days to induce colitis and explants of distal and proximal colon were cultured for 24 hours in complete medium and the levels of IL-1α, IL-1β, IL-5, IL-6, IL-10, IFNγ and TNFα were determined by Luminex analysis. Results show the mean + 1 SD of 5 mice per group.

Two way Anova with Bonferroni post tests *$p<0.05$ ***$p<0.001$

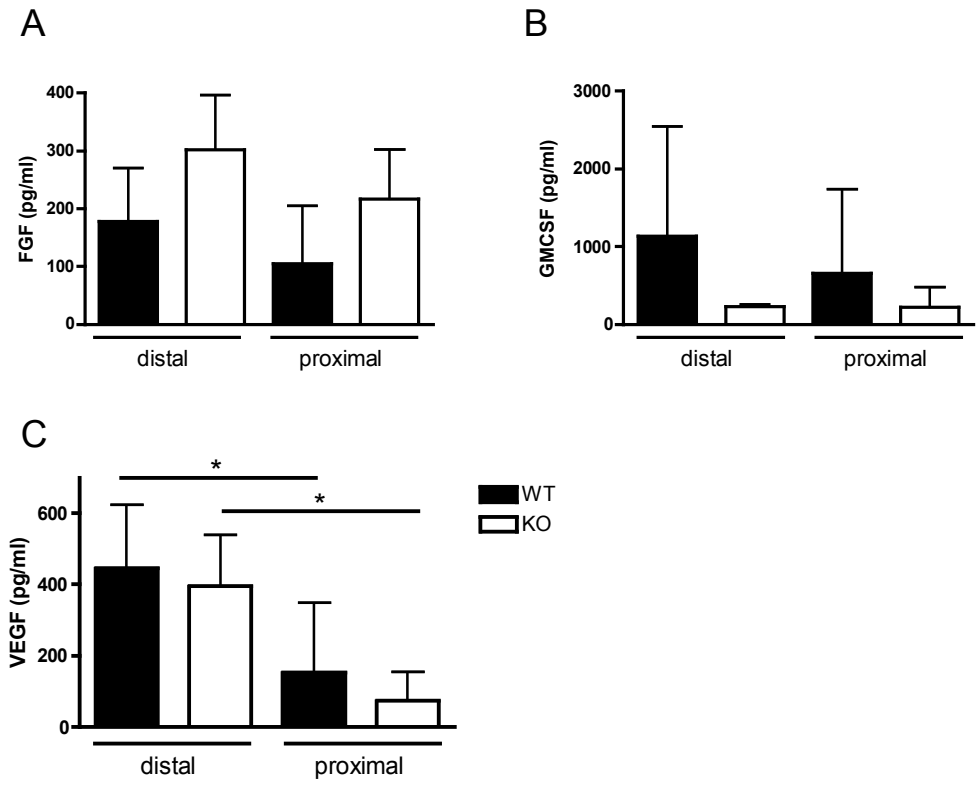

Figure 5.18
Production of Growth Factors by Colon Explants from CCX-CKR KO and WT Mice with DSS Colitis
CCX-CKR KO and WT mice received 2% DSS in their drinking water for 7 days to induce colitis and explants of distal and proximal colon were cultured for 24 hours in complete medium and the levels of FGF, GMCSF and VEGF were determined by Luminex analysis. Results show the mean + 1 SD of 5 mice per group.

Two way Anova with Bonferroni post tests *$p<0.05$

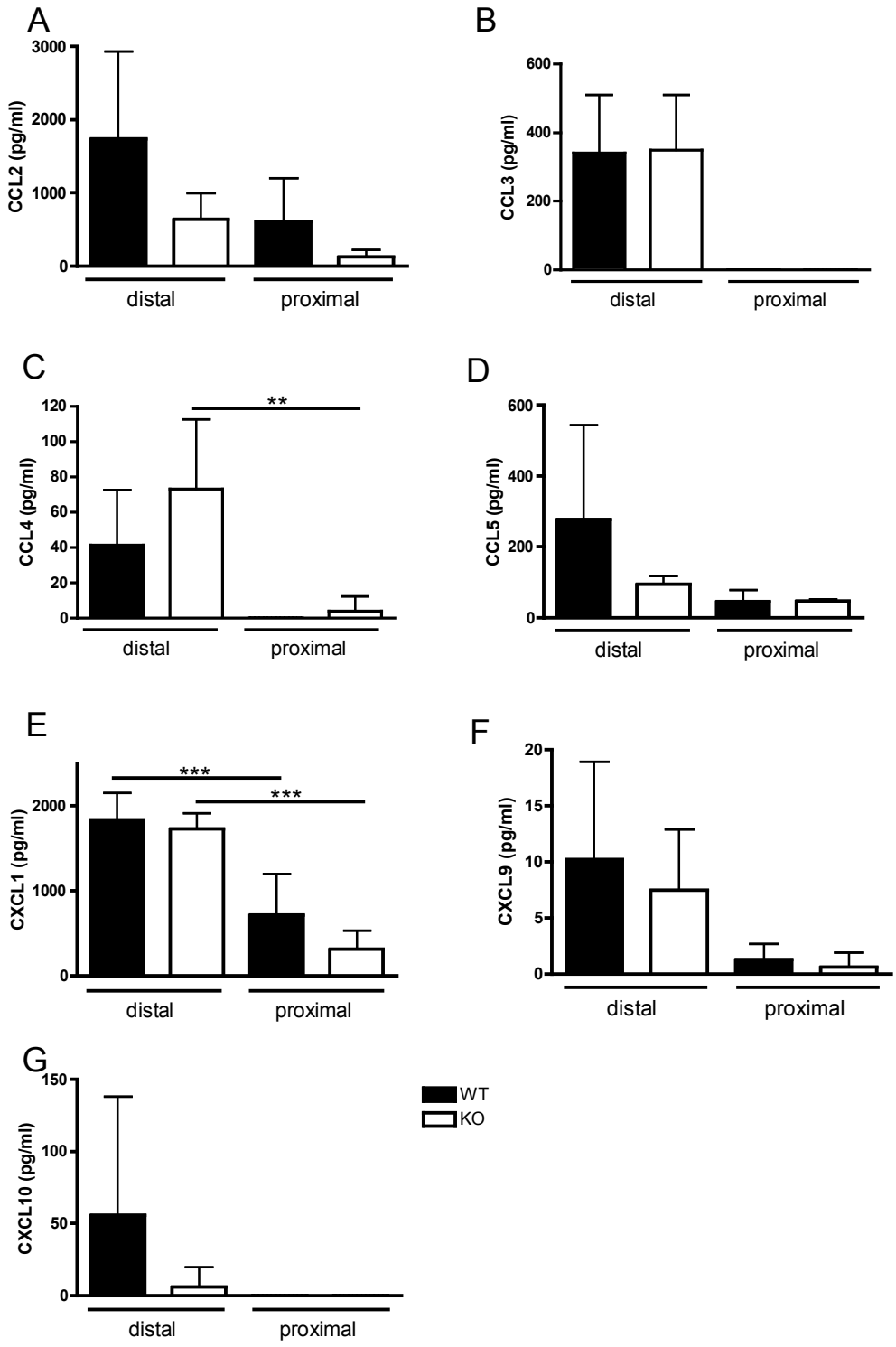

Figure 5.19
Production of Chemokines by Colon Explants from CCX-CKR KO and WT Mice with DSS Colitis
CCX-CKR KO and WT mice received 2% DSS in their drinking water for 7 days to induce colitis and explants of distal and proximal colon were cultured for 24 hours in complete medium and the levels of CCL2, CCL3, CCL4, CCL5, CXCL1, CXCL9 and CXCL10 were determined by Luminex analysis. Results show the mean + 1 SD of 5 mice per group.

Two way Anova with Bonferroni post tests **p<0.01 ***p<0.001

Chapter 6

Analysis of DC Function in CCX-CKR KO Mice

Introduction

So far my data have shown that CCX-CKR deficiency causes a significant reduction in pDC proportions and numbers in MLN. In addition, the induction of oral tolerance is defective in CCX-CKR KO mice, while both local and systemic antibody production suggests enhanced priming by oral administration of antigen and adjuvant. In this chapter, I have tried to connect these findings by conducting preliminary studies of the function and distribution of DC in CCX-CKR KO mice.

6.1 Intrinsic functions of CCX-CKR KO DC *in vitro*

In the first experiment, I examined the intrinsic functions of DC by comparing the responses of GM-CSF derived bone marrow DC from CCX-CKR KO and WT mice to stimulation with LPS *in vitro*. CD40, CD86 and class II MHC expression were moderately up-regulated in both CCX-CKR KO and WT bone marrow derived DC (BMDC) after stimulation with 1μg/ml LPS overnight compared with BMDC cultured in medium alone, and there were no differences between the strains. CD80 expression was not altered by LPS stimulation of either CCX-CKR KO or WT BMDC (Fig 6.1).

I next investigated the endocytic activity of CCX-CKR KO and WT BMDC by incubating them with 1mg/ml FITC-dextran at 37°C for 10-60 minutes and analysing the uptake by flow cytometry. Both CCX-CKR KO and WT BMDC showed time and temperature dependent uptake of FITC dextran, with no consistent differences between the strains (Fig 6.2).

To assess the ability of CCX-CKR KO and WT BMDC to process and present antigen, BMDC were pulsed with either OVA or OVA 323-339 peptide, irradiated and cultured with LN cells from OT2 mice which have a transgenic TCR on $CD4^+$ cells specific for OVA 323-339 peptide. Both CCX-CKR KO and WT BMDC could present OVA peptide efficiently to OT2 cells at 1:5 and 1:10 ratios. Although CCX-CKR KO DC induced significantly more T cell proliferation at the 1:5 ratio, no differences were seen at the 1:10 ratio. WT BMDC also presented intact protein to OT2 cells with moderate efficiency, but CCX-CKR KO BMDC were significantly less effective at presenting intact protein at both ratios (Fig 6.3). Taken together, these data suggest that CCX-CKR KO BMDC can effectively present peptide bound in class II MHC, but may be defective in their ability to process intact antigens.

To extend these results, I examined the antigen presenting activity of tissue derived APC obtained from the spleens of CCX-CKR KO and WT mice. Spleen cells were pulsed with OVA protein or peptide, irradiated and cultured with LN cells or purified $CD4^+$ cells from OT2 mice. Splenic APC from WT mice induced excellent proliferative responses by both unpurified OT2 cells and purified $CD4^+$ T cells when either protein or peptide were used as antigen. All these responses were markedly and significantly reduced when CCX-CKR KO spleen cells were used as the APC (Fig 6.4). Overall these findings suggest there may be defective APC activity in CCX-CKR KO mice.

6.2 Responses of DC from resting mice to TLR 7 stimulation *in vitro*

Having explored conventional DC activity, I next attempted to examine pDC more specifically, focussing particularly on the MLN where the most significant defect was found in CCX-CKR KO mice. One of the most potent ways of stimulating pDC is via TLR7 which recognises single stranded RNA (ssRNA) from viruses and induces the production of type 1 IFN. To mimic the effects of ssRNA on pDC, I used R848 as a synthetic agonist of TLR7 and TLR8, which has been used widely to investigate pDC function (121, 248, 249).

Firstly, I examined the effects of R848 *in vitro* using MLN cells from resting mice which were cultured for 20 hours with or without 5μg/ml R848. After culture, the cells were analysed by flow cytometry for CD11c and PDCA-1 expression to identify DC subsets, and CD40 and CD86 to assess activation status. $CD11c^+$ cells were divided into $CD11c^+PDCA\text{-}1^-$, $CD11c^{lo}PDCA\text{-}1^+$ and $CD11c^{hi}PDCA\text{-}1^+$ cell subsets to identify conventional DC, pDC and PDCA-1 expressing conventional DC respectively (Fig 6.5).

Approximately 80% of $CD11c^+$ cells from resting CCX-CKR KO and WT MLN were conventional $CD11c^+PDCA\text{-}1^-$ DC, and there was only a small population of $CD11c^{lo}PDCA\text{-}1^+$ pDC. As I found previously, the numbers of pDC were drastically and significantly reduced amongst CCX-CKR KO $CD11c^+$ MLN cells compared with WT MLN. The proportions of conventional DC and pDC were not significantly altered by R848 stimulation *in vitro*. However, the proportions of $CD11c^{hi}PDCA\text{-}1^+$ cells which I putatively defined as activated conventional DC, were found rarely amongst CCX-CKR KO and WT MLN $CD11c^+$ cells although were significantly increased in both strains of mice after R848 stimulation. This may

reflect the effects of R848 induced type 1 IFN which has been shown to induce expression of PDCA-1 on conventional DC (250) (Fig 6.6).

The expression of CD40 and CD86 on $CD11c^{hi}PDCA\text{-}1^{-}$ conventional DC was low and comparable in resting CCX-CKR KO and WT MLN, and these did not change after R848 stimulation. Similar results were obtained for $CD11c^{lo}PDCA\text{-}1^{+}$ pDC in resting animals. CD40 and CD86 expression levels were higher on unstimulated $CD11c^{hi}PDCA\text{-}1^{+}$ cells compared with the other two $CD11c^{+}$ cell subsets, suggesting this may represent a partially activated subset. R848 stimulation did not alter the expression of CD40 by these DC amongst either CCX-CKR KO or WT MLN cells. However R848 stimulation induced a significant increase in CD86 expression by CCX-CKR $CD11c^{hi}PDCA\text{-}1^{+}$ DC. Although CD86 expression levels also increased on WT $CD11c^{hi}PDCA\text{-}1^{+}$ cells stimulated with R848, this was not statistically significant (Fig 6.7).

6.3 Responses of DC from Flt3L treated mice to TLR 7 stimulation *in vitro*

Due to the scarcity of the DC subsets in resting MLN, it was often difficult to determine precisely the phenotypic changes in these DC after R848 stimulation *in vitro*. Therefore, I extended these studies by expanding DC numbers *in vivo* using Flt3L. As I found previously in Chapter 4, treatment with Flt3L produced a marked expansion of all DC subsets in the MLN of CCX-CKR KO and WT mice (Figs 6.6A and 6.8A). The proportions of $CD11c^{+}PDCA\text{-}1^{-}$ cells in the MLN of Flt3L treated mice were comparable in CCX-CKR KO and WT mice, with approximately 80% of total $CD11c^{+}$ cells having this phenotype, as was seen in resting MLN. However, in contrast to what I found in resting mice, stimulation of Flt3L treated MLN cells with R848 *in vitro* reduced the proportion of $CD11c^{+}PDCA\text{-}1^{-}$ DC by about half (Fig 6.8B). As before, Flt3L treatment did not overcome the defect in the numbers of $CD11c^{lo}PDCA\text{-}1^{+}$ pDC in CCX-CKR KO MLN and although R848 stimulation *in vitro* led to a significant increase in the proportion of pDC amongst CCX-CKR KO MLN cells, they still did not attain the levels seen after R848 treatment of Flt3L expanded WT DC (Fig 6.8C). As in resting mice, the proportions of $CD11c^{hi}PDCA\text{-}1^{+}$ conventional DC amongst total $CD11c^{+}$ cells were dramatically elevated after R848 stimulation of MLN cells from Flt3L treated CCX-CKR KO and WT mice, and this effect was much more clearly visible using Flt3L treated animals (Fig 6.8D).

In contrast to what I found in resting MLN, stimulation of Flt3L treated MLN cells with R848 *in vitro* reduced the expression of CD40 and CD86 on conventional $CD11c^{+}PDCA\text{-}1^{-}$ DC in both CCX-CKR KO and WT mice. Interestingly however, CD40 appeared to be expressed at higher levels on unstimulated $CD11c^{+}PDCA\text{-}1^{-}$ DC from CCX-CKR KO mice compared with these DC in WT MLN (Fig 6.9A). R848 stimulation induced significant increases in CD40 expression by $CD11c^{lo}PDCA\text{-}1^{+}$ pDC from Flt3L treated CCX-CKR KO and WT mice. Similar effects were seen with CD86 expression by pDC, although this increase was only statistically significant for CCX-CKR KO cells, which showed higher CD86 expression than R848 stimulated WT pDC (Fig 6.9B). R848 also induced significant increases in the expression of CD40 and CD86 by $CD11c^{hi}PDCA\text{-}1^{+}$ MLN DC from Flt3L treated CCX-CKR KO and WT mice, although again, CD86 was expressed at higher levels by $CD11c^{hi}PDCA\text{-}1^{+}$ DC from CCX-CKR KO MLN than WT MLN both before and after R848 stimulation (Fig 6.9C).

To try to expand on these phenotypic effects, I made several attempts to assess IFNα production by MLN DC in response to R848 stimulation using ELISA. However, these experiments were unsuccessful due to the ELISA being unreliable and due to time constraints, I could not establish an intracellular staining protocol for this cytokine.

6.4 Effects of R848 on MLN DC *in vivo*

Previous studies have shown that feeding R848 induces the migration of conventional DC out of the gut wall and that this is dependent on tissue resident pDC (121). I next examined the effects of R848 on DC in CCX-CKR KO and WT mice *in vivo*. As well as assessing evidence of activation, this allowed me to study how the pDC deficiency in CCX-CKR KO mice might affect the migration of DC from the small intestinal lamina propria to the MLN. These migratory, tissue derived DC can be identified in the MLN by their $CD11c^{hi}classIIMHC^{hi}CD103^{+}$ phenotype, whereas resident DC are characterised as $CD11c^{hi}classIIMHC^{lo}CD103^{-}$ cells.

18 hours after oral administration of 100μg of R848, there were no changes in the overall numbers of MLN cells in either CCX-CKR KO or WT mice compared with resting MLN. However, there were significant increases in the proportions of CD11c expressing cells in the MLN of both strains (Figs 6.10A and 6.10B). The absolute numbers of $CD11c^{+}$ cells in the

MLN of CCX-CKR KO and WT mice also increased after R848 feeding, although this was only statistically significant for WT mice. However, overall there were no major differences in the proportions or absolute numbers of $CD11c^+$ cells in the MLN after feeding R848 to CCX-CKR KO or WT mice (Fig 6.10C).

Clear populations of migratory and LN resident DC could be defined in the MLN of control CCX-CKR KO and WT mice fed with PBS, with all $CD11c^{hi}CD103^{hi}$ cells expressing high levels of class II MHC (Fig 6.11). As the representative FACS profiles shown in Fig 6.11 illustrate, feeding 100μg R848 altered these proportions dramatically, with a large increase in the proportion of migratory DC seen 18 hours after feeding. These effects were confirmed when the overall results from groups of three mice were analysed, with significant increases in the proportions of migratory $CD11c^{hi}$classIIMHC^{hi} DC amongst $CD11c^+$ cells after R848 feeding in both strains. The absolute numbers of these cells in the MLN also increased with R848 feeding in both strains, although this was only statistically significant for WT mice (Fig 6.12A). In parallel, the proportions of LN resident $CD11c^{hi}$classIIMHC^{lo} DC amongst $CD11c^+$ cells in the MLN of CCX-CKR KO and WT mice were decreased significantly after R848 feeding, although this did not translate into significant changes in the absolute numbers of these cells in either strain (Fig 6.12B). In addition, the proportions and absolute numbers of CD103 expressing DC amongst $CD11c^+$ cells increased significantly in R848 fed CCX-CKR KO and WT mice compared with PBS fed controls (Fig 6.12C).

As well as changes in the proportions of migratory and LN resident DC, the expression of class II MHC and CD103 was significantly increased on $CD11c^+$ cells from the MLN of R848 fed CCX-CKR KO and WT mice compared with PBS fed controls (Fig 6.13). There were no significant differences between CCX-CKR KO and WT mice in their responses to R848 *in vivo* in any of these analyses. I also attempted to examine the effects of R848 feeding on pDC numbers in the MLN, but this proved impossible, as although $CD11c^{lo}$PDCA-1^+ pDC were readily found in the MLN of PBS fed mice, this population was not clearly definable in R848 fed mice (Fig 6.14).

Thus both CCX-CKR KO and WT mice showed significant responses to R848 *in vivo* which occurred identically in both strains. Next, I carried out a more extensive analysis of how

widespread the defect in pDC numbers might be by examining the bone marrow (BM) and non-lymphoid tissues such as the liver and blood of CCX-CKR KO mice.

6.5 Analysis of DC composition in the liver of CCX-CKR KO mice

There is considerable evidence that the liver may play an important role in oral tolerance and recent studies have linked this specifically to pDC in the liver (226). Therefore, having observed a defect in the establishment of oral tolerance coupled with a depletion of pDC in CCX-CKR KO mice, I decided to analyse the pDC composition of the liver directly.

Live leukocytes were isolated from the livers of CCX-CKR KO and WT mice, and analysed for CD11c and PDCA-1 expression to identify pDC. Total leukocyte numbers recovered from livers were comparable in resting CCX-CKR KO and WT mice, as were the proportion and absolute numbers of $CD11c^+$ cells. Although there seemed to be decreases in the proportions and absolute numbers of $CD11c^{lo}PDCA\text{-}1^+$ pDC in the liver of CCX-CKR KO mice, this was not statistically significant (Fig 6.15). Similar results were obtained using liver cells from Flt3L treated mice, suggesting there is no significant defect in total DC or pDC in the liver of CCX-CKR KO mice (Fig 6.16).

6.6 Analysis of pDC from the bone marrow and blood of CCX-CKR KO mice

pDC begin life in the bone marrow (BM) and migrate to secondary lymphoid organs and other tissues via the blood (106, 112). The reduction in pDC proportions and numbers I observed in CCX-CKR KO MLN could be caused by an intrinsic deficiency in pDC differentiation or by defective migration from the bone marrow into the blood or from the bloodstream into MLN. To begin to examine these possibilities, I assessed the prevalence of pDC in the bone marrow and blood of CCX-CKR KO mice.

The combined expression of B220 and PDCA-1 was used to identify pDC in the BM, as most $CD11c^+$ cells in this tissue expressed PDCA-1 to some extent. There were no differences in the proportions of $CD11c^+$ cells or $B220^+PDCA\text{-}1^+$ cells in resting CCX-CKR KO mice (Fig 6.17). I also examined the effects of Flt3L treatment on DC subsets in the BM, which showed a dramatic expansion in the proportions of $CD11c^+$ cells and $CD11c^{lo}B220^+PDCA\text{-}1^+$ pDC in the BM of both CCX-CKR KO and WT mice. Again there were no differences between these populations in the two strains (Fig 6.18). Live blood leukocytes were isolated from WT and

CCX-CKR KO mice and analysed for CD11c, B220 and PDCA-1 surface expression by flow cytometry. The concentrations of live leukocytes were comparable in the blood of CCX-CKR KO and WT mice, as were the proportions of $CD11c^+$ cells. Although the absolute numbers of $CD11c^+$ cells were significantly increased in CCX-CKR KO blood, there were no significant differences in the proportions or absolute numbers of $CD11c^{lo}B220^+PDCA\text{-}1^+$ pDC between CCX-CKR KO and WT mice (Fig 6.19).

Flt3L treated WT mice had a significant increase in the total blood leukocyte count compared with controls, with 25 fold and 60 fold increases in the numbers of $CD11c^+$ cells and pDC respectively (Figs 6.19A,D,F and 6.20A,D,F). In comparison, although the total leukocyte count increased in CCX-CKR KO mice treated with Flt3L, this was significantly less marked than in Flt3L treated WT mice. In addition, Flt3L treatment had much less effect on the numbers of $CD11c^+$ cells and pDC in the blood of CCX-CKR KO mice, with only 7 fold and 20 fold increases in these cells in Flt3L treated mice compared with controls. However, these differences in $CD11c^+$ cell and pDC numbers in the blood of Flt3L treated CCX-CKR KO and WT mice were not statistically significant (Figs 6.19D,F and 6.20D,F).

Thus despite normal numbers and proportions of pDC in the BM and blood of resting CCX-CKR KO mice and a normal response of pDC precursors in the BM to Flt3L, there seems to be a defect in the mobilisation of pDC into the bloodstream of CCX-CKR KO mice after administration of Flt3L.

6.7 Adoptive transfer of pDC between CCX-CKR KO and WT mice

To try and determine whether the deficiency in pDC in CCX-CKR KO MLN was a property of the lymphoid tissue environment, or if CCX-CKR KO pDC themselves are inherently unable to migrate effectively into WT LN, I carried out reciprocal adoptive transfer experiments using CCX-CKR KO and WT pDC (Table 6.1).

Table 6.1: Donor and recipient combinations

Donor	Recipient
CD45.1$^+$ WT	CD45.2$^+$ WT
CD45.1$^+$ WT	CD45.2$^+$ CCX-CKR KO
CD45.2$^+$ WT	CD45.1$^+$ WT
CD45.2$^+$ CCX-CKR KO	CD45.1$^+$ WT

In the first experiment, I followed a published protocol in which unseparated resting spleen cells were used as a source of donor pDC (121) and used WT CD45.1$^+$ mice as donors so that transferred cells could be identified in WT CD45.2$^+$ recipient mice. The equivalent of 1x10^6 CD11c^{lo}PDCA-1$^+$ cells were transferred into recipients and 20 hours later, cells from the MLN, ILN and spleens of recipients were analysed for CD11c, PDCA-1 and CD45.1 expression to identify transferred pDC. However, very few donor derived pDC could be seen in the spleens of recipient mice using this protocol and there were virtually none in the MLN or ILN (Fig 6.21).

I therefore altered the protocol and purified pDC from the spleens of mice that had been expanded *in vivo* with Flt3L. pDC were enriched by negative selection using magnetic beads, yielding a purity of 50-70% (Fig 6.22). 1x10^6 pDC were then transferred into recipients and the presence of donor cells within secondary lymphoid organs was assessed 20 hours later (Fig 6.23). This protocol also yielded sufficient pDC to allow a full transfer experiment in which both WT and CCX-CKR KO pDC were transferred into each strain of recipients.

Donor pDC could be identified in all secondary lymphoid organs of recipients, irrespective of which donor/recipient combination was used. When the numbers of donor pDC were expressed as a proportion of total pDC, WT CD45.1$^+$ or CD45.2$^+$ pDC appeared to re-populate WT lymphoid tissues to similar extents. A similar difference was seen between the entry of WT pDC into CCX-CKR KO ILN compared with WT ILN, although this was not statistically significant. These differences did not translate into significant differences in the absolute numbers of donor pDC suggesting that the proportional increase of donor pDC in CCX-CKR KO tissues is likely to reflect the decreased numbers of pDC in CCX-CKR KO mice and indicating that CCX-CKR KO tissues are permissive to the entry of normal pDC. CCX-CKR

KO pDC were also able to migrate into the lymphoid organs of WT mice, although these pDC did seem to show some decreased ability to enter WT MLN compared with WT pDC, although this was not statistically significant (Fig 6.24).

6.8 Assesment of CCL21 protein levels in CCX-CKR KO tissues

As CCX-CKR has been proposed to regulate levels of its chemokine ligands *in vivo*, I decided to assess the levels of CCL21 protein in CCX-CKR KO ILN, MLN, spleen, PP, lower small intestine and upper small intestine by ELISA. The levels of CCL21 protein relative to total protein across all tissues examined were not significantly altered by CCX-CKR deletion.

Summary

The results in this chapter suggest that CCX-CKR KO BMDC are activated by LPS and endocytose FITC-dextran particles in a similar manner to WT BMDC. However, CCX-CKR KO BMDC and splenic APC did not process and present antigen as effectively as WT cells. MLN cells from resting and Flt3L treated CCX-CKR KO mice appeared to respond normally to the synthetic TLR7 agonist, R848 with an expansion in the numbers of $CD11c^{hi}PDCA\text{-}1^{+}$ cells that nearly all expressed CD40 and CD86. In addition, R848 triggered identical migration of $CD11c^{hi}classIIMHC^{hi}CD103^{+}$ DC into the MLN of CCX-CKR KO and WT mice. There were no differences in the proportions or absolute numbers of pDC in the liver or bone marrow of resting or Flt3L treated CCX-CKR KO and WT mice. However, the expansion of $CD11c^{+}$ cells and pDC found in the blood in response to Flt3L treatment appeared to be less effective in CCX-CKR KO mice than WT. Experiments using the adoptive transfer of pDC were somewhat inconclusive but suggested that WT pDC could enter the MLN and other lymphoid tissues of CCX-CKR KO mice normally. However, pDC from CCX-CKR KO mice may have a defective ability to enter WT MLN compared with WT pDC. In addition, the levels of CCL21 protein in secondary lymphoid organs and the small intestine do not appear to be affected by CCX-CKR deletion.

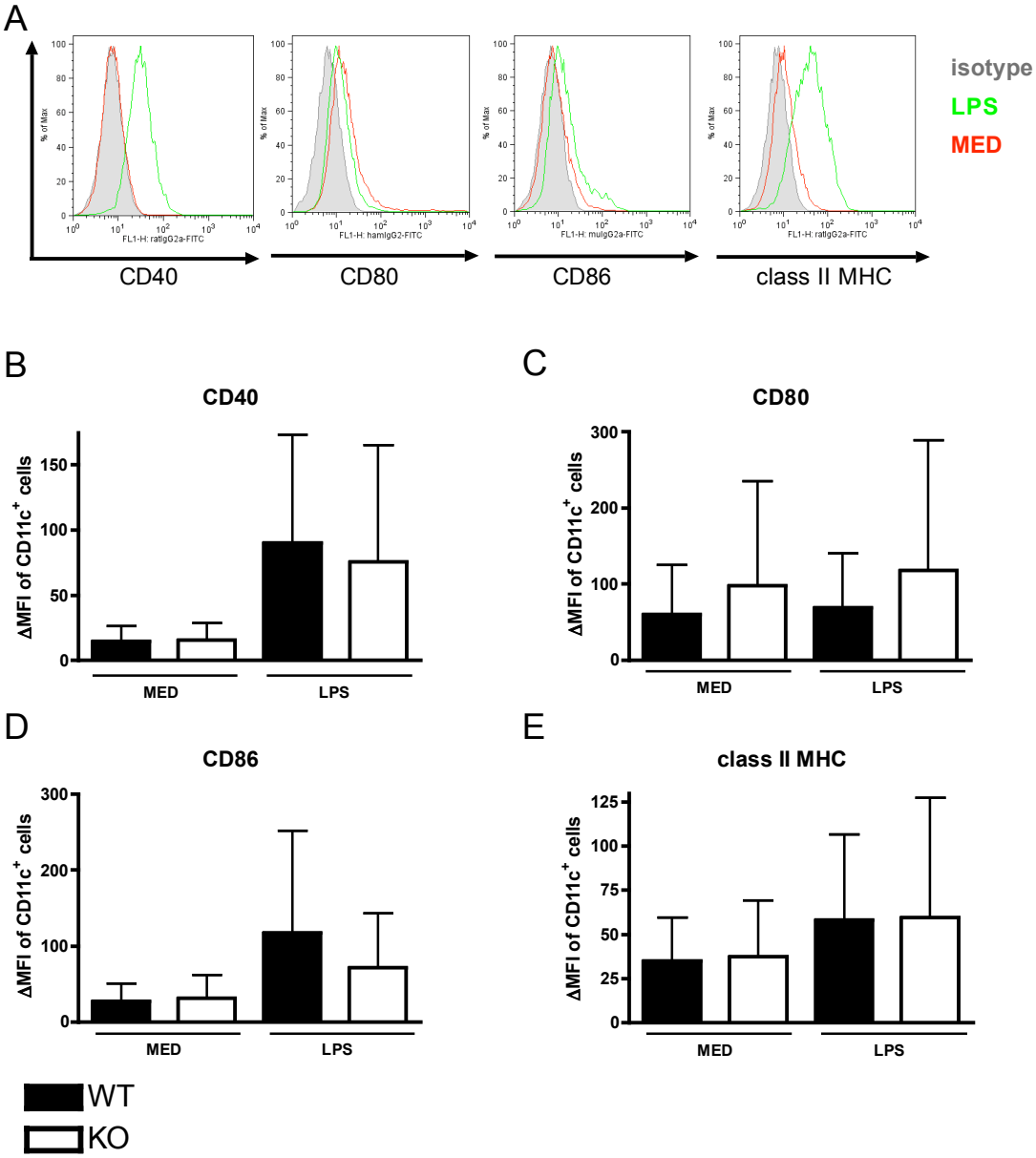

Figure 6.1
Activation of Bone Marrow Derived CCX-CKR KO and WT DC by LPS
Bone marrow (BM) DC from CCX-CKR KO and WT mice were cultured overnight either in medium alone or with 1μg/ml LPS. The expression of CD40, CD80, CD86 and class II MHC was then determined by flow cytometry. (A) Representative histograms show CD40, CD80, CD86 and class II MHC expression by WT BMDC and appropriate isotype controls after culture in medium alone or with LPS. The ΔMFI of (B) CD40, (C) CD80, (D) CD86 and (E) class II MHC expression on $CD11c^+$ cells show the means +1 SD of 3 mice per group.

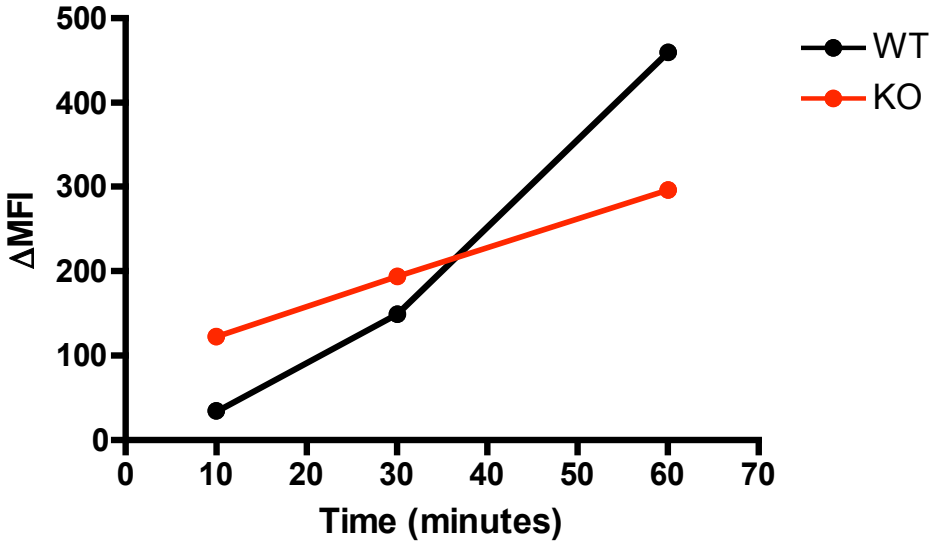

Figure 6.2
Endocytic Activity of Bone Marrow Derived CCX-CKR KO and WT DC
Bone marrow (BM) DC from CCX-CKR KO and WT mice were cultured with 1mg/ml FITC-dextran at 37^{o}C or 4^{o}C for 10-60 minutes. The specific uptake of FITC dextran (ΔMFI) was calculated by subtracting the MFI of control cells incubated at 4^{o}C from the MFI readings obtained from cultures at 37^{o}C.

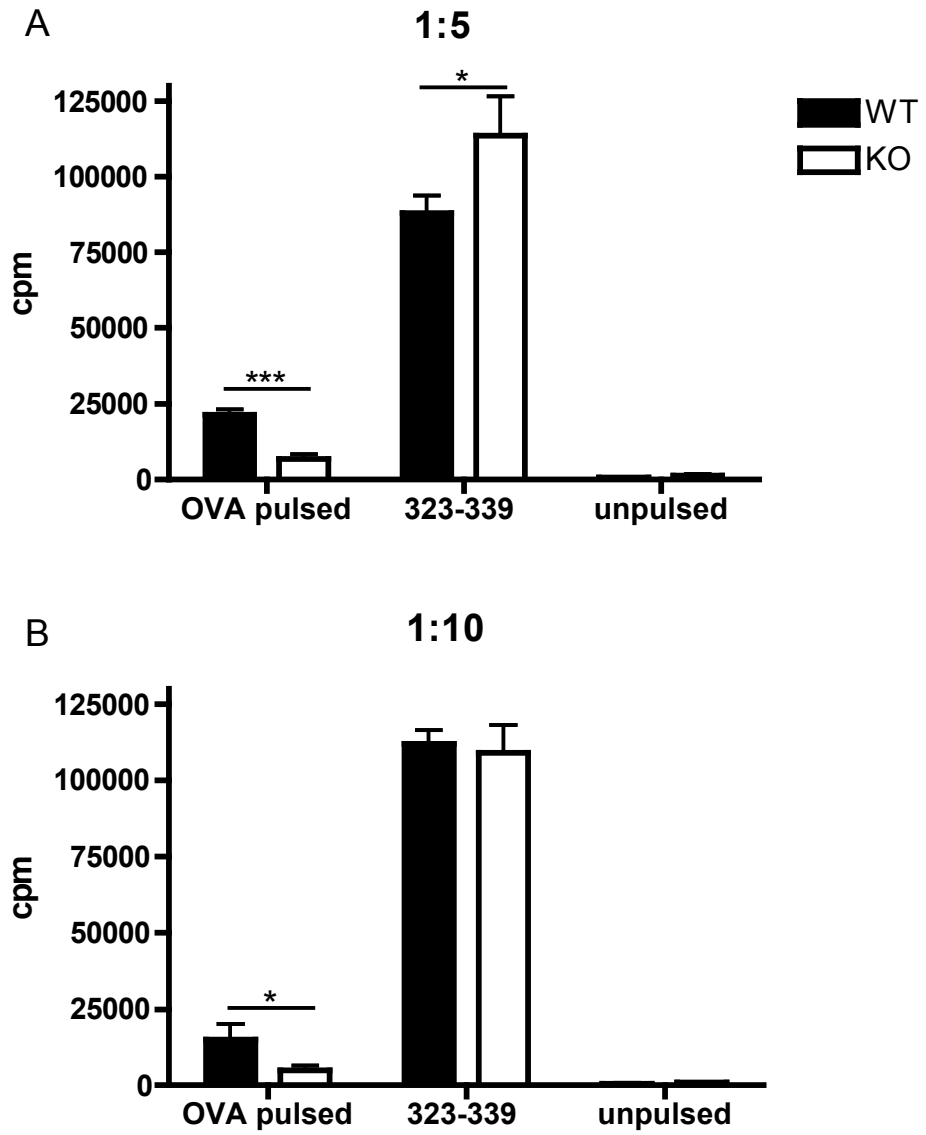

Figure 6.3
Antigen Presenting Cell Activity of Bone Marrow Derived CCX-CKR KO and WT DC
Bone marrow (BM) DC from CCX-CKR KO and WT mice were irradiated and pulsed with 5mg/ml OVA for 2 hours before being cultured for 72 hours with OT2 LN cells at 1:5 (A) and 1:10 (B) responder cell:BMDC ratios. OT2 LN cells were also cultured with unpulsed BMDC and OVA 323-339 peptide as a control. ^{3}H-TdR was added for the last 18 hours of culture and the results show means +1 SD of 3 mice per group.

*p<0.05 ***p<0.001 Unpaired t test

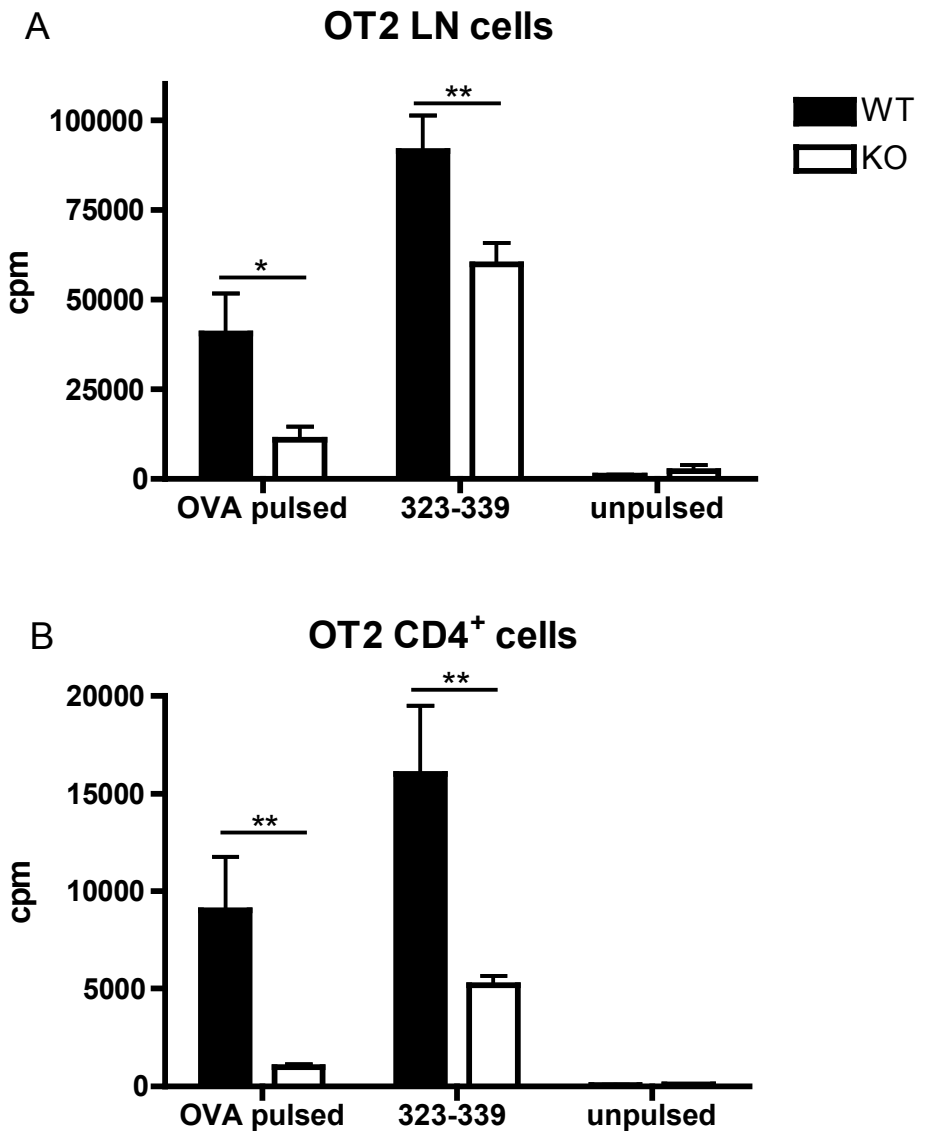

Figure 6.4
Antigen Presenting Cell Activity of Tissue Derived CCX-CKR KO and WT DC
Whole splenocytes from CCX-CKR KO and WT mice were irradiated and pulsed with 5mg/ml OVA for 2 hours before being cultured for 72 hours with OT2 LN cells (A) or purified OT2 $CD4^+$ LN cells (B) at a 1:1 ratio. OT2 cells were also cultured with unpulsed splenocytes and OVA 323-339 as a control. ^{3}H-TdR was added for the last 18 hours of culture and the results show means +1 SD of 3 mice per group.

*$p<0.05$ **$p<0.01$ Unpaired t test

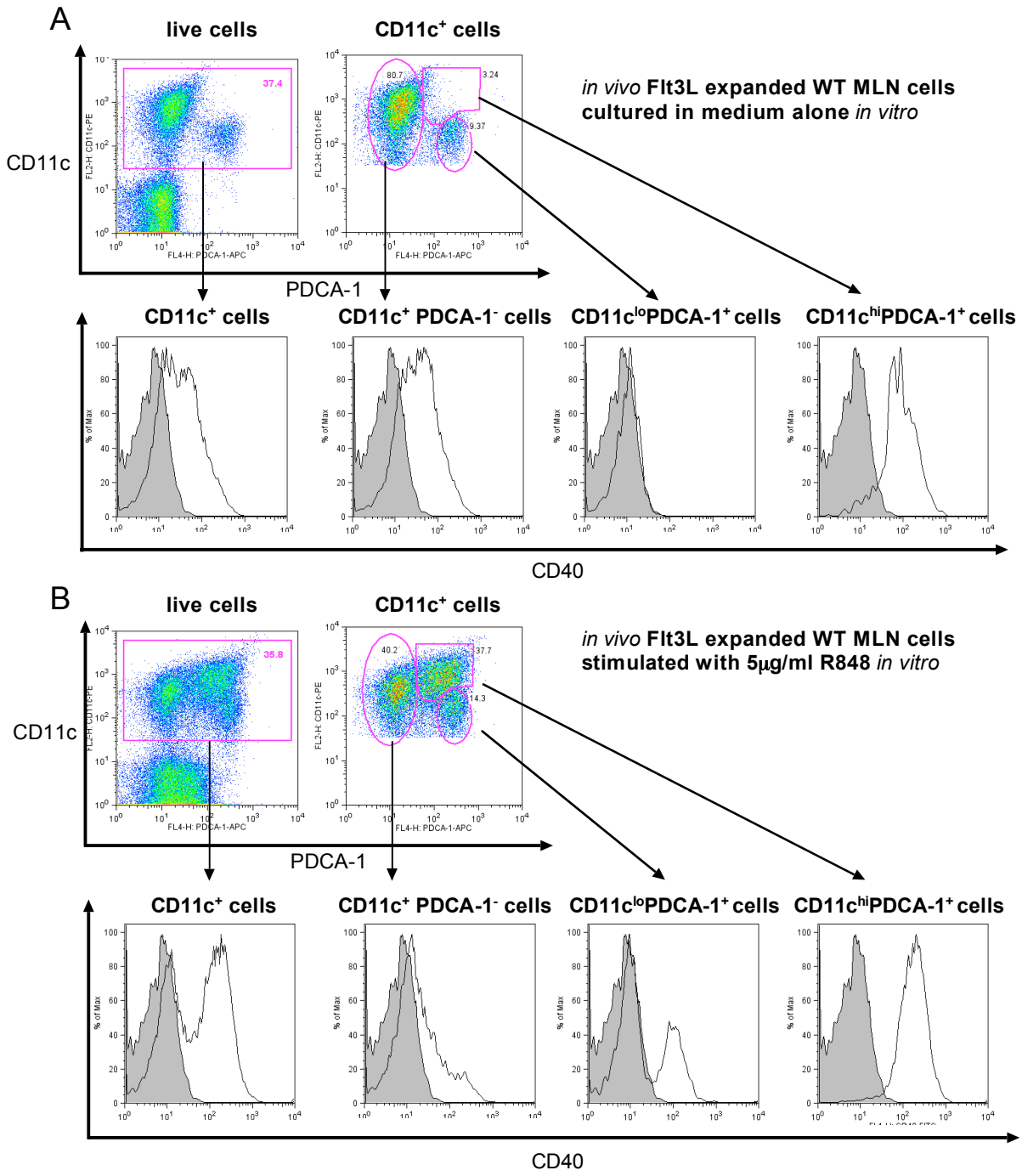

Figure 6.5
Effects of R848 on DC from CCX-CKR KO and WT MLN *In Vitro*
MLN cells were isolated from resting and Flt3L treated CCX-CKR KO and WT mice and cultured either in medium alone, or with 5μg/ml R848 for 20 hours. DC subsets were identified by expression of CD11c and PDCA-1 and their expression of co-stimulatory molecules assessed. Representative FACS plots show the proportion of total MLN cells from Flt3L treated WT mice expressing CD11c and the proportions of DC subsets within the $CD11c^+$ cell population. Histograms show isotype (shaded) and CD40 specific staining of total $CD11c^+$, $CD11c^+PDCA\text{-}1^-$, $CD11c^{lo}PDCA\text{-}1^+$ and $CD11c^{hi}PDCA\text{-}1^+$cell populations after culture in medium alone (A) or with R848 (B).

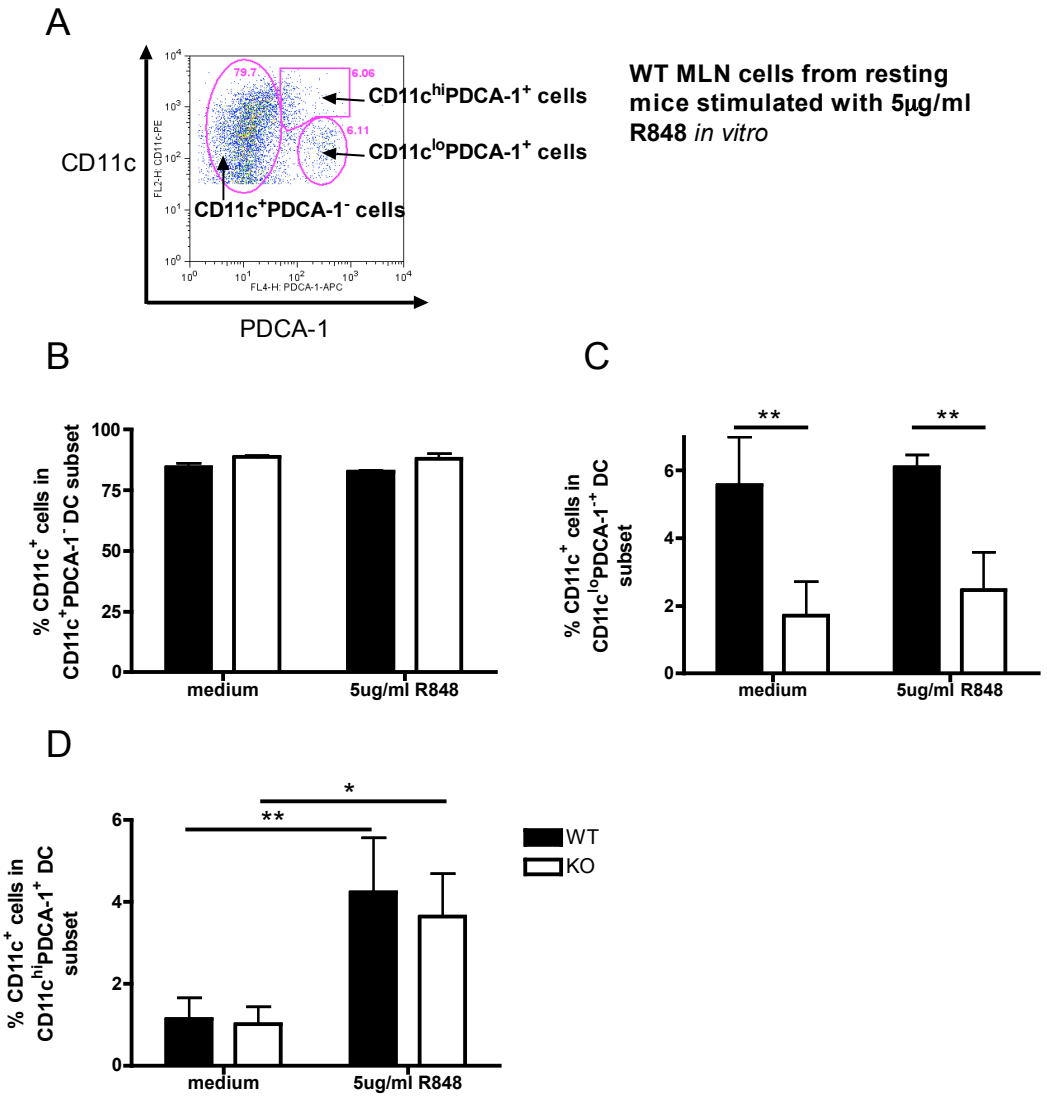

Figure 6.6
Effects of R848 on MLN DC from Resting CCX-CKR KO and WT Mice *In Vitro*

MLN cells were isolated from resting CCX-CKR KO and WT mice and cultured either in medium alone, or with 5μg/ml R848 and analysed 20 hours later for cell surface expression of CD11c and PDCA-1 to identify DC subsets. (A) Representative FACS plot showing $CD11c^{+}PDCA\text{-}1^{-}$, $CD11c^{lo}PDCA\text{-}1^{+}$ and $CD11c^{hi}PDCA\text{-}1^{+}$ DC subsets amongst WT $CD11c^{+}$ MLN cells after stimulation with R848. The proportions of $CD11c^{+}$ cells within the $CD11c^{+}PDCA\text{-}1^{-}$ (B), $CD11c^{lo}PDCA\text{-}1^{+}$ (C) and $CD11c^{hi}PDCA\text{-}1^{+}$ (D) cell subsets for unstimulated and R848 stimulated cells are shown. Results show means +1 SD of 3 mice per group.

Two way Anova with Bonferroni post tests *p<0.05 **p<0.01

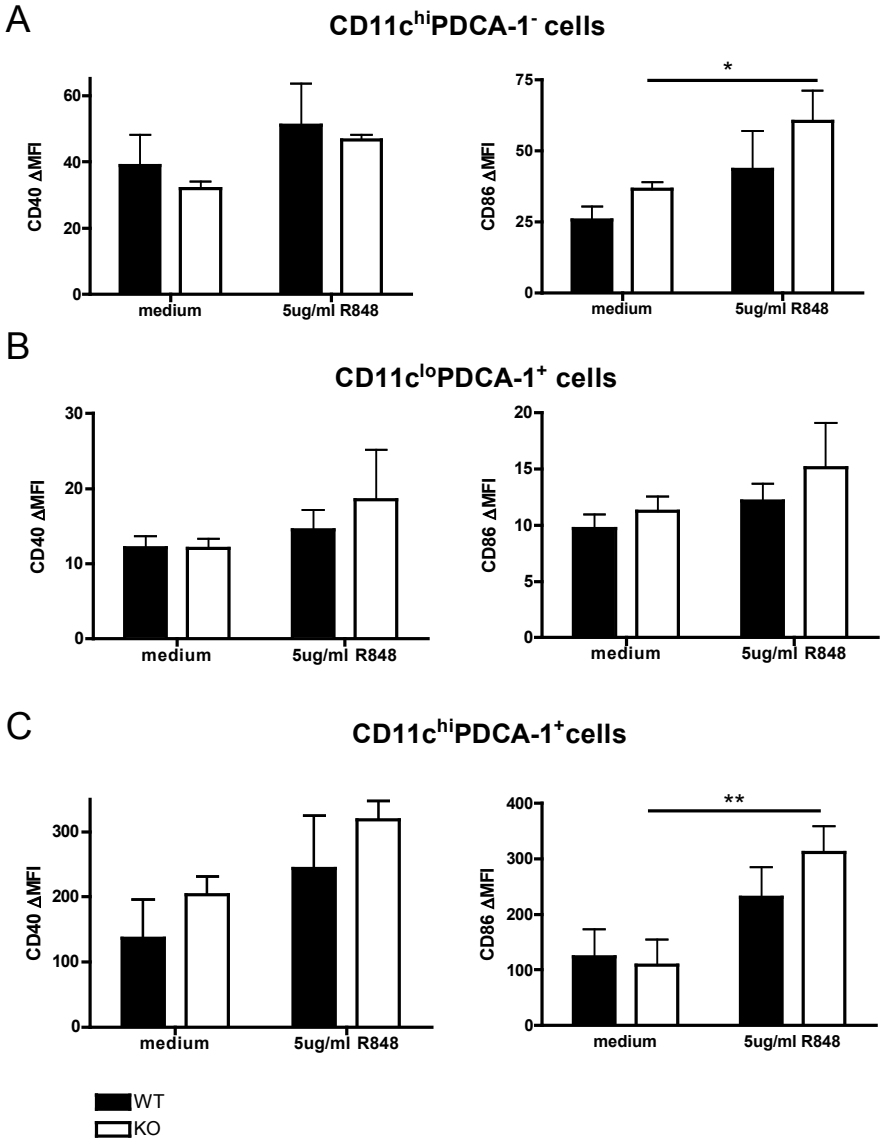

Figure 6.7
Effects of R848 on MLN DC from Resting CCX-CKR KO and WT Mice *In Vitro*
MLN cells were isolated from resting CCX-CKR KO and WT mice and cultured either in medium alone, or with 5μg/ml R848 and analysed 20 hours later for cell surface expression of CD11c and PDCA-1 to identify DC subsets and CD40 and CD86. The expression of CD40 (left graphs) and CD86 (right graphs) on (A) $CD11c^{+}PDCA\text{-}1^{-}$, (B) $CD11c^{lo}PDCA\text{-}1^{+}$ and (C) $CD11c^{hi}PDCA\text{-}1^{+}$ cells is shown. Results show mean ΔMFI +1 SD of 3 mice per group.

Two way Anova with Bonferroni post tests *p<0.05 **p<0.01

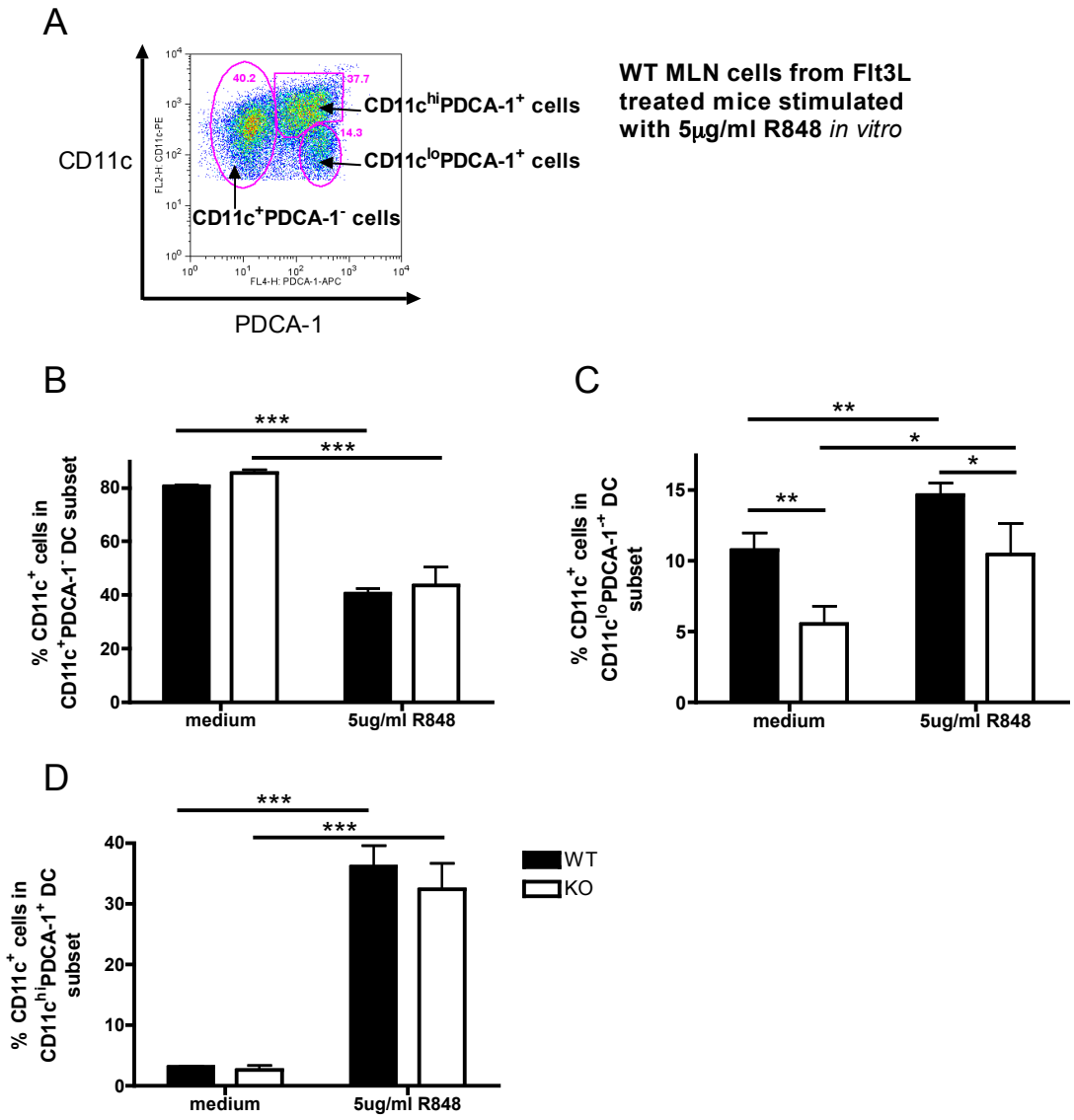

Figure 6.8
Effects of R848 on MLN DC from Flt3L Treated CCX-CKR KO and WT Mice *In Vitro*

MLN cells were isolated from Flt3L treated CCX-CKR KO and WT mice and cultured either in medium alone, or with 5μg/ml R848 and analysed 20 hours later for cell surface expression of CD11c and PDCA-1 to identify DC subsets. (A) Representative FACS plot showing $CD11c^{+}PDCA\text{-}1^{-}$, $CD11c^{lo}PDCA\text{-}1^{+}$ and $CD11c^{hi}PDCA\text{-}1^{+}$ DC subsets amongst WT $CD11c^{+}$ MLN cells after stimulation with R848. The proportions of $CD11c^{+}PDCA\text{-}1^{-}$ (B), $CD11c^{lo}PDCA\text{-}1^{+}$ (C) and $CD11c^{hi}PDCA\text{-}1^{+}$ (D) cells within the $CD11c^{+}$ cell population for unstimulated and R848 stimulated cells are shown. Results show means +1 SD of 3 mice per group.

Two way Anova with Bonferroni post tests *p<0.05 **p<0.01 ***p<0.001

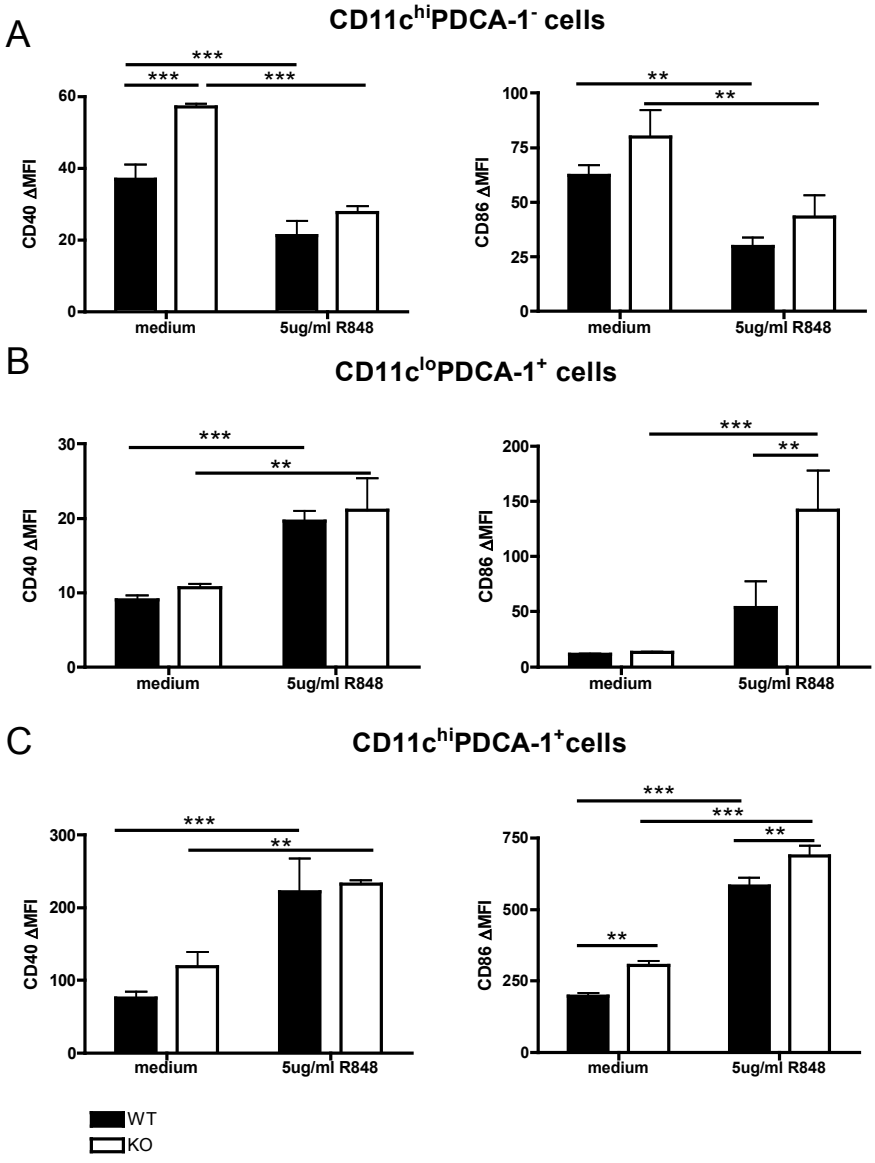

Figure 6.9
Effects of R848 on MLN DC from Flt3L Treated CCX-CKR KO and WT Mice *In Vitro*
MLN cells were isolated from Flt3L treated CCX-CKR KO and WT mice and cultured either in medium alone, or with 5μg/ml R848 and analysed 20 hours later for cell surface expression of CD11c and PDCA-1 to identify DC subsets and CD40 and CD86. The expression of CD40 (left graphs) and CD86 (right graphs) on (A) $CD11c^{+}PDCA\text{-}1^{-}$, (B) $CD11c^{lo}PDCA\text{-}1^{+}$ and (C) $CD11c^{hi}PDCA\text{-}1^{+}$ cells is shown. Results show mean ΔMFI +1 SD of 3 mice per group.

Two way Anova with Bonferroni post tests **p<0.01 ***p<0.001

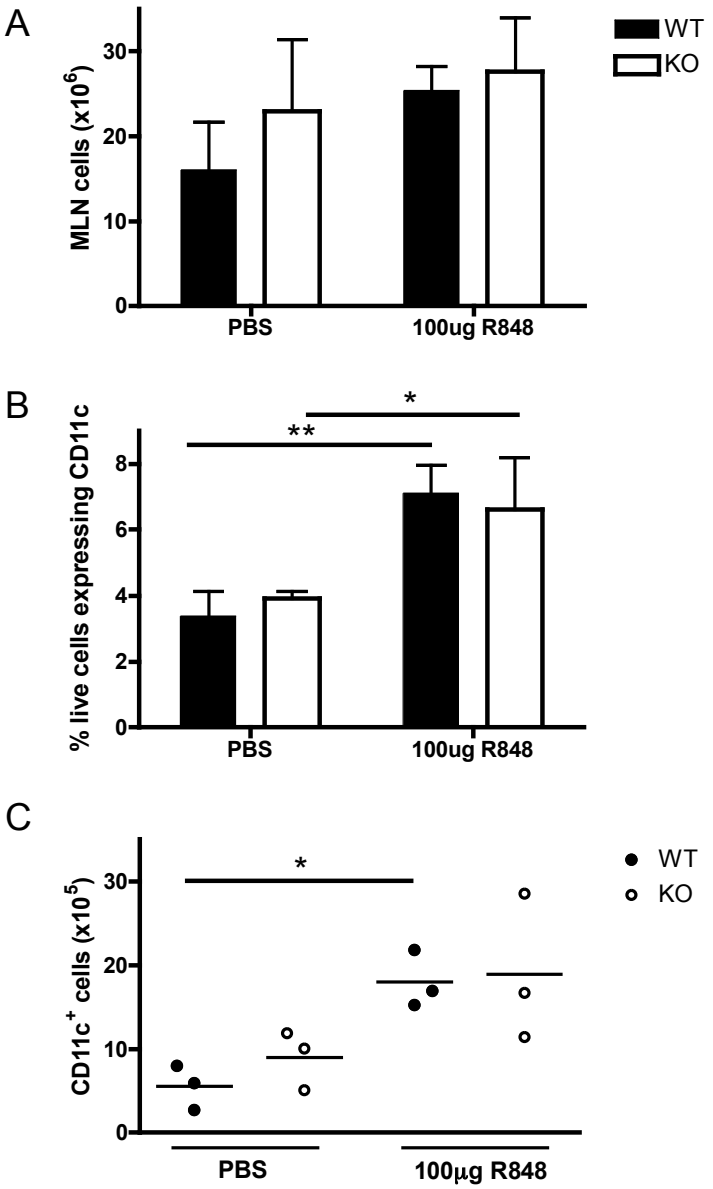

Figure 6.10
Effects of Oral Administration of R848 on DC Populations in the MLN of CCX-CKR KO and WT Mice
CCX-CKR KO and WT mice were fed 100μg R848 or PBS, sacrificed 18 hours later and MLN cells analysed for cell surface expression of CD11c, class II MHC and CD103 to identify DC subsets. (A) Total numbers of live MLN cells and the (B) proportion and (C) absolute numbers of live cells expressing CD11c are shown. Results show means +1 SD of 3 mice.

Two way Anova with Bonferroni post tests *$p<0.05$ **$p<0.01$

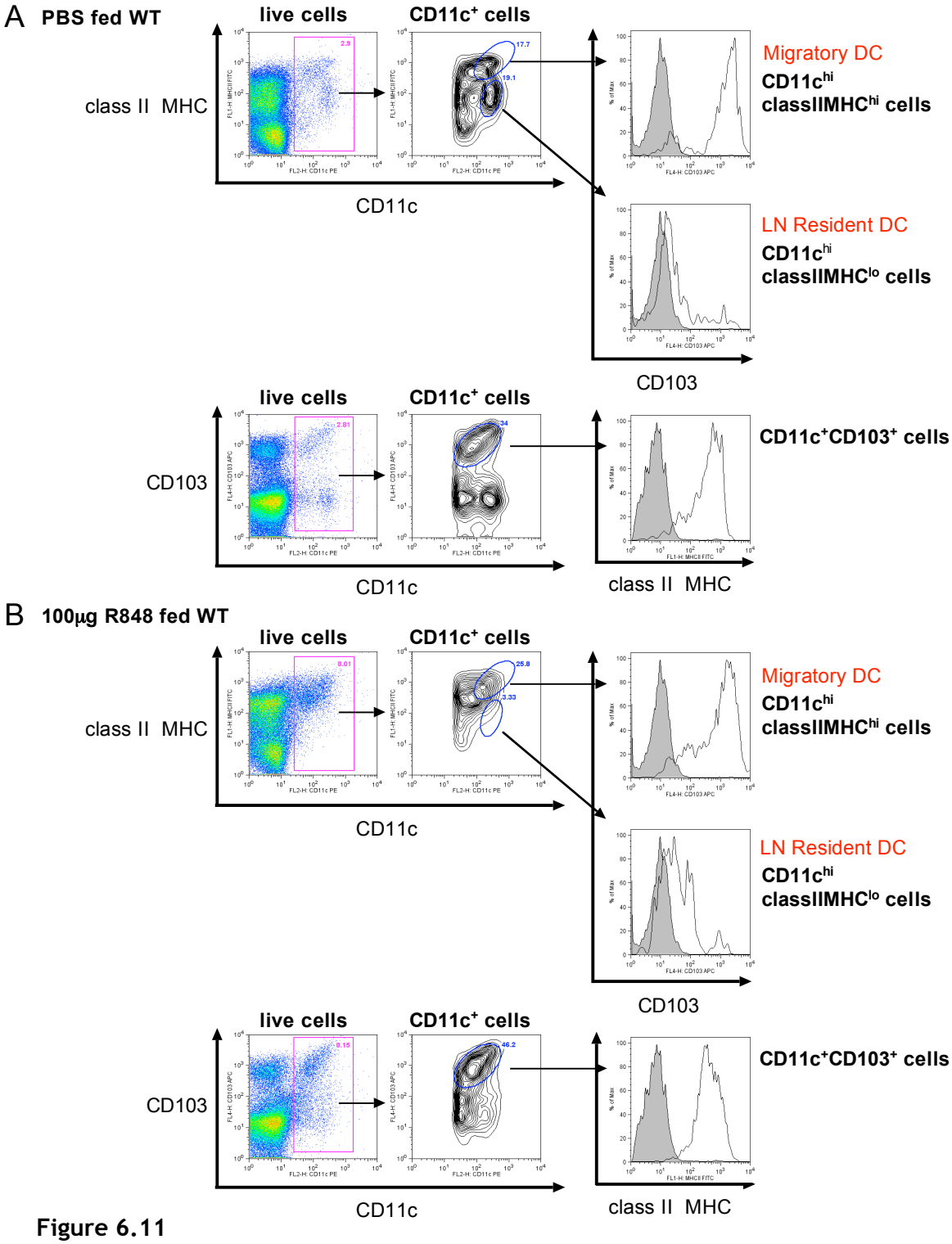

Figure 6.11
Effects of Oral Administration of R848 on DC Populations in the MLN of CCX-CKR KO and WT Mice
CCX-CKR KO and WT mice were fed 100µg R848 or PBS, sacrificed 18 hours later and MLN cells analysed for surface expression of CD11c, class II MHC and CD103 by flow cytometry. Representative FACS plots show the proportion of total live cells expressing CD11c from (A) PBS and (B) R848 fed WT mice. $CD11c^+$ cells were separated into class II MHC^{hi} and class II MHC^{lo} sub-populations to identify migratory and lymph node resident DC respectively. Histograms show isotype staining (shaded) and specific CD103 expression by these DC subsets (top panels of each data set). $CD11c^+CD103^+$ cells were also identifed amongst $CD11c^+$ cells and histograms show isotype staining (shaded) and specific class II MHC expression on these cells (bottom panels of each data set).

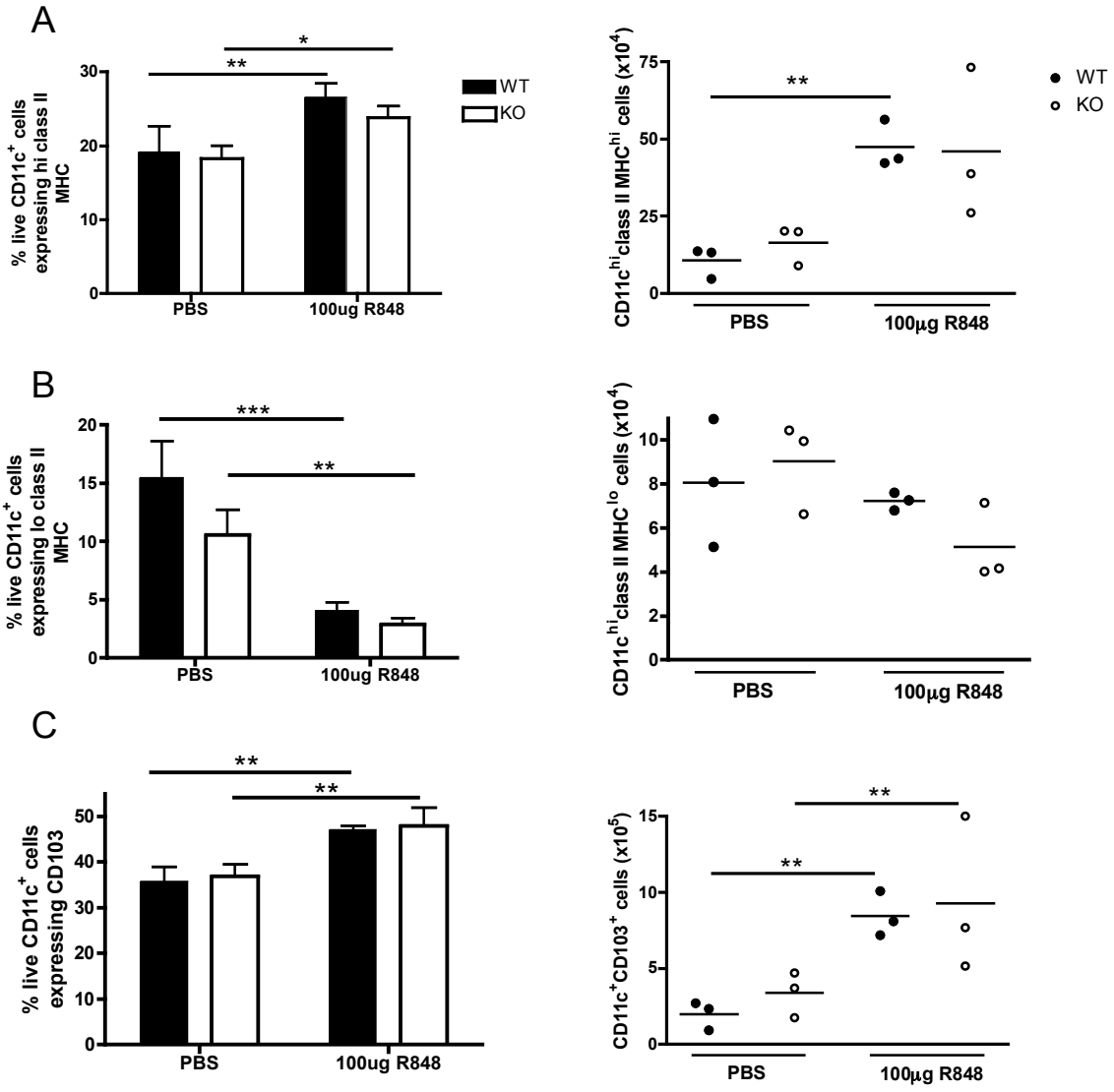

Figure 6.12
Effects of Oral Adminstration of R848 on DC Populations in the MLN of CCX-CKR KO and WT Mice
CCX-CKR KO and WT mice were fed 100µg R848 or PBS, sacrificed 18 hours later and MLN cells analysed for cell surface expression of CD11c, class II MHC and CD103 to identify DC subsets. The proportions (left) and numbers (right) of (A) migratory DC ($CD11c^{hi}$class II MHC^{hi}) and (B) LN resident ($CD11c^{hi}$class II MHC^{lo}) sub-populations are shown. The proportions (left) and numbers (right) of $CD11c^{+}$ cells expressing CD103 are also shown (C). Results show means +1 SD of 3 mice.

Two way Anova with Bonferroni post tests *p<0.05 **p<0.01 ***p<0.001

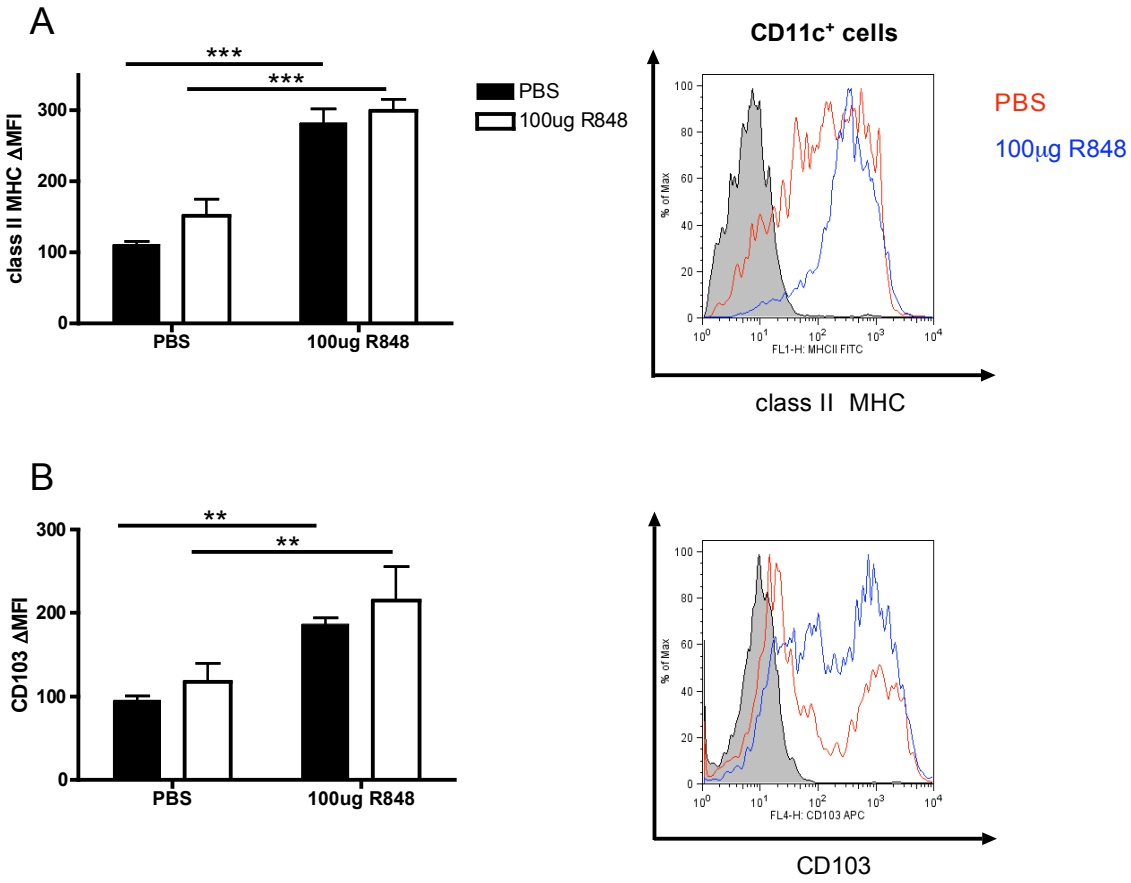

Figure 6.13
Effects of Oral Administration of R848 on Class II MHC and CD103 Expression by MLN DC from CCX-CKR KO and WT Mice
CCX-CKR KO and WT mice were fed 100μg R848 and sacrificed 18 hours later. MLN cells were isolated and analysed for cell surface expression of CD11c, class II MHC and CD103 by flow cytometry. The ΔMFI of (A) class II MHC and (B) CD103 expression on $CD11c^+$ cells is shown. The right panels show representative histograms of isotype staining (shaded) and specific class II MHC and CD103 expression by $CD11c^+$ cells from PBS (red) and R848 (blue) fed WT mice. Results show means +1 SD of 3 mice per group.

Two way Anova with Bonferroni post tests **p<0.01 ***p<0.001

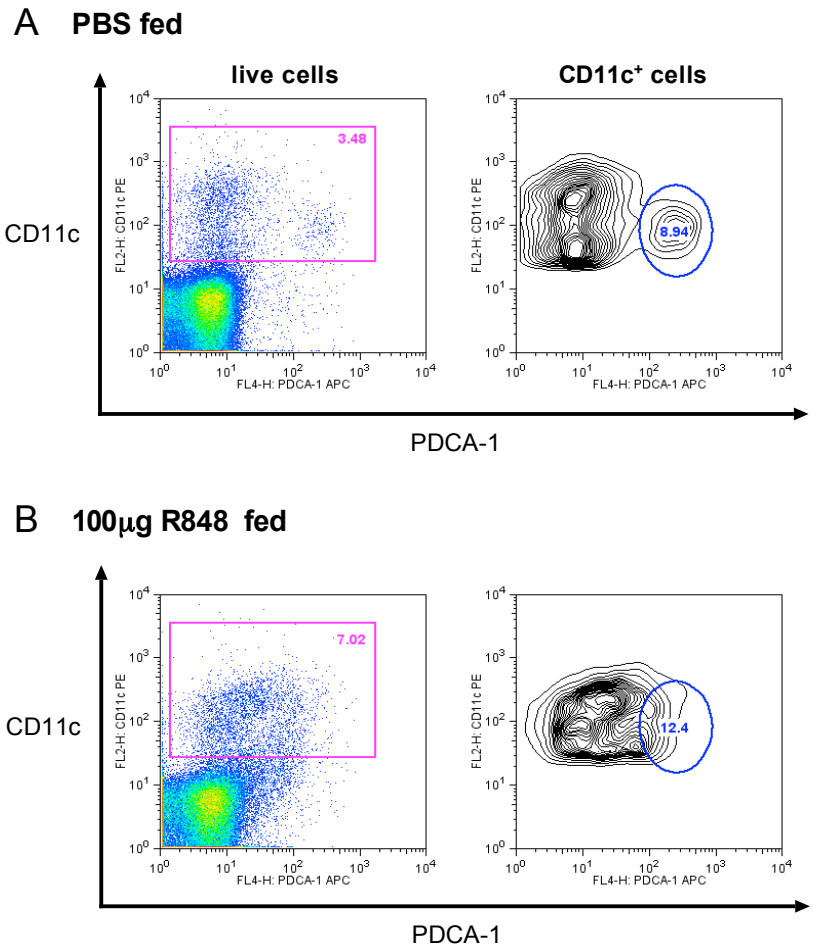

Figure 6.14
pDC from CCX-CKR KO and WT Mice MLN After Oral Administration of R848
CCX-CKR KO and WT mice were fed 100μg R848 or PBS and sacrificed 18 hours later. MLN cells were isolated and analysed for cell surface expression of CD11c and PDCA-1 by flow cytometry. Representative FACS plots of cells from the MLN of (A) PBS and (B) R848 fed WT mice show the proportion of total live cells expressing CD11c (left) and the proportion of $CD11c^+$ cells co-expressing PDCA-1 (right).

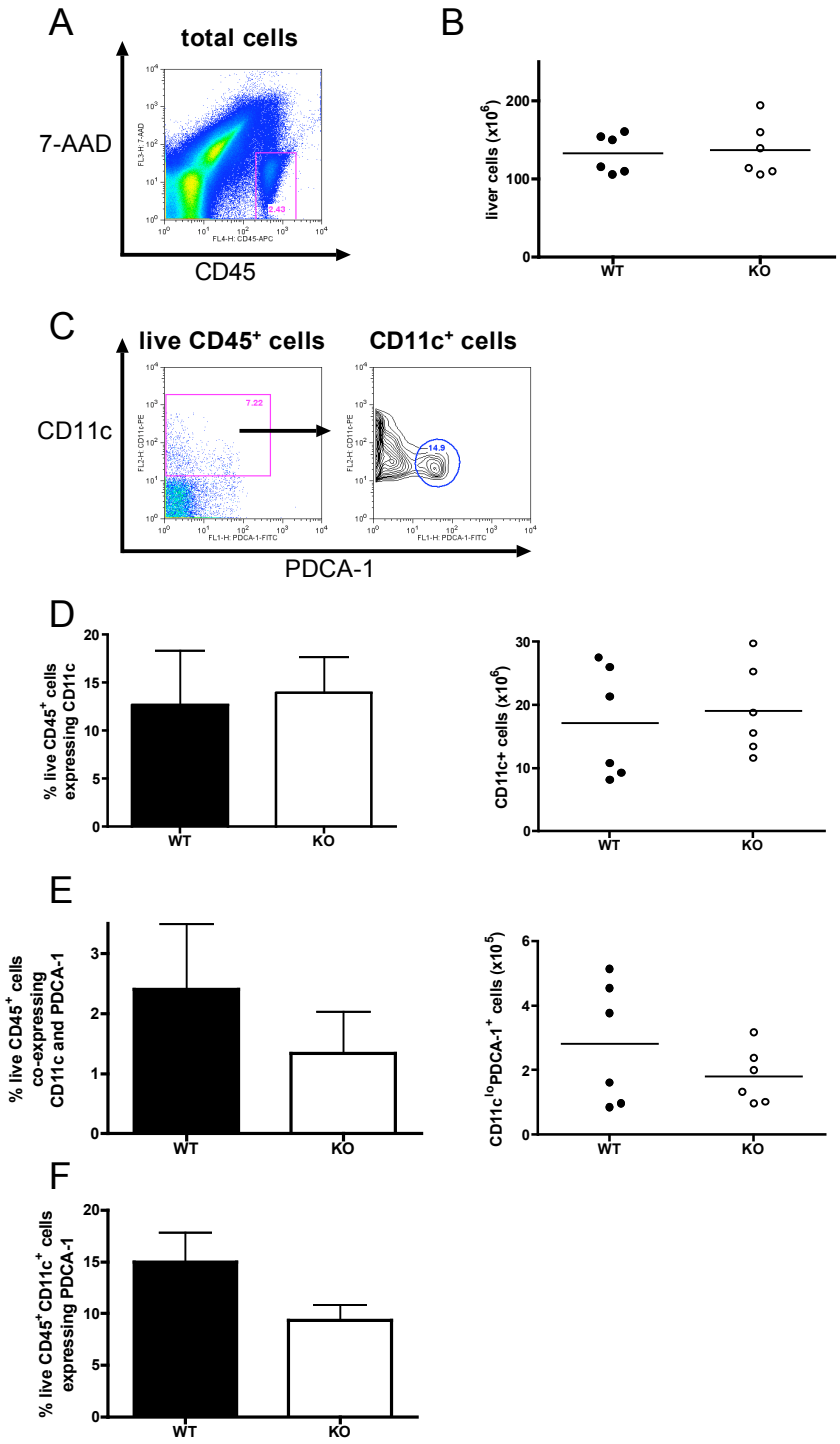

Figure 6.15
pDC in the Liver of Resting CCX-CKR KO and WT Mice
Liver cells from resting CCX-CKR KO and WT mice were analysed for 7-AAD uptake and expression of CD45 to identify 7-AAD$^-$CD45$^+$ live leukocytes (A). The total numbers of live leukocytes were calculated (B) and analysed for expression of CD11c and PDCA-1 to identify pDC. (C) Representative FACS plots show the proportion of live leukocytes expressing CD11c (left) and the proportion of CD11c$^+$ cells expressing PDCA-1 (right). The proportions and numbers of live leukocytes in CCX-CKR KO and WT mice expressing CD11c (D) or CD11c and PDCA-1 (E) are shown. The proportions of CD11c$^+$ cells which co-express PDCA-1 are shown in (F). Results show means +1 SD of 6 mice per group and are pooled from 2 separate experiments.

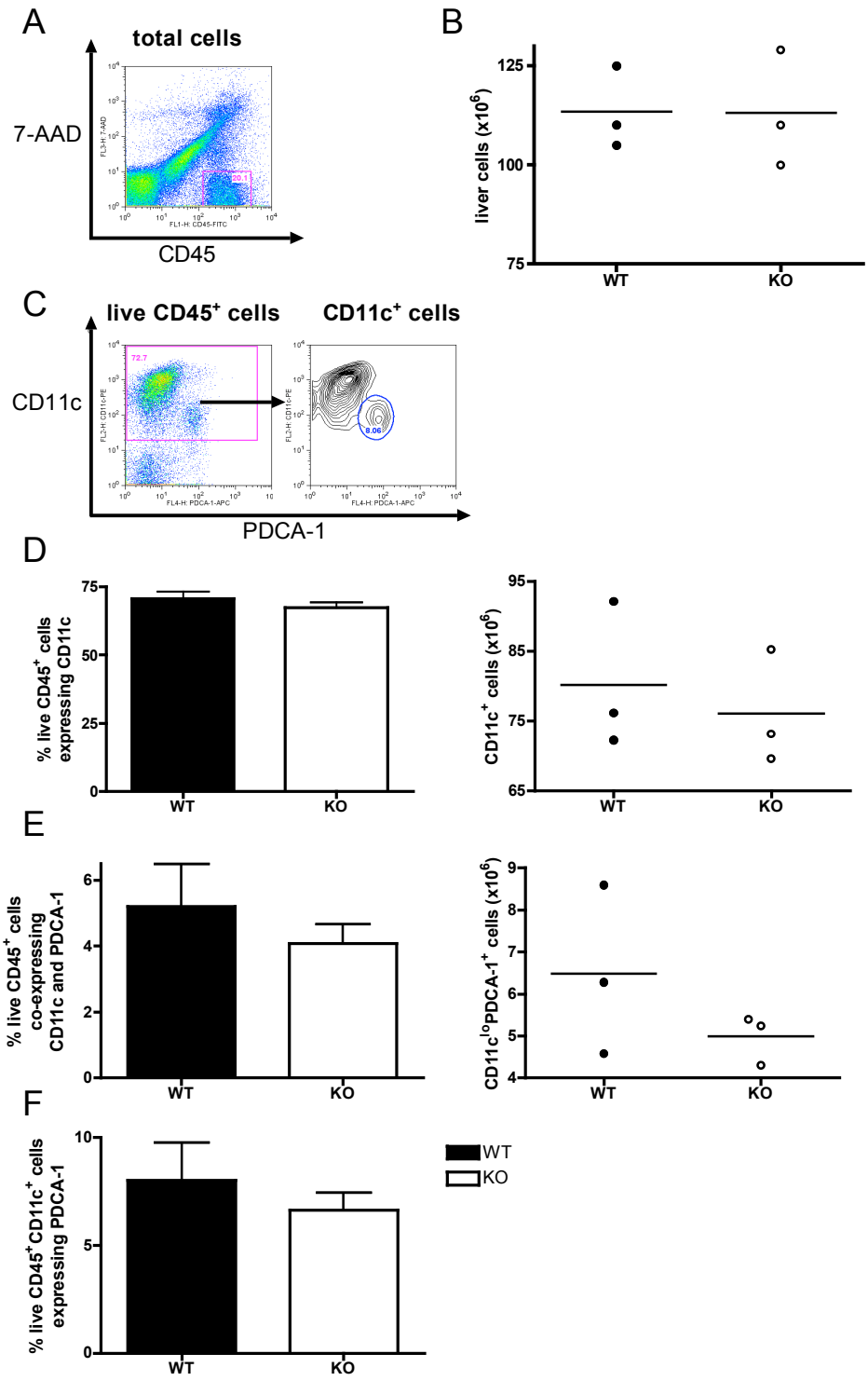

Figure 6.16
pDC in the Liver of Flt3L Treated CCX-CKR KO and WT Mice
Liver cells from Flt3L treated CCX-CKR KO and WT mice were analysed for 7-AAD uptake and expression of CD45 to identify 7-AAD$^-$CD45$^+$ live leukocytes (A). The total numbers of live leukocytes were calculated (B) and analysed for expression of CD11c and PDCA-1 to identify pDC. (C) Representative FACS plots show the proportion of live leukocytes expressing CD11c (left) and the proportion of CD11c$^+$ cells expressing PDCA-1 (right). The proportions and numbers of live leukocytes in CCX-CKR KO and WT expressing CD11c (D) or CD11c and PDCA-1 (E) are shown. The proportions of CD11c$^+$ cells which co-express PDCA-1 are shown in (F). Results show means +1 SD of 6 mice per group and are pooled from 2 separate experiments.

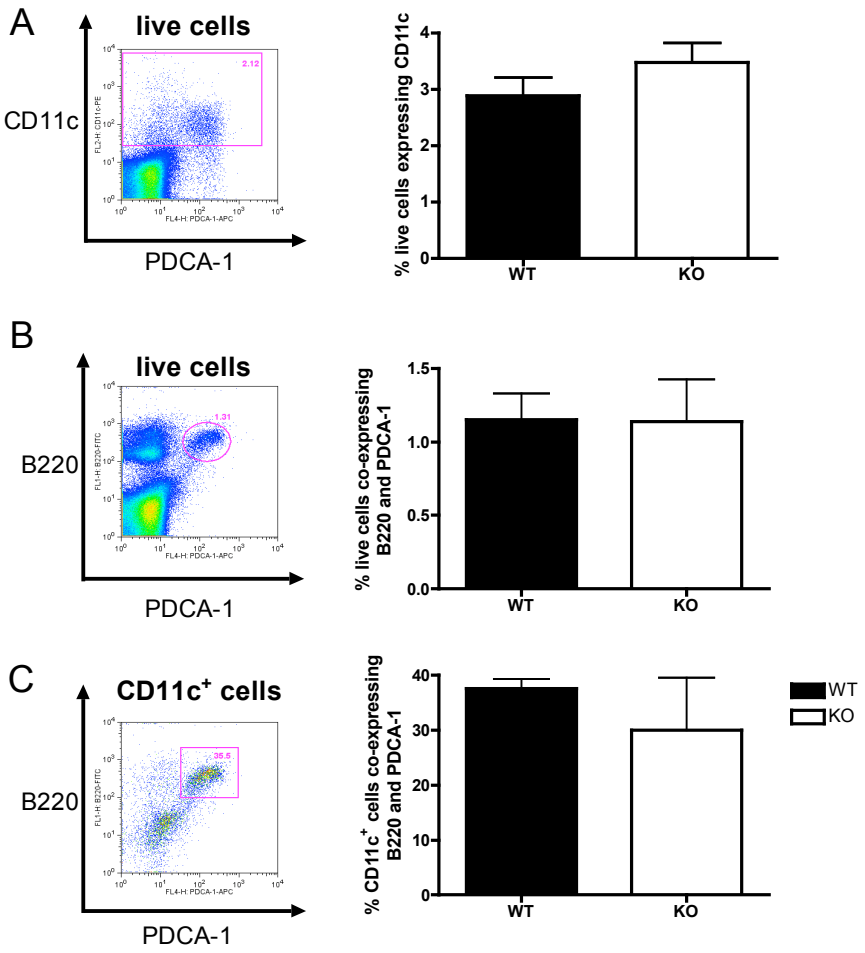

Figure 6.17
pDC in the Bone Marrow of Resting CCX-CKR KO and WT Mice
BM cells were isolated from the femurs of resting WT and CCX-CKR KO mice and analysed for cell surface expression of CD11c, B220 and PDCA-1 to identify pDC. (A) Representative FACS plot of live WT BM cells showing the $CD11c^+$ cell gate and the proportions of live cells expressing CD11c. (B) Representative FACS plot of live WT BM cells showing the $PDCA\text{-}1^+B220^+$ cell gate and the proportions of live cells co-expressing PDCA-1 and B220. (C) Representative FACS plot of live WT BM $CD11c^+$ cells showing the $PDCA\text{-}1^+B220^+$ cell gate and the proportions of $CD11c^+$ cells co-expressing PDCA-1 and B220. Results show means +1 SD of 3 mice per group.

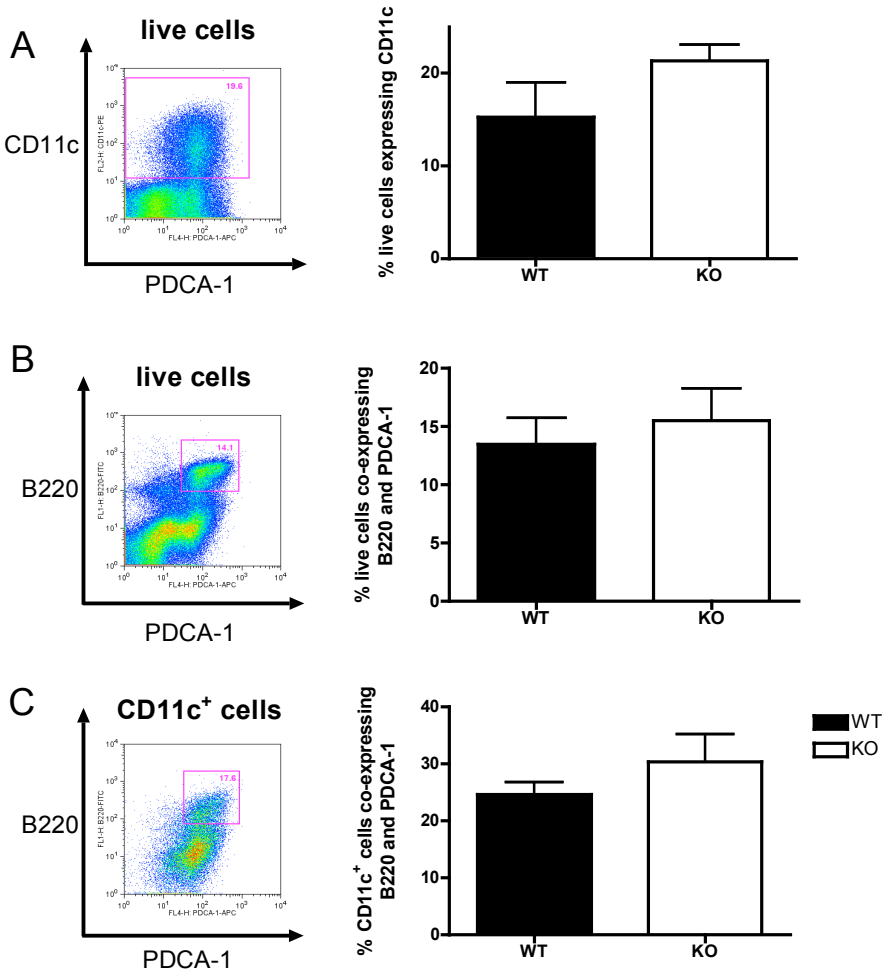

Figure 6.18
pDC in the Bone Marrow of Flt3L Treated CCX-CKR KO and WT Mice
BM cells were isolated from the femurs of Flt3L treated WT and CCX-CKR KO mice and analysed for cell surface expression of CD11c, B220 and PDCA-1 to identify pDC. (A) Representative FACS plot of live WT BM cells showing the $CD11c^+$ cell gate and the proportions of live cells expressing CD11c. (B) Representative FACS plot of live WT BM cells showing the $PDCA\text{-}1^+B220^+$ cell gate and the proportions of live cells co-expressing PDCA-1 and B220. (C) Representative FACS plot of live WT BM $CD11c^+$ cells showing the $PDCA\text{-}1^+B220^+$ cell gate and the proportions of $CD11c^+$ cells co-expressing PDCA-1 and B220. Results show means +1 SD of 3 mice per group.

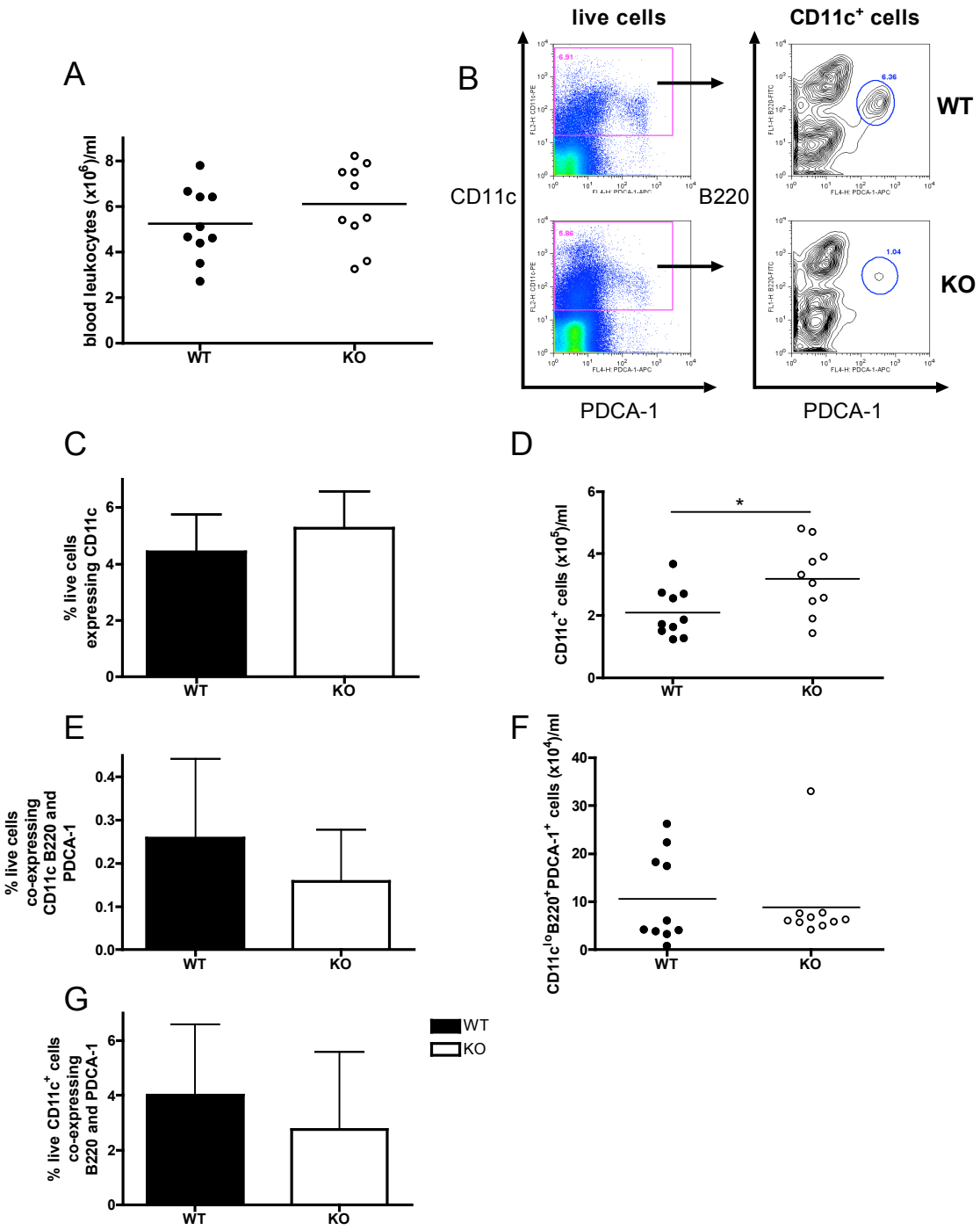

Figure 6.19
pDC in the Peripheral Blood of Resting CCX-CKR KO and WT Mice
The concentration of leukocytes in the blood of resting CCX-CKR KO and WT mice was calculated (A) and cells analysed for surface expression of CD11c, B220 and PDCA-1 to identify pDC. Representative FACS plots of WT and CCX-CKR KO blood leukocytes show the proportion of $CD11c^+$ cells within total live cells and the proportion of $B220^+PDCA\text{-}1^+$ cells in this $CD11c^+$ cell population (B). The proportions (C,E) and absolute numbers (D,F) of total $CD11c^+$ cells and $CD11c^{lo}B220^+$ $PDCA\text{-}1^+$ cells are shown as well as the proportion of pDC within live $CD11c^+$ cells (G). Results show means + 1 SD of 4 or 5 mice per group.

*$p<0.05$ Unpaired t test

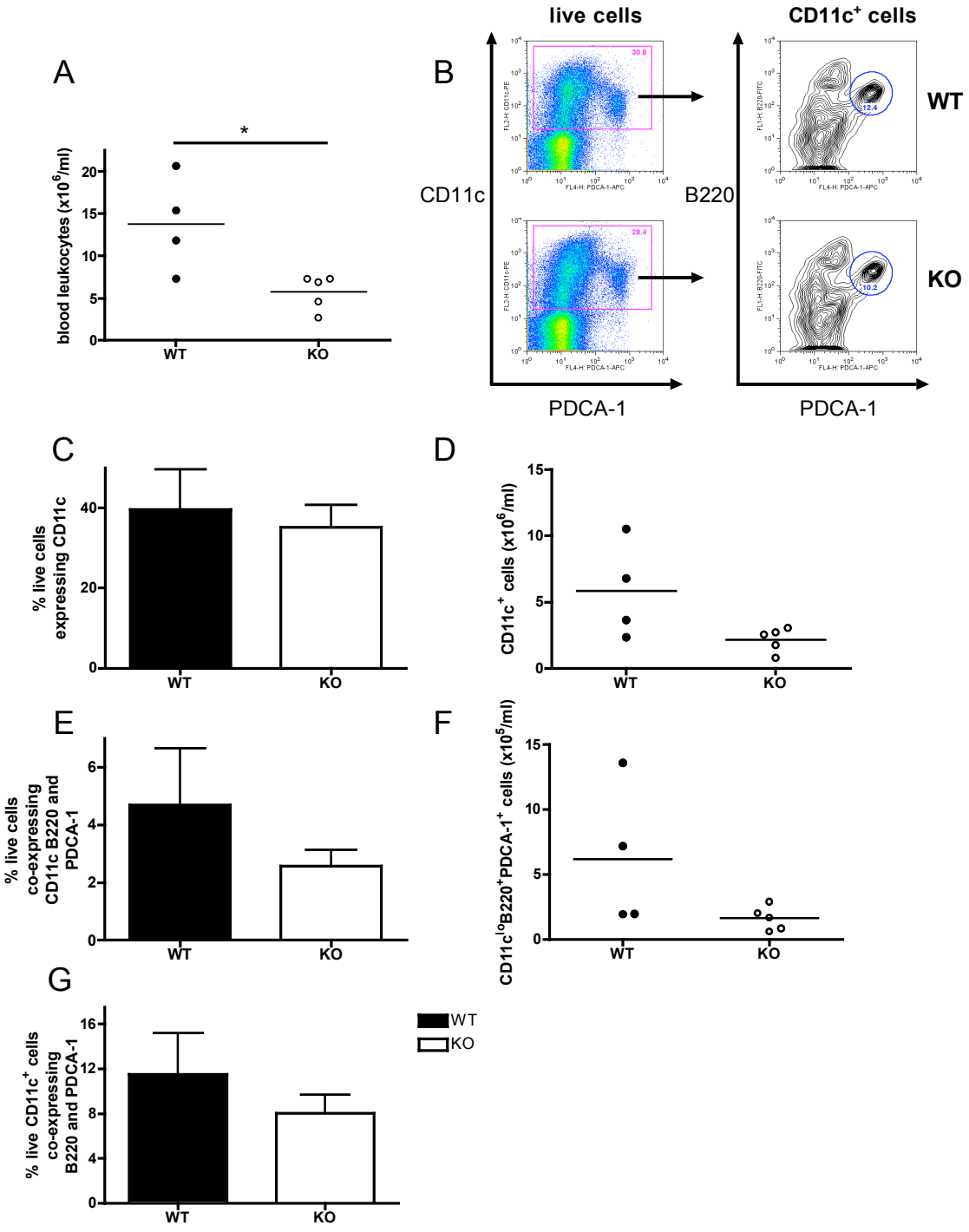

Figure 6.20
pDC in the Peripheral Blood of Flt3L Treated CCX-CKR KO and WT Mice

The concentration of leukocytes in the blood of Flt3L treated CCX-CKR KO and WT mice was calculated (A) and cells analysed for surface expression of CD11c, B220 and PDCA-1 to identify pDC. Representative FACS plots of WT and CCX-CKR KO blood leukocytes show the proportion of $CD11c^+$ cells within total live cells and the proportion of $B220^+PDCA\text{-}1^+$ cells in this $CD11c^+$ cell population (B). The proportions (C,E) and absolute numbers (D,F) of total $CD11c^+$ cells and $CD11c^{lo}B220^+$ $PDCA\text{-}1^+$ cells are shown as well as the proportion of pDC within live $CD11c^+$ cells (G). Results show means + 1 SD of 4 or 5 mice per group.

*p<0.05 Unpaired t test

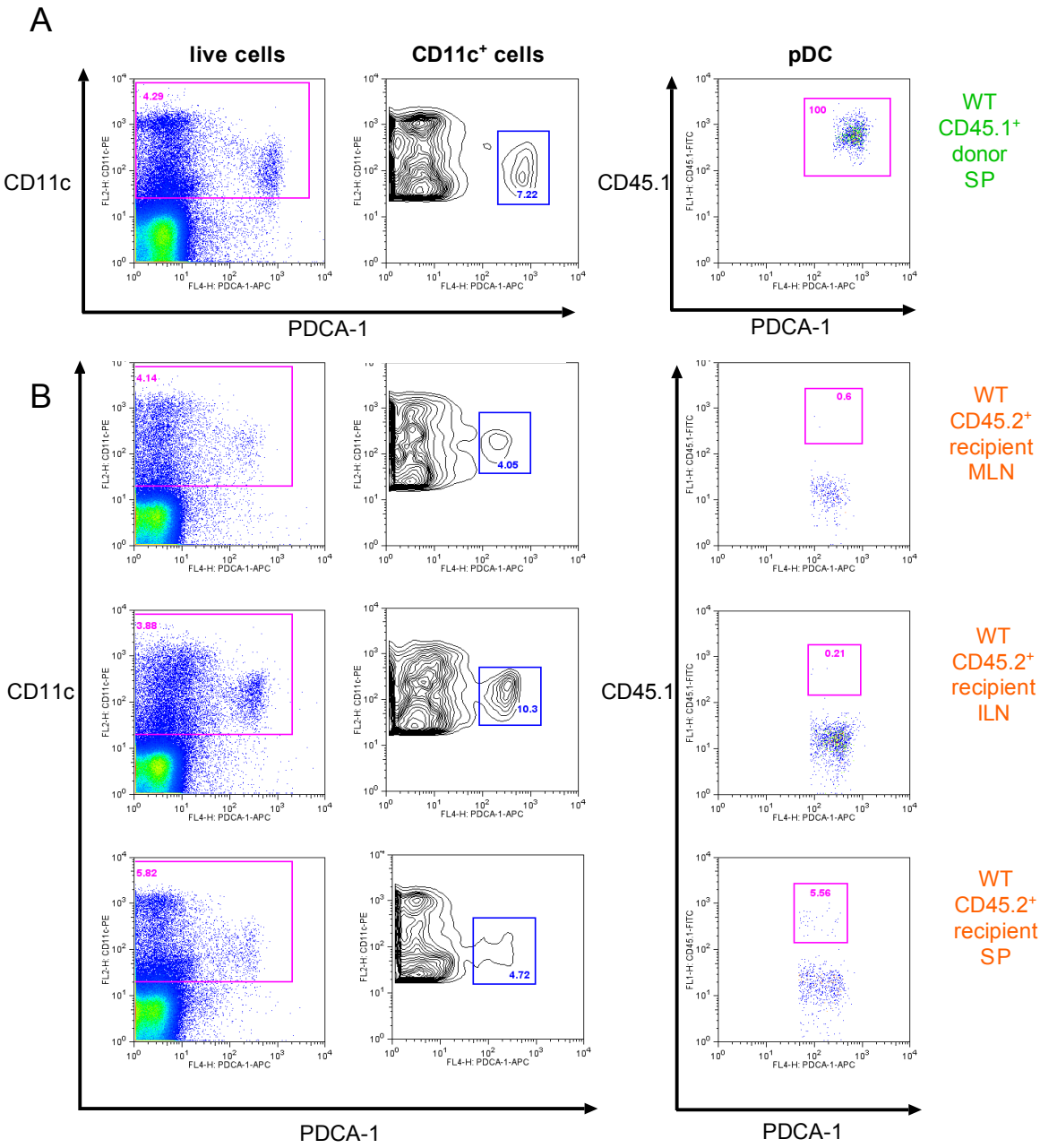

Figure 6.21
Migration of Donor Derived pDC into Tissues of Recipient Mice
WT CD45.1$^+$ splenocytes were stained for CD11c and PDCA-1 to identify pDC as CD11c^{lo}PDCA-1$^+$ cells. CD45.1 expression by all donor pDC was then confirmed by flow cytometry (A). The equivalent of 1x10^6 pDC were adoptively transferred i.p. into CD45.2$^+$ WT mice and 20 hours later, the MLN, ILN and spleens or recipient mice were removed, cells isolated and stained for CD11c, PDCA-1 and CD45.1 to identify transferred pDC. (B) Representative FACS plots show the proportions of total cells expressing CD11c (left), the proportions of CD11c$^+$ cells expressing PDCA-1 (middle) and the proportions of CD11c^{lo}PDCA-1$^+$ pDC expressing CD45.1 to identify donor pDC in the MLN (top), ILN (middle) and spleens (bottom) of CD45.2$^+$ recipient mice.

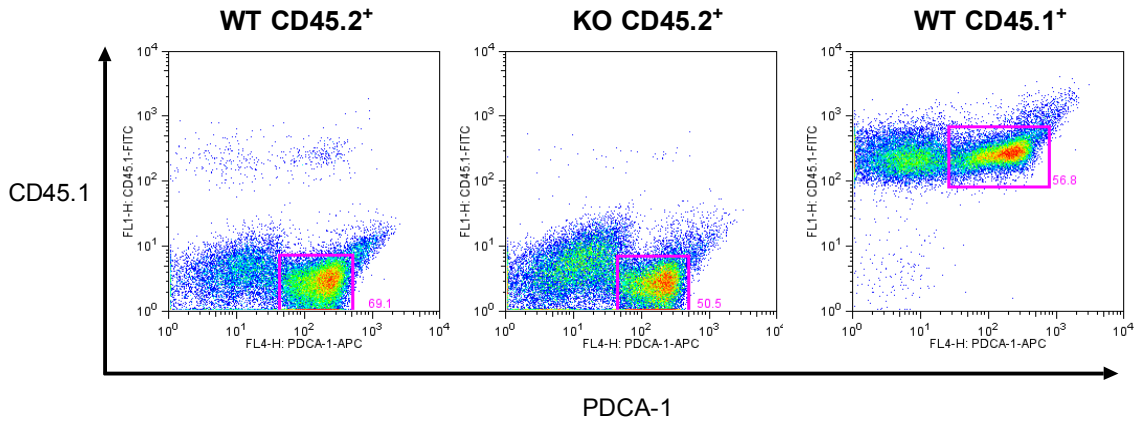

Figure 6.22
Purification of Splenic pDC from Flt3L Treated WT CD45.2$^+$, CCX-CKR KO CD45.2$^+$ and WT CD45.1$^+$ Mice
pDC were isolated from the spleens of Flt3L treated WT CD45.2$^+$, CCX-CKR KO CD45.2$^+$ and WT CD45.1$^+$ mice by negative selection using magnetic beads. Cells were then analysed for surface expression of CD45.1 and PDCA-1 by flow cytometry. Representative FACS plots show the proportion of pDC within the negative fraction of splenocytes from WT CD45.2$^+$, CCX-CKR KO CD45.2$^+$ and WT CD45.1$^+$ donor mice.

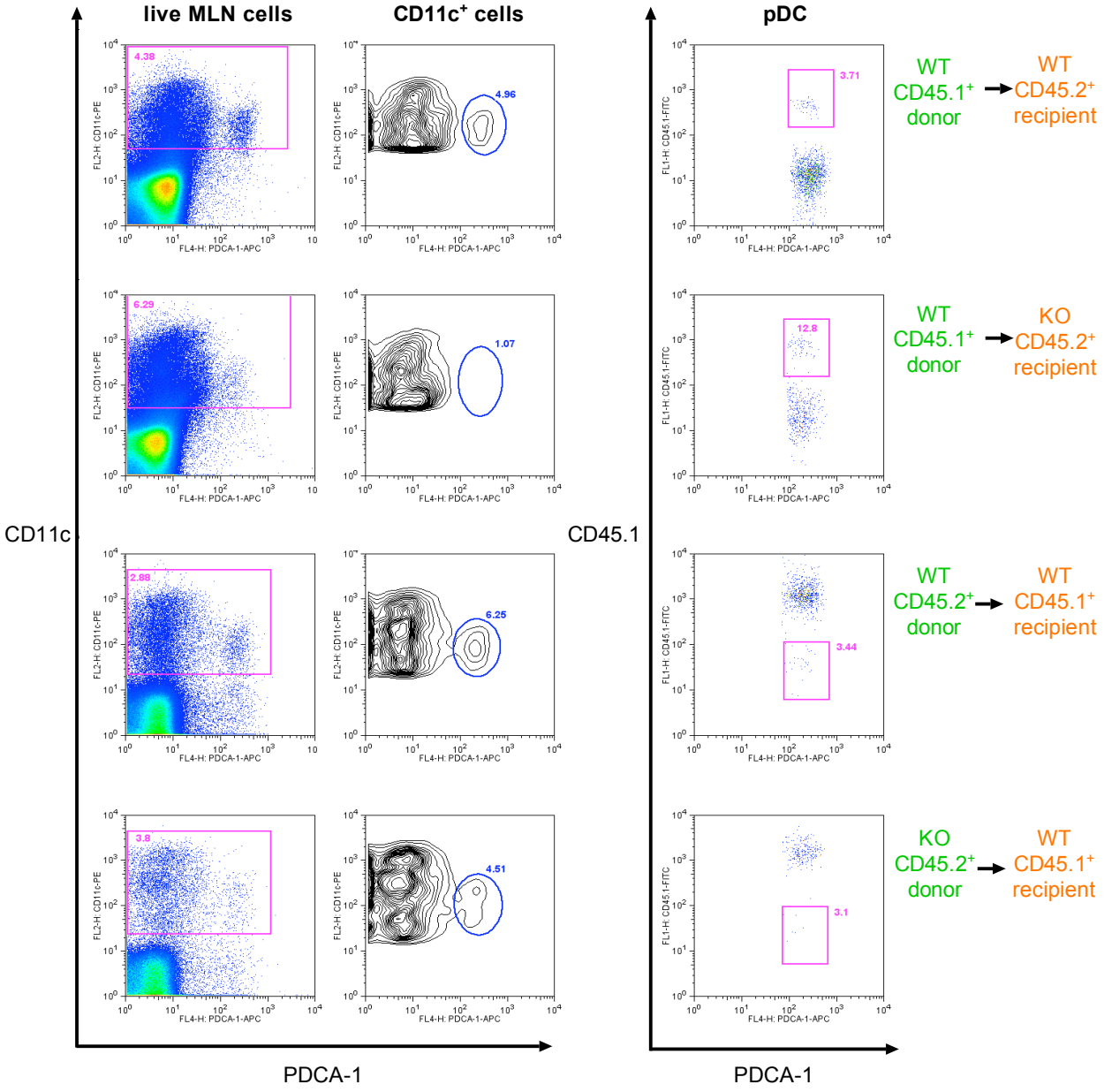

Figure 6.23
Adoptive Transfer of Flt3L Expanded WT and CCX-CKR KO pDC into WT and CCX-CKR KO Recipients

$1x10^6$ pDC from the spleens of Flt3L treated WT CD45.2$^+$, CCX-CKR KO CD45.2$^+$ and WT CD45.1$^+$ donor mice were transferred i.v. into WT CD45.2$^+$, CCX-CKR KO CD45.2$^+$ and WT CD45.1$^+$ recipient mice. 20 hours later, the MLN, ILN and spleens of recipient mice were removed, cells isolated and stained for CD11c, PDCA-1 and CD45.1 to identify transferred pDC. Representative FACS plots show the proportions of recipient live MLN cells expressing CD11c (left panels) and the proportion of these live CD11c$^+$ cells expressing PDCA-1 to identify pDC (middle panels). The proportion of donor pDC within the total MLN pDC population is shown as the proportion of cells expressing CD45.1 or 2 as congenic markers (right panels). Donor mice are indicated in green and recipients in orange alongside plots.

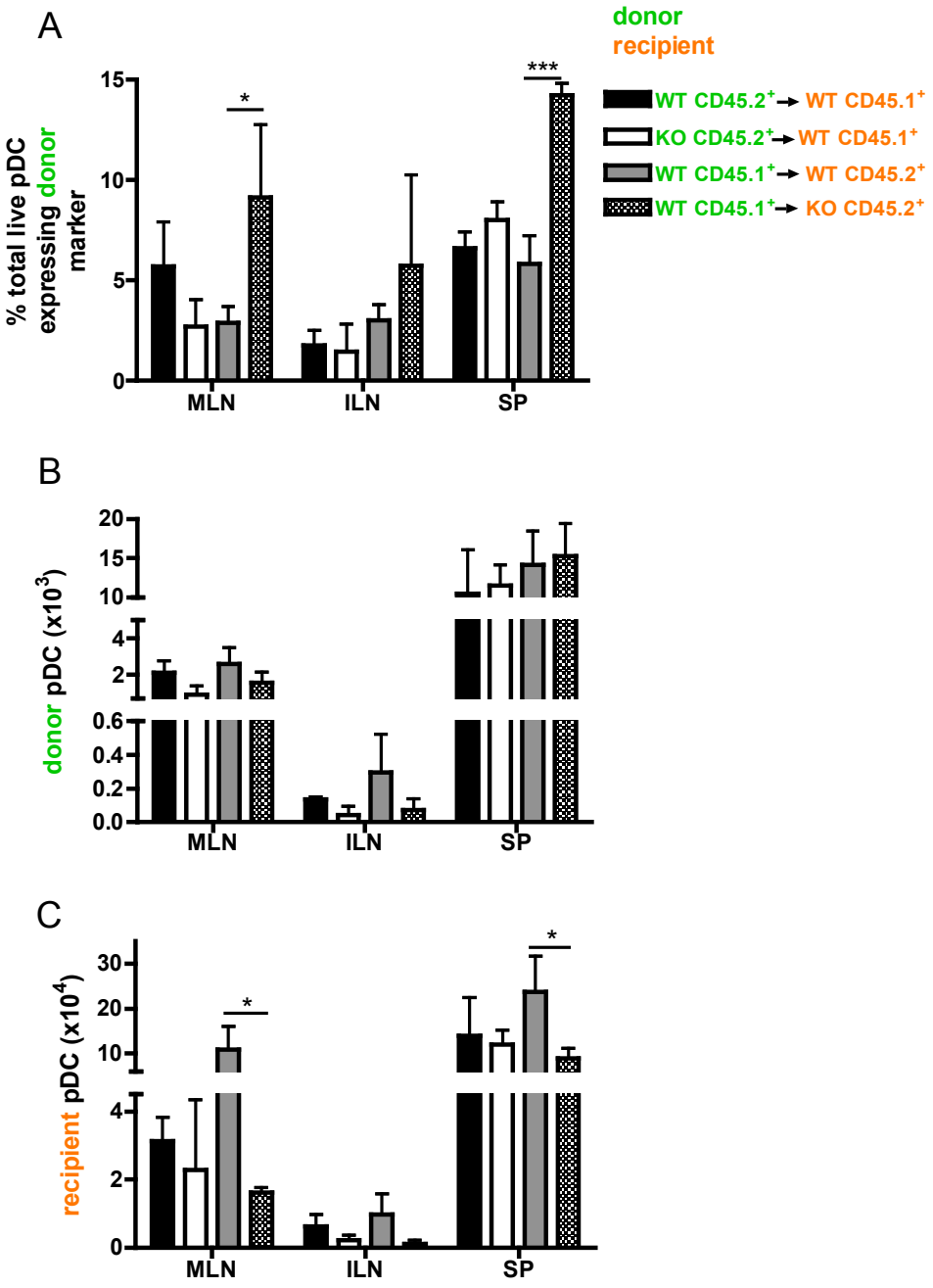

Figure 6.24
Migration of Adoptively Transferred pDC into Secondary Lymphoid Organs of Recipient Mice
$1x10^6$ pDC from the spleens of Flt3L treated WT CD45.2$^+$, CCX-CKR KO CD45.2$^+$ and WT CD45.1$^+$ donor mice were transferred i.v. into WT CD45.2$^+$, CCX-CKR KO CD45.2$^+$ and WT CD45.1$^+$ recipient mice. 20 hours later, MLN, ILN and spleens of recipient mice were removed and cells stained for CD11c, PDCA-1 and CD45.1 to identify transferred pDC. The proportions of donor pDC within total pDC in the MLN, ILN and spleens of recipient mice are shown in (A). The absolute numbers of (B) donor and (C) recipient pDC are also shown. Donor mice are indicated in green and recipients in orange. Results show means +1 SD of between 3 and 4 mice per group.

One-way Anova with Bonferroni post tests *p<0.05 ***p<0.001

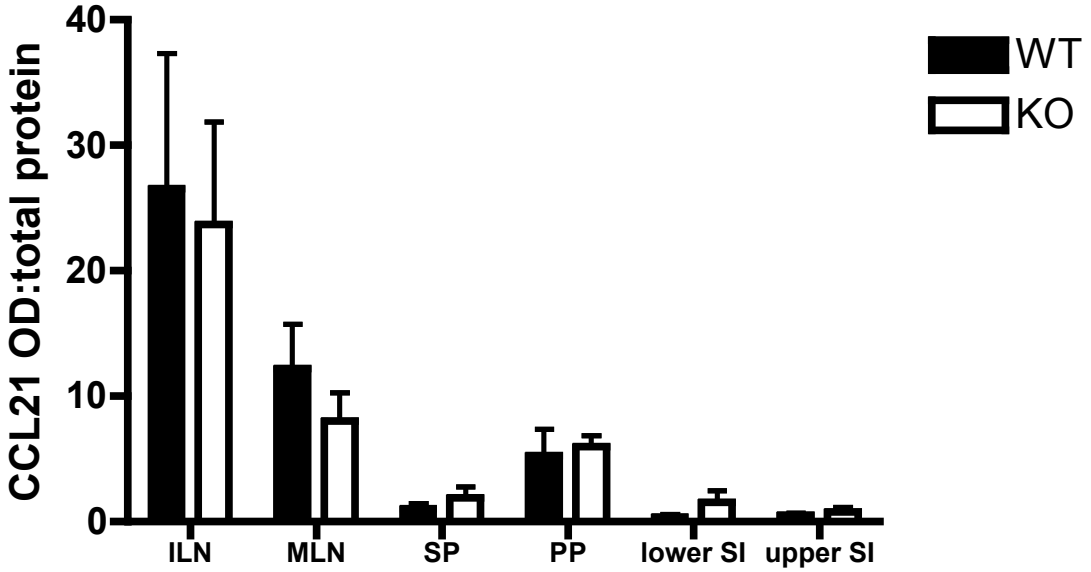

Figure 6.25
CCL21 Protein Levels in CCX-CKR KO and WT Tissues
ILN, MLN, SP,PP and 3cm sections of lower and upper small intestine were isolated from CCX-CKR KO and WT mice and homogenised in TPER protein extraction solution with protease inhibitors. CCL21 levels were determined by ELISA and total protein by BCA assay. Results show the mean ratios + 1 SD of the CCL21 specific OD at 630nm relative to total protein within tissue samples of 5 mice per group.

Chapter 7
Discussion

Introduction

The immune system is constantly interacting with our environment and reacting to the bombardment of antigen it faces every day. The innate immune cells in peripheral tissues, along with the naïve lymphocytes re-circulating throughout secondary lymphoid organs are essential in the establishment of a targeted, antigen specific and efficient immune response that can be re-deployed promptly during re-infection. The organisation of these cells is crucially dependent on chemokines, which must be tightly regulated so that they in turn may regulate leukocyte migration appropriately. Atypical chemokine receptors are proposed to contribute to this organisation by scavenging and/or presenting chemokines and have been studied extensively in recent years. However, the *in vivo* role of the atypical chemokine receptor, CCX-CKR, has remained unclear and at the time of starting my project, there were no publications on this subject. As CCX-CKR binds the homeostatic chemokines, CCL19, CCL21 and CCL25, I aimed to characterise antigen specific immune responses in CCX-CKR KO mice, paying particular attention to the intestinal immune compartment, where all three ligands are involved in the regulation of immunity and tolerance.

7.1 The role of CCX-CKR in steady state lymphocyte trafficking

My initial experiments described in Chapter 3, examined the architecture and cellular composition of secondary lymphoid organs in CCX-CKR KO mice, as CCL19 and CCL21 have important roles in the recruitment and organisation of the cells that initiate and occupy these structures (47). The architecture of the MLN, ILN and spleens of CCX-CKR KO mice appeared normal on H&E stained tissue sections. Secondary lymphoid organs were densely populated and as expected, the LN appeared to be organised into T cell areas and B cell follicles. In addition, white pulp lymphoid areas were also obvious in the spleen. Immunofluorescence staining of tissue sections analysing the expression of T and B cell markers such as CD3 and CD19 would be a logical next step to assess the compartmentalisation of lymphocytes in CCX-CKR KO secondary lymphoid organs more thoroughly.

The cellularity of secondary lymphoid organs appeared to be normal in the large cohort of CCX-CKR KO mice that I examined. This contradicts reports by a previous PhD student which suggested reduced LN cellularity and size in the absence of CCX-CKR. One possible explanation for this discrepancy may be differences in the mouse strains examined, as I used

CCX-CKR KO mice backcrossed on to the C57/Bl6 genetic background, whereas the previous studies were carried out using CCX-CKR KO mice backcrossed on to the FVB genetic background. I also found that the proportions and absolute numbers of $CD4^+$ or $CD8^+$ T and $CD19^+$ B cells were completely normal in the MLN, ILN and spleens of CCX-CKR KO mice, despite their dependence on CCR7 and its ligands for their entry and positioning (22, 66, 71, 76).

As increased concentrations of chemokine can potentially desensitize chemokine receptor activity and CCX-CKR is hypothesised to scavenge excess CCL19, CCL21 and CCL25 (192), I decided to assess lymphocyte expression of CCR7 and CCR9 in CCX-CKR KO mice. CCR9 expression by $CD4^+$ or $CD8^+$ T cells and B cells was not affected by CCX-CKR deletion, suggesting that CCX-CKR does not regulate CCR9 expression directly, despite binding the only known CCR9 ligand, CCL25. However, I did not assess whether or not CCR9 was functional on these cells, for instance, by assessing chemotaxis potential *in vitro*. Unfortunately, my attempts to assess CCR7 expression on these lymphocytes by flow cytometry were unsuccessful despite repeated efforts. Quantification of CCR7 mRNA presents an alternative approach to investigate this and is currently being pursued by another PhD student in the group, who has also developed an assay using biotinylated-CCL19 and flow cytometry to detect CCR7 activity on primary lymphoid cells. In addition, chemotaxis assays could be used to assess CCR7 function *in vitro*.

T regs are essential mediators of peripheral tolerance and are dependent on their expression of CCR7 for their effective function *in vivo*. The suppressive function of CCR7 deficient T regs *in vivo* is profoundly perturbed due to their inability to access secondary lymphoid organs, the T cell zones of which are the major site of T reg mediated suppression (12, 90, 251). There were no differences in the proportions of $CD4^+CD25^+FoxP3^+$ T regs when calculated as a proportion of $CD4^+CD25^+$ T cells that express FoxP3 in the MLN, ILN or spleens of resting CCX-CKR KO mice. However, the absolute numbers and proportions of $CD4^+CD25^+FoxP3^+$ cells amongst total live spleen cells appeared to be slightly elevated in CCX-CKR KO mice although only the increase in proportions attained statistical significance. This suggests that although there is a normal frequency of FoxP3 expressing cells amongst $CD4^+CD25^+$ T cells in the ILN, MLN and spleens of CCX-CKR KO mice, overall there is a greater proportion of $CD4^+CD25^+FoxP3^+$ T regs in the CCX-CKR KO spleen. Perhaps, this reflects an aberrant re-

circulation or distribution of T regs in CCX-CKR KO mice, a possibility that might be better addressed using models of tolerance where the induction of T regs can be assessed, for instance during the induction of oral tolerance.

The proliferative responses of T cells to anti-CD3/CD28 and to the mitogen, Con A, were normal in the absence of CCX-CKR. However, IFNγ production by cells from the MLN and spleens of CCX-CKR KO mice was significantly reduced compared with WT cells when stimulated with anti-CD3/CD28. Furthermore, $CD4^+$ T cells from the MLN and spleens of CCX-CKR KO mice were less efficient than WT in their production of IFNγ in response to stimulation with PMA/ionomycin. IFNγ production by MLN cells from CCX-CKR KO mice stimulated with Con A was also significantly reduced compared with WT MLN cells. This suggests that the *in vitro* production of the Th_1 type cytokine, IFNγ may be affected by CCX-CKR deletion. It would be interesting therefore, to investigate Th_2 or Th_{17} type responses in CCX-CKR KO mice (252-256). Effector T cell functions in CCX-CKR KO mice have not been examined in any detail but it has been published very recently that CCX-CKR KO mice develop exaggerated Th_{17} responses during EAE (257).

Thus the lymphocyte composition of secondary lymphoid organs is normal in CCX-CKR KO mice, with the exception of slightly but significantly elevated proportions of $CD4^+CD25^+FoxP3^+$ T regs in the spleen. Proliferative responses of polyclonal T cells were normal when stimulated with anti-CD3/CD28 or ConA, but the production of IFNγ under such circumstances and in response to PMA/ionomycin stimulation were impaired, suggesting that T cells may be polarised differently in resting CCX-CKR KO mice.

7.2 Conventional DC in CCX-CKR KO mice

The CCR7 and CCX-CKR ligands CCL19 and CCL21 have crucial roles in the recruitment of antigen loaded CCR7 expressing DC from peripheral tissues to secondary lymphoid organs and are essential for the development of antigen specific adaptive immunity and tolerance (60, 62, 125, 258). All mouse DC express CD11c and class II MHC to varying extents, but class II MHC is also highly expressed by B cells and activated macrophages, while CD11c may also be present on some NK cells and even a few T cells in secondary lymphoid organs (259). However during my project, only four colour flow cytometry was available in the department and therefore I was limited in the number of parameters I could use to discriminate different

cell populations. Therefore I decided to use CD11c expression as the consistent marker of DC in all the tissues I examined. My initial results suggested there might be a significant reduction of $CD11c^+$ cells in the MLN, but not the ILN or spleens of CCX-CKR KO mice compared with WT. However this difference was not consistent when the experiments were repeated. Overall, the proportions and absolute numbers of $CD11c^+$ cells in the MLN, ILN and spleens of CCX-CKR KO mice were almost identical to those in WT mice. Despite this, I decided to pursue a more thorough characterisation of the DC subsets in CCX-CKR KO mice, as some DC subsets constitute a relatively minor fraction of total DC and so any differences in their numbers may be very subtle and difficult to detect.

Due to my initial observations of reduced $CD11c^+$ cell numbers in the MLN of CCX-CKR KO mice and difficulties in obtaining sufficient DC from other tissues for analysis, most of my subsequent investigations were focussed on the MLN. Conventional DC can be broadly divided into $CD11c^+CD8^+$ and $CD11c^+CD11b^+$ cell subsets, the latter of which also usually expresses CD4 (55). Therefore it was somewhat surprising that although I found the proportions of $CD11c^+CD11b^+$ DC amongst total live cells to be normal in CCX-CKR KO MLN, the proportion of $CD11c^+CD4^+$ DC were decreased under the same conditions. The proportion of $CD11c^+CD8^+$ DC amongst total live cells was also reduced in CCX-CKR KO MLN. I also assessed the prevalence of the individual DC subsets amongst $CD11c^+$ cells themselves, so as to examine the relative contributions of any given DC subset to the total $CD11c^+$ cell population. By doing this, I hoped to increase the accuracy and sensitivity of my analyses as it meant that DC subsets that made up a relatively minor proportion of total live cells would constitute a significant fraction of $CD11c^+$ cells. When I expressed the results in this way, the proportion of $CD8^+$ DC amongst CD11c expressing cells was still significantly reduced in CCX-CKR KO MLN, but the apparent defect in $CD4^+$ DC disappeared and $CD11b^+$ DC remained normal. The absolute numbers of $CD4^+$, $CD8^+$ or $CD11b^+$ DC were not significantly decreased in CCX-CKR KO MLN, although the absolute numbers of $CD8^+$ DC did appear to be reduced. Further investigations using larger sample sizes and the nine colour flow cytometry which became available in the department after my project finished would be valuable in determining any affect of CCX-CKR deletion on the $CD8^+$ DC subset.

As $CD8^+$ DC gain access to LN via HEV, this suggests that CCX-CKR may play a role in regulating trans-migration of DC into LN. Interestingly, an as yet unidentified receptor has

been shown to transcytose CCL19 across the endothelial cells lining the HEV and in doing so, regulates the recruitment of leukocytes into LN (72). The possibility that CCX-CKR may serve such a purpose is intriguing. Adoptive transfer experiments using WT $CD8^+$ DC may help to determine whether or not there is a defect in $CD8^+$ DC migration across HEV in CCX-CKR KO mice.

In the experiments described in Chapter 6, I performed some preliminary investigations in to the function of CCX-CKR KO DC. Firstly, I compared the intrinsic responses of CCX-CKR KO and WT BMDC to stimulation with the TLR ligand, LPS. No differences were found between the different sources of BMDC in this experiment, but these studies were only partially successful as there were no statistically significant increases in the expression of co-stimulatory molecules or class II MHC after LPS stimulation of either kind of BMDC. Therefore these experiments need to be repeated and it would be important to assess other responses to BMDC activation, such as CCR7 up-regulation and cytokine production, as well as other TLR ligands. Although the endocytic capacity of CCX-CKR KO BMDC appeared to be normal, their ability to process and present OVA to OT2 LN cells was significantly reduced compared with WT BMDC. However, the capacity of BMDC to present OVA 323-339 peptide was not impaired by CCX-CKR deletion and in fact was significantly enhanced at a 1:5 DC:T cell ratio. Splenic DC from CCX-CKR KO mice also showed a significantly reduced capacity to process and present either intact OVA or OVA peptide to T cells. These findings of reduced APC activity by CCX-CKR KO DC are difficult to reconcile with the apparently exaggerated susceptibility to oral priming that I observed. However, it should be noted that immune responses to systemic immunisation were normal in CCX-CKR KO mice and therefore any defect in antigen presentation may be restricted to the intestinal immune compartment. As this may not be replicated by splenic DC or BMDC, it would be important to assess APC activity of MLN or lamina propria derived DC directly. In addition, I would have liked to examine the antigen presentation capacity of pDC from CCX-CKR KO mice by generating BMDC *in vitro* using Flt3L as an alternative to GMCSF (279).

7.3 CCX-CKR KO mice have a selective defect in pDC in secondary lymphoid organs

The most dramatic effect of CCX-CKR deletion I found on DC populations was a consistent defect in pDC numbers in the MLN. I defined pDC as $CD11c^{lo}PDCA\text{-}1^+$ cells, because

although pDC are $B220^+$, a recent report has identified some $CD11c^+B220^+$ cells in LN as being precursors of conventional DC rather than genuine pDC. The absolute numbers and proportions of all $CD11c^{lo}B220^+$ cells amongst $CD11c^+$ cells were reduced in the MLN of CCX-CKR KO mice and closer examination showed that this was due to dramatic decreases in the proportions and absolute numbers of pDC as defined by the $CD11c^{lo}PDCA\text{-}1^+$ and $CD11c^{lo}B220^+PDCA\text{-}1^+$ phenotype. In contrast, the absolute numbers and proportions of the $CD11c^{lo}B220^+PDCA\text{-}1^-$ putative precursor DC were not different between the strains.

This marked defect in pDC in CCX-CKR KO MLN was highly reproducible in repeated experiments. The proportions of pDC amongst total live cells and $CD11c^+$ cells were also significantly reduced in the ILN of CCX-CKR KO mice and the absolute numbers of pDC were also reduced here, but this did not attain statistical significance. In addition, the proportions and absolute numbers of pDC were normal in the spleen of CCX-CKR KO mice, suggesting that the defect in pDC numbers is selective to lymphoid organs where pDC must migrate across HEV to gain access (123, 124) and that this is particularly manifest in the MLN. This is supported by the deficiency in the proportions of $CD8^+$ DC in CCX-CKR KO MLN that I also observed. However, as some pDC are reported to express CD8 (55), it is possible that the apparent decrease in $CD11c^+CD8^+$ cells I found in CCX-CKR KO MLN could be accounted for by the large defect in pDC. It has been shown that pDC are found in the T cell zone near to HEV in WT LN (117) and it would be important to perform immunohistological analysis to determine the distribution of pDC in the lymphoid tissues of CCX-CKR KO mice. Unfortunately, I did not have time to carry out studies of this kind.

PDCA-1, is also known as BST-2, CD317 or 120G8 (250, 260) and binds ILT7 which inhibits type 1 IFN and pro-inflammatory cytokine production by pDC. The co-expression of PDCA-1 and ILT7 on human pDC is believed to co-operate in a negative feedback loop that limits their cytokine production (261, 262). The apparent decrease in pDC numbers in CCX-CKR KO MLN did not appear to be an artefact of decreased PDCA-1 expression, as the numbers of pDC were similarly altered when using B220 and CCR9 expression as pDC markers. Unfortunately, I was unable to examine the levels of CCR9 expression on $PDCA\text{-}1^+$ pDC, due to technical difficulties and the lack of sufficient flow cytometry colours, but this would have been interesting in view of the possibility that CCX-CKR may regulate the functional expression of this receptor.

Although macrophages and NK cells do not express CCR7 or CCR9 they do respond to the cytokines that are secreted by activated pDC such as type 1 IFN (115). However, the proportions and absolute numbers of $F480^+$ macrophages in the MLN, ILN and spleens of CCX-CKR KO mice were entirely normal, as were the proportions and absolute numbers of $CD3^-DX5^+$ NK cells in CCX-CKR KO MLN.

7.4 Composition of leukocytes in the intestinal immune compartment of CCX-CKR KO mice

All three CCX-CKR ligands are expressed in the intestinal immune compartment and have established roles in the development of mucosal immunity and tolerance. My experiments in Chapter 4 indicated that the architecture of the small intestine and colon was normal in the absence of CCX-CKR. One abnormality in the small intestine was that although IEL were positioned normally in CCX-CKR KO mice, their numbers were significantly reduced in comparison to WT mice. CCL25 secretion by the epithelial layer recruits CCR9 expressing IEL and is thought to induce the CD103 mediated adhesion of IEL to the E-cadherin expressed on the intestinal epithelium (199-201, 263). As CCL25 availability and/or distribution may be affected by CCX-CKR deletion, it would therefore be of interest to examine CD103 expression on IEL in CCX-CKR KO mice. I did attempt to analyse IEL from CCX-CKR KO and WT mice by flow cytometry, but was unable to produce consistent results and as this was not a major aim of my work, I did not take this further.

CCR9 is expressed on most lamina propria lymphocytes (214, 264) and its expression is imprinted by lamina propria derived $CD103^+$ DC that are dependent on CCR7 for their migration to the MLN. Thus, the ligands of CCR7 and CCR9, CCL19, CCL21 and CCL25 all have important roles in the induction and recruitment of gut homing effector lymphocytes to the small intestinal lamina propria (125, 132, 133, 210). The proportions and numbers of T cells in the lamina propria as defined by CD3, CD4 or CD8 expression were normal in the absence of CCX-CKR suggesting that the migration of effector T cells to this site is not dependent on CCX-CKR. Again, I was unable to confirm the expression levels of CCR9 on these cells which would be important to determine. It would also be informative to assess the levels of CCL25 protein in the mucosa of CCX-CKR KO mice to gain some insight into how CCX-CKR might function as a chemokine scavenger. I did begin preliminary studies of this, but other work going on in the laboratory at the same time showed that the commercially

available ELISA kit was unreliable. As other reagents were not available, I did not pursue this line of investigation and unfortunately as this was towards the end of my project, I did not have time to assess CCL25 mRNA levels.

Interestingly, the proportions of $CD11c^+$ cells and $CD19^+$ B cells were significantly increased and decreased respectively in CCX-CKR KO small intestinal lamina propria, although these differences did not translate into differences in absolute numbers. As many $CD11c^+$ cells in the lamina propria are likely to be macrophages rather than genuine DC (265), it was important to determine if this finding might be related to the requirement for CCR7 ligands in the migration of $CD11c^+$ DC from the lamina propria to the MLN. Therefore, I decided to analyse the numbers of individual DC subsets in the lamina propria of CCX-CKR KO mice. Assessing the numbers and phenotype of conventional DC in this tissue proved impossible due to the limitations of four colour flow cytometry, but I was able to examine pDC in the CCX-CKR KO lamina propria. This was important as pDC at this site express high levels of CCR9 and are absent from the small intestine of CCR9 KO mice, suggesting an essential role for CCR9 and CCL25 in their accumulation at this site (121). I was unable to use CD11c and PDCA-1 alone as markers of pDC in the mucosa as a significant proportion of $CD45^+CD11c^-$ cells in the lamina propria seemed to express PDCA-1, making gating difficult. I therefore defined pDC as $CD11c^{lo}B220^+$ cells. Although not a perfect strategy for the reasons discussed above, a clear population of $CD11c^{lo}B220^+$ cells was apparent in the small intestinal lamina propria of both CCX-CKR KO and WT mice, with their proportions being identical between strains. This requires confirmation using more sophisticated flow cytometry. I was able to examine CD103 expression by $CD11c^+$ cells in the lamina propria and could distinguish two subsets within this population, one $CD11c^{hi}CD103^{hi}$ and the other, $CD11c^{int}CD103^{lo}$. The proportions and absolute numbers of both subsets of $CD103^+$ DC were unaltered in the lamina propria in the absence of CCX-CKR. As $CD103^+$ DC migrate from the lamina propria to MLN, I also examined the numbers of these cells in CCX-CKR KO MLN. Again, the absolute numbers and proportions of $CD103^+$ DC were normal in the absence of CCX-CKR, suggesting that CCX-CKR plays little or no role in regulating the constitutive migration of DC from the lamina propria to MLN.

I also examined the numbers of migratory and LN resident DC in resting CCX-CKR KO MLN using a phenotypic strategy that defined them on the basis of their levels of CD11c and class II

MHC expression. I found that the proportions and absolute numbers of DC in CD11c^{hi}classIIMHC^{lo} LN resident and CD11c^{hi}classII^{hi} migratory DC subsets in the MLN were unaffected under resting conditions by CCX-CKR deletion, which was consistent with the normal numbers of CD103^{+} DC I observed in the small intestinal lamina propria of CCX-CKR KO mice. While I was carrying out these investigations, it was reported that there was a trend towards lower numbers of CD11c^{hi}classIIMHC^{hi} migratory DC in the skin draining brachial, axillary and inguinal LN of CCX-CKR KO mice. However, this trend vanished following FITC sensitisation of the skin, when normal numbers of CD11c^{hi}classIIMHC^{hi} migratory DC accumulated in the draining LN with similar kinetics as those seen in WT mice (191). These results suggest that any defect in DC migration via afferent lymphatics (a process which is dependent on CCR7 and its ligands) in CCX-CKR KO mice is only subtle and apparent under steady state conditions. One possible explanation for the discrepancy between my findings and those published could be that the MLN are not draining a truly resting tissue as the small intestine harbours a massive antigen load. Therefore, the normal proportions of migratory DC I observed in the MLN in CCX-CKR KO mice would be consistent with the normal proportions reported in the skin draining LN after FITC sensitisation. Although to investigate the migratory responses of CCX-CKR KO small intestinal lamina propria DC under inflammatory conditions, I used R848 as a synthetic TLR 7 agonist which I discuss later.

The PP are a major inductive site of adaptive immunity in the small intestine and differ significantly from MLN in being devoid of afferent lymphatics. Instead PP DC sample luminal antigens that have been directly transcytosed across M cells into the SED, although naive lymphocytes and pDC enter PP across HEV as they do in LN (197). Because of the significant reduction of pDC in the MLN of CCX-CKR KO mice, I decided to focus on assessing pDC numbers in the PP of these animals using the combination of CD11c, PDCA-1 and B220 expression to identify pDC. The proportions of total CD11c^{+} cells in CCX-CKR KO PP were significantly increased compared with WT PP and a similar but not statistically significant trend was seen when absolute numbers were calculated. CD11c^{lo}PDCA-1^{+} cells in the PP all expressed B220 and these were significantly reduced as both a proportion of total live cells and of CD11c^{+} cells in CCX-CKR KO PP compared with WT PP. The absolute numbers of pDC appeared to be decreased in CCX-CKR KO PP, although this was not statistically

significant, perhaps reflecting the overall increase in total $CD11c^+$ cells I found in CCX-CKR KO PP.

7.5 Effects of Flt3L administration in CCX-CKR KO mice

Together these results suggested some selective defects in DC localisation in resting CCX-CKR KO mice, particularly with regard to pDC. However several of the effects were subtle and were compromised by difficulties in obtaining sufficient $CD11c^+$ cells to carry out a detailed analysis of DC subsets across tissues. Therefore I decided to expand DC numbers *in vivo* using the DC differentiation cytokine, Flt3L. Flt3L acts through the Flt3 receptor that is expressed by DC committed precursors and drives the expansion of both cDC and pDC (246, 247, 266, 267). As well as expanding DC numbers, this also allowed me to investigate if the pDC defect in CCX-CKR KO mice was apparent at the precursor level. In keeping with published reports (245, 267), Flt3L caused a dramatic expansion of $CD11c^+$ DC in all the tissues of WT and CCX-CKR KO mice that I examined. This protocol allowed the clear identification of CD4, CD8, CD11b or CD103 expressing DC subsets, as well as $CD11c^{lo}B220^+$ cells and $CD11c^{lo}$PDCA-1^+ pDC in the lamina propria. Although the proportions and absolute numbers of all these DC subsets were identical in CCX-CKR KO and WT mice, the distribution of the $CD11c^{hi}CD103^{hi}$ and $CD11c^{int}CD103^{lo}$ subsets within the $CD103^+$ DC population was different between the two strains, with a significant increase in the proportion of $CD11c^{hi}CD103^{hi}$ cells in CCX-CKR KO lamina propria compared with WT. However, this did not translate into differences in the absolute numbers of these subsets and is difficult to interpret, as I was unable to find previous literature on the functions of these subsets. Recently, it has been shown in the laboratory that $CD103^+$ DC may contain $CD11b^+$ and $CD8\alpha^+$ subsets and it would be interesting to assess these in CCX-CKR KO mice.

$CD11c^+$ DC were expanded to similar extents by Flt3L in CCX-CKR KO and WT PP, although, as I had found in resting CCX-CKR KO PP, the absolute numbers of $CD11c^+$ cells were slightly elevated in CCX-CKR KO PP compared to WT PP after administration of Flt3L. Although this increase was not statistically significant, it may explain the statistically significant increase I found in the absolute numbers of B220 or PDCA-1 expressing DC in the PP of Flt3L treated CCX-CKR KO mice. Although the absolute numbers of $CD103^+$ DC were also increased in the PP of CCX-CKR KO mice compared with WT PP, this did not attain statistical significance. The absolute numbers of $CD11c^{lo}B220^+$ cells and $CD11c^{lo}$PDCA-1^+

pDC were significantly increased in CCX-CKR KO PP compared to WT PP, which contrasts with the decreased numbers of pDC I observed in resting CCX-CKR KO PP compared to WT. Thus, Flt3L treatment can overcome the defects in pDC numbers in the PP of resting CCX-CKR KO mice.

In contrast, the absolute numbers of $CD11c^{lo}PDCA\text{-}1^{+}$ pDC in CCX-CKR KO MLN remained significantly reduced despite Flt3L treatment, emphasising the extent of this defect. This was particularly notable given that the numbers of B220, CD8 or CD11b expressing DC expanded normally in response to Flt3L treatment in CCX-CKR KO MLN. However, $CD11c^{+}CD103^{+}$ "migratory" DC did not appear to expand in CCX-CKR KO MLN to the same extent as in WT MLN, suggesting a defect in this population that was not apparent in resting mice as the relative frequency of these cells amongst the total live cells in CCX-CKR KO MLN was reduced significantly. However, caution must be exercised in interpreting these results as the absolute numbers of $CD11c^{+}CD103^{+}$ DC and their proportions amongst $CD11c^{+}$ cells, were not significantly different between CCX-CKR KO and WT MLN, suggesting that it is in fact changes in other cell populations that are responsible for this apparent difference in the proportions of $CD11c^{+}CD103^{+}$ DC after Flt3L treatment. In support of this, the proportions and absolute numbers of $CD11c^{hi}CD103^{hi}$ and $CD11c^{int}CD103^{lo}$ cells amongst $CD103^{+}$ DC subsets were expanded similarly in CCX-CKR KO and WT MLN in response to Flt3L treatment.

The expansion of $CD11c^{+}$ DC in the ILN and spleens of Flt3L treated CCX-CKR KO and WT mice allowed me to examine the proportions and absolute numbers of $CD8^{+}$, $CD11b^{+}$ and $PDCA\text{-}1^{+}$ DC in these tissues, which were similar in the two strains. Thus, most CCX-CKR KO DC subsets responded normally to Flt3L, except for pDC in the MLN, which retained their defect in absolute numbers that was seen in resting CCX-CKR KO mice.

In a bid to address whether the reduced pDC numbers observed in CCX-CKR KO mice were due to a defect in their generation and/or release from the bone marrow, I analysed CCX-CKR KO bone marrow from resting and Flt3L treated mice for the presence of pDC. The pDC marker, PDCA-1 is also known as bone marrow stromal cell antigen-2 (BST-2) and is thought to be involved in the stromal cell interactions required for B cell development (268). Interestingly, my first observation was that virtually all $CD11c^{+}$ cells in both CCX-CKR KO

and WT bone marrow expressed PDCA-1. Because of this, I had to define bone marrow pDC as $CD11c^{lo}B220^{+}PDCA\text{-}1^{+}$ which were not different in their proportions in CCX-CKR KO and WT mice. In addition, $CD11c^{lo}B220^{+}PDCA\text{-}1^{+}$ pDC expanded normally in response to Flt3L *in vivo* in both CCX-CKR KO and WT bone marrow indicating that pDC can develop in the bone marrow in the absence of CCX-CKR and that the precursors respond normally to this major growth factor. Interestingly however, the absolute numbers of circulating pDC in the blood of resting CCX-CKR KO mice appeared to be reduced compared with WT mice, although this was not statistically significant perhaps because of the overall increase in the numbers of total $CD11c^{+}$ cells in the blood of CCX-CKR KO mice. In addition, CCX-CKR KO mice did not show the same expansion of total leukocytes, $CD11c^{+}$ cells or pDC in the blood in response to Flt3L as was found in WT mice. Although the differences in pDC numbers between the blood of CCX-CKR KO and WT mice were not statistically significant, it should be noted that there was only an approximate 25 fold increase in pDC numbers in the blood of CCX-CKR KO mice after Flt3L treatment compared to a 60 fold increase in pDC numbers in the blood of WT mice. Together these results suggest that there may be a defect in mobilisation of pDC precursors from the bone marrow into the blood stream in the resting state and after Flt3L treatment in CCX-CKR KO mice. Alternatively, there may be a defect in survival of pDC in the absence of CCX-CKR.

7.6 The role of CCX-CKR in antigen specific immune responses

CCR7 and its ligands, CCL19 and CCL21 are critical in organising lymphocytes and DC in secondary lymphoid organs, driving the development of adaptive immune responses (22, 67, 80, 269). Thus any disruption in the distribution of CCL19 and CCL21 may perturb antigen specific immune responses. The experiments described in Chapter 5 were designed to assess if any such disruption could be seen in CCX-CKR KO mice. Systemic antigen specific DTH responses and humoral immunity developed normally in CCX-CKR KO mice after subcutaneous immunisation with OVA emulsified in CFA. In addition, the numbers and proportions of lymphocyte subsets in the draining popliteal LN were normal in CCX-CKR KO mice, as were antigen specific and DC dependent proliferative and IFNγ responses after re-stimulation of popliteal LN cells with OVA *in vitro*. This is in contrast to results described in Chapter 3 that suggested a defect in IFNγ production by polyclonally activated T cells from CCX-CKR KO MLN, ILN and spleens. This evidence that CCX-CKR is not essential in the priming of systemic antigen specific immune responses by subcutaneous immunisation, which

is supported by other preliminary data from a previous PhD student and by the published report of normal migration of DC from inflamed skin draining LN (191).

7.7 The role of CCX-CKR in oral tolerance

As CCR7 and its ligands are important in the development of oral tolerance (12, 125, 258) and CCX-CKR also binds CCL25, the ligand for CCR9 which is induced on gut tropic effector cells (82, 211, 212, 221), I decided to examine the development of oral tolerance in CCX-CKR KO mice. In these experiments, I examined the effects of high and low doses of antigen which have been proposed to induce clonal deletion/anergy of reactive T cells and the induction of T regs respectively (227).

In WT mice, a single high dose feed of OVA resulted in the significant suppression of OVA specific DTH responses and IgG2a antibody, confirming the induction of oral tolerance. This suppression was not apparent in OVA fed CCX-CKR KO mice in any of the three experiments I performed. In contrast, both strains seemed to show the same degree of oral tolerance of proliferative and IFNγ responses *in vitro,* while OVA specific IgG1 antibody production was not suppressed in either CCX-CKR KO or WT mice in any of the three experiments I carried out. A similar pattern of results were obtained when multiple low doses of antigen were used to induce oral tolerance, with no suppression of either OVA specific DTH responses or IgG2a seen in OVA fed mice. However, the suppression of DTH responses in WT mice was not statistically significant in this experiment and I was unable to obtain successful antigen specific T cell responses after re-stimulation of draining popliteal LN cells *in vitro*. I had insufficient time to repeat this experiment and this would clearly be necessary before any conclusions can be drawn regarding T cell tolerance in response to low dose antigen feeds in CCX-CKR KO mice.

Shortly after I carried out these experiments, it was reported that pDC mediate the suppression of antigen specific T cells during the induction of oral tolerance and that oral tolerance cannot be induced after depleting pDC *in vivo* (226). Furthermore, these effects were attributed to pDC in the gut associated lymphoid tissue, particularly the liver, which were shown to induce $CD4^+CD25^+$ T regs capable of inhibiting systemic immune responses (225). However, I found no differences in the absolute numbers or proportions of pDC in the livers of CCX-CKR KO mice under resting conditions, or after Flt3L treatment. I therefore attempted to extend my

studies by examining whether antigen specific FoxP3$^+$ T regs could be induced normally in the MLN of CCX-CKR KO mice fed OVA after the adoptive transfer of OVA specific CD4$^+$ T cells from OT2 mice. However, this experiment was unsuccessful and would be important to repeat.

7.8 The role of CCX-CKR in priming mucosal immune responses

Having observed a defect in the development of oral tolerance in CCX-CKR KO mice I next assessed the efficiency of mucosal priming in these animals using cholera toxin (CT), which has been widely used as a mucosal adjuvant (270-276). I carried out three separate experiments to examine oral priming and although the results varied somewhat between each study, CCX-CKR KO mice more consistently readily primed than WT mice. This affected most kinds of responses, including OVA specific systemic DTH, serum IgG, IgG2a and IgA antibodies, as well as intestinal OVA specific IgA production. CCX-CKR KO mice also generated low levels of OVA specific serum antibody when fed OVA in the absence of CT. In comparison, WT mice fed OVA+CT only appeared to show priming of Th_2 dependent IgG1 antibody responses and had no evidence of responses to OVA alone. Importantly, CCX-CKR KO mice had normal levels of total IgG in their serum and total IgA in secretions, ruling out the possibility that these mice are inherently more prone to generating antibody in general.

Despite the evidence that CCX-CKR influences the induction of antigen specific immunity and tolerance to protein antigens, CCX-CKR KO mice developed acute colitis normally after oral administration of DSS, with identical weight loss, clinical disease scores, colon shortening and local production of inflammatory mediators seen in CCX-CKR KO and WT mice. This is perhaps not surprising given that CCL25 is not produced in the colon and suggests that antigen specific immune responses in the small intestine are selectively affected by CCX-CKR deletion.

Together, these results suggest that in CCX-CKR KO mice, the environment of the CCX-CKR KO MLN has unusual effects on the differentiation of T cells after oral administration of antigen. Therefore it would be interesting to examine the phenotype of adoptively transferred OVA transgenic CD4$^+$ and CD8$^+$ T cells in CCX-CKR KO mice to examine the development of antigen specific effector or regulatory T cells cells directly, in particular their induction of CCR9 and FoxP3 expression. This approach could also be used to assess the subsequent

localisation of efector $CD4^+$ and $CD8^+$ T cells in the lamina propria. It would also be of interest to compare the the numbers of plasma cells in the small intestines of primed CCX-CKR KO and WT mice and examine their expression levels of CCR9 to determine if these correlate with the elevated levels of OVA specific intestinal IgA in orally primed CCX-CKR KO mice.

7.9 pDC function in CCX-CKR KO mice

The tolerogenic properties of pDC have been described in several models in addition to the work on oral tolerance described above. Specifically, pDC have been shown to induce tolerance to cardiac grafts and suppress graft versus host disease, with the latter phenomenon being associated with CCR9 expressing pDC in particular (118, 277). Furthermore, pDC have been linked to a spontaneous breach of self-tolerance in a model of autoimmune arthritis (119). Together, these findings support my own observations that reduced pDC numbers in the MLN of CCX-CKR KO mice correlates with abrogated oral tolerance and enhanced oral priming.

Despite their relatively low expression of class II MHC, pDC have been reported to process and present antigen to T cells directly *in vivo,* although not as effectively as conventional DC (113, 116). Imaging studies have revealed that mature pDC maintain sustained contacts with T cells while interactions between immature pDC and T cells are less stable. Consequently, mature pDC were found to induce immunogenic responses whereas their immature counterparts showed a very limited immunogenic capacity (278) and their low expression of class II MHC and co-stimulatory molecules, induce T regs that control inflammatory immune responses in EAE (117). Despite the decreased numbers, I found that pDC in the MLN, ILN and spleens of resting CCX-CKR KO mice expressed significantly higher levels of class II MHC than WT pDC. Thus pDC in the secondary lymphoid organs of resting CCX-CKR KO mice may be of a more mature phenotype and this may be related to the functional defects in oral tolerance I observed.

In an effort to investigate whether there was a causative relationship between reduced pDC numbers and dysregulated immune responses to intestinal antigen in the mucosa, I began to investigate pDC function in CCX-CKR KO mice. pDC are potent producers of type 1 IFN which are important in the development of anti-viral immunity and DC activation (280-283). Therefore I stimulated MLN cells or sorted pDC with CpG or R848 as agonists of TLR9 and

7 respectively, which are expressed by pDC and can induce their production of type 1 IFN (248, 261, 281, 282, 284). I also stimulated cells in medium alone or with LPS or PolyI:C as TLR4 and 3 ligands that are not reported to activate pDC. Unfortunately, I was unable to detect any IFNα in supernatants from any of these cells by ELISA and it appears this may be a general problem with immunoassays for this cytokine. At the end of my project, I was made aware of a new antibody that is suitable for intracellular detection of type 1 IFN produced by pDC that would provide a feasible alternative to ELISA (285).

To gain some insight into the functional potential of MLN pDC in CCX-CKR KO mice, I analysed their phenotype after culture with R848 *in vitro*. MLN cells from resting mice cultured in medium alone revealed $CD11c^{hi}PDCA\text{-}1^{-}$ and $CD11c^{lo}PDCA\text{-}1^{+}$ cell populations and a minor $CD11c^{hi}$ population of cells that expressed very low levels of PDCA-1, that I termed $CD11c^{hi}PDCA\text{-}1^{+}$. The proportions of $CD11c^{hi}PDCA\text{-}1^{-}$ cells amongst total $CD11c^{+}$ cells did not alter after R848 stimulation of either CCX-CKR KO or WT MLN cells. However in both strains, the proportions of $CD11c^{lo}PDCA\text{-}1^{+}$ cells and $CD11c^{hi}PDCA\text{-}1^{+}$ cells significantly decreased and increased respectively after R848 stimulation. The $CD11c^{hi}PDCA\text{-}1^{+}$ cell population was far more striking amongst cells from Flt3L treated mice stimulated with R848 *in vitro* and was found to express high levels of CD40 and CD86 suggesting an activated phenotype. The dramatic expansion of this population after R848 stimulation is indirect evidence for the presence of type 1 IFN in these cultures as PDCA-1 has been shown to be induced on conventional DC activated by type 1 IFN (250). Although the increase in the proportions of $CD11c^{lo}PDCA\text{-}1^{+}$ pDC after Flt3L expansion *in vivo* and stimulation with R848 *in vitro* occurred in both CCX-CKR KO and WT MLN cells, this was less marked amongst CCX-CKR KO MLN cells, supporting my previous finding that the deficit in pDC in resting CCX-CKR KO MLN could not be overcome with Flt3L treatment. Overall however, there were no major differences between CCX-CKR KO and WT mice in their response to stimulation with the synthetic TLR7 agonist, R848 *in vitro*.

Next I used R848 to explore pDC functions *in vivo* as previous work has shown that R848 drives a dramatic recruitment of lamina propria $CD103^{+}$ DC into the MLN, secondary to the production of type 1 IFN and TNFα from lamina propria pDC (121, 223, 224). This effect is not seen in CCR9 KO mice due to the lack of pDC in their lamina propria (121). Thus I hoped this would give me some indirect information on the biological role of pDC in the lamina

propria of CCX-CKR KO mice. As expected, feeding R848 to WT mice led to increased proportions of migratory CD11c^{hi}classIIMHC^{hi}CD103^{+} DC in the MLN, consistent with mobilisation of lamina propria DC to the MLN and suggested that pDC function in the lamina propria in response to R848 *in vivo* is normal in the absence of CCX-CKR. However, it would be important to examine pDC function in the CCX-CKR KO small intestine more directly, as well as assessing the antigen uptake and presentation ability of mucosal CD103^{+} DC. Further studies in the Nibbs group also plan to assess the migration of CD103^{+} DC into pseudo-afferent lymph of CCX-CKR KO and WT mice that have had their MLN surgically removed.

7.10 Transfer of pDC between CCX-CKR KO and WT mice

In my final experiments, I attempted to explore the *in vivo* behaviour of CCX-CKR KO pDC more directly. Specifically, I attempted to determine whether the defective numbers of pDC in CCX-CKR KO MLN were because the CCX-CKR KO pDC have an intrinsic failure to migrate to MLN, or whether the environment of CCX-CKR KO MLN is not permissive to pDC entry. To do this, I performed adoptive transfer experiments with pDC between CCX-CKR KO and WT mice. Although I was able to detect transferred pDC in recipient tissues, the results of my initial studies using resting mice were somewhat inconclusive and I went on to use Flt3L treated mice as a source of pDC in order to obtain sufficient cells. The findings, suggested that WT pDC could enter CCX-CKR KO MLN normally, but that CCX-CKR KO pDC may not be as efficient at entering WT MLN as WT pDC. These experiments clearly need to be repeated and should incorporate competitive co-transfers in which WT and CCX-CKR KO pDC are given together. In addition, time course studies should be used to distinguish between failure of entry by pDC versus their failure to survive once there. The generation of bone marrow chimera mice could give further insights into whether it is pDC, stromal elements or both that is defective in CCX-CKR KO MLN. It would be particularly interesting to conduct oral tolerance experiments in these bone marrow chimera mice to determine if reconstitution with WT bone marrow would be sufficient to restore oral tolerance in CCX-CKR KO mice and whether this is abrogated in WT mice receiving CCX-CKR KO bone marrow.

Conclusions and future directions

These preliminary studies provide intriguing evidence that there may be a defect in the environment of CCX-CKR KO MLN which limits entry and/or survival of pDC. An obvious

candidate for this might be dysregulation of CCR7 and CCL19/CCL21 mediated pathways, due to a lack of CCX-CKR mediated scavenging. Although my preliminary results suggested there were no differences in the levels of CCL21 in the MLN, ILN, spleen, PP and small intestine of CCX-CKR KO mice, it has been reported that the levels of CCL19 and CCL21 protein are significantly elevated in the LN of CCX-CKR KO mice, supporting the hypothesis that CCX-CKR scavenges excess chemokine (257). It will be important to carry out more detailed studies of CCL19, CCL21 and CCL25 in CCX-CKR KO mice. This is currently under investigation by another PhD student in the group. In addition, recent work suggests that chemerin on HEV may be a further mediator that recruits ChemR23 expressing pDC into LN and it would be interesting to explore ChemR23 and chemerin expression in CCX-CKR KO mice (286). It will also be essential to examine exactly where CCX-CKR is expressed in the normal immune system. Despite several attempts, I was unable to obtain sufficient mRNA from pDC to determine whether they themselves express CCX-CKR. However, preliminary data from the Agace group in Lund (personal communication) suggest that CCX-CKR is expressed only by the stromal compartment of organised lymphoid tissues and that no CCX-CKR mRNA is detectable in $CD45^+$ cells, suggesting that pDC do not express this receptor.

Thus my studies have revealed a selective and robust defect in the numbers of pDC in the MLN of CCX-CKR KO mice that cannot be overcome by the differentiation factor, Flt3L. This was associated with an inability to induce oral tolerance and an abnormal susceptibility to priming of systemic and mucosal immune responses after oral administration of antigen with adjuvant. These abnormalities did not affect peripheral immune responses. Although I obtained some evidence that CCX-CKR KO DC had a defective APC capacity, my preliminary findings suggest that the dysregulation of small intestinal immune responses in CCX-CKR KO mice was not due to a failure of $CD103^+$ DC to migrate to the MLN. However, there may be a selective defect in the recruitment of pDC precursors from the bone marrow and/or a failure of pDC to enter and/or survive in MLN. How this may relate to defective tolerance remains to be determined. In conclusion, my project has revealed important roles for the atypical chemokine receptor, CCX-CKR in the regulation of mucosal immune responses and pDC positioning. In addition, it has also provided some insight into how pDC may regulate immune responses *in vivo*.

References

1. Allen, S. J., S. E. Crown, and T. M. Handel. 2007. Chemokine: receptor structure, interactions, and antagonism. *Annual review of immunology* 25:787-820.

2. Murphy, P. M., M. Baggiolini, I. F. Charo, C. A. Hebert, R. Horuk, K. Matsushima, L. H. Miller, J. J. Oppenheim, and C. A. Power. 2000. International union of pharmacology. XXII. Nomenclature for chemokine receptors. *Pharmacological reviews* 52:145-176.

3. Rossi, D., and A. Zlotnik. 2000. The biology of chemokines and their receptors. *Annual review of immunology* 18:217-242.

4. Charo, I. F., and R. M. Ransohoff. 2006. The many roles of chemokines and chemokine receptors in inflammation. *The New England journal of medicine* 354:610-621.

5. Salanga, C. L., M. O'Hayre, and T. Handel. 2009. Modulation of chemokine receptor activity through dimerization and crosstalk. *Cell Mol Life Sci* 66:1370-1386.

6. Schumann, K., T. Lammermann, M. Bruckner, D. F. Legler, J. Polleux, J. P. Spatz, G. Schuler, R. Forster, M. B. Lutz, L. Sorokin, and M. Sixt. 2010. Immobilized chemokine fields and soluble chemokine gradients cooperatively shape migration patterns of dendritic cells. *Immunity* 32:703-713.

7. Comerford, I., and R. J. Nibbs. 2005. Post-translational control of chemokines: a role for decoy receptors? *Immunology letters* 96:163-174.

8. Handel, T. M., Z. Johnson, S. E. Crown, E. K. Lau, and A. E. Proudfoot. 2005. Regulation of protein function by glycosaminoglycans--as exemplified by chemokines. *Annual review of biochemistry* 74:385-410.

9. Middleton, J., A. M. Patterson, L. Gardner, C. Schmutz, and B. A. Ashton. 2002. Leukocyte extravasation: chemokine transport and presentation by the endothelium. *Blood* 100:3853-3860.

10. Lau, E. K., C. D. Paavola, Z. Johnson, J. P. Gaudry, E. Geretti, F. Borlat, A. J. Kungl, A. E. Proudfoot, and T. M. Handel. 2004. Identification of the glycosaminoglycan binding site of the CC chemokine, MCP-1: implications for structure and function in vivo. *The Journal of biological chemistry* 279:22294-22305.

11. Shamri, R., V. Grabovsky, J. M. Gauguet, S. Feigelson, E. Manevich, W. Kolanus, M. K. Robinson, D. E. Staunton, U. H. von Andrian, and R. Alon. 2005. Lymphocyte arrest requires instantaneous induction of an extended LFA-1 conformation mediated by endothelium-bound chemokines. *Nature immunology* 6:497-506.

12. Forster, R., A. C. Davalos-Misslitz, and A. Rot. 2008. CCR7 and its ligands: balancing immunity and tolerance. *Nature reviews* 8:362-371.

13. Vicente-Manzanares, M., C. K. Choi, and A. R. Horwitz. 2009. Integrins in cell migration--the actin connection. *Journal of cell science* 122:199-206.

14. Mackay, C. R. 2001. Chemokines: immunology's high impact factors. *Nature immunology* 2:95-101.

15. Rot, A., and U. H. von Andrian. 2004. Chemokines in innate and adaptive host defense: basic chemokinese grammar for immune cells. *Annual review of immunology* 22:891-928.

16. Nieto, M., J. M. Frade, D. Sancho, M. Mellado, A. C. Martinez, and F. Sanchez-Madrid. 1997. Polarization of chemokine receptors to the leading edge during lymphocyte chemotaxis. *The Journal of experimental medicine* 186:153-158.

17. Kinashi, T. 2005. Intracellular signalling controlling integrin activation in lymphocytes. *Nature reviews* 5:546-559.

18. Thelen, M., and J. V. Stein. 2008. How chemokines invite leukocytes to dance. *Nature immunology* 9:953-959.

19. Miyasaka, M., and T. Tanaka. 2004. Lymphocyte trafficking across high endothelial venules: dogmas and enigmas. *Nature reviews* 4:360-370.

20. Lammermann, T., B. L. Bader, S. J. Monkley, T. Worbs, R. Wedlich-Soldner, K. Hirsch, M. Keller, R. Forster, D. R. Critchley, R. Fassler, and M. Sixt. 2008. Rapid leukocyte migration by integrin-independent flowing and squeezing. *Nature* 453:51-55.

21. Woolf, E., I. Grigorova, A. Sagiv, V. Grabovsky, S. W. Feigelson, Z. Shulman, T. Hartmann, M. Sixt, J. G. Cyster, and R. Alon. 2007. Lymph node chemokines promote sustained T lymphocyte motility without triggering stable integrin adhesiveness in the absence of shear forces. *Nature immunology* 8:1076-1085.

22. Cyster, J. G. 1999. Chemokines and cell migration in secondary lymphoid organs. *Science (New York, N.Y* 286:2098-2102.

23. Link, A., T. K. Vogt, S. Favre, M. R. Britschgi, H. Acha-Orbea, B. Hinz, J. G. Cyster, and S. A. Luther. 2007. Fibroblastic reticular cells in lymph nodes regulate the homeostasis of naive T cells. *Nature immunology* 8:1255-1265.

24. Pribila, J. T., A. C. Quale, K. L. Mueller, and Y. Shimizu. 2004. Integrins and T cell-mediated immunity. *Annual review of immunology* 22:157-180.

25. Tomei, A. A., S. Siegert, M. R. Britschgi, S. A. Luther, and M. A. Swartz. 2009. Fluid flow regulates stromal cell organization and CCL21 expression in a tissue-engineered lymph node microenvironment. *J Immunol* 183:4273-4283.

26. Worbs, T., T. R. Mempel, J. Bolter, U. H. von Andrian, and R. Forster. 2007. CCR7 ligands stimulate the intranodal motility of T lymphocytes in vivo. *The Journal of experimental medicine* 204:489-495.

27. Patel, D. D., W. Koopmann, T. Imai, L. P. Whichard, O. Yoshie, and M. S. Krangel. 2001. Chemokines have diverse abilities to form solid phase gradients. *Clinical immunology (Orlando, Fla* 99:43-52.

28. Premont, R. T., and R. R. Gainetdinov. 2007. Physiological roles of G protein-coupled receptor kinases and arrestins. *Annual review of physiology* 69:511-534.

29. Randolph, G. J., J. Ochando, and S. Partida-Sanchez. 2008. Migration of dendritic cell subsets and their precursors. *Annual review of immunology* 26:293-316.

30. Cotton, M., and A. Claing. 2009. G protein-coupled receptors stimulation and the control of cell migration. *Cellular signalling* 21:1045-1053.

31. Vroon, A., C. J. Heijnen, and A. Kavelaars. 2006. GRKs and arrestins: regulators of migration and inflammation. *Journal of leukocyte biology* 80:1214-1221.

32. Serra, H. M., C. E. Baena-Cagnani, and Y. Eberhard. 2004. Is secondary lymphoid-organ chemokine (SLC/CCL21) much more than a constitutive chemokine? *Allergy* 59:1219-1223.

33. Rangel-Moreno, J., J. E. Moyron-Quiroz, L. Hartson, K. Kusser, and T. D. Randall. 2007. Pulmonary expression of CXC chemokine ligand 13, CC chemokine ligand 19, and CC chemokine ligand 21 is essential for local immunity to influenza. *Proceedings of the National Academy of Sciences of the United States of America* 104:10577-10582.

34. Nitta, T., S. Murata, T. Ueno, K. Tanaka, and Y. Takahama. 2008. Thymic microenvironments for T-cell repertoire formation. *Advances in immunology* 99:59-94.

35. Krueger, A., S. Willenzon, M. Lyszkiewicz, E. Kremmer, and R. Forster. 2010. CC chemokine receptor 7 and 9 double-deficient hematopoietic progenitors are severely impaired in seeding the adult thymus. *Blood* 115:1906-1912.

36. Uehara, S., A. Grinberg, J. M. Farber, and P. E. Love. 2002. A role for CCR9 in T lymphocyte development and migration. *J Immunol* 168:2811-2819.

37. Zlotoff, D. A., A. Sambandam, T. D. Logan, J. J. Bell, B. A. Schwarz, and A. Bhandoola. 2010. CCR7 and CCR9 together recruit hematopoietic progenitors to the adult thymus. *Blood* 115:1897-1905.

38. Rodewald, H. R. 2008. Thymus organogenesis. *Annual review of immunology* 26:355-388.

39. Liu, C., F. Saito, Z. Liu, Y. Lei, S. Uehara, P. Love, M. Lipp, S. Kondo, N. Manley, and Y. Takahama. 2006. Coordination between CCR7- and CCR9-mediated chemokine signals in prevascular fetal thymus colonization. *Blood* 108:2531-2539.

40. Misslitz, A., O. Pabst, G. Hintzen, L. Ohl, E. Kremmer, H. T. Petrie, and R. Forster. 2004. Thymic T cell development and progenitor localization depend on CCR7. *The Journal of experimental medicine* 200:481-491.

41. Kwan, J., and N. Killeen. 2004. CCR7 directs the migration of thymocytes into the thymic medulla. *J Immunol* 172:3999-4007.

42. Anderson, G., P. J. Lane, and E. J. Jenkinson. 2007. Generating intrathymic microenvironments to establish T-cell tolerance. *Nature reviews* 7:954-963.

43. Ueno, T., F. Saito, D. H. Gray, S. Kuse, K. Hieshima, H. Nakano, T. Kakiuchi, M. Lipp, R. L. Boyd, and Y. Takahama. 2004. CCR7 signals are essential for cortex-medulla migration of developing thymocytes. *The Journal of experimental medicine* 200:493-505.

44. Kurobe, H., C. Liu, T. Ueno, F. Saito, I. Ohigashi, N. Seach, R. Arakaki, Y. Hayashi, T. Kitagawa, M. Lipp, R. L. Boyd, and Y. Takahama. 2006. CCR7-dependent cortex-to-medulla migration of positively selected thymocytes is essential for establishing central tolerance. *Immunity* 24:165-177.

45. Witt, C. M., and E. A. Robey. 2004. The ins and outs of CCR7 in the thymus. *The Journal of experimental medicine* 200:405-409.

46. Davalos-Misslitz, A. C., J. Rieckenberg, S. Willenzon, T. Worbs, E. Kremmer, G. Bernhardt, and R. Forster. 2007. Generalized multi-organ autoimmunity in CCR7-deficient mice. *European journal of immunology* 37:613-622.

47. Randall, T. D., D. M. Carragher, and J. Rangel-Moreno. 2008. Development of secondary lymphoid organs. *Annual review of immunology* 26:627-650.

48. Ansel, K. M., V. N. Ngo, P. L. Hyman, S. A. Luther, R. Forster, J. D. Sedgwick, J. L. Browning, M. Lipp, and J. G. Cyster. 2000. A chemokine-driven positive feedback loop organizes lymphoid follicles. *Nature* 406:309-314.

49. Forster, R., A. E. Mattis, E. Kremmer, E. Wolf, G. Brem, and M. Lipp. 1996. A putative chemokine receptor, BLR1, directs B cell migration to defined lymphoid organs and specific anatomic compartments of the spleen. *Cell* 87:1037-1047.

50. Luther, S. A., K. M. Ansel, and J. G. Cyster. 2003. Overlapping roles of CXCL13, interleukin 7 receptor alpha, and CCR7 ligands in lymph node development. *The Journal of experimental medicine* 197:1191-1198.

51. Chensue, S. W. 2001. Molecular machinations: chemokine signals in host-pathogen interactions. *Clinical microbiology reviews* 14:821-835, table of contents.

52. Power, C. A. 2003. Knock out models to dissect chemokine receptor function in vivo. *Journal of immunological methods* 273:73-82.

53. Gu, L., S. Tseng, R. M. Horner, C. Tam, M. Loda, and B. J. Rollins. 2000. Control of TH2 polarization by the chemokine monocyte chemoattractant protein-1. *Nature* 404:407-411.

54. Karpus, W. J., N. W. Lukacs, K. J. Kennedy, W. S. Smith, S. D. Hurst, and T. A. Barrett. 1997. Differential CC chemokine-induced enhancement of T helper cell cytokine production. *J Immunol* 158:4129-4136.

55. Alvarez, D., E. H. Vollmann, and U. H. von Andrian. 2008. Mechanisms and consequences of dendritic cell migration. *Immunity* 29:325-342.

56. Serbina, N. V., and E. G. Pamer. 2006. Monocyte emigration from bone marrow during bacterial infection requires signals mediated by chemokine receptor CCR2. *Nature immunology* 7:311-317.

57. Sanchez-Sanchez, N., L. Riol-Blanco, and J. L. Rodriguez-Fernandez. 2006. The multiple personalities of the chemokine receptor CCR7 in dendritic cells. *J Immunol* 176:5153-5159.

58. Campbell, D. J., C. H. Kim, and E. C. Butcher. 2003. Chemokines in the systemic organization of immunity. *Immunological reviews* 195:58-71.

59. Sato, A., and A. Iwasaki. 2005. Peyer's patch dendritic cells as regulators of mucosal adaptive immunity. *Cell Mol Life Sci* 62:1333-1338.

60. Lutz, M. B., and G. Schuler. 2002. Immature, semi-mature and fully mature dendritic cells: which signals induce tolerance or immunity? *Trends in immunology* 23:445-449.

61. Steinman, R. M., D. Hawiger, and M. C. Nussenzweig. 2003. Tolerogenic dendritic cells. *Annual review of immunology* 21:685-711.

62. Marsland, B. J., P. Battig, M. Bauer, C. Ruedl, U. Lassing, R. R. Beerli, K. Dietmeier, L. Ivanova, T. Pfister, L. Vogt, H. Nakano, C. Nembrini, P. Saudan, M. Kopf, and M. F. Bachmann. 2005. CCL19 and CCL21 induce a potent proinflammatory differentiation program in licensed dendritic cells. *Immunity* 22:493-505.

63. Muller, G., U. E. Hopken, and M. Lipp. 2003. The impact of CCR7 and CXCR5 on lymphoid organ development and systemic immunity. *Immunological reviews* 195:117-135.

64. Rosen, H., G. Sanna, and C. Alfonso. 2003. Egress: a receptor-regulated step in lymphocyte trafficking. *Immunological reviews* 195:160-177.

65. Sallusto, F., and C. R. Mackay. 2004. Chemoattractants and their receptors in homeostasis and inflammation. *Current opinion in immunology* 16:724-731.

66. Cyster, J. G. 2005. Chemokines, sphingosine-1-phosphate, and cell migration in secondary lymphoid organs. *Annual review of immunology* 23:127-159.

67. Bromley, S. K., S. Y. Thomas, and A. D. Luster. 2005. Chemokine receptor CCR7 guides T cell exit from peripheral tissues and entry into afferent lymphatics. *Nature immunology* 6:895-901.

68. Debes, G. F., C. N. Arnold, A. J. Young, S. Krautwald, M. Lipp, J. B. Hay, and E. C. Butcher. 2005. Chemokine receptor CCR7 required for T lymphocyte exit from peripheral tissues. *Nature immunology* 6:889-894.

69. Forster, R., A. Schubel, D. Breitfeld, E. Kremmer, I. Renner-Muller, E. Wolf, and M. Lipp. 1999. CCR7 coordinates the primary immune response by establishing functional microenvironments in secondary lymphoid organs. *Cell* 99:23-33.

70. Asperti-Boursin, F., E. Real, G. Bismuth, A. Trautmann, and E. Donnadieu. 2007. CCR7 ligands control basal T cell motility within lymph node slices in a phosphoinositide 3-kinase-independent manner. *The Journal of experimental medicine* 204:1167-1179.

71. Luther, S. A., A. Bidgol, D. C. Hargreaves, A. Schmidt, Y. Xu, J. Paniyadi, M. Matloubian, and J. G. Cyster. 2002. Differing activities of homeostatic chemokines

CCL19, CCL21, and CXCL12 in lymphocyte and dendritic cell recruitment and lymphoid neogenesis. *J Immunol* 169:424-433.

72. Baekkevold, E. S., T. Yamanaka, R. T. Palframan, H. S. Carlsen, F. P. Reinholt, U. H. von Andrian, P. Brandtzaeg, and G. Haraldsen. 2001. The CCR7 ligand elc (CCL19) is transcytosed in high endothelial venules and mediates T cell recruitment. *The Journal of experimental medicine* 193:1105-1112.

73. Stein, J. V., A. Rot, Y. Luo, M. Narasimhaswamy, H. Nakano, M. D. Gunn, A. Matsuzawa, E. J. Quackenbush, M. E. Dorf, and U. H. von Andrian. 2000. The CC chemokine thymus-derived chemotactic agent 4 (TCA-4, secondary lymphoid tissue chemokine, 6Ckine, exodus-2) triggers lymphocyte function-associated antigen 1-mediated arrest of rolling T lymphocytes in peripheral lymph node high endothelial venules. *The Journal of experimental medicine* 191:61-76.

74. Unsoeld, H., K. Mueller, U. Schleicher, C. Bogdan, J. Zwirner, D. Voehringer, and H. Pircher. 2007. Abrogation of CCL21 chemokine function by transgenic over-expression impairs T cell immunity to local infections. *International immunology* 19:1281-1289.

75. Schwab, S. R., and J. G. Cyster. 2007. Finding a way out: lymphocyte egress from lymphoid organs. *Nature immunology* 8:1295-1301.

76. Mebius, R. E., and G. Kraal. 2005. Structure and function of the spleen. *Nature reviews* 5:606-616.

77. Gunn, M. D., S. Kyuwa, C. Tam, T. Kakiuchi, A. Matsuzawa, L. T. Williams, and H. Nakano. 1999. Mice lacking expression of secondary lymphoid organ chemokine have defects in lymphocyte homing and dendritic cell localization. *The Journal of experimental medicine* 189:451-460.

78. Mori, S., H. Nakano, K. Aritomi, C. R. Wang, M. D. Gunn, and T. Kakiuchi. 2001. Mice lacking expression of the chemokines CCL21-ser and CCL19 (plt mice)

demonstrate delayed but enhanced T cell immune responses. *The Journal of experimental medicine* 193:207-218.

79. Fazilleau, N., L. Mark, L. J. McHeyzer-Williams, and M. G. McHeyzer-Williams. 2009. Follicular helper T cells: lineage and location. *Immunity* 30:324-335.

80. Hardtke, S., L. Ohl, and R. Forster. 2005. Balanced expression of CXCR5 and CCR7 on follicular T helper cells determines their transient positioning to lymph node follicles and is essential for efficient B-cell help. *Blood* 106:1924-1931.

81. Sallusto, F., D. Lenig, C. R. Mackay, and A. Lanzavecchia. 1998. Flexible programs of chemokine receptor expression on human polarized T helper 1 and 2 lymphocytes. *The Journal of experimental medicine* 187:875-883.

82. Agace, W. W. 2006. Tissue-tropic effector T cells: generation and targeting opportunities. *Nature reviews* 6:682-692.

83. Masopust, D., J. Jiang, H. Shen, and L. Lefrancois. 2001. Direct analysis of the dynamics of the intestinal mucosa CD8 T cell response to systemic virus infection. *J Immunol* 166:2348-2356.

84. Sallusto, F., and A. Lanzavecchia. 1999. Mobilizing dendritic cells for tolerance, priming, and chronic inflammation. *The Journal of experimental medicine* 189:611-614.

85. Menning, A., U. E. Hopken, K. Siegmund, M. Lipp, A. Hamann, and J. Huehn. 2007. Distinctive role of CCR7 in migration and functional activity of naive- and effector/memory-like Treg subsets. *European journal of immunology* 37:1575-1583.

86. Lanzavecchia, A., and F. Sallusto. 2005. Understanding the generation and function of memory T cell subsets. *Current opinion in immunology* 17:326-332.

87. Kunkel, E. J., and E. C. Butcher. 2003. Plasma-cell homing. *Nature reviews* 3:822-829.

88. Hargreaves, D. C., P. L. Hyman, T. T. Lu, V. N. Ngo, A. Bidgol, G. Suzuki, Y. R. Zou, D. R. Littman, and J. G. Cyster. 2001. A coordinated change in chemokine responsiveness guides plasma cell movements. *The Journal of experimental medicine* 194:45-56.

89. Vlad, G., R. Cortesini, and N. Suciu-Foca. 2005. License to heal: bidirectional interaction of antigen-specific regulatory T cells and tolerogenic APC. *J Immunol* 174:5907-5914.

90. Schneider, M. A., J. G. Meingassner, M. Lipp, H. D. Moore, and A. Rot. 2007. CCR7 is required for the in vivo function of CD4+ CD25+ regulatory T cells. *The Journal of experimental medicine* 204:735-745.

91. Wei, S., I. Kryczek, and W. Zou. 2006. Regulatory T-cell compartmentalization and trafficking. *Blood* 108:426-431.

92. Cools, N., P. Ponsaerts, V. F. Van Tendeloo, and Z. N. Berneman. 2007. Balancing between immunity and tolerance: an interplay between dendritic cells, regulatory T cells, and effector T cells. *Journal of leukocyte biology* 82:1365-1374.

93. Coquerelle, C., and M. Moser. 2010. DC subsets in positive and negative regulation of immunity. *Immunological reviews* 234:317-334.

94. Paul, W. E., and J. Zhu. 2010. How are T(H)2-type immune responses initiated and amplified? *Nature reviews* 10:225-235.

95. Schulz, O., E. Jaensson, E. K. Persson, X. Liu, T. Worbs, W. W. Agace, and O. Pabst. 2009. Intestinal CD103+, but not CX3CR1+, antigen sampling cells migrate in lymph and serve classical dendritic cell functions. *The Journal of experimental medicine* 206:3101-3114.

96. Niess, J. H., S. Brand, X. Gu, L. Landsman, S. Jung, B. A. McCormick, J. M. Vyas, M. Boes, H. L. Ploegh, J. G. Fox, D. R. Littman, and H. C. Reinecker. 2005. CX3CR1-

mediated dendritic cell access to the intestinal lumen and bacterial clearance. *Science (New York, N.Y* 307:254-258.

97. Shortman, K., and Y. J. Liu. 2002. Mouse and human dendritic cell subtypes. *Nature reviews* 2:151-161.

98. Iwasaki, A. 2007. Mucosal dendritic cells. *Annual review of immunology* 25:381-418.

99. Pulendran, B., J. L. Smith, G. Caspary, K. Brasel, D. Pettit, E. Maraskovsky, and C. R. Maliszewski. 1999. Distinct dendritic cell subsets differentially regulate the class of immune response in vivo. *Proceedings of the National Academy of Sciences of the United States of America* 96:1036-1041.

100. Hildner, K., B. T. Edelson, W. E. Purtha, M. Diamond, H. Matsushita, M. Kohyama, B. Calderon, B. U. Schraml, E. R. Unanue, M. S. Diamond, R. D. Schreiber, T. L. Murphy, and K. M. Murphy. 2008. Batf3 deficiency reveals a critical role for CD8alpha+ dendritic cells in cytotoxic T cell immunity. *Science (New York, N.Y* 322:1097-1100.

101. Lopez-Bravo, M., and C. Ardavin. 2008. In vivo induction of immune responses to pathogens by conventional dendritic cells. *Immunity* 29:343-351.

102. Dudziak, D., A. O. Kamphorst, G. F. Heidkamp, V. R. Buchholz, C. Trumpfheller, S. Yamazaki, C. Cheong, K. Liu, H. W. Lee, C. G. Park, R. M. Steinman, and M. C. Nussenzweig. 2007. Differential antigen processing by dendritic cell subsets in vivo. *Science (New York, N.Y* 315:107-111.

103. Skokos, D., and M. C. Nussenzweig. 2007. CD8- DCs induce IL-12-independent Th1 differentiation through Delta 4 Notch-like ligand in response to bacterial LPS. *The Journal of experimental medicine* 204:1525-1531.

104. Sponaas, A. M., E. T. Cadman, C. Voisine, V. Harrison, A. Boonstra, A. O'Garra, and J. Langhorne. 2006. Malaria infection changes the ability of splenic dendritic cell

populations to stimulate antigen-specific T cells. *The Journal of experimental medicine* 203:1427-1433.

105. Heath, W. R., G. T. Belz, G. M. Behrens, C. M. Smith, S. P. Forehan, I. A. Parish, G. M. Davey, N. S. Wilson, F. R. Carbone, and J. A. Villadangos. 2004. Cross-presentation, dendritic cell subsets, and the generation of immunity to cellular antigens. *Immunological reviews* 199:9-26.

106. Martin-Fontecha, A., A. Lanzavecchia, and F. Sallusto. 2009. Dendritic cell migration to peripheral lymph nodes. *Handbook of experimental pharmacology*:31-49.

107. Smit, J. J., D. M. Lindell, L. Boon, M. Kool, B. N. Lambrecht, and N. W. Lukacs. 2008. The balance between plasmacytoid DC versus conventional DC determines pulmonary immunity to virus infections. *PloS one* 3:e1720.

108. Smit, J. J., B. D. Rudd, and N. W. Lukacs. 2006. Plasmacytoid dendritic cells inhibit pulmonary immunopathology and promote clearance of respiratory syncytial virus. *The Journal of experimental medicine* 203:1153-1159.

109. Lund, J. M., M. M. Linehan, N. Iijima, and A. Iwasaki. 2006. Cutting Edge: Plasmacytoid dendritic cells provide innate immune protection against mucosal viral infection in situ. *J Immunol* 177:7510-7514.

110. Zhang, Z., and F. S. Wang. 2005. Plasmacytoid dendritic cells act as the most competent cell type in linking antiviral innate and adaptive immune responses. *Cellular & molecular immunology* 2:411-417.

111. Yoneyama, H., K. Matsuno, E. Toda, T. Nishiwaki, N. Matsuo, A. Nakano, S. Narumi, B. Lu, C. Gerard, S. Ishikawa, and K. Matsushima. 2005. Plasmacytoid DCs help lymph node DCs to induce anti-HSV CTLs. *The Journal of experimental medicine* 202:425-435.

112. Sathe, P., and K. Shortman. 2008. The steady-state development of splenic dendritic cells. *Mucosal immunology* 1:425-431.

113. Blasius, A. L., and M. Colonna. 2006. Sampling and signaling in plasmacytoid dendritic cells: the potential roles of Siglec-H. *Trends in immunology* 27:255-260.

114. Marshall, J. D., D. S. Heeke, C. Abbate, P. Yee, and G. Van Nest. 2006. Induction of interferon-gamma from natural killer cells by immunostimulatory CpG DNA is mediated through plasmacytoid-dendritic-cell-produced interferon-alpha and tumour necrosis factor-alpha. *Immunology* 117:38-46.

115. Fitzgerald-Bocarsly, P., J. Dai, and S. Singh. 2008. Plasmacytoid dendritic cells and type I IFN: 50 years of convergent history. *Cytokine & growth factor reviews* 19:3-19.

116. Villadangos, J. A., and L. Young. 2008. Antigen-presentation properties of plasmacytoid dendritic cells. *Immunity* 29:352-361.

117. Irla, M., N. Kupfer, T. Suter, R. Lissilaa, M. Benkhoucha, J. Skupsky, P. H. Lalive, A. Fontana, W. Reith, and S. Hugues. MHC class II-restricted antigen presentation by plasmacytoid dendritic cells inhibits T cell-mediated autoimmunity. 2010. *The Journal of experimental medicine* 207:1891-1905.

118. Hadeiba, H., T. Sato, A. Habtezion, C. Oderup, J. Pan, and E. C. Butcher. 2008. CCR9 expression defines tolerogenic plasmacytoid dendritic cells able to suppress acute graft-versus-host disease. *Nature immunology* 9:1253-1260.

119. Jongbloed, S. L., R. A. Benson, M. B. Nickdel, P. Garside, I. B. McInnes, and J. M. Brewer. 2009. Plasmacytoid dendritic cells regulate breach of self-tolerance in autoimmune arthritis. *J Immunol* 182:963-968.

120. Matta, B. M., A. Castellaneta, and A. W. Thomson. 2010. Tolerogenic plasmacytoid DC. *European journal of immunology*.

121. Wendland, M., N. Czeloth, N. Mach, B. Malissen, E. Kremmer, O. Pabst, and R. Forster. 2007. CCR9 is a homing receptor for plasmacytoid dendritic cells to the small intestine. *Proceedings of the National Academy of Sciences of the United States of America* 104:6347-6352.

122. Penna, G., S. Sozzani, and L. Adorini. 2001. Cutting edge: selective usage of chemokine receptors by plasmacytoid dendritic cells. *J Immunol* 167:1862-1866.

123. Yoneyama, H., K. Matsuno, Y. Zhang, T. Nishiwaki, M. Kitabatake, S. Ueha, S. Narumi, S. Morikawa, T. Ezaki, B. Lu, C. Gerard, S. Ishikawa, and K. Matsushima. 2004. Evidence for recruitment of plasmacytoid dendritic cell precursors to inflamed lymph nodes through high endothelial venules. *International immunology* 16:915-928.

124. Matsutani, T., T. Tanaka, K. Tohya, K. Otani, M. H. Jang, E. Umemoto, K. Taniguchi, H. Hayasaka, K. Ueda, and M. Miyasaka. 2007. Plasmacytoid dendritic cells employ multiple cell adhesion molecules sequentially to interact with high endothelial venule cells - molecular basis of their trafficking to lymph nodes. *International immunology* 19:1031-1037.

125. Worbs, T., U. Bode, S. Yan, M. W. Hoffmann, G. Hintzen, G. Bernhardt, R. Forster, and O. Pabst. 2006. Oral tolerance originates in the intestinal immune system and relies on antigen carriage by dendritic cells. *The Journal of experimental medicine* 203:519-527.

126. Mahnke, K., J. Knop, and A. H. Enk. 2003. Induction of tolerogenic DCs: 'you are what you eat'. *Trends in immunology* 24:646-651.

127. Siddiqui, K. R., and F. Powrie. 2008. CD103+ GALT DCs promote Foxp3+ regulatory T cells. *Mucosal immunology* 1 Suppl 1:S34-38.

128. Smits, H. H., E. C. de Jong, E. A. Wierenga, and M. L. Kapsenberg. 2005. Different faces of regulatory DCs in homeostasis and immunity. *Trends in immunology* 26:123-129.

129. MacPherson, G. G., C. D. Jenkins, M. J. Stein, and C. Edwards. 1995. Endotoxin-mediated dendritic cell release from the intestine. Characterization of released dendritic cells and TNF dependence. *J Immunol* 154:1317-1322.

130. Jakubzick, C., M. Bogunovic, A. J. Bonito, E. L. Kuan, M. Merad, and G. J. Randolph. 2008. Lymph-migrating, tissue-derived dendritic cells are minor constituents within steady-state lymph nodes. *The Journal of experimental medicine* 205:2839-2850.

131. Hintzen, G., L. Ohl, M. L. del Rio, J. I. Rodriguez-Barbosa, O. Pabst, J. R. Kocks, J. Krege, S. Hardtke, and R. Forster. 2006. Induction of tolerance to innocuous inhaled antigen relies on a CCR7-dependent dendritic cell-mediated antigen transport to the bronchial lymph node. *J Immunol* 177:7346-7354.

132. Jang, M. H., N. Sougawa, T. Tanaka, T. Hirata, T. Hiroi, K. Tohya, Z. Guo, E. Umemoto, Y. Ebisuno, B. G. Yang, J. Y. Seoh, M. Lipp, H. Kiyono, and M. Miyasaka. 2006. CCR7 is critically important for migration of dendritic cells in intestinal lamina propria to mesenteric lymph nodes. *J Immunol* 176:803-810.

133. Johansson-Lindbom, B., M. Svensson, O. Pabst, C. Palmqvist, G. Marquez, R. Forster, and W. W. Agace. 2005. Functional specialization of gut CD103+ dendritic cells in the regulation of tissue-selective T cell homing. *The Journal of experimental medicine* 202:1063-1073.

134. Bonifaz, L., D. Bonnyay, K. Mahnke, M. Rivera, M. C. Nussenzweig, and R. M. Steinman. 2002. Efficient targeting of protein antigen to the dendritic cell receptor DEC-205 in the steady state leads to antigen presentation on major histocompatibility complex class I products and peripheral CD8+ T cell tolerance. *The Journal of experimental medicine* 196:1627-1638.

135. Mahnke, K., E. Schmitt, L. Bonifaz, A. H. Enk, and H. Jonuleit. 2002. Immature, but not inactive: the tolerogenic function of immature dendritic cells. *Immunology and cell biology* 80:477-483.

136. Steinman, R. M., S. Turley, I. Mellman, and K. Inaba. 2000. The induction of tolerance by dendritic cells that have captured apoptotic cells. *The Journal of experimental medicine* 191:411-416.

137. Munn, D. H., M. D. Sharma, B. Baban, H. P. Harding, Y. Zhang, D. Ron, and A. L. Mellor. 2005. GCN2 kinase in T cells mediates proliferative arrest and anergy induction in response to indoleamine 2,3-dioxygenase. *Immunity* 22:633-642.

138. Kushwah, R., J. Wu, J. R. Oliver, G. Jiang, J. Zhang, K. A. Siminovitch, and J. Hu. Uptake of apoptotic DC converts immature DC into tolerogenic DC that induce differentiation of Foxp3+ Treg. *European journal of immunology* 40:1022-1035.

139. Braun, D., R. S. Longman, and M. L. Albert. 2005. A two-step induction of indoleamine 2,3 dioxygenase (IDO) activity during dendritic-cell maturation. *Blood* 106:2375-2381.

140. Orabona, C., P. Puccetti, C. Vacca, S. Bicciato, A. Luchini, F. Fallarino, R. Bianchi, E. Velardi, K. Perruccio, A. Velardi, V. Bronte, M. C. Fioretti, and U. Grohmann. 2006. Toward the identification of a tolerogenic signature in IDO-competent dendritic cells. *Blood* 107:2846-2854.

141. von Bergwelt-Baildon, M. S., A. Popov, T. Saric, J. Chemnitz, S. Classen, M. S. Stoffel, F. Fiore, U. Roth, M. Beyer, S. Debey, C. Wickenhauser, F. G. Hanisch, and J. L. Schultze. 2006. CD25 and indoleamine 2,3-dioxygenase are up-regulated by prostaglandin E2 and expressed by tumor-associated dendritic cells in vivo: additional mechanisms of T-cell inhibition. *Blood* 108:228-237.

142. Sharma, M. D., B. Baban, P. Chandler, D. Y. Hou, N. Singh, H. Yagita, M. Azuma, B. R. Blazar, A. L. Mellor, and D. H. Munn. 2007. Plasmacytoid dendritic cells from mouse tumor-draining lymph nodes directly activate mature Tregs via indoleamine 2,3-dioxygenase. *The Journal of clinical investigation* 117:2570-2582.

143. Furrie, E., R. E. Smith, M. W. Turner, S. Strobel, and A. M. Mowat. 2002. Induction of local innate immune responses and modulation of antigen uptake as mechanisms underlying the mucosal adjuvant properties of immune stimulating complexes (ISCOMS). *Vaccine* 20:2254-2262.

144. Iliev, I. D., E. Mileti, G. Matteoli, M. Chieppa, and M. Rescigno. 2009. Intestinal epithelial cells promote colitis-protective regulatory T-cell differentiation through dendritic cell conditioning. *Mucosal immunology* 2:340-350.

145. Min, S. Y., K. S. Park, M. L. Cho, J. W. Kang, Y. G. Cho, S. Y. Hwang, M. J. Park, C. H. Yoon, J. K. Min, S. H. Lee, S. H. Park, and H. Y. Kim. 2006. Antigen-induced, tolerogenic CD11c+,CD11b+ dendritic cells are abundant in Peyer's patches during the induction of oral tolerance to type II collagen and suppress experimental collagen-induced arthritis. *Arthritis and rheumatism* 54:887-898.

146. Mowat, A. M. 2003. Anatomical basis of tolerance and immunity to intestinal antigens. *Nature reviews* 3:331-341.

147. Rutella, S., S. Danese, and G. Leone. 2006. Tolerogenic dendritic cells: cytokine modulation comes of age. *Blood* 108:1435-1440.

148. Mortier, A., J. Van Damme, and P. Proost. 2008. Regulation of chemokine activity by posttranslational modification. *Pharmacology & therapeutics* 120:197-217.

149. Comerford, I., W. Litchfield, Y. Harata-Lee, R. J. Nibbs, and S. R. McColl. 2007. Regulation of chemotactic networks by 'atypical' receptors. *Bioessays* 29:237-247.

150. Blanpain, C., I. Migeotte, B. Lee, J. Vakili, B. J. Doranz, C. Govaerts, G. Vassart, R. W. Doms, and M. Parmentier. 1999. CCR5 binds multiple CC-chemokines: MCP-3 acts as a natural antagonist. *Blood* 94:1899-1905.

151. Ogilvie, P., G. Bardi, I. Clark-Lewis, M. Baggiolini, and M. Uguccioni. 2001. Eotaxin is a natural antagonist for CCR2 and an agonist for CCR5. *Blood* 97:1920-1924.

152. Ogilvie, P., S. Paoletti, I. Clark-Lewis, and M. Uguccioni. 2003. Eotaxin-3 is a natural antagonist for CCR2 and exerts a repulsive effect on human monocytes. *Blood* 102:789-794.

153. Petkovic, V., C. Moghini, S. Paoletti, M. Uguccioni, and B. Gerber. 2004. Eotaxin-3/CCL26 is a natural antagonist for CC chemokine receptors 1 and 5. A human chemokine with a regulatory role. *The Journal of biological chemistry* 279:23357-23363.

154. Loetscher, P., A. Pellegrino, J. H. Gong, I. Mattioli, M. Loetscher, G. Bardi, M. Baggiolini, and I. Clark-Lewis. 2001. The ligands of CXC chemokine receptor 3, I-TAC, Mig, and IP10, are natural antagonists for CCR3. *The Journal of biological chemistry* 276:2986-2991.

155. Nibbs, R. J., T. W. Salcedo, J. D. Campbell, X. T. Yao, Y. Li, B. Nardelli, H. S. Olsen, T. S. Morris, A. E. Proudfoot, V. P. Patel, and G. J. Graham. 2000. C-C chemokine receptor 3 antagonism by the beta-chemokine macrophage inflammatory protein 4, a property strongly enhanced by an amino-terminal alanine-methionine swap. *J Immunol* 164:1488-1497.

156. Xanthou, G., C. E. Duchesnes, T. J. Williams, and J. E. Pease. 2003. CCR3 functional responses are regulated by both CXCR3 and its ligands CXCL9, CXCL10 and CXCL11. *European journal of immunology* 33:2241-2250.

157. Mantovani, A., R. Bonecchi, and M. Locati. 2006. Tuning inflammation and immunity by chemokine sequestration: decoys and more. *Nature reviews* 6:907-918.

158. Graham, G. J. 2009. D6 and the atypical chemokine receptor family: novel regulators of immune and inflammatory processes. *European journal of immunology* 39:342-351.

159. Hansell, C., and R. Nibbs. 2007. Professional and part-time chemokine decoys in the resolution of inflammation. *Sci STKE* 2007:pe18.

160. Hansell, C. A., C. V. Simpson, and R. J. Nibbs. 2006. Chemokine sequestration by atypical chemokine receptors. *Biochemical Society transactions* 34:1009-1013.

161. Haraldsen, G., and A. Rot. 2006. Coy decoy with a new ploy: interceptor controls the levels of homeostatic chemokines. *European journal of immunology* 36:1659-1661.

162. Nibbs, R., G. Graham, and A. Rot. 2003. Chemokines on the move: control by the chemokine "interceptors" Duffy blood group antigen and D6. *Seminars in immunology* 15:287-294.

163. Collins, C. B., E. N. McNamee, J. D. Wermers, M. D. Lebsack, and J. Rivera-Nieves. 2010. Chemokine decoy receptor D6 in inflammatory bowel disease (IBD) and IBD-associated colon cancer. *Gut* 59:151-152.

164. Pruenster, M., L. Mudde, P. Bombosi, S. Dimitrova, M. Zsak, J. Middleton, A. Richmond, G. J. Graham, S. Segerer, R. J. Nibbs, and A. Rot. 2009. The Duffy antigen receptor for chemokines transports chemokines and supports their promigratory activity. *Nature immunology* 10:101-108.

165. Kashiwazaki, M., T. Tanaka, H. Kanda, Y. Ebisuno, D. Izawa, N. Fukuma, N. Akimitsu, K. Sekimizu, M. Monden, and M. Miyasaka. 2003. A high endothelial venule-expressing promiscuous chemokine receptor DARC can bind inflammatory, but not lymphoid, chemokines and is dispensable for lymphocyte homing under physiological conditions. *International immunology* 15:1219-1227.

166. Lu, Z. H., Z. X. Wang, R. Horuk, J. Hesselgesser, Y. C. Lou, T. J. Hadley, and S. C. Peiper. 1995. The promiscuous chemokine binding profile of the Duffy antigen/receptor for chemokines is primarily localized to sequences in the amino-terminal domain. *The Journal of biological chemistry* 270:26239-26245.

167. Chakera, A., R. M. Seeber, A. E. John, K. A. Eidne, and D. R. Greaves. 2008. The duffy antigen/receptor for chemokines exists in an oligomeric form in living cells and

functionally antagonizes CCR5 signaling through hetero-oligomerization. *Molecular pharmacology* 73:1362-1370.

168. Dawson, T. C., A. B. Lentsch, Z. Wang, J. E. Cowhig, A. Rot, N. Maeda, and S. C. Peiper. 2000. Exaggerated response to endotoxin in mice lacking the Duffy antigen/receptor for chemokines (DARC). *Blood* 96:1681-1684.

169. Lee, J. S., M. M. Wurfel, G. Matute-Bello, C. W. Frevert, M. R. Rosengart, M. Ranganathan, V. W. Wong, T. Holden, S. Sutlief, A. Richmond, S. Peiper, and T. R. Martin. 2006. The Duffy antigen modifies systemic and local tissue chemokine responses following lipopolysaccharide stimulation. *J Immunol* 177:8086-8094.

170. Madigan, J., D. J. Freeman, F. Menzies, S. Forrow, S. M. Nelson, A. Young, A. Sharkey, A. Moffett, G. J. Graham, I. A. Greer, A. Rot, and R. J. Nibbs. 2010. Chemokine scavenger D6 is expressed by trophoblasts and aids the survival of mouse embryos transferred into allogeneic recipients. *J Immunol* 184:3202-3212.

171. Weber, M., E. Blair, C. V. Simpson, M. O'Hara, P. E. Blackburn, A. Rot, G. J. Graham, and R. J. Nibbs. 2004. The chemokine receptor D6 constitutively traffics to and from the cell surface to internalize and degrade chemokines. *Molecular biology of the cell* 15:2492-2508.

172. McCulloch, C. V., V. Morrow, S. Milasta, I. Comerford, G. Milligan, G. J. Graham, N. W. Isaacs, and R. J. Nibbs. 2008. Multiple roles for the C-terminal tail of the chemokine scavenger D6. *The Journal of biological chemistry* 283:7972-7982.

173. Galliera, E., V. R. Jala, J. O. Trent, R. Bonecchi, P. Signorelli, R. J. Lefkowitz, A. Mantovani, M. Locati, and B. Haribabu. 2004. beta-Arrestin-dependent constitutive internalization of the human chemokine decoy receptor D6. *The Journal of biological chemistry* 279:25590-25597.

174. Fra, A. M., M. Locati, K. Otero, M. Sironi, P. Signorelli, M. L. Massardi, M. Gobbi, A. Vecchi, S. Sozzani, and A. Mantovani. 2003. Cutting edge: scavenging of

inflammatory CC chemokines by the promiscuous putatively silent chemokine receptor D6. *J Immunol* 170:2279-2282.

175. Jamieson, T., D. N. Cook, R. J. Nibbs, A. Rot, C. Nixon, P. McLean, A. Alcami, S. A. Lira, M. Wiekowski, and G. J. Graham. 2005. The chemokine receptor D6 limits the inflammatory response in vivo. *Nature immunology* 6:403-411.

176. Martinez de la Torre, Y., M. Locati, C. Buracchi, J. Dupor, D. N. Cook, R. Bonecchi, M. Nebuloni, D. Rukavina, L. Vago, A. Vecchi, S. A. Lira, and A. Mantovani. 2005. Increased inflammation in mice deficient for the chemokine decoy receptor D6. *European journal of immunology* 35:1342-1346.

177. Di Liberto, D., M. Locati, N. Caccamo, A. Vecchi, S. Meraviglia, A. Salerno, G. Sireci, M. Nebuloni, N. Caceres, P. J. Cardona, F. Dieli, and A. Mantovani. 2008. Role of the chemokine decoy receptor D6 in balancing inflammation, immune activation, and antimicrobial resistance in Mycobacterium tuberculosis infection. *The Journal of experimental medicine* 205:2075-2084.

178. Bordon, Y., C. A. Hansell, D. P. Sester, M. Clarke, A. M. Mowat, and R. J. Nibbs. 2009. The atypical chemokine receptor D6 contributes to the development of experimental colitis. *J Immunol* 182:5032-5040.

179. Liu, L., G. J. Graham, A. Damodaran, T. Hu, S. A. Lira, M. Sasse, C. Canasto-Chibuque, D. N. Cook, and R. M. Ransohoff. 2006. Cutting edge: the silent chemokine receptor D6 is required for generating T cell responses that mediate experimental autoimmune encephalomyelitis. *J Immunol* 177:17-21.

180. Vetrano, S., E. M. Borroni, A. Sarukhan, B. Savino, R. Bonecchi, C. Correale, V. Arena, M. Fantini, M. Roncalli, A. Malesci, A. Mantovani, M. Locati, and S. Danese. 2010. The lymphatic system controls intestinal inflammation and inflammation-associated Colon Cancer through the chemokine decoy receptor D6. *Gut* 59:197-206.

181. Zabel, B. A., Y. Wang, S. Lewen, R. D. Berahovich, M. E. Penfold, P. Zhang, J. Powers, B. C. Summers, Z. Miao, B. Zhao, A. Jalili, A. Janowska-Wieczorek, J. C. Jaen, and T. J. Schall. 2009. Elucidation of CXCR7-mediated signaling events and inhibition of CXCR4-mediated tumor cell transendothelial migration by CXCR7 ligands. *J Immunol* 183:3204-3211.

182. Miao, Z., K. E. Luker, B. C. Summers, R. Berahovich, M. S. Bhojani, A. Rehemtulla, C. G. Kleer, J. J. Essner, A. Nasevicius, G. D. Luker, M. C. Howard, and T. J. Schall. 2007. CXCR7 (RDC1) promotes breast and lung tumor growth in vivo and is expressed on tumor-associated vasculature. *Proceedings of the National Academy of Sciences of the United States of America* 104:15735-15740.

183. Naumann, U., E. Cameroni, M. Pruenster, H. Mahabaleshwar, E. Raz, H. G. Zerwes, A. Rot, and M. Thelen. 2010. CXCR7 functions as a scavenger for CXCL12 and CXCL11. *PloS one* 5:e9175.

184. Zabel, B. A., A. M. Silverio, and E. C. Butcher. 2005. Chemokine-like receptor 1 expression and chemerin-directed chemotaxis distinguish plasmacytoid from myeloid dendritic cells in human blood. *J Immunol* 174:244-251.

185. Borroni, E. M., and R. Bonecchi. 2009. Shaping the gradient by nonchemotactic chemokine receptors. *Cell adhesion & migration* 3:146-147.

186. Zabel, B. A., S. Nakae, L. Zuniga, J. Y. Kim, T. Ohyama, C. Alt, J. Pan, H. Suto, D. Soler, S. J. Allen, T. M. Handel, C. H. Song, S. J. Galli, and E. C. Butcher. 2008. Mast cell-expressed orphan receptor CCRL2 binds chemerin and is required for optimal induction of IgE-mediated passive cutaneous anaphylaxis. *The Journal of experimental medicine* 205:2207-2220.

187. Hartmann, T. N., M. Leick, S. Ewers, A. Diefenbacher, I. Schraufstatter, M. Honczarenko, and M. Burger. 2008. Human B cells express the orphan chemokine receptor CRAM-A/B in a maturation-stage-dependent and CCL5-modulated manner. *Immunology* 125:252-262.

188. Leick, M., J. Catusse, M. Follo, R. J. Nibbs, T. N. Hartmann, H. Veelken, and M. Burger. 2009. CCL19 is a specific ligand of the constitutively recycling atypical human chemokine receptor CRAM-B. *Immunology*.

189. Gosling, J., D. J. Dairaghi, Y. Wang, M. Hanley, D. Talbot, Z. Miao, and T. J. Schall. 2000. Cutting edge: identification of a novel chemokine receptor that binds dendritic cell- and T cell-active chemokines including ELC, SLC, and TECK. *J Immunol* 164:2851-2856.

190. Townson, J. R., and R. J. Nibbs. 2002. Characterization of mouse CCX-CKR, a receptor for the lymphocyte-attracting chemokines TECK/mCCL25, SLC/mCCL21 and MIP-3beta/mCCL19: comparison to human CCX-CKR. *European journal of immunology* 32:1230-1241.

191. Heinzel, K., C. Benz, and C. C. Bleul. 2007. A silent chemokine receptor regulates steady-state leukocyte homing in vivo. *Proceedings of the National Academy of Sciences of the United States of America* 104:8421-8426.

192. Comerford, I., S. Milasta, V. Morrow, G. Milligan, and R. Nibbs. 2006. The chemokine receptor CCX-CKR mediates effective scavenging of CCL19 in vitro. *European journal of immunology* 36:1904-1916.

193. Kohout, T. A., S. L. Nicholas, S. J. Perry, G. Reinhart, S. Junger, and R. S. Struthers. 2004. Differential desensitization, receptor phosphorylation, beta-arrestin recruitment, and ERK1/2 activation by the two endogenous ligands for the CC chemokine receptor 7. *The Journal of biological chemistry* 279:23214-23222.

194. Bardi, G., M. Lipp, M. Baggiolini, and P. Loetscher. 2001. The T cell chemokine receptor CCR7 is internalized on stimulation with ELC, but not with SLC. *European journal of immunology* 31:3291-3297.

195. Feng, L. Y., Z. L. Ou, F. Y. Wu, Z. Z. Shen, and Z. M. Shao. 2009. Involvement of a novel chemokine decoy receptor CCX-CKR in breast cancer growth, metastasis and patient survival. *Clin Cancer Res* 15:2962-2970.

196. Marchiando, A. M., W. V. Graham, and J. R. Turner. 2010. Epithelial barriers in homeostasis and disease. *Annual review of pathology* 5:119-144.

197. Newberry, R. D., and R. G. Lorenz. 2005. Organizing a mucosal defense. *Immunological reviews* 206:6-21.

198. Eberl, G., and M. Lochner. 2009. The development of intestinal lymphoid tissues at the interface of self and microbiota. *Mucosal immunology* 2:478-485.

199. Ericsson, A., A. Arya, and W. Agace. 2004. CCL25 enhances CD103-mediated lymphocyte adhesion to E-cadherin. *Annals of the New York Academy of Sciences* 1029:334-336.

200. Ericsson, A., M. Svensson, A. Arya, and W. W. Agace. 2004. CCL25/CCR9 promotes the induction and function of CD103 on intestinal intraepithelial lymphocytes. *European journal of immunology* 34:2720-2729.

201. Wurbel, M. A., M. Malissen, D. Guy-Grand, E. Meffre, M. C. Nussenzweig, M. Richelme, A. Carrier, and B. Malissen. 2001. Mice lacking the CCR9 CC-chemokine receptor show a mild impairment of early T- and B-cell development and a reduction in T-cell receptor gammadelta(+) gut intraepithelial lymphocytes. *Blood* 98:2626-2632.

202. Macpherson, A. J., and T. Uhr. 2004. Induction of protective IgA by intestinal dendritic cells carrying commensal bacteria. *Science (New York, N.Y* 303:1662-1665.

203. Cerutti, A., and M. Rescigno. 2008. The biology of intestinal immunoglobulin A responses. *Immunity* 28:740-750.

204. Cerutti, A. 2008. The regulation of IgA class switching. *Nature reviews* 8:421-434.

205. Coombes, J. L., and F. Powrie. 2008. Dendritic cells in intestinal immune regulation. *Nature reviews* 8:435-446.

206. del Rio, M. L., G. Bernhardt, J. I. Rodriguez-Barbosa, and R. Forster. 2010. Development and functional specialization of CD103+ dendritic cells. *Immunological reviews* 234:268-281.

207. Pabst, O., L. Ohl, M. Wendland, M. A. Wurbel, E. Kremmer, B. Malissen, and R. Forster. 2004. Chemokine receptor CCR9 contributes to the localization of plasma cells to the small intestine. *The Journal of experimental medicine* 199:411-416.

208. Jaensson, E., H. Uronen-Hansson, O. Pabst, B. Eksteen, J. Tian, J. L. Coombes, P. L. Berg, T. Davidsson, F. Powrie, B. Johansson-Lindbom, and W. W. Agace. 2008. Small intestinal CD103+ dendritic cells display unique functional properties that are conserved between mice and humans. *The Journal of experimental medicine* 205:2139-2149.

209. Bogunovic, M., F. Ginhoux, J. Helft, L. Shang, D. Hashimoto, M. Greter, K. Liu, C. Jakubzick, M. A. Ingersoll, M. Leboeuf, E. R. Stanley, M. Nussenzweig, S. A. Lira, G. J. Randolph, and M. Merad. 2009. Origin of the lamina propria dendritic cell network. *Immunity* 31:513-525.

210. Johansson-Lindbom, B., and W. W. Agace. 2007. Generation of gut-homing T cells and their localization to the small intestinal mucosa. *Immunological reviews* 215:226-242.

211. Johansson-Lindbom, B., M. Svensson, M. A. Wurbel, B. Malissen, G. Marquez, and W. Agace. 2003. Selective generation of gut tropic T cells in gut-associated lymphoid tissue (GALT): requirement for GALT dendritic cells and adjuvant. *The Journal of experimental medicine* 198:963-969.

212. Agace, W. 2010. Generation of gut-homing T cells and their localization to the small intestinal mucosa. *Immunology letters* 128:21-23.

213. Svensson, M., J. Marsal, A. Ericsson, L. Carramolino, T. Broden, G. Marquez, and W. W. Agace. 2002. CCL25 mediates the localization of recently activated CD8alphabeta(+) lymphocytes to the small-intestinal mucosa. *The Journal of clinical investigation* 110:1113-1121.

214. Papadakis, K. A., J. Prehn, V. Nelson, L. Cheng, S. W. Binder, P. D. Ponath, D. P. Andrew, and S. R. Targan. 2000. The role of thymus-expressed chemokine and its receptor CCR9 on lymphocytes in the regional specialization of the mucosal immune system. *J Immunol* 165:5069-5076.

215. Mora, J. R., M. R. Bono, N. Manjunath, W. Weninger, L. L. Cavanagh, M. Rosemblatt, and U. H. Von Andrian. 2003. Selective imprinting of gut-homing T cells by Peyer's patch dendritic cells. *Nature* 424:88-93.

216. Feng, N., M. C. Jaimes, N. H. Lazarus, D. Monak, C. Zhang, E. C. Butcher, and H. B. Greenberg. 2006. Redundant role of chemokines CCL25/TECK and CCL28/MEC in IgA+ plasmablast recruitment to the intestinal lamina propria after rotavirus infection. *J Immunol* 176:5749-5759.

217. Hieshima, K., Y. Kawasaki, H. Hanamoto, T. Nakayama, D. Nagakubo, A. Kanamaru, and O. Yoshie. 2004. CC chemokine ligands 25 and 28 play essential roles in intestinal extravasation of IgA antibody-secreting cells. *J Immunol* 173:3668-3675.

218. Mora, J. R., and U. H. von Andrian. 2009. Role of retinoic acid in the imprinting of gut-homing IgA-secreting cells. *Seminars in immunology* 21:28-35.

219. Stenstad, H., A. Ericsson, B. Johansson-Lindbom, M. Svensson, J. Marsal, M. Mack, D. Picarella, D. Soler, G. Marquez, M. Briskin, and W. W. Agace. 2006. Gut-associated lymphoid tissue-primed CD4+ T cells display CCR9-dependent and -independent homing to the small intestine. *Blood* 107:3447-3454.

220. Coombes, J. L., K. R. Siddiqui, C. V. Arancibia-Carcamo, J. Hall, C. M. Sun, Y. Belkaid, and F. Powrie. 2007. A functionally specialized population of mucosal CD103+ DCs induces Foxp3+ regulatory T cells via a TGF-beta and retinoic acid-dependent mechanism. *The Journal of experimental medicine* 204:1757-1764.

221. Iwata, M., A. Hirakiyama, Y. Eshima, H. Kagechika, C. Kato, and S. Y. Song. 2004. Retinoic acid imprints gut-homing specificity on T cells. *Immunity* 21:527-538.

222. Hammerschmidt, S. I., M. Ahrendt, U. Bode, B. Wahl, E. Kremmer, R. Forster, and O. Pabst. 2008. Stromal mesenteric lymph node cells are essential for the generation of gut-homing T cells in vivo. *The Journal of experimental medicine* 205:2483-2490.

223. Yrlid, U., V. Cerovic, S. Milling, C. D. Jenkins, L. S. Klavinskis, and G. G. MacPherson. 2006. A distinct subset of intestinal dendritic cells responds selectively to oral TLR7/8 stimulation. *European journal of immunology* 36:2639-2648.

224. Yrlid, U., S. W. Milling, J. L. Miller, S. Cartland, C. D. Jenkins, and G. G. MacPherson. 2006. Regulation of intestinal dendritic cell migration and activation by plasmacytoid dendritic cells, TNF-alpha and type 1 IFNs after feeding a TLR7/8 ligand. *J Immunol* 176:5205-5212.

225. Dubois, B., G. Joubert, M. Gomez de Aguero, M. Gouanvic, A. Goubier, and D. Kaiserlian. 2009. Sequential role of plasmacytoid dendritic cells and regulatory T cells in oral tolerance. *Gastroenterology* 137:1019-1028.

226. Goubier, A., B. Dubois, H. Gheit, G. Joubert, F. Villard-Truc, C. Asselin-Paturel, G. Trinchieri, and D. Kaiserlian. 2008. Plasmacytoid dendritic cells mediate oral tolerance. *Immunity* 29:464-475.

227. Garside, P., and A. M. Mowat. 2001. Oral tolerance. *Seminars in immunology* 13:177-185.

228. Leishman, A. J., P. Garside, and A. M. Mowat. 2000. Induction of oral tolerance in the primed immune system: influence of antigen persistence and adjuvant form. *Cellular immunology* 202:71-78.

229. Fleeton, M., N. Contractor, F. Leon, J. He, D. Wetzel, T. Dermody, A. Iwasaki, and B. Kelsall. 2004. Involvement of dendritic cell subsets in the induction of oral tolerance and immunity. *Annals of the New York Academy of Sciences* 1029:60-65.

230. Kelsall, B. L., and F. Leon. 2005. Involvement of intestinal dendritic cells in oral tolerance, immunity to pathogens, and inflammatory bowel disease. *Immunological reviews* 206:132-148.

231. Mayer, L., and L. Shao. 2004. Therapeutic potential of oral tolerance. *Nature reviews* 4:407-419.

232. Mowat, A. M. 2005. Dendritic cells and immune responses to orally administered antigens. *Vaccine* 23:1797-1799.

233. Mowat, A. M., A. M. Donachie, L. A. Parker, N. C. Robson, H. Beacock-Sharp, L. J. McIntyre, O. Millington, and F. Chirdo. 2003. The role of dendritic cells in regulating mucosal immunity and tolerance. *Novartis Foundation symposium* 252:291-302; discussion 302-295.

234. Mowat, A. M., L. A. Parker, H. Beacock-Sharp, O. R. Millington, and F. Chirdo. 2004. Oral tolerance: overview and historical perspectives. *Annals of the New York Academy of Sciences* 1029:1-8.

235. Peron, J. P., A. P. de Oliveira, and L. V. Rizzo. 2009. It takes guts for tolerance: the phenomenon of oral tolerance and the regulation of autoimmune response. *Autoimmunity reviews* 9:1-4.

236. Mestecky, J., Z. Moldoveanu, and C. O. Elson. 2005. Immune response versus mucosal tolerance to mucosally administered antigens. *Vaccine* 23:1800-1803.

237. Miller, A., O. Lider, A. B. Roberts, M. B. Sporn, and H. L. Weiner. 1992. Suppressor T cells generated by oral tolerization to myelin basic protein suppress both in vitro and in vivo immune responses by the release of transforming growth factor beta after antigen-specific triggering. *Proceedings of the National Academy of Sciences of the United States of America* 89:421-425.

238. Rizzo, L. V., R. A. Morawetz, N. E. Miller-Rivero, R. Choi, B. Wiggert, C. C. Chan, H. C. Morse, 3rd, R. B. Nussenblatt, and R. R. Caspi. 1999. IL-4 and IL-10 are both required for the induction of oral tolerance. *J Immunol* 162:2613-2622.

239. Whitacre, C. C., I. E. Gienapp, C. G. Orosz, and D. M. Bitar. 1991. Oral tolerance in experimental autoimmune encephalomyelitis. III. Evidence for clonal anergy. *J Immunol* 147:2155-2163.

240. Melamed, D., and A. Friedman. 1993. Direct evidence for anergy in T lymphocytes tolerized by oral administration of ovalbumin. *European journal of immunology* 23:935-942.

241. Kunkel, D., D. Kirchhoff, S. Nishikawa, A. Radbruch, and A. Scheffold. 2003. Visualization of peptide presentation following oral application of antigen in normal and Peyer's patches-deficient mice. *European journal of immunology* 33:1292-1301.

242. Spahn, T. W., H. Herbst, P. D. Rennert, N. Lugering, C. Maaser, M. Kraft, A. Fontana, H. L. Weiner, W. Domschke, and T. Kucharzik. 2002. Induction of colitis in mice deficient of Peyer's patches and mesenteric lymph nodes is associated with increased disease severity and formation of colonic lymphoid patches. *The American journal of pathology* 161:2273-2282.

243. Segura, E., J. Wong, and J. A. Villadangos. 2009. Cutting edge: B220+CCR9- dendritic cells are not plasmacytoid dendritic cells but are precursors of conventional dendritic cells. *J Immunol* 183:1514-1517.

244. Sun, J., B. Dirden-Kramer, K. Ito, P. B. Ernst, and N. Van Houten. 1999. Antigen-specific T cell activation and proliferation during oral tolerance induction. *J Immunol* 162:5868-5875.

245. Miller, G., V. G. Pillarisetty, A. B. Shah, S. Lahrs, and R. P. DeMatteo. 2003. Murine Flt3 ligand expands distinct dendritic cells with both tolerogenic and immunogenic properties. *J Immunol* 170:3554-3564.

246. Onai, N., A. Obata-Onai, R. Tussiwand, A. Lanzavecchia, and M. G. Manz. 2006. Activation of the Flt3 signal transduction cascade rescues and enhances type I interferon-producing and dendritic cell development. *The Journal of experimental medicine* 203:227-238.

247. Waskow, C., K. Liu, G. Darrasse-Jeze, P. Guermonprez, F. Ginhoux, M. Merad, T. Shengelia, K. Yao, and M. Nussenzweig. 2008. The receptor tyrosine kinase Flt3 is required for dendritic cell development in peripheral lymphoid tissues. *Nature immunology* 9:676-683.

248. Gibson, S. J., J. M. Lindh, T. R. Riter, R. M. Gleason, L. M. Rogers, A. E. Fuller, J. L. Oesterich, K. B. Gorden, X. Qiu, S. W. McKane, R. J. Noelle, R. L. Miller, R. M. Kedl, P. Fitzgerald-Bocarsly, M. A. Tomai, and J. P. Vasilakos. 2002. Plasmacytoid dendritic cells produce cytokines and mature in response to the TLR7 agonists, imiquimod and resiquimod. *Cellular immunology* 218:74-86.

249. Yrlid, U., V. Cerovic, S. Milling, C. D. Jenkins, J. Zhang, P. R. Crocker, L. S. Klavinskis, and G. G. MacPherson. 2006. Plasmacytoid dendritic cells do not migrate in intestinal or hepatic lymph. *J Immunol* 177:6115-6121.

250. Blasius, A. L., E. Giurisato, M. Cella, R. D. Schreiber, A. S. Shaw, and M. Colonna. 2006. Bone marrow stromal cell antigen 2 is a specific marker of type I IFN-producing cells in the naive mouse, but a promiscuous cell surface antigen following IFN stimulation. *J Immunol* 177:3260-3265.

251. Ueha, S., H. Yoneyama, S. Hontsu, M. Kurachi, M. Kitabatake, J. Abe, O. Yoshie, S. Shibayama, T. Sugiyama, and K. Matsushima. 2007. CCR7 mediates the migration of Foxp3+ regulatory T cells to the paracortical areas of peripheral lymph nodes through high endothelial venules. *Journal of leukocyte biology* 82:1230-1238.

252. Bettelli, E., Y. Carrier, W. Gao, T. Korn, T. B. Strom, M. Oukka, H. L. Weiner, and V. K. Kuchroo. 2006. Reciprocal developmental pathways for the generation of pathogenic effector TH17 and regulatory T cells. *Nature* 441:235-238.

253. Bettelli, E., T. Korn, and V. K. Kuchroo. 2007. Th17: the third member of the effector T cell trilogy. *Current opinion in immunology* 19:652-657.

254. Bettelli, E., T. Korn, M. Oukka, and V. K. Kuchroo. 2008. Induction and effector functions of T(H)17 cells. *Nature* 453:1051-1057.

255. Nurieva, R., X. O. Yang, Y. Chung, and C. Dong. 2009. Cutting edge: in vitro generated Th17 cells maintain their cytokine expression program in normal but not lymphopenic hosts. *J Immunol* 182:2565-2568.

256. Veldhoen, M., C. Uyttenhove, J. van Snick, H. Helmby, A. Westendorf, J. Buer, B. Martin, C. Wilhelm, and B. Stockinger. 2008. Transforming growth factor-beta 'reprograms' the differentiation of T helper 2 cells and promotes an interleukin 9-producing subset. *Nature immunology* 9:1341-1346.

257. Comerford, I., R. J. Nibbs, W. Litchfield, M. Bunting, Y. Harata-Lee, S. Haylock-Jacobs, S. Forrow, H. Korner, and S. R. McColl. 2010. The atypical chemokine receptor CCX-CKR scavenges homeostatic chemokines in circulation and tissues and suppresses Th17 responses. *Blood*.

258. Worbs, T., and R. Forster. 2007. A key role for CCR7 in establishing central and peripheral tolerance. *Trends in immunology* 28:274-280.

259. Liu, K., C. Waskow, X. Liu, K. Yao, J. Hoh, and M. Nussenzweig. 2007. Origin of dendritic cells in peripheral lymphoid organs of mice. *Nature immunology* 8:578-583.

260. Asselin-Paturel, C., G. Brizard, J. J. Pin, F. Briere, and G. Trinchieri. 2003. Mouse strain differences in plasmacytoid dendritic cell frequency and function revealed by a novel monoclonal antibody. *J Immunol* 171:6466-6477.

261. Cao, W., L. Bover, M. Cho, X. Wen, S. Hanabuchi, M. Bao, D. B. Rosen, Y. H. Wang, J. L. Shaw, Q. Du, C. Li, N. Arai, Z. Yao, L. L. Lanier, and Y. J. Liu. 2009. Regulation of TLR7/9 responses in plasmacytoid dendritic cells by BST2 and ILT7 receptor interaction. *The Journal of experimental medicine* 206:1603-1614.

262. Cao, W. 2009. Molecular characterization of human plasmacytoid dendritic cells. *Journal of clinical immunology* 29:257-264.

263. Wurbel, M. A., J. M. Philippe, C. Nguyen, G. Victorero, T. Freeman, P. Wooding, A. Miazek, M. G. Mattei, M. Malissen, B. R. Jordan, B. Malissen, A. Carrier, and P. Naquet. 2000. The chemokine TECK is expressed by thymic and intestinal epithelial cells and attracts double- and single-positive thymocytes expressing the TECK receptor CCR9. *European journal of immunology* 30:262-271.

264. Kunkel, E. J., J. J. Campbell, G. Haraldsen, J. Pan, J. Boisvert, A. I. Roberts, E. C. Ebert, M. A. Vierra, S. B. Goodman, M. C. Genovese, A. J. Wardlaw, H. B. Greenberg, C. M. Parker, E. C. Butcher, D. P. Andrew, and W. W. Agace. 2000. Lymphocyte CC chemokine receptor 9 and epithelial thymus-expressed chemokine (TECK) expression distinguish the small intestinal immune compartment: Epithelial expression of tissue-specific chemokines as an organizing principle in regional immunity. *The Journal of experimental medicine* 192:761-768.

265. Pabst, O., and G. Bernhardt. 2010. The puzzle of intestinal lamina propria dendritic cells and macrophages. *European journal of immunology* 40:2107-2111.

266. Kingston, D., M. A. Schmid, N. Onai, A. Obata-Onai, D. Baumjohann, and M. G. Manz. 2009. The concerted action of GM-CSF and Flt3-ligand on in vivo dendritic cell homeostasis. *Blood* 114:835-843.

267. Laouar, Y., T. Welte, X. Y. Fu, and R. A. Flavell. 2003. STAT3 is required for Flt3L-dependent dendritic cell differentiation. *Immunity* 19:903-912.

268. Ishikawa, J., T. Kaisho, H. Tomizawa, B. O. Lee, Y. Kobune, J. Inazawa, K. Oritani, M. Itoh, T. Ochi, K. Ishihara, and et al. 1995. Molecular cloning and chromosomal mapping of a bone marrow stromal cell surface gene, BST2, that may be involved in pre-B-cell growth. *Genomics* 26:527-534.

269. Randolph, G. J., V. Angeli, and M. A. Swartz. 2005. Dendritic-cell trafficking to lymph nodes through lymphatic vessels. *Nature reviews* 5:617-628.

270. Williamson, E., G. M. Westrich, and J. L. Viney. 1999. Modulating dendritic cells to optimize mucosal immunization protocols. *J Immunol* 163:3668-3675.

271. Grdic, D., R. Smith, A. Donachie, M. Kjerrulf, E. Hornquist, A. Mowat, and N. Lycke. 1999. The mucosal adjuvant effects of cholera toxin and immune-stimulating complexes differ in their requirement for IL-12, indicating different pathways of action. *European journal of immunology* 29:1774-1784.

272. Hornquist, E., and N. Lycke. 1993. Cholera toxin adjuvant greatly promotes antigen priming of T cells. *European journal of immunology* 23:2136-2143.

273. Vajdy, M., and N. Lycke. 1995. Mucosal memory B cells retain the ability to produce IgM antibodies 2 years after oral immunization. *Immunology* 86:336-342.

274. Vajdy, M., and N. Y. Lycke. 1992. Cholera toxin adjuvant promotes long-term immunological memory in the gut mucosa to unrelated immunogens after oral immunization. *Immunology* 75:488-492.

275. Vajdy, M., and M. Singh. 2005. The role of adjuvants in the development of mucosal vaccines. *Expert opinion on biological therapy* 5:953-965.

276. Sanchez, J., and J. Holmgren. 2008. Cholera toxin structure, gene regulation and pathophysiological and immunological aspects. *Cell Mol Life Sci* 65:1347-1360.

277. Ochando, J. C., C. Homma, Y. Yang, A. Hidalgo, A. Garin, F. Tacke, V. Angeli, Y. Li, P. Boros, Y. Ding, R. Jessberger, G. Trinchieri, S. A. Lira, G. J. Randolph, and J. S. Bromberg. 2006. Alloantigen-presenting plasmacytoid dendritic cells mediate tolerance to vascularized grafts. *Nature immunology* 7:652-662.

278. Mittelbrunn, M., G. Martinez del Hoyo, M. Lopez-Bravo, N. B. Martin-Cofreces, A. Scholer, S. Hugues, L. Fetler, S. Amigorena, C. Ardavin, and F. Sanchez-Madrid. 2009. Imaging of plasmacytoid dendritic cell interactions with T cells. *Blood* 113:75-84.

279. Bonasio, R., and U. H. von Andrian. 2006. Generation, migration and function of circulating dendritic cells. *Current opinion in immunology* 18:503-511.

280. Asselin-Paturel, C., A. Boonstra, M. Dalod, I. Durand, N. Yessaad, C. Dezutter-Dambuyant, A. Vicari, A. O'Garra, C. Biron, F. Briere, and G. Trinchieri. 2001. Mouse type I IFN-producing cells are immature APCs with plasmacytoid morphology. *Nature immunology* 2:1144-1150.

281. Asselin-Paturel, C., and G. Trinchieri. 2005. Production of type I interferons: plasmacytoid dendritic cells and beyond. *The Journal of experimental medicine* 202:461-465.

282. Gilliet, M., W. Cao, and Y. J. Liu. 2008. Plasmacytoid dendritic cells: sensing nucleic acids in viral infection and autoimmune diseases. *Nature reviews* 8:594-606.

283. Tailor, P., T. Tamura, and K. Ozato. 2006. IRF family proteins and type I interferon induction in dendritic cells. *Cell research* 16:134-140.

284. Marshall, J. D., D. S. Heeke, M. L. Gesner, B. Livingston, and G. Van Nest. 2007. Negative regulation of TLR9-mediated IFN-alpha induction by a small-molecule, synthetic TLR7 ligand. *Journal of leukocyte biology* 82:497-508.

285. Seeds, R. E., S. Gordon, and J. L. Miller. 2009. Characterisation of myeloid receptor expression and interferon alpha/beta production in murine plasmacytoid dendritic cells by flow cytomtery. *Journal of immunological methods* 350:106-117.

286. Vermi, W., E. Riboldi, V. Wittamer, F. Gentili, W. Luini, S. Marrelli, A. Vecchi, J. D. Franssen, D. Communi, L. Massardi, M. Sironi, A. Mantovani, M. Parmentier, F. Facchetti, and S. Sozzani. 2005. Role of ChemR23 in directing the migration of myeloid and plasmacytoid dendritic cells to lymphoid organs and inflamed skin. *The Journal of experimental medicine* 201:509-515.